Year : 2016

Study of the rôle of PHO1 and PHO1;H1 in phosphate homeostasis in seeds and leaves of Arabidopsis thaliana

Vogiatzaki Evangelia

UNIL | Université de Lausanne
Faculté de biologie
et de médecine

Département de Biologie Moléculaire Végétal

Study of the role of *PHO1* and *PHO1;H1* in phosphate homeostasis in seeds and leaves of *Arabidopsis thaliana*

Thèse de doctorat ès sciences de la vie (PhD)

présentée à la

Faculté de biologie et de médecine
de l'Université de Lausanne

par

Evangelia VOGIATZAKI

Master de l'université de Crète – Grèce

Jury

Prof. Alexandre Roulin, Président
Prof. Yves Poirier, Directeur de thèse
Prof. Doris Rentsch, expert
Prof. Michael Broberg Palmgren, expert

Lausanne 2016

UNIL | Université de Lausanne
Faculté de biologie
et de médecine

Ecole Doctorale

Doctorat ès sciences de la vie

Imprimatur

Vu le rapport présenté par le jury d'examen, composé de

Président · e	Monsieur	Prof. Alexandre **Roulin**
Directeur · rice de thèse	Monsieur	Prof. Yves **Poirier**
Experts · es	Madame	Prof. Doris **Rentsch**
	Monsieur	Prof. Michael **Broberg Palmgren**

le Conseil de Faculté autorise l'impression de la thèse de

Madame Evangelia Vogiatzaki

Master of Science University of Crete, Grèce

intitulée

Study on the role of PH01 and PH01; H1 in phosphate homeostasis in seeds and leaves of *Arabidopsis thaliana*

Lausanne, le 15 décembre 2016

pour le Doyen
de la Faculté de biologie et de médecine

Prof. Alexandre Roulin

Contents

Summary

The *PHO1* gene was first described in the plant *Arabidposis thaliana* as a gene involved in the export of phosphate (Pi) into the root xylem vessel. The *pho1* mutant of *Arabidopsis* is deficient in phosphate loading to the xylem and has low shoot Pi and high root Pi. PHO1 can trigger Pi export in ectopic plant cells, strongly indicating that PHO1 is itself a Pi exporter and PHO1-mediated Pi export was associated with its localization to the Golgi and trans-Golgi networks, revealing a role for these organelles in Pi transport. Another interesting role of *PHO1* was also revealed by Zimmerli and colleagues, who showed that *PHO1* expression in guard cells is involved in the stomatal response to abscisic acid (ABA) in *Arabidopsis*.

The *Arabidopsis PHO1* gene family comprises of 11 members. One of these homologues, called *PHO1;H1*, is expressed in the vascular tissue of root and shoot and is regulated by the plant Pi status. Out of the set of *Arabidopsis PHO1* homologues, only *PHO1;H1* can functionally replace *PHO1* in the transfer of Pi into the root xylem vessel when its expression is under the regulation of the *PHO1* promoter. The role of *PHO1;H1* in the aerial part of the plant is currently unknown. Apart from one other homologue, called *PHO1;H4*, that probably plays a role in the hypocotyl growth under the blue light, the role of the other members of the *PHO1* family has not been identified yet.

Mining of the RNAseq data revealed that *PHO1* (seed coat) and *PHO1;H1* (both embryo and seed coat) are both expressed in the seed. Consequently, the aim of this thesis project was to identify the exact cell type(s) in which these genes are expressed and the role of *PHO1* and *PHO1;H1* in the leaves and the seeds of *Arabidopsis* plants.

Regarding the role of these genes in the seeds, we report that *PHO1* does play a bigger role than *PHO1;H1* in exporting Pi into the seed apoplast. *PHO1;H1*, as it was shown for the roots, also contributes to the Pi export into the seed apoplast but less than *PHO1* or probably under specific conditions. Furthermore, another important finding of this study was that the chalazal region of the seed coat is important for *PHO1* to be expressed in order to off-load Pi into the seed apoplast. After fusing a chalazal specific promoter in front of the genomic sequence of *PHO1* we also proved that the expression of PHO1 specifically in the chalazal seed coat is enough for Pi export into the apoplast so as the embryo to develop properly. Finally, we show that the expression of PHO1 under Pi starvation conditions increases in the micropylar region of the seed coat, something that raises interesting questions about the possible function of the micropylar region under abiotic or biotic stress.

Résumé

Le gène *PHO1* a été décrit la première fois chez la plante *Arabidposis thaliana* comme étant impliqué dans l'export de phosphate inorganique (Pi) vers le xylème de la racine. Le mutant *pho1* d'*Arabidopsis* est déficient pour le chargement du phosphate dans le xylème et contient une faible concentration de Pi dans les feuilles et une forte concentration dans les racines. L'expression de *PHO1* peut déclencher l'export du Pi dans des cellules végétales ectopiques, indiquant que *PHO1* est lui-même un exporteur de Pi. L'export du Pi médié par *PHO1* est associé à sa localisation aux réseaux de Golgi et trans-Golgi, révélant le rôle de ces organes dans le transport du Pi. Un autre rôle intéressant de *PHO1* a également été révélé par Zimmerli et collègues, montrant que l'expression de *PHO1* dans les cellules de garde médie la réponse stomatique à l'acide abscissique (ABA) chez *Arabidopsis*.

La famille du gène *Arabidopsis PHO1* comprend 11 membres. L'un de ces homologues, appelé *PHO1;H1*, est exprimé dans le tissu vasculaire des racines et des feuilles et est régulé par la concentration en Pi. Sur l'ensemble des homologues de PHO1 chez *Arabidopsis*, seulement *PHO1;H1* peut remplacer fonctionnellement *PHO1* dans le transfert de Pi vers le xylème de la racine lorsque son expression est sous le contrôle du promoteur de *PHO1*. Le rôle de *PHO1;H1* dans les feuilles est actuellement inconnu. Mis à part un autre homologue, appelé *PHO1;H4*, qui joue probablement un rôle dans la croissance de l'hypocotyle en présence de lumière bleue, le rôle des autres membres de la famille de *PHO1* n'a pas encore été identifié.

L'exploitation d'une base de données d'expression de gènes a révélé que PHO1 et *PHO1;H1* sont tous les deux exprimés dans la graine (PHO1 dans le tégument et PHO1;H1 dans l'embryon et le tégument). Par conséquent, l'objectif de ce projet de thèse était d'identifier le type exact de cellules dans lesquelles ces gènes sont exprimés ainsi que de clarifier le rôle de *PHO1* et *PHO1; H1* dans les feuilles et les graines de la plante *Arabidopsis.*

Concernant les graines, nous avons montré que PHO1 joue un rôle plus important que PHO1;H1 dans l'export de Pi vers l'apoplaste des graines. PHO1; H1, comme il a été montré pour les racines, contribue également à l'export du Pi vers l'apoplaste des graines, mais moins que PHO1 ou probablement dans des conditions spécifiques. Une autre conclusion importante de cette étude est que la région chalaze de l'enveloppe de la graine est importante pour l'export du Pi vers l'apoplaste des graines médié par PHO1. Par fusion d'un promoteur spécifique chalaze en amont de la séquence génomique de *PHO1*, nous avons

également prouvé que l'expression de PHO1 spécifiquement dans le tégument de chalaze est suffisante pour l'export du Pi dans l'apoplaste, afin que l'embryon se développe correctement. Enfin, nous montrons qu'en condition de carence en Pi, l'expression de PHO1 augmente dans la région micropylaire de l'enveloppe de la graine, ce qui soulève des questions intéressantes sur la fonction possible de la région micropylaire en réponse à des stress biotiques ou abiotiques.

Abbreviations

ATP	Adenosine triphosphate
amiRNA	Artificial microRNA
BiFC	Bimolecular fluorescence complementation
CZSC	Chalazal Seed Coat
DIC	Differential Interference Contrast method
DNA	Deoxy-ribonucleic acid
DM	Double mutant (*pho1.1/pho1.1 pho1;h1.1/pho1;h1.1*)
DM2.4	Double mutant (*pho1.2/pho1.2 pho1;h1.4/pho1;h1.4)*
E	Embryo
FM	Female gametophyte
GEN	General endosperm
GUS	β-glucuronidase
GSC	General seed coat
I.I.	Inner Integuments
O.I.	Outer Integuments
P	Phosphorus
PA	Phytic acid
PEN	Peripheral Endosperm
PM	Plasma membrane
Pi	Inorganic Phosphate
PUE	Phosphorus-use efficiency
qPCR	Quantitative PCR
RNA	Ribonucleic acid
RT	Room temperature
SC	Seed coat
TGN	trans-Golgi

CHAPTER 1

Introduction

The importance of Phosphate in our life

Plants require mineral nutrients to complete their life cycle. Mineral nutrients are divided into two categories, namely macronutrients (nitrogen, phosphorus, potassium, calcium, magnesium and sulfur) and micronutrients (boron, copper, iron, chloride, manganese, molybdenum and zinc), and they are required in large and small quantities, respectively, for normal plant development.

The macronutrient Phosphorus (P) is present in all living cells and is vital for life. Providing P to every living being is critical for their survival and reproduction, as P is an essential macronutrient required for many physiological and metabolic processes. It serves various basic biological functions as a structural element in nucleic acids (DNA, RNA) and phospholipids. Furthermore, P is involved in signaling mechanisms by phosphorylation and dephosphorylation of proteins. P also plays a very important role in photosynthesis and respiration, the two key processes for the survival of plants (Poirier and Bucher, 2002). Moreover, P cannot be found in nature as a free element because it is highly reactive, combining rapidly with oxygen and hydrogen. Depending on the rhizosphere pH, P can be found in many different forms including $(H_2PO_4)^-$, $(HPO_4)^{-2}$ and $(PO_4)^{-3}$, however in plants, it is mainly assimilated via the root system in the form of inorganic phosphate $(H_2PO_4)^-$ (Pi). Within the plant, Pi is distributed from cell to cell and to different organs to maintain Pi homeostasis at the whole organism level.

Several reviews have reported a potential P crisis because future sustainability of crop yields will be challenged, as global P resources are finite and rapidly diminishing. Depending on where they are found, high quality, economically viable phosphate rock reserves, which the U.S. Geological Survey estimated totaled 69 billion tons this year, will last only 50 to 200 years, if current levels of use are maintained or increased (U.S., Geological Survey 2016). However, when the global need for Pi fertilizer and its impact on the lifetime of P reserves is evaluated, only cropland is taken into account. Recently, and interesting study by Sattari et al. (2016) estimated the P fertilizer needed to sustain not only cropland, but also grassland used to meet the growing needs for meat and milk production. Globally, soils that are permanently

used as grassland cover approximately 3.3 billion hectares or 26% of the Earth's ice-free land. These lands are expected to diminish in nutritional quality, as nutrients are permanently being removed from these soils in the form of livestock products and these lands are generally not fertilized. Therefore, if we take into account the continuous removal of Pi from grassland soils through the withdrawal of livestock products and the input of manure as an organic fertilizer for cropland, these authors estimated that mineral P fertilizer consumption should double by 2050 to sustain crop and grassland productivity.

The shortage of P in the future, also known as "P crisis", is much more complicated as many proposals suggest that organic agriculture, using manure as a main external source of nutrients, is an effective alternative that can reduce the need for chemical P fertilizer. However, the supporters of organic farming do not take into account that nutrients present in manure were previously removed from grassland by the form of livestock (Fig. 1). Therefore, as proposed by Sattari et al. (2016) food production can only be sustainable if it is addressed in the context of Pi supply in global terms, taking into account land used for both crop and grass production. Doubling our needs for P fertilizer seems unfeasible, because P reserves are not infinite and irreplaceable. Thus, it is very likely that very soon, the humanity will face a food production crisis due to a lack of sufficient chemical or organic P fertilizer (Herrera-Estrella and Lopez-Arredondo, 2016).

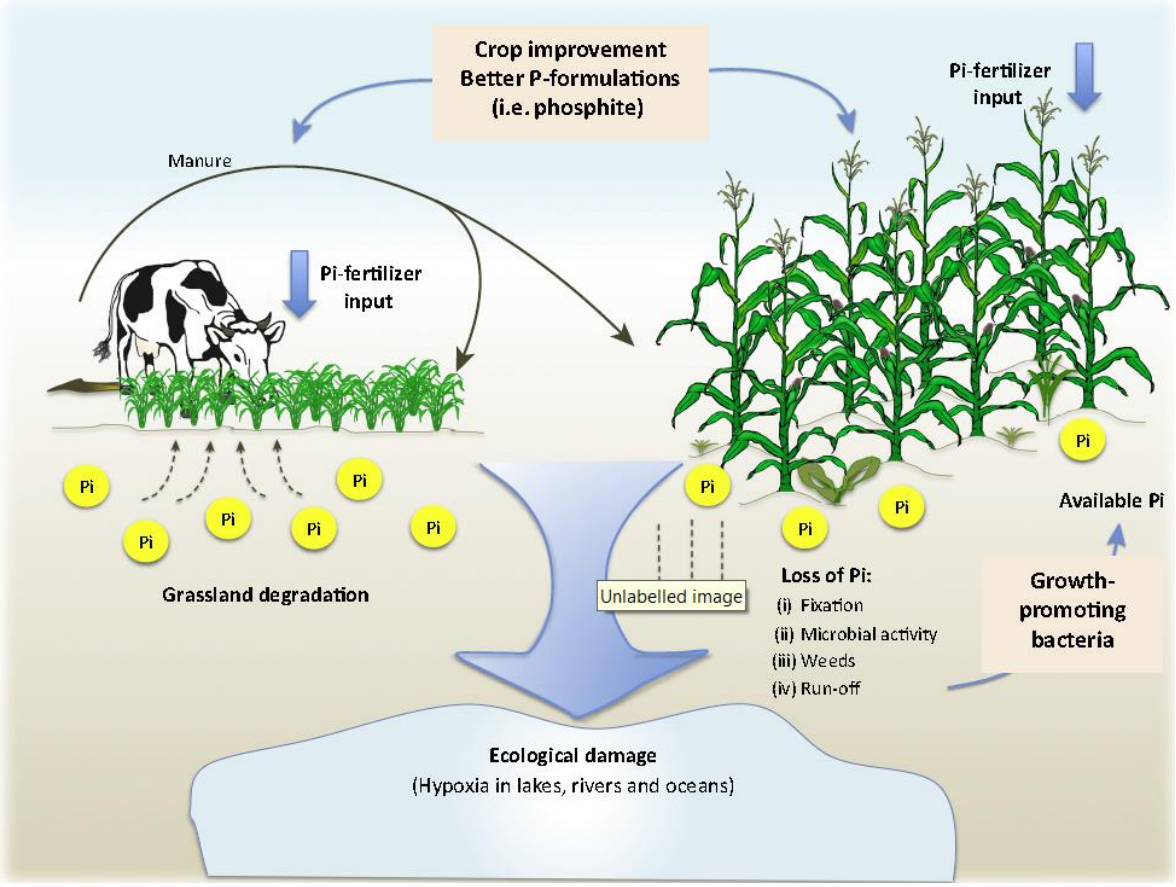

Figure 1: Factors influencing the global need for phosphate fertilizers. Currently, livestock production including milk and meat is mainly sustained by the phosphate (Pi) present in the soil. In addition to Pi-fertilizers, a large percentage of the Pi consumed by cattle is discarded in manure, which in turn is used as source of Pi for crop production leading to grassland degradation. Moreover, a large percentage of the Pi applied in the field is lost due to biological and physicochemical factors, causing irreversible ecological damage. The use of Pi-fertilizers is crucial to sustain food production and it is predicted that in order to sustain productivity, in both grass land and cropland, the need of chemical Pi-fertilizer will need to be doubled by 2050, therefore aggravating environmental contamination. Technologies including the design and use of better phosphorus (P)-fertilizers, improved plants, and growth-promoting bacteria would help to optimize the use of P-fertilizers and increase the lifetime of P reserves [from:(Herrera-Estrella and Lopez-Arredondo, 2016)].

Another important aspect of phosphate fertilization is eutrophication, or more precisely hypertrophication, which is the depletion of oxygen in a body of water, that kills aquatic animals. This usually happens due to a dramatic increase of plant nutrient concentrations, mainly phosphates, in water bodies which induces explosive growth of plants and algae, the decaying of which consumes oxygen from the water. Natural eutrophication is a slow and gradual process, typically occurring over a period of many centuries as nutrient-rich soil washes into lakes. In contrast, human-induced eutrophication can occur over time frames as short as a decade (Addy and Green, 1996). Although it has taken only 60 years for humans to turn many freshwater lakes eutrophic, studies suggest their recovery may take

1000 years under the best of circumstances (Carpenter and Lathrop, 2008). At present, nearly 38% of US lakes are experiencing eutrophic conditions affecting aquatic life and watershed ecosystems (SAMAB, 1996). Runoff, especially from urban and agricultural areas, carries fertilizers, pesticides, sediment, and/or industrial sewage that accelerate eutrophication when vacated into a water body (Smith et al., 1999). During severe eutrophication, there are hypoxic conditions which disrupt normal food chain and ecosystem processes by creating a "dead zone" where no animal life can be sustained (Smaya, TJ. 2008). As seen in Figure 2, "cultural eutrophication" is caused by human land use, including agriculture and residential or industrial developments. On a global basis, researchers have demonstrated a strong correlation between total phosphorus inputs and algal biomass in lakes (Anderson et al., 2002). Since 1950, phosphorus inputs to the environment have been increasing as the use of phosphate-containing fertilizer, manure, and laundry detergent has become more common (Litke, 1999). Consequently, humans release of phosphorus to the soil and the water is 75% more than would be naturally deposited by weathering of rock (Bennet et al., 2001). Even increases in minute amounts of the nutrient can stimulate tremendous growth and productivity (Addy and Green, 1996). According to an estimate, 400 grams of phosphates could potentially induce an algal bloom to the extent of 350 tons (Sharma, 2009). Although a need for a solution to eutrophication, especially in the developing countries has been highlighted since the 70s (Beeton and Edmondso, 1972; Lund, 1974), more research is needed in order to feed the continuous population growth and new regulations have to be implemented from the governments in order to control the industrial and agricultural sectors to reduce activities that contribute to eutrophication.

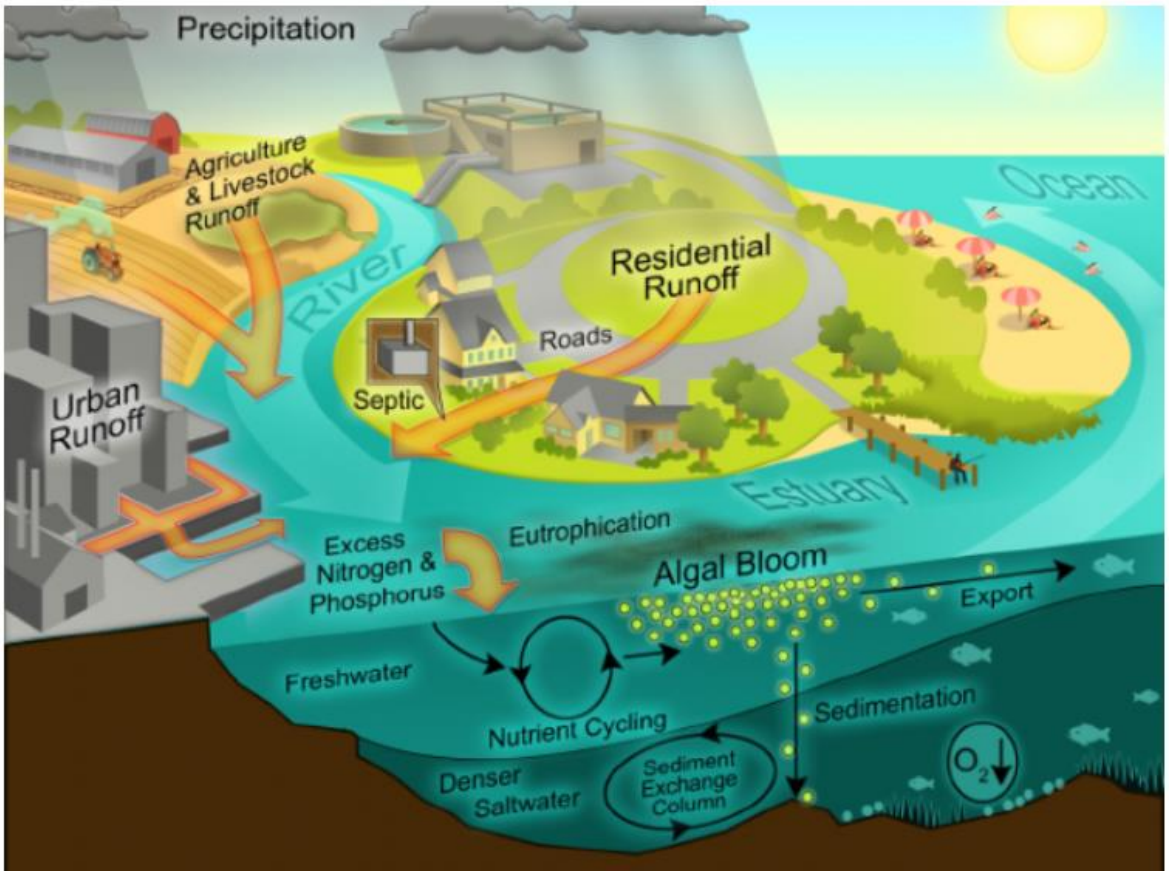

Figure 2: Numerous sources from the watershed of the lake contribute to nutrient inputs and eutrophication (http://projecteutrophication.weebly.com/sources-of-cultural-eutrophication.html).

Phosphate acquisition and transport in plants

Phosphate from the soil is absorbed and assimilated from plants in the form of soluble inorganic orthophosphate (Pi), which has low availability and mobility in most soils. Although P is an abundant element in nature, its' bioavailability in the form of utilizable Pi is often suboptimal for crop productivity (Lin et al., 2009; Marschner, 1995; Raghothama, 1999; Ticconi and Abel, 2004). This happens because Pi is rapidly fixed in the soil due to its high reactivity with cations such as calcium and magnesium in alkaline soils or aluminum and iron in acidic soils. Since Pi concentrations in soil solution rarely exceed 10uM and cellular Pi concentrations are greater than 10mM, plants must acquire Pi in roots against a steep concentration gradient (Mimura, 1999; Raghothama, 2000).

Ion uptake across the membrane follows Michaelis-Menten kinetics, thus allowing us to calculate functional parameters such as pH optimum, Michaelis-Menten constant K_m, uptake velocity V_{max} and minimal concentration of the ion at which transport occurs (Epstein and Hagen, 1952; Epstein et al., 1963). In 1998 Schachtman et al. showed that Pi uptake can be mediated by high- and low-affinity transport mechanisms. However, at Pi concentrations in

the μM range, which corresponds to the soil used naturally for cultivation reasons, only high-affinity transport occurs (Cogliatti and Clarkson, 1983; Drew et al., 1984). As there are extremely low (usually at micromolar level) concentrations of available Pi at the root-soil interface, but much higher ones (millimolar) of intracellular Pi, its' uptake across the cell boundary has to be effected against a steep concentration gradient. This is achived by transport of the anion across the membrane coupled to the transport of protons (H^+-symport). Plants and fungi use a proton P-type ATPase pump to generate an electrochemical gradient across the plasma membrane at the expense of ATP (Fig. 3). This leads to the formation of a large membrane potential with the cytoplasm having a negative potential of about -120mV on average. Consequently, the transport of anions, such as Pi, is usually coupled to protons in a secondary transport process. Thus, the driving force for Pi influx is the proton gradient generated by the P-type H^+-ATPase, with a stoichiometry of two to four protons per Pi (Sakano, 1990; Schachtman et al., 1998; Sze et al., 1999; Thibaud et al., 1988; Ullrich-Eberius et al., 1984).

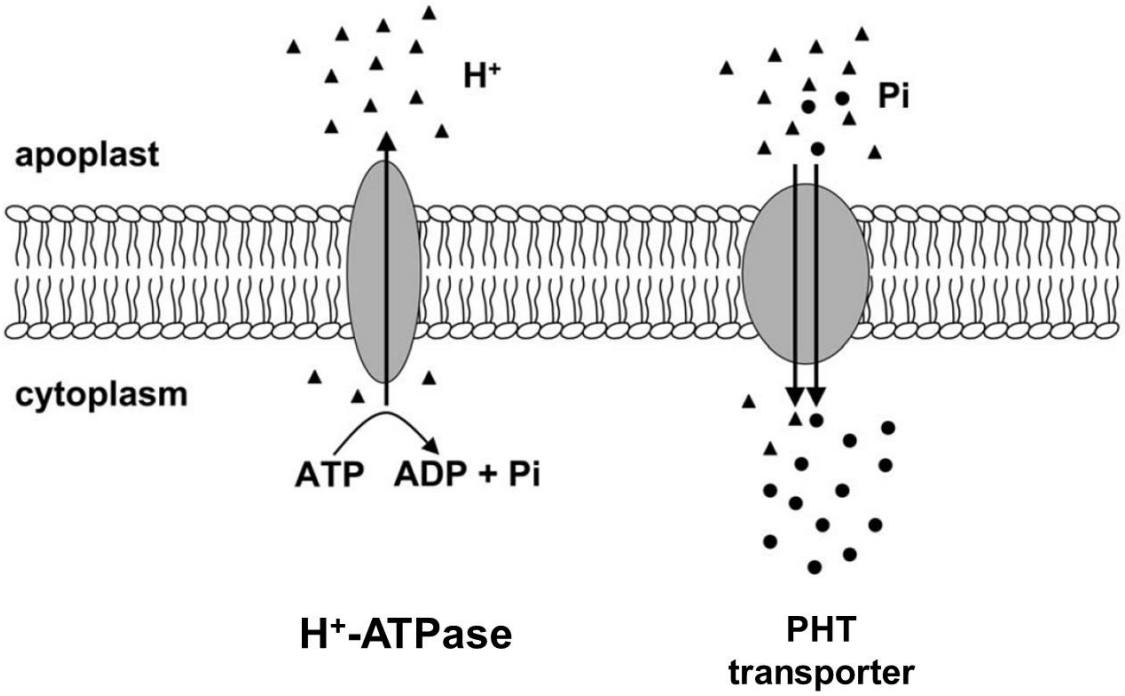

Figure 3: A model for secondary Pi transport across the plasma membrane. The H^+ (triangles) gradient across the lipid bilayer is generated by the activity of the H^+-ATPase at the expense of ATP. H^+/Pi (circles) co-transport is mediated by the Pi transporter protein (PHT). The orientation of the transport is marked by arrows. The orientation of the plasma membrane is as indicated (apoplast, cytoplasm). Modified from (Poirier and Bucher, 2002)

Today, after many years of research using electrophysiological techniques on several cell types, a variety of plasma membrane ion channels and transporters have been revealed. These transporters are either constitutively active or are activated by membrane depolarization, hyperpolarization, light, or expansion (for more information see reviews: (Barbier-Brygoo et al., 2000; Krol and Trebacz, 2000; Poirier and Jung, 2015; Roberts, 2006; Schroeder, 1995; Teakle and Tyerman, 2010; Tyerman, 1992; White and Broadley, 2001).

In order to modulate P homeostasis, plants must balance P uptake, mobilization, and partitioning to various organs. The most known plasma membrane-localized high affinity $H_2PO_4^-/H^+$ symporters that mediate Pi acquisition belong to the PHOSPHATE TRANSPORTER1 (*PHT1*) family (Chiou et al., 2001; Muchhal et al., 1996; Poirier and Bucher, 2002; Raghothama, 2000). These proteins are characterized by 12 membrane spanning domains that are similar to the yeast Pho84p high-affinity Pi transporter (Muchhal et al., 1996; Rausch and Bucher, 2002). In *Arabidopsis*, there are nine such PHT1 proteins with 60% to 95% sequence similarity, and their homologs have been identified in several crop species (rice [*Oryza sativa*], wheat [*Triticum aestivum*], potato [*Solanum tuberosum*], tomato [*Solanum lycopersicum*], and tobacco [*Nicotiana tabacum*]; (Rausch and Bucher, 2002). Promoter-reporter fusions of PHT1 members in *Arabidopsis* demonstrated the Pi deficiency-induced expression of eight of the nine members in roots (Karthikeyan et al., 2002; Mudge et al., 2002). Plasma membrane localized Pi transporters can take up Pi from soil in the epidermis cells or root cap.

Furthermore, another factor that also affects Pi nutrition in a complex manner is the abundance and diversity of soil microorganisms. Some organisms (arbuscular mycorrhizal fungi and plant growth–promoting rhizobacteria) may enhance plant Pi acquisition. However, other microbial species compete with plant roots for Pi uptake and convert it into organic forms that are not directly available for plant uptake. Thus, all these factors impact negatively the P use efficiency of plants, as crops assimilate only between 20 to 30% of the applied Pi (Herrera-Estrella and Lopez-Arredondo, 2016).

Once Pi is absorbed into the root by epidermis or root hairs, it will be transferred across the root to the stele by the appoplastic, the symplastic or the coupled trans-cellular pathway. Through the apoplastic pathway water and nutrients are diffused towards the stele through free spaces and cell walls of the epidermis and cortex (Fig. 4A). The rate of diffusion depends upon the ionic gradient between the external solution and the apoplastic free space. As pectins in the cell walls can act as cation exchangers due to the negatively charged carboxylic

groups (R.COO2) in the galacturonic acid monomers of pectin, cations from the external solution can accumulate in the root apoplast, whereas anions are kept away. The symplastic route to the vasculature implicates cell-to-cell movement via plasmodesmata (Fig. 4A). Plant cells are surrounded by a cell wall, creating a burden and thus a challenge for individual cells to directly communicate and exchange nutrients. Therefore, plasmodesmata, connections providing cytoplasmic continuity between each cell and its immediate neighbor, enable transport and communication between them (Burch-Smith and Zambryski, 2012). The rate of symplastic transport, depends on the size exclusion limit and the frequency of plasmodesmata between the cells, features that can be controlled by certain stress conditions. However, while the role of plasmodesmata for transporting large molecules such as RNA, proteins, and viral RNA-protein complexes is well understood (Burch-Smith and Zambryski, 2012), not much is known regarding the transport of metal-chelate complexes or macronutrients. Considering that the passage through the plasmodesmata is dependent upon regulated size exclusion limits, the transport of metal-chelate complexes or of macronutrients between cells could be a fine-tuned and regulated process. Hence, plasmodesmata could modulate metal-chelate transport either by blocking them or facilitating their transport in a selective way. Finally, the coupled trans-cellular pathway relates to a trans-epithelial transport (paracellular) with influx and efflux transporters, where nutrients are being transported from one cell to the other (Fig. 4). In this pathway, transporters are polarly distributed, not only in the endodermis but also in cortical and epidermal cells. Thus, nutrients are transported from one cell to the other, passing repeatedly from symplast to apoplast, in a mechanism similar to auxin polar transport (Lofke et al., 2013). Such a mechanism provides directional long-distance transport towards the stele and offers the advantage of a control mechanism over multiple cell layers, regardless of the mass flow of nutrients (Barberon and Geldner, 2014).

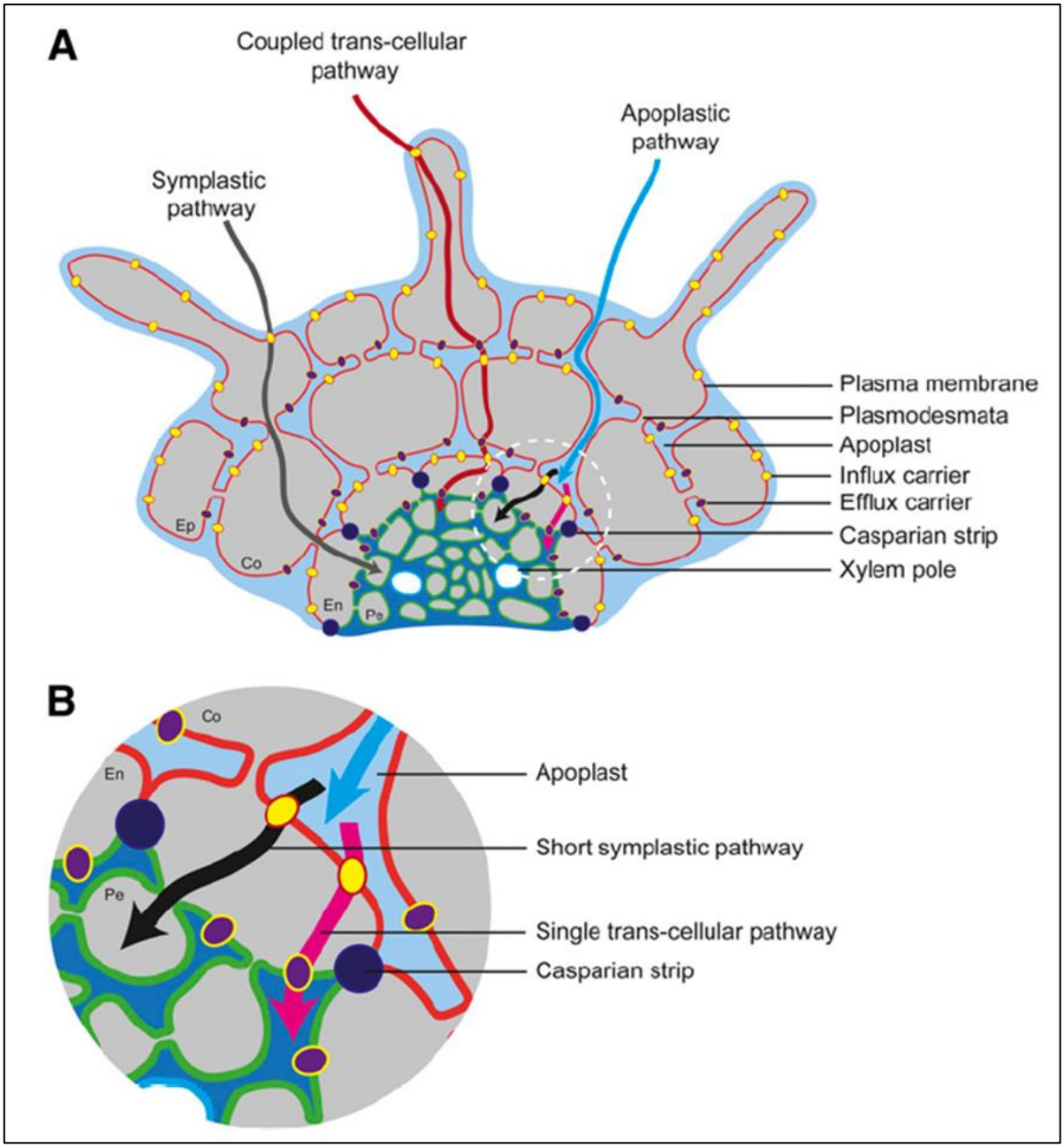

Figure 4: Transport of nutrients in roots: three different pathways. **A**, Schematic view of the three different pathways involved in the transport of nutrients from the soil to the endodermis. The symplastic pathway (in gray) requires at first a selective uptake into a cell and then transport from one cell to the other through plasmodesmata. The coupled transcellular pathway (in red) involves influx (in yellow) and efflux (in purple) carriers to transport nutrients from one cell to the other. The apoplastic pathway (in blue) corresponds to a passive transport in the extracellular space and is blocked by the CS at the level of the endodermis.**B**, Magnification of the circled area in A, focusing on the transport of nutrients from the apoplast to the endodermis. Transport routes through the endodermis involve a short symplastic pathway (in black) and a single trans-cellular pathway (in pink), restricted at the level of the endodermis. Co, Cortex; En, endodermis; Ep, epidermis; Pe, pericycle [from (Barberon and Geldner, 2014)].

Once in the stele, Pi is exported into the xylem (apoplast), where Pi is transported from the root to the shoot following the transpiration stream. The only Pi exporter in plants known so far is PHOSPHATE1 (PHO1) (Hamburger et al., 2002). The PHO1 protein (Fig. 5) contains an SPX (for SYG1/PHO81/XPR1) domain in the N-terminal hydrophilic region, an EXS (for ERD1/XPR1/SYG1) domain in the C-terminal hydrophobic tail and four transmembrane domains (Arpat et al., 2012; Hamburger et al., 2002; Wang et al., 2004; Wege et al., 2016). Knowing all this information regarding the function of phosphate importers (Fig. 3) and having in mind the structure of PHO1 protein (Fig. 5), the question of what kind of exporter could PHO1 be is raised.

Arpat et al. (2012) expressed PHO1 under an estradiol-inducible promoter and showed that PHO1 expression in leaf mesophyll cells leads to a specific export of Pi to the apoplast. This Pi export was only marginally affected by the addition of a proton-ionophore, indicating that Pi export was not coupled to the proton gradient. Examination of the localization of PHO1 using a PHO1:GFP chimeric protein able to complement the *pho1* mutant and shown to mediate Pi export revealed that, contrary to expectation, PHO1 was not localized to the plasma membrane (PM) but to the Golgi and trans-Golgi network (TGN) (Arpat et al., 2012). Thus, one possibility is that, at steady-state level, only a minor fraction of PHO1 is localized at the PM and that it is this minor fraction that is responsible for Pi export. Such a mechanism has been postulated for the iron importer IRT1 that shows a similar localization to the Golgi/TGN (Barberon et al., 2011). Alternatively, it is possible that PHO1 loads Pi into vesicles and that Pi export is mediated by vesicle fusion with the PM. Clearly, further research on PHO1 trafficking is required to clarify its' actual mode of action.

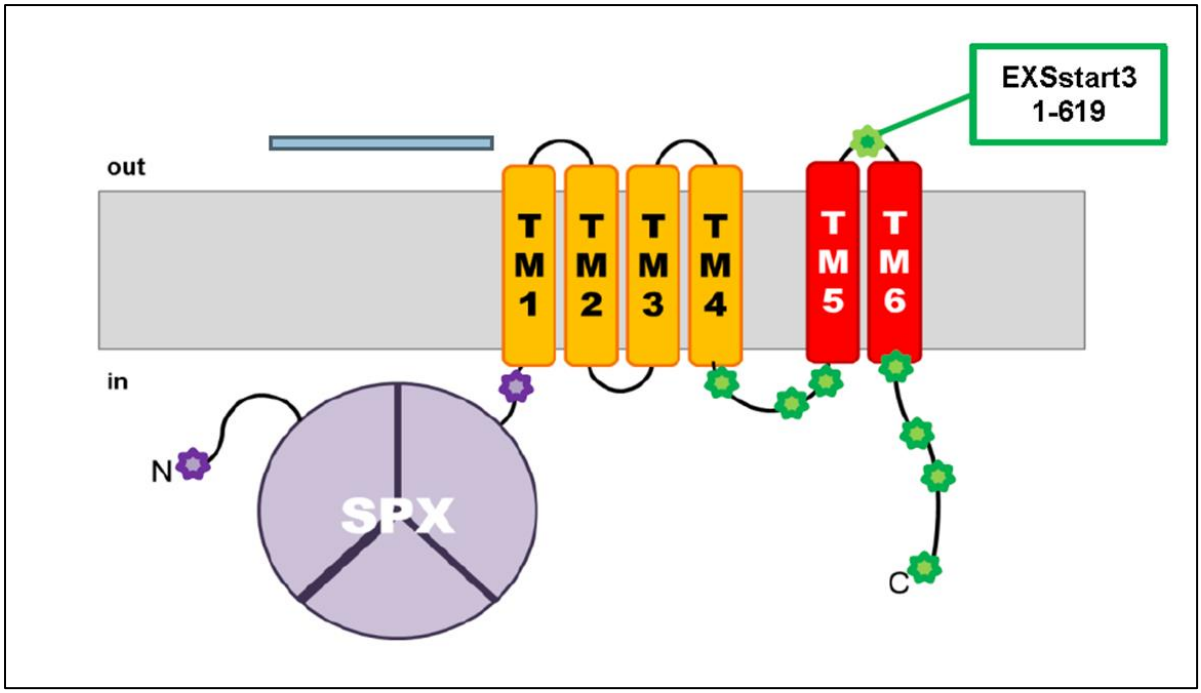

Figure 5: Model of PHO1 topology according to BiFC and roGFP2 data with both termini localized in the cytosol and a total of 6 transmembrane spanning segments. SPX domain displayed in purple, 4TM in orange, transmembrane part of EXS domain in red, N-terminal truncations indicated as purple stars, C-terminal truncations as green stars, lumen-localized truncation EXSstart3 indicated in box [from:(Wege et al., 2016)].

pho1 mutants were first isolated in a screen for low shoot Pi contents and are shoot Pi deficient with reduced shoot growth (Fig. 6) (Hamburger et al., 2002; Poirier et al., 1991; Stefanovic et al., 2007). These mutants are impaired in xylem loading of Pi, leading to plants, that are Pi deficient in shoots but accumulate more Pi in roots. *pho1* mutants show all the hallmarks associated with Pi deficiency including reduced shoot growth and increased anthocyanin accumulation (Poirier et al., 1991). In Arabidopsis, *PHO1* has 10 homologues making it a multigenic family of 11 members (*PHO1, PHO1;H1-H10*, see Fig. 7). In roots, *PHO1* is expressed primarily in the root stellar cells including pericycle as well as endodermal passage cells (Fig. 8) (Hamburger et al., 2002). This pattern of expression is consistent with the role of PHO1 in Pi loading into xylem cells. Pi export activity of PHO1 was demonstrated by transiently expressing PHO1 in leaf mesophyll cells (Arpat et al., 2012). Several members of the *PHO1* gene family are transcriptionally activated upon different nutrient starvation stresses. Among them, only *PHO1;H1* is strongly up regulated under Pi starvation (Stefanovic et al., 2007) and it was shown that it can complement the *pho1* mutant phenotype when expressed under *PHO1* promoter, suggesting a role in Pi export, although it seems to be regulated differently comparing to *PHO1* probably at the promoter level. Consequently, *PHO1* is the key player of Pi export into the apoplast in the roots and *PHO1;H1* plays a minor role. The implication of *PHO1;H1* in Pi export into the root xylem

was also shown by the analysis of *pho1 pho1;h1* double mutant. These mutants have highly reduced shoot growth and reduced Pi transfer to the shoot (Stefanovic et al., 2007). Finally, PHO1;H1 is also expressed in the same tissues as PHO1, i.e: shoot and root vasculature (Fig. 8). Regarding, the rest of the homologues they are expressed in a range of different tissues and organs (Fig. 9) (Wang et al., 2004).

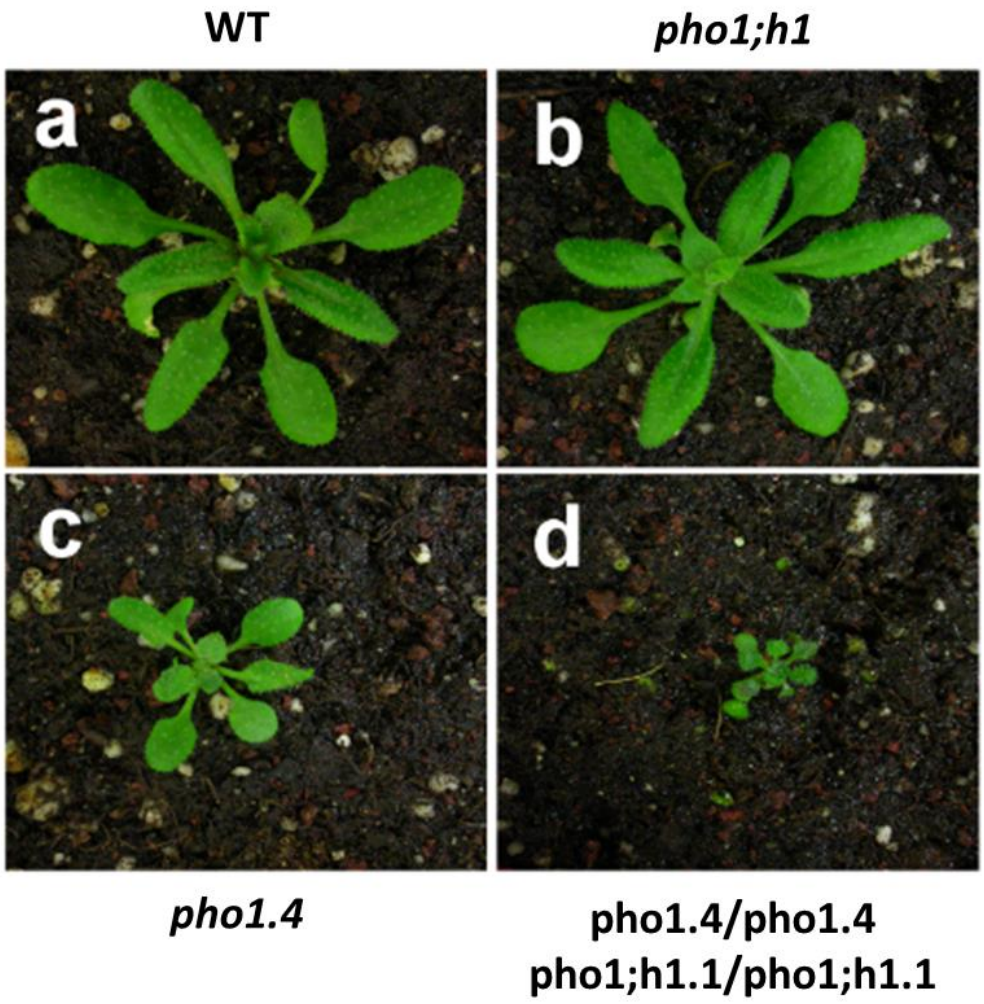

Figure 6: Characterization of the *pho1;h1-1* mutant and *pho1-4/pho1;h1-1* double mutant. Wild-type accession Columbia (a), *pho1;h1-1* (b), *pho1-4* (c) and *pho1-4/pho1;h1-1* double mutant (d) were grown for 1 week in MS solid medium, followed by 3 weeks in soil under continuous light [from (Stefanovic et al., 2007)].

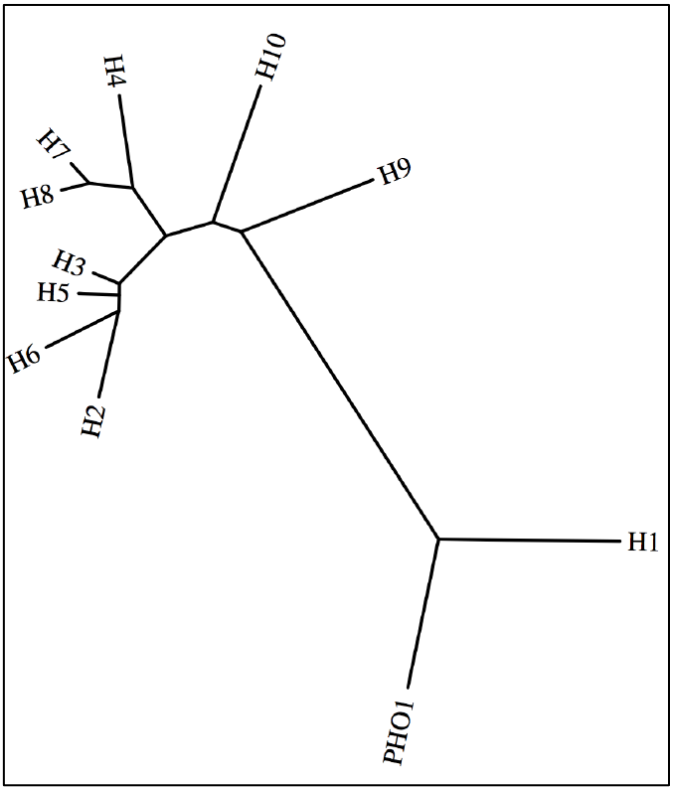

Figure 7: Unrooted phylogenetic tree of the *Arabidopsis PHO1* family. The tree was made using the MUSCLE alignment method of http://www.phylogeny.fr and the protein sequences of all the gene members of *PHO1* family.

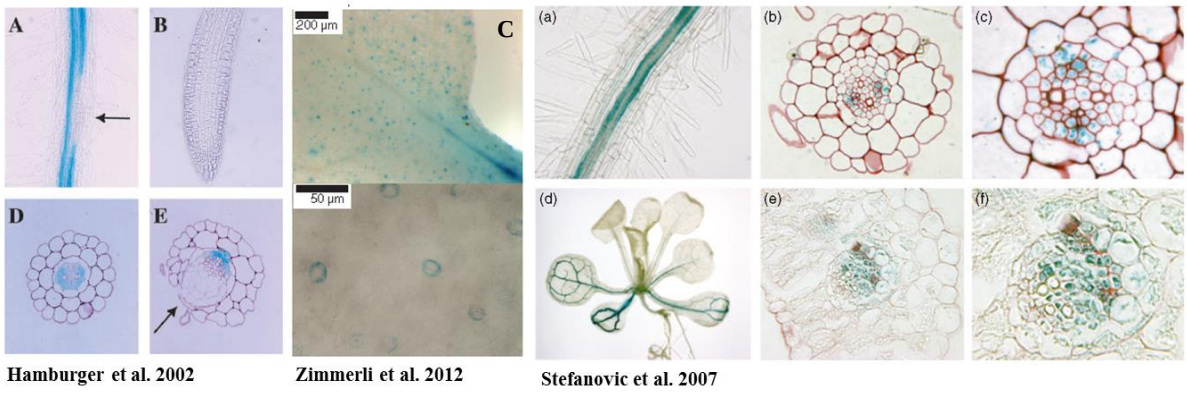

Figure 8: *Left:* Expression Pattern of the *PHO1* promoter (A,B,D,E), and *PHO1* protein (C-D). Longitudinal and transverse views of the mature zone of roots (A, D, and E), root tip and elongation zone (B), leaf vascular tissue (C, up) and guard cells of stomata (C, down) are shown. *Right:* Expression pattern of *PHO1;H1* promoter. Longitudinal and transverse views of the root (a–c) and shoot (d–f) of inorganic phosphate (Pi)-replete plants are shown (Hamburger et al., 2002; Stefanovic et al., 2007; Zimmerli et al., 2012).

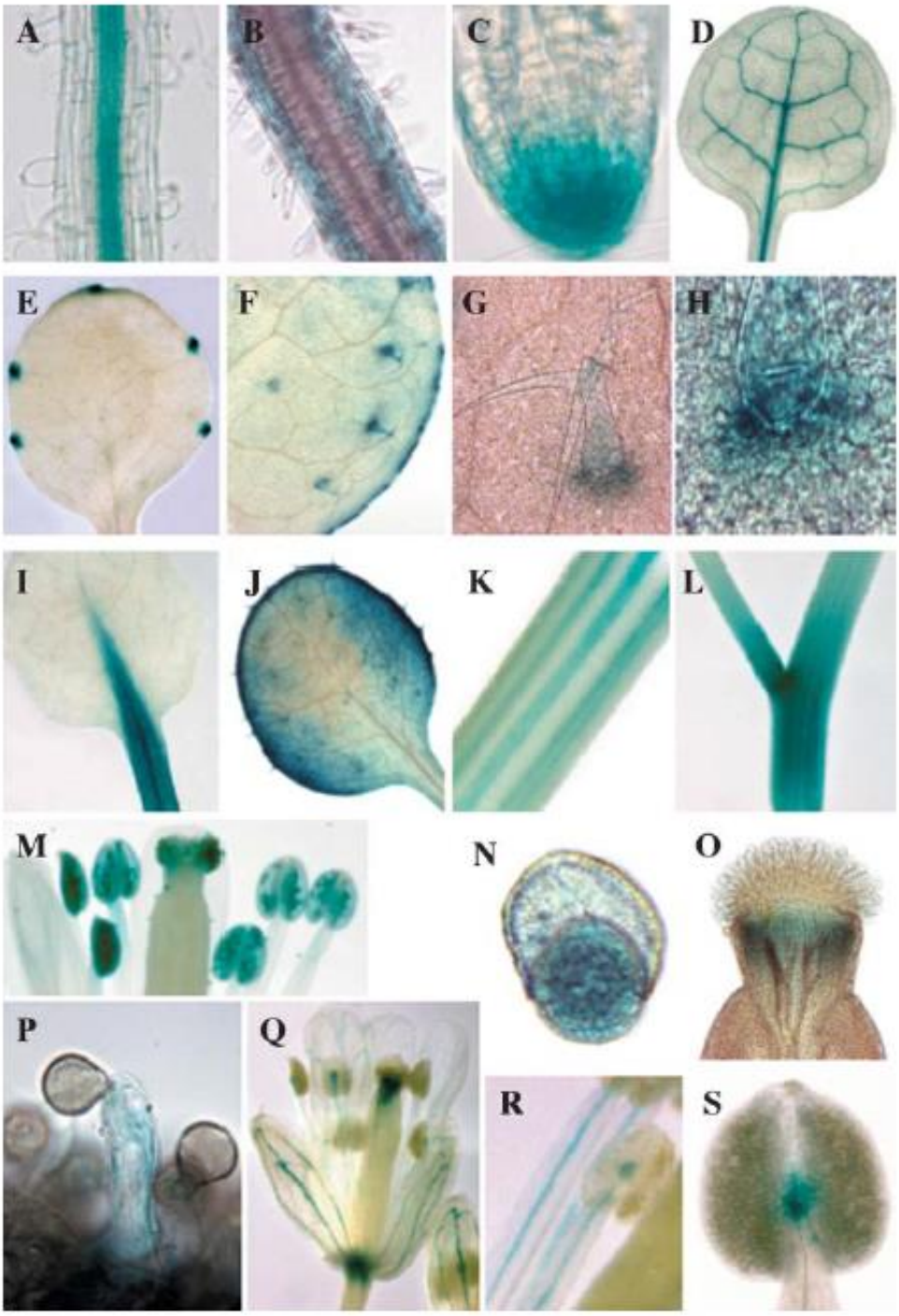

Figure 9: Expression pattern of *PHO1* gene family.
Expression of *PHO1:H3* (A), *PHO1:H10* (B) and *PHO1:H7* (C) in the root. *PHO1;H1* expression in the leaf vascular tissue (D). *PHO1;H7* activity in hydathodes (E), *PHO1;H8* expression in trichomes (F–H), *PHO1;H5* expression in leaf petioles (I), *PHO1;H10* expression in leaf blade (J), *PHO1;H1* expression in the vascular tissue of stem (K), *PHO1;H7* expression in stem (L), *PHO1;H10* expression in mature pollen grains (M), *PHO1;H9* expression in mature pollen grain (N), *PHO1;H8* expression in the stigma (O), *PHO1;H9* expression in germinating pollen grain (P), *PHO1;H1* expression in vascular tissue of sepals, petals, and filaments (Q), *PHO1;H1* expression in the vascular tissue of anther filament (R), and *PHO1;H6* expression in the connective tissue of the anther (S) (Wang et al., 2004).

Seed Development

A. Embryogenesis

Ovules of higher plants are the precursors of seeds and emerge from placental tissue inside the gynoecium of flowers. Prior to fertilization, the mature ovule consists of a haploid multicellular embryo sac or female gametophyte (FM), surrounded by diploid or sporophytic tissue (Schneitz et al., 1998). Right after pollination, the female gametophyte sends signals that participate in guiding the pollen tube growth towards the ovule (Hulskamp et al., 1995). The female gametophyte gets fertilized; a procedure that is controlled by molecular processes (Dresselhaus, 2006; Russell, 1993; Willemse and van Went, 1984). Upon fertilization, the embryo and the endosperm develop into a seed (Maheshwari and Johri, 1950) a process induced by female gametophyte expressed genes (Kermicle, 1969; Kobayashi and Tsunewaki, 1980; Ohad et al., 1996; Tsunewaki and Mukai, 1990).

Embryogenesis begins with double fertilization in which one sperm cell fuses with the egg cell and another with the central cell to form the zygote and the endosperm mother cell, respectively. In the zygote asymmetrical divisions lead to an apical cell that develops into an embryo proper and a basal cell that generates the hypophysis and the suspensor (Park and Harada, 2008). The archesporial cell functions directly as the megaspore mother cell (Schneitz et al., 1995; Webb and Gunning, 1990) and the megaspore mother cell is in direct contact with the nucellar epidermis (Christensen et al., 1997). The majority of angiosperms produce monosporic embryo sacs (Fig. 10A, stage FG1), in which three of the four megaspores undergo programmed cell death (apoptosis), and only one (usually the chalazal megaspore) subsequently is mitotically divided to produce a megagametophyte (Fig. 10A, stage FG3). Thus, polarity between chalaza and micropyle is established at an early stage. The Polygonum-type of megagametophyte is typical of more than 70% of flowering plant species examined thus far, including the archetypal model organism *Arabidopsis*. In this type, the single functional megaspore undergoes three mitoses to produce an eight-nucleate structure, arranged in two four-nucleate groups at opposite poles of the embryo sac (Fig. 10B). One nucleus from each group migrates to the centre, and the other three become cellularized, resulting in three antipodal cells at the chalazal pole and a three-celled egg apparatus (two synergids and an egg cell) at the micropylar pole (Fig. 10B, stage FG5). Thus, the coenocytic phase is followed very rapidly by a cellular phase and the resulting seven-celled (eight-nucleate) structure is highly modular, consisting of two mirror-image domains.

The two central nuclei fuse to form a diploid polar nucleus that ultimately fuses with a secondary sperm cell to form a triploid endosperm (Rudall, 2006).

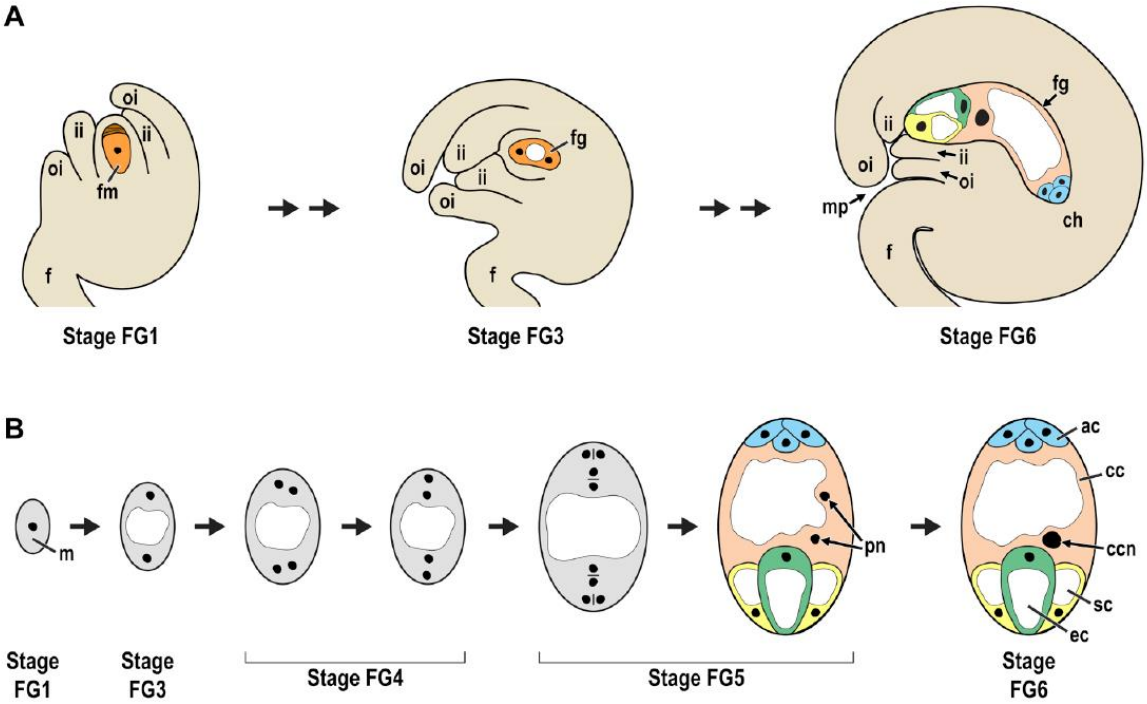

Figure 10: Megagametogenesis in *Arabidopsis*.
(A) Steps of megagametogenesis emphasizing development within the ovule.
(B) Stages of megagametogenesis (Christensen et al., 1997). The megaspore contains a single nucleus (stage FG1). This nucleus undergoes two rounds of mitosis, producing a four-nucleate coenocyte, with two nuclei at each pole separated by a large central vacuole (stage FG4). During a third mitosis, phragmoplasts and cell plates form between sister and non-sister nuclei and the nuclei become completely surrounded by cell walls (Stage FG5). During cellularization, the polar nuclei migrate toward the center of the female gametophyte and fuse before fertilization. These events produce a seven-celled structure consisting of three antipodal cells, one central cell, two synergid cells, and one egg cell. If the female gametophyte is not fertilized, the antipodal cells eventually degenerate (Stage FG7, not shown).
White areas represent vacuoles and black circles/ovals represent nuclei.
Abbreviations: ac, antipodal cells; cc, central cell; ccn; central cell nucleus; ch, chalazal region of the ovule; ec, egg cell; f, funiculus; fg, female gametophyte; fm, functional megaspore; ii, inner integument; m, megaspore; mp, micropyle; oi, outer integument; pn, polar nuclei; sc, synergid cells [from: (Drews and Koltunow, 2011)].

B. Seed development

In many plants, including *Arabidopsis* the embryo undergoes several cell-divisions, differentiating into the embryo proper which then gives the new progeny and the suspensor, a temporary structure that serves as a channel between the embryo proper and the seed coat (Fig. 11). The primary endosperm cell undergoes nuclear but not cell divisions and nuclei migrate to form three sub-regions: the micropylar, which is the closest to the young embryo; the peripheral, in the center of the endosperm region; and the chalazal, at the pole opposite to the embryo. Cellularization of the endosperm proceeds in a wave-like manner from the micropylar to chalazal end (Brown et al., 1999). The cells of the ovule integuments divide

and differentiate into distinct cell types of the seed coat that encircle the embryo and the endosperm. Late in seed development during the maturation phase, the embryo accumulates storage macromolecules and becomes tolerant of desiccation. Although development of these sub-regions has been well-characterized morphologically, little is known of the cellular processes that occur in these sub-regions or how their development is coordinated within the context of seed development (Belmonte et al., 2013).

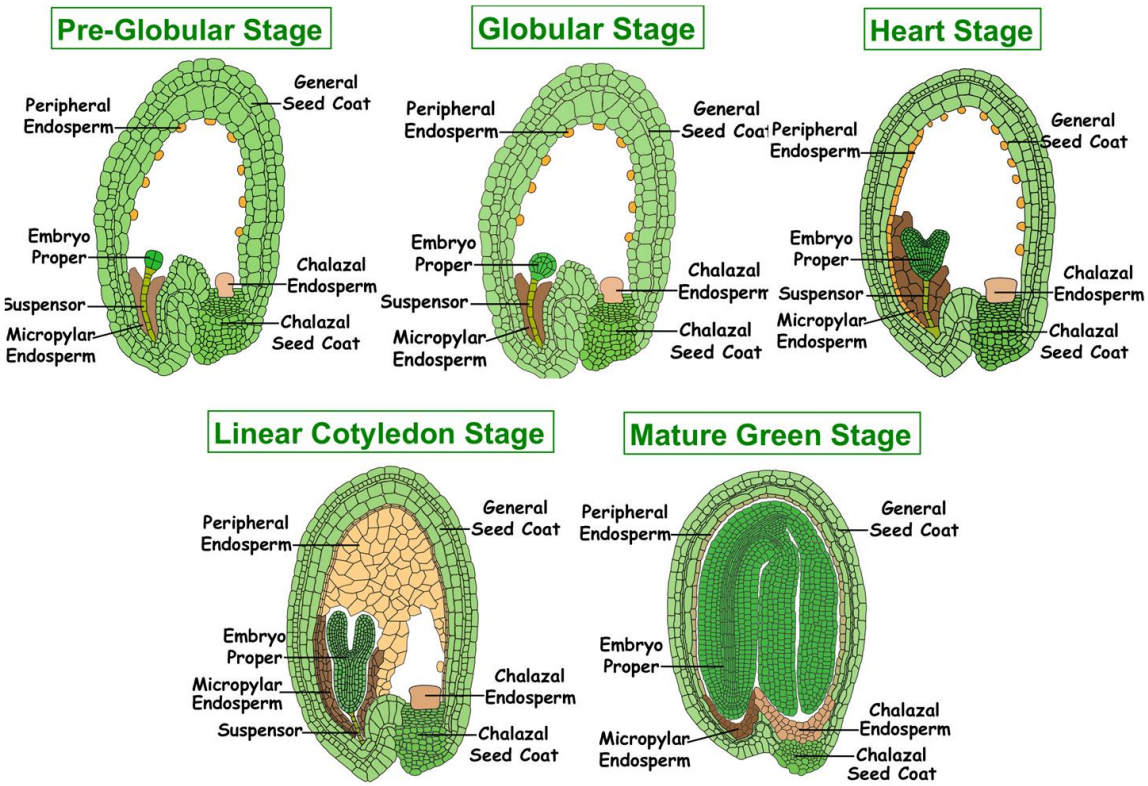

Figure 11: Embryo development in *Arabidopsis thaliana*. Representation of *Arabidopsis* seeds at the pre-globular stage, globular stage, heart stage, linear cotyledon stage, and mature green stage. (http://seedgenenetwork.net/arabidopsis).

C. Seed coat development

In order to understand the seed coat development, genetics and physiology it is necessary to understand the seed coat morphology. Seed coats develop from the integuments that surround the ovule before fertilization. Prior to fertilization, cells of the integuments are rather undifferentiated. However, after fertilization, in order for the seed coat to be developed extensive differentiation of the cell layers into specialized cell types is needed. In addition, some cell layers in the seed coats of several species may accumulate large quantities of certain substances, such as mucilage or pigments which play a role to the overall seed morphology. Many seed coats of both the *Brassicaceae* and *Fabaceae* share common cell types. The layers that are often crushed at maturity usually do not undergo any significant differentiation and remain parenchymatous. Other cells undergo a slight thickening of the cell wall and thus become collenchymatous. Some cell layers undergo extensive secondary thickening of some parts of the cell walls and thus, become sclerotic. These cell layers are known as palisade layers, especially if the cells become elongated in the radial plane. In figure 12 the positioning of different cell layer types in *Arabidopsis* and soybean is depicted. Seed coats separate one generation of plants from the next and ensure the survival of the embryo that they surround. The embryos need to be protected during dormancy and a conducive environment for quiescence has to be maintained around them, so plants often build strong impermeable seed coats (Bewley, 1997). However, during germination the seed coat weakens and breaks open in order to provide nutrients and other substances that contribute to biotic and abiotic stress resistance of the embryo. Many studies have shown that the seed coat is vital for directing the nutrient supply to the embryo during seed development (Weber et al., 2005). By controlling seed dormancy and germination it plays an important role in providing the optimal environmental conditions for the viability and growth of the next plant generation. An understanding of these roles is essential for developing crops suitable for a sustainable agricultural production.

The seed coat is also a rich source of many valuable naturally occurring compounds and the use of transgenic technologies can greatly expand and diversify them. Generally, the seed coat has not been characterized at the molecular level to the extent of the embryo and endosperm. It is now recognized that such knowledge is a prerequisite for the development of plants with modified seed coat traits and only lately there have been some studies that characterized the expression of some genes in the seed coat and their role in transferring nutrients into the seeds (Chen et al., 2015; Muller et al., 2015; Olsen et al., 2016).

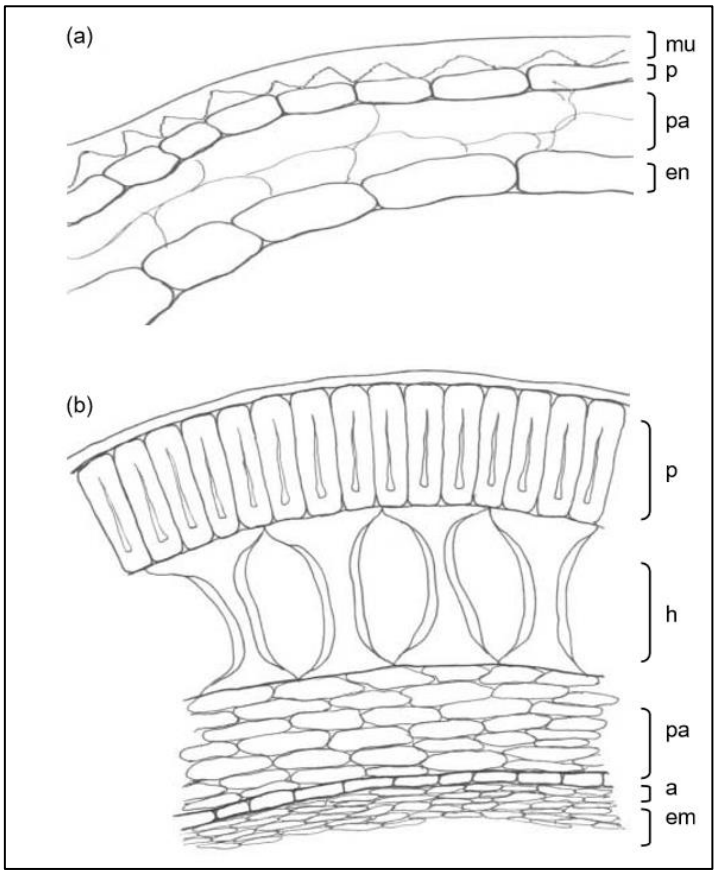

Figure 12: Schematic diagrams illustrating the general organization of the seed coat of *Arabidopsis thaliana* and soybean (*G. max L. Merrill*). a, *A. thaliana*. The seed coat at the torpedo stage. mu, Mucilaginous epidermal cells; p, palisade layer with thickened inner cell walls; pa, parenchymatous cells; en, endothelium layer. The mucilaginous cells and the palisade layer comprise the outer integument while the inner integument consists of parenchymatous cells and the endothelium layer. Adapted from (Beeckman et al., 2000); b, Soybean. A mature seed coat. p, Palisade layer; h, hourglass cells; pa, partially crushed parenchyma; a, aleurone; em, crushed endosperm. The palisade layer and the hourglass cells comprise the outer integument while the inner integument consists of parenchymatous cells. Adapted from (Miller et al., 1999).

The *Arabidopsis* testa is maternally derived and is formed from two integuments of epidermal origin that surround the mature ovule. The development of the integuments surrounding the *Arabidopsis* ovule has been well studied (Gasser and Robinson-Beers, 1993; Robinson-Beers et al., 1992; Schneitz et al., 1995) and several mutants in integument development have been characterized. The integuments of a mature ovule at the time of anthesis consist of a two cell-layered outer integument and a mostly three cell-layered inner integument. At the micropyle end, an endothelium apparently does not form and the inner integument may be only one cell layer at that end grading to two and then three cells thick at the opposite, chalazal, end.

In response to fertilization, the *Arabidopsis* seed coat differentiates primarily from cells of the ovule integuments (Fig. 13a) over a period of 2–3 weeks (Beeckman et al., 2000; Debeaujon et al., 2003; Western et al., 2000; Windsor et al., 2000). Cells in both layers of the

outer integument (Fig. 13a, layers 1,2) and all three layers of the inner integument (Fig. 13a, layers 3–5) go through a dramatic period of growth in the first few days after fertilization through both cell division and expansion (Fig. 13b). The five cell layers follow one of four distinct fates (Fig. 13c–e). Cells of the innermost layer (the endothelium; Fig. 13a, layer 5) synthesize proanthocyanidin (PA) flavonoid compounds, also known as condensed tannins (Dixon et al., 2005), which accumulate in the central vacuole during the first week after fertilization and later oxidize, imparting a brown color to the seed coat. By contrast, cells of the other two inner integument layers (Fig. 13a, layers 3,4) do not appear to differentiate further and are crushed together as the seed develops (Fig. 13d,e). Cells of both outer integument layers (Fig. 13a, layers 1,2) accumulate starch-containing epidermal layer (Fig. 13a, layer 1) synthesize and secrete a large quantity of mucilage (a pectinaceous carbohydrate) into the apoplast specifically at the junction of the outer tangential and radial cell walls (Fig. 13c). As mucilage deposition precedes, the vacuole contracts, leaving a cytoplasmic column in the center of the cell surrounded by a donut-shaped apoplastic space filled with mucilage. Following mucilage synthesis, a secondary cell wall is deposited that completely fills the space occupied by the cytoplasmic column, forming the columella (Fig. 13d,e). During the later stages of seed development, the cells of all seed coat layers die, except the aleurone or endothelium which remains alive during the whole maturity (Bradford and H., 2007). The structure of the epidermal cells is preserved by the mucilage and columella, and the remaining layers are crushed together by the end of seed maturation. PAs are apparently released from the endothelial cells and impregnate the inner three cell layers during this period (Fig. 13e).

The roles typically ascribed to the seed coat include the promotion of dormancy, protection, longevity, vigor of the seedling and dispersal. In the *Arabidopsis* seed coat, the special features attained through differentiation include inner cell walls impregnated with PA, two sets of thickened secondary cell walls in the outer two layers, and mucilage in the apoplast of the epidermis that is extruded upon exposure to water. In other species, the presence of PA has been associated with resistance to pathogens and herbivores. Secondary cell walls are assumed to provide support, protection and impermeability to water and oxygen. It has been proposed that mucilage assists germination and protects the seed against toxic chemicals. The availability of mutants defective in the seed coat epidermis, palisade and endothelium has been useful in testing some of these hypotheses concerning seed coat function (Haughn and Chaudhury, 2005).

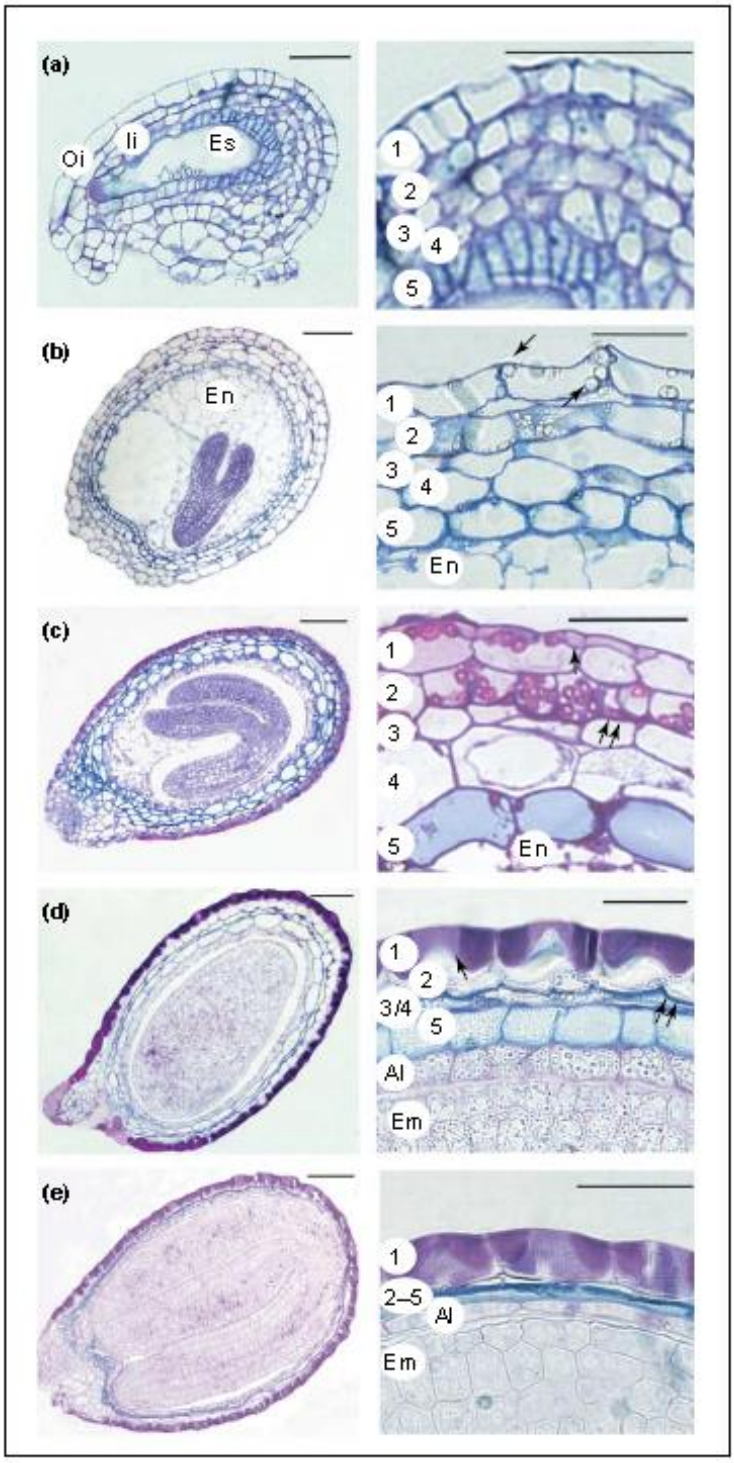

Figure 13: Development of the ovule integuments into a seed coat following fertilization. This figure shows several stages (a–e) of seed development for the whole seed (left) and a detail of the developing seed coat (right). The two cell layers of the ovule outer integument [(a), right, 1,2] and three cell layers of the inner integument [(a), right, 3–5] undergo a period of growth within the first 5 days after fertilization (b). Cells of individual layers differentiate (c) into specialized cell types including endothelium (5), palisade (2) and epidermis (1), a process that is almost complete 10 days after fertilization (d). By seed maturity (15 days) (e), cells of all layers are dead and have been crushed together, except for the epidermis, the shape of which is maintained by the thick secondary cell wall of the columella. Single arrows indicate starch-containing plastids (b), mucilage in the apoplast (c) or secondary cell wall forming in the epidermis (d). The double arrows indicate the secondary cell wall of the palisade (c,d). Abbreviations: Al, endosperm aleurone; Em, embryo; En, endosperm; Es, embryo sac; Ii, inner integument; Oi, outer integument. Scale bar*Z*80 mm (b–d, left); 40 mm (a, left, a–d, right). Adapted from (Haughn and Chaudhury, 2005).

Nutrient translocation into the developing seeds

Seeds are major sources of human and animal foods, and also the basic material for cultivating most agricultural crops. Seed quality determines if these seeds are suitable for both of these purposes. The maternal plant supplies the metabolic building blocks that ultimately make up the seed. These inputs are influenced by environmental conditions and by the genetic makeup of the maternal plant. An increased understanding of control over supply of nutrients to developing seeds will allow development of improved varieties that can respond favorably to maintain seed production and quality in adverse environments. This understanding will also allow production of biofortified seeds with increased concentrations of micronutrients (Waters and Sankaran, 2011b).

In higher plants species, nutrients are commonly delivered to growth and storage organs (sinks) via the phloem (Patrick, 1997). From sites of nutrient assimilation (sources) to sites of nutrient utilization, there is an interconnected network of sieve elements which forms a supracellular compartment for the transport of nutrients, phytohormones and macromolecules (Lalonde et al., 1999). The precursors of starch, oil and protein are sucrose, amino acids and amides which, together with mineral elements, are imported into seeds through the maternal vascular system (Patrick and Offler, 2001).

In the xylem, the mineral-containing sap moves as an upward bulk flow. The power that makes this flow to move is the evaporative loss of water from aerial organs which reduces pressure in their cell walls. By contrast, through the phloem osmotically generated pressure differences move photosynthetic products by bulk flow from leaves (sources- net assimilate exporters) to heterotrophic organ (sinks-net assimilate importers). The sieve element/companion cell (se/cc) complex is the long-distance transport unit. Most assimilates are delivered through the phloem to the sink tissues as these organs characteristically have low rates of transpiration and hence xylem import (Lalonde et al., 2003).

Seeds contain filial tissues (embryo and endosperm, aleurone) surrounded by maternal tissues (seed coat). The developing seed is connected to the maternal plant by a single vascular trace (Thorne, 1985; Zhang et al., 2007). This vascular bundle ends at the seed coat and is not symplastically connected to the endosperm or embryo. Nutrients moving to the seed are unloaded from the phloem, while excess water is thought to move in the opposite direction in this vascular strand, through the xylem or suberized cells (Oparka and Gates, 1984). Phloem derived nutrients are distributed in the maternal tissue surrounding the seed, and are eventually effluxed into an apoplastic space that separates the maternal and the filial

tissues. Thus, specific micronutrient efflux transporters are likely to be required for this action, as well as for uptake into cells of the endosperm and/or embryo (Fig. 14). The endosperm tissue is present in mature cereals, but is consumed by the embryo in legumes and *Arabidopsis* during seed maturation (Thorne, 1985). For mineral micronutrients, the transporters that are involved in phloem unloading and uptake by the filial tissues are not well defined, but likely belong to the families discussed as transporters in other parts of the plant (Waters and Sankaran, 2011a).

Nutrients and assimilates are constantly distributed in different organs and tissues via efflux mechanisms during the whole growth and development of a plant. At key stages of plant life cycle profound changes occur, with one of the most critical of these being the seed filling. Plants accumulate and re-translocate macro- and micronutrients throughout their life cycle. Ideally, the plant is in a quest of optimizing the way it responds to environmental cues and integrating these with the genetically determined elements of development in order to reach a maximum of its reproductive potential and secure the production and survival of the next generation. In order to ensure the highest reproductive potential, plants need to (re)mobilize nutrients from sources to sinks in a very controlled manner. This process is also dependent on the stage of the plant's life cycle, the reproductive strategy of the plant as well as on the space and time. For instance, an annual plant like *Arabidopsis* will ultimately die after seed filling is complete; in this example, the seeds are the resources by which the genetic information of an individual over-winters and survives until the environmental conditions become favorable once again. In some species, seed dormancy can last months or even years, and provides a highly effective means of spreading the timing of germination and potentially avoiding adverse environmental challenges (Barton, 1961). Thus, under optimal growth conditions, the process of nutrient allocation ensures that eventually nearly all the nutrient resources produced during the photosynthetic period will be recycled from the vegetative tissues into the developing seeds.

In contrast, perennial plants commit a more limited proportion of resources to the reproductive phase of their life cycle as it is advantageous to retain some photosynthetic capacity for as long as the environmental conditions allow. For this reason, it has been speculated that the anthocyanins produced in autumnal leaves provide photoprotection to enable maximal re-absorption during times when the leaves are vulnerable to the effects of high light accompanied by low temperatures (Archetti et al., 2009). For a perennial plant it is less essential to ensure reproductive success every year due to their longer life spans, and tolerance to environmental stress is often achieved by slower growth in addition to niche

adaptations such as an evergreen habit. Grime (1977) proposed that resource allocation strategies in plants could be divided into three categories: competitive, stress-tolerant, and ruderal strategies (denoted C-, S-, and R-strategies respectively). Grime summarized the consequences of C-, S-, and R-strategies on resource allocation for plants growing in three broad habitat categories (Table 1), and it is interesting to review these in the light of considering crop plants and the habitats under which they are grown in a modern agricultural environment.

Table 1: Morphogenetic responses to desiccation, shading, or mineral nutrient stress of competitive, stress-tolerant , and ruderal plants and their ecological consequences of three types of habitat [from: (Grime, 1977)].

Strategy	Response to stress	Habitat 1[a]	Habitat 2[b]	Habitat 3[c]
Competitive	Large and rapid changes in root:shoot ratio, leaf area, and root surface area	Tendency to sustain high rates of uptake of water and mineral nutrients to maintain dry matter production under stress and to succeed in competition	Tendency to exhaust reserves of water and/or mineral nutrients both in the rhizoshere and within the plant; etiolation in response to shade increases susceptibility to fungal attack	Failure rapidly to produce seeds reduces chance of rehabilitation after disturbance
Stress tolerant	Changes in morphology slow and often small in magnitude	Overgrown by competitors	Conservative utilization of water, mineral nutrients, and photosynthate allows survival over long periods in which little dry matter production is possible	Failure rapidly to produce seeds reduces chance of rehabilitation after disturbance
Ruderal plants	Rapid curtailment of vegetative growth and diversion of resources into seed production	Overgrown by competitors	Chronically low seed production fails to compensate for high rate of mortality	Rapid production of seeds ensures rehabilitation after disturbance

[a] In the early stages of productive, undisturbed habitats (stresses mainly plant induced) and coinciding with competition.
[b] In other continuously unproductive habitats (stresses more or less constant and due to unfavourable climate and/or soil) or in the late stages of succession to productive habitats.
[c] In severely disturbed, potentially productive habitats (stresses either a prelude to disturbance, e.g. moisture stress preceding plant fatalities, or plant induced) between periods of disturbance.
Reproduced from JP Grime. 1977. Evidence for the existence of three primary strategies in plants and its relevance to ecological and evolutionary theory. *American Naturalist* 111, 1169–1194, with permission of the University of Chicago Press.

Nutrient loading of seeds is a spatially and temporally dynamic process. The latter is inextricably linked with their development (Weber et al., 2005). Of relevance to nutrient loading, seeds advance through three main stages of development. Immediately after fertilization, seed development is dominated by cell division before a storage phase when most nutrients are loaded as their cells expand. For a period, cell division, cell expansion and storage overlap temporally as sequential waves of these phenomena progress through the tissues of developing seeds in distinctive spatio-termporal patterns (Jenner et al., 1991; Weber et al., 2005). Nutrient loading rates per seed reach a plateau which overlaps with attaining final seed volume. Thereafter, loading rates are constant during the remainder of storage product accumulation before declining precipitously as seed maturity is approached. During seed development, dominant sinks for nutrient loading shift from maternal tissues

early in development, to filial tissues during later stages of development. However, exceptions to this generalization exist, as illustrated by predominant allocation of biomass into maternal fibrous cells of cotton seeds (Ruan, 2005). During the storage phase, nutrients are partitioned between endosperm and embryo. In non-endospermic seeds of dicots the endosperm functions as a nutrient source for the developing embryo during the pre-storage phase of seed development and, by the onset of the storage phase, is completely depleted (Weber et al., 2005). By contrast, endospermic seeds harbor a diminutive embryo and the endosperm is the major sink for nutrient loading throughout seed development. This developmental pattern is characteristic of all cereal grains (Jenner et al., 1991).

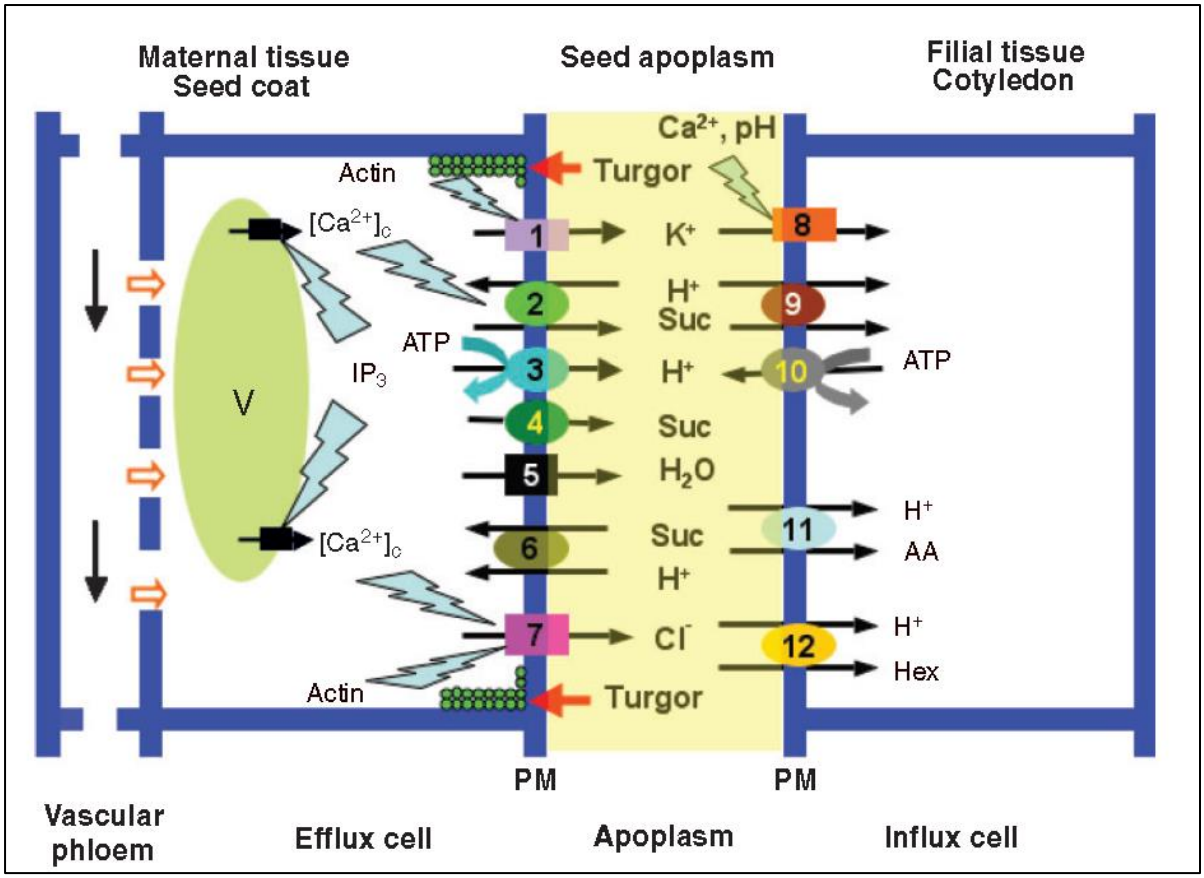

Figure 14: Schematic diagram showing membrane transporters involved in transferring phloem-imported nutrients from seed coats to cotyledons of developing grain legume seeds [from (Zhang et al., 2007)].

A lot of progress has been done the last years towards the discovery of molecular mechanisms that regulate nutrient loading of seeds during the storage phase of their development. However, there are still many open questions regarding the membrane proteins facilitating the release of nutrients from maternal seed tissues as well as their cellular localization(s). Although there is quite some work done on sucrose transporters in several plant species we still know very little about other macro- and micro- nutrient transporters. Evidence from studies on pea (*Pisum sativum*) and bean (*Phaseolus vulgaris*) seed coats

implicated SUF transporters, which appear to have lost proton coupling to act as uniporters, in sucrose efflux from seed coat (Ritchie et al., 2003; Zhou et al., 2007) and they appear to have evolved from recent gene duplications and likely represent a specific adaptation in legumes to sustain the large seeds but they have not yet been found in other plants, such as *Arabidopsis* or maize (*Zea mays*) (Zhou et al., 2007). The recently identified SWEET sugar transporters of eukaryotes have seven transmembrane domains and function mainly in cellular efflux (Chen et al., 2010; Xu et al., 2014). It was also lately (Chen et al., 2015) that three of them, SWEET11, 12, and 15, are actually expressed in developing seeds and are involved in sucrose efflux transfering sugars from the seed coat to embryo. Using promoter fusions with GFP Chen et al. (2015) showed that SWEET11 is expressed in the endosperm at the linear cotelydon stage, SWEET12 at the micropylar seed coat from the preglobular throughout the green mature stage and SWEET15 at the epidermal cells of the seed coat at the preglobular stage, which then faded from globular stage to heart stage, but appeared bright again from the linear cotyledon stage throughout the maturation stage, as well as in the micropylar endosperm layer closest to the embryo at the linear cotyledon stage.

However sucrose is a big molecule that can be transported with very different mechanisms comparing to other nutrients such as nitrate or phosphate for example. Regarding, such nutrients there is no information related to transporters that could facilitate their loading into the seeds. Only recently, Muller et al. (2015) characterized four members (UmamiT11, 14, 28 and 29) of the plant-specific UmamiT transporter family in *Arabidopsis*. The authors showed that the proteins transport amino acids along their (electro) chemical potential across the plasma membrane and that they are expressed in seeds, in tissues where amino acids could be exported (like the chalazal seed coat). Loss-of-function mutants of these transporters accumulate high levels of free amino acids in fruits and produce smaller seeds. Moreover, another very interesting paper from Olsen et al. (2016) showed that two zinc transporting P1B-ATPases (HMA2 and 4), belonging to a family which is known for heavy metal transport, actively export zinc (Zn) from the mother plant to the filial tissues. Mutant plants that lack both zinc pumps (*hma2 hma4*) accumulated zinc in the seed coat and consequently had very reduced amounts of zinc inside the seed. Furthermore, blockage of zinc transport was observed at both high and low external zinc supplies and the phenotype was determined by the mother plant and was thus due to a lack of zinc pump activity in the seed coat and not in the filial tissues. Seed P is the only P source available to sustain the initial growth of seedlings and, upon germination seed P reserves are rapidly mobilized and translocated to emerging root and shoot tissues. This P source is subsequently supplemented

by P uptake by the developing root system. Although the P contained in a seed contributes little to the final P content of the mature plant, it contributes significantly to the P nutrition of a young seedling. Greater seed P reserves allow seedlings to establish faster and ultimately produce plants with higher yields (Bolland and Baker, 1988; De Marco, 1990; Grant et al., 2001; Ros et al., 1997; Thompson et al., 1991; Thomson and Bolger, 1993; Zhang et al., 1990; Zhu and Smith, 2001). However, there are not any known transporters that have been shown to transport P into the developing seeds.

Furthermore, large amounts of mineral nutrients, notably K+ and Cl−, are released from legumes seed coats to the seed apoplasm (Walker et al., 1995). Preliminary studies on bean seed coats using the patch clamp technique showed that non-selective ion channels might be responsible for K+ release from the maternal tissue into the seed apoplast (Zhang et al., 2007).The characteristics and function of these channels are analogous to those of non-selective cation channels in the xylem parenchyma and the genes that encode such channels have yet to be identified.

Communication of the seed compartments in *Arabidopsis thaliana*

Developing *Arabidopsis* seeds and embryos represent a complex set of cell layers and tissues that mediate the transport and partitioning of carbohydrates, amino acids, hormones, and signaling molecules from the terminal end of the funicular phloem to and between these seed tissues and eventually to the growing embryo.

In angiosperm seeds, after double fertilization of the egg cell and the two polar nuclei the embryo and the endosperm are created, respectively. These filial organs are enclosed by a maternal seed coat, derived from the one or both ovular integuments. The seed coat is comprised of a vascular compartment embedded in ground tissues. The latter serves as a symplasmic compartment to process and deliver imported nutrients to the underlying filial tissues (Murray, 1987). Nutrients are released from specialized maternal cells in the region of the chalazal seed coat into the seed apoplasm (Patrick and Offler, 1995). Current knowledge shows that in legumes as well as in other seeds early embryo growth is subject to maternal control. This can be due to physical restriction, which determines how far the embryo can realize its growth potential later on [discussed in (Wang and Hedley, 1993)]. Transient storage products within the seed coat could play the role of a buffer and are subsequently mobilized to supply the embryo and promote its growth (Borisjuk L., 1995; Dejardin et al., 1997; Heim et al., 1993; Rochat et al., 1995). In addition, seed coat invertases are key players

for the modification of the seed coat and the control of the nutrient supply to the embryo (Weber et al., 1995).

The symplasmically-isolated tissues collectively function as a compartment committed to storage of nutrients released from the seed coat (Fig. 15C). Nutrients are retrieved from the seed apoplasm by specialized filial cells located at the maternal/filial interface and are moved syplasmically to the cellular sites of storage [Fig. 15C; (Patrick and Offler, 1995)]. Storage products accumulate in either the embryo (Fig. 15A- principally the cotyledons) or endosperm (Fig. 15B). Where the endosperm acts as the principal storage organ, its outer layer develops into the aleurone (Fig. 15B) at the beginning of seed filling, the remaining endosperm is cellularized (e.g. cereals) or forms a liquid syncytium (e.g. coconut; Lopes and Larkins, 1993). In contrast, when cotyledons form the final storage organ, the endosperm is substantially degraded during cotyledon expansion (e.g. grain legumes). Cotyledons are enclosed by a dermal cell layer and are mostly comprised of storage parenchyma cells with a pro-vascular network located in their center (Offler et al., 1989).

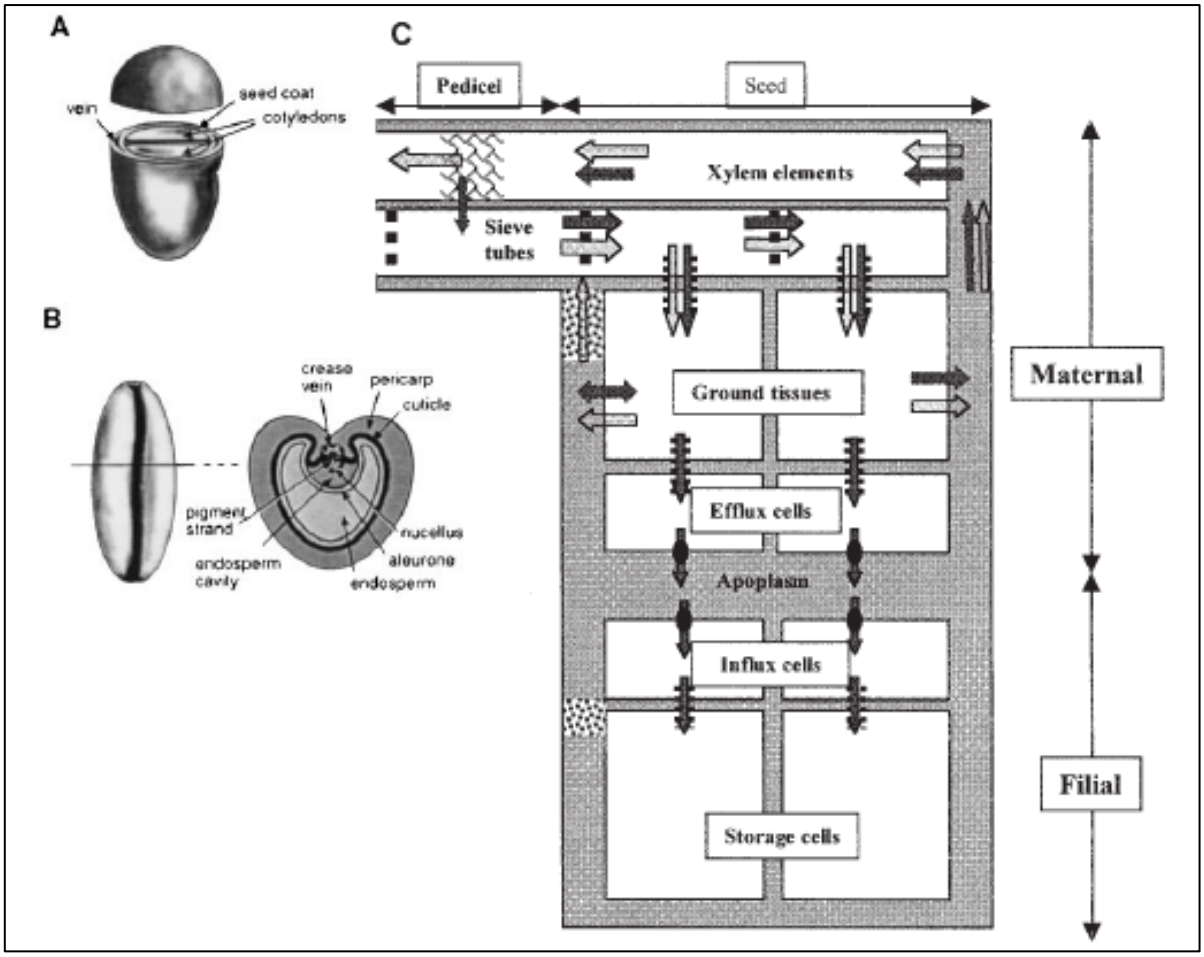

Figure 15: Key structural features of (A, B), and generalized cellular pathways (C) followed by water and nutrients imported into developing seeds. Diagrammatic representation of (A) grain legume and (B) wheat seed structure. (C) Block diagram showing water (white arrows) and nutrient (black arrows) transport in a developing seed. Nutrients and water exit the importing phloem by bulk flow. Water returns to the parent plant in the xylem while nutrient loss is prevented by selectively-permeable apoplasmic barriers and xylem discontinuities. Nutrients move through extensive symplasmic paths via interconnecting plasmodesmata in maternal and filial tissues. Nutrient exchange to and from the seed apoplasm, by cells specialized for efflux and influx, occurs at the maternal/filial interface. Finally, nutrients accumulate in filial cells supporting storage product biosynthesis.

The seed anatomy in *Arabidopsis* differs strongly from that described for cereals and legumes. There is no vascular tissue within the developing *Arabidopsis* seed, a nucellar projection is not formed, and most of the nucellar cells have degenerated in the fully developed seed. The unique vascular bundle that translocates photoassimilates to an *Arabidopsis* seed terminates at the end of the funiculus and releases its content into the testa proximal to the micropyle, where the abscission zone (the hilum) will be formed in the mature seed (Robinson-Beers et al., 1992).

Stadler et al. in (2005) studied the cell-to-cell movement of the green fluorescent protein of mobile and non-mobile green fluorescent protein fusions in seeds and embryos of plants expressing the corresponding cDNAs under the control of various promoters shown to be active in defined seed or embryo cell layers (SUC3,TT12, and GL2) or only outside the

developing *Arabidopsis* seed (AtSUC2). Cell-to-cell movement was also analyzed with the low-molecular-weight fluorescent dye 8-hydroxypyrene-1,3,6-trisulfonate. They showed that there are only three apoplastic borders between the phloem and the embryo: (1) between the outer and inner integument; (2) between the inner integument and the endosperm; and (3) between the endosperm and the embryo (Fig. 16). Only for these apoplastic steps does a carrier-mediated transport (e.g. for Suc or amino acids) seem necessary. In a recent paper from the same laboratory (Werner et al., 2011) it was shown that symplastic phloem unloading which occurs in young developing seeds of flowers up to stage 11 is switched off in stage 12 flowers and switched on again in developing seeds of stage 13 flowers (globular stage of embryo development).

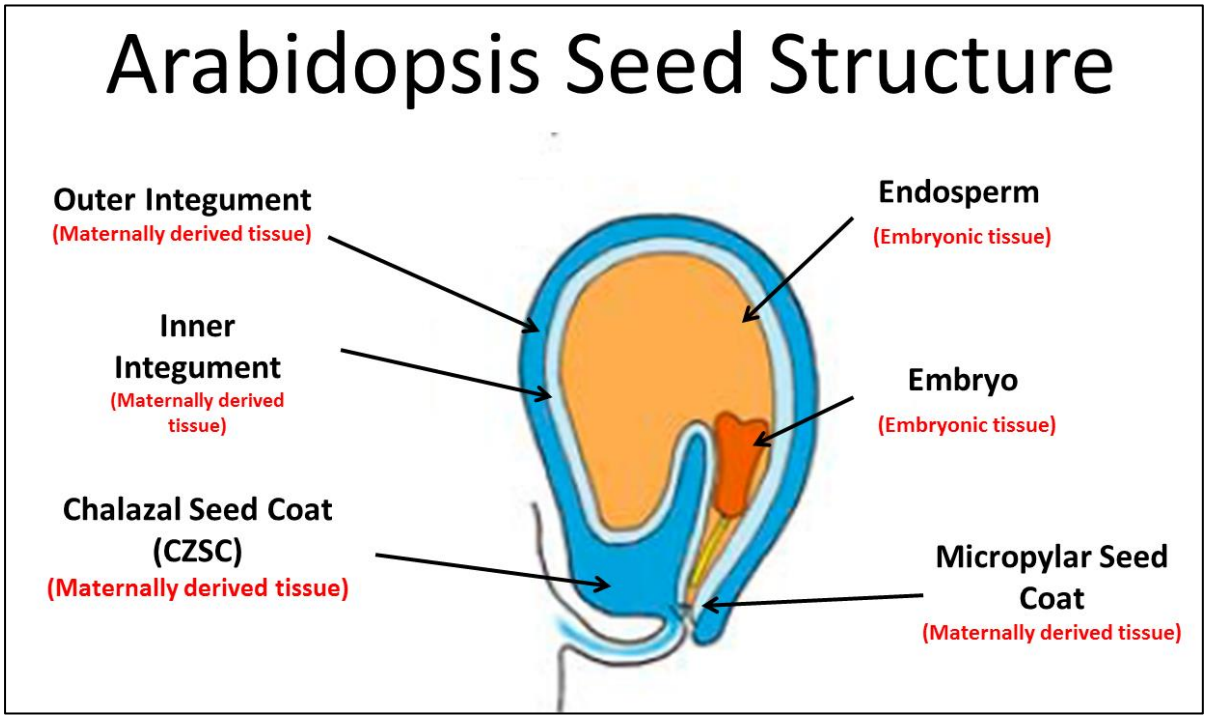

Figure 16: *Arabidopsis* seed structure. There are only 3 apoplastic barriers between the phloem of the mother plant and the embryo: (1) between the outer and inner integument (2) between the inner integument and the endosperm (3) between the endosperm and the embryo. Modified from (Stadler et al., 2005).

Nutrient exchange between maternal, endosperm and embryo compartments of developing seeds has directed attention to membrane transport events and how these interface with nutrient import by, and nutrient metabolism/compartmentation within, developing seeds. These issues have been addressed in past reviews of nutrient loading of developing seeds with a particular focus on sugar transport [see (Patrick and Offler, 1995, 2001; Thorne, 1985; Weber et al., 1997; Wolswinkel et al., 1992).

Seeds are heterotrophic organs, totally dependent on nutrients imported (nutrient loading) from the parent plant for their growth and development. Nutrient loading of seeds influences seed number at seed set and determines their final size, which are properties of key biological and agronomic significance. In terms of reproductive success, an evolutionary trade-off exists between seed number and size (Fenner 2005). Although it is well accepted that phloem unloading plays a key role in the partitioning of photoassimilate (Fisher and Oparka, 1996; Patrick, 1997; Viola et al., 2001) and the process of phloem unloading has been studied extensively over the last 20 years [for review, see (Oparka, 1990; Patrick, 1997; Schulz et al., 1998) it still remains poorly understood. According to Zhang et al. (2007) some nutrients and mainly sucrose, are transported through the plasmodesmata to the seed coat efflux cells, from where they are released to the seed apoplasm and taken up from the embryo by membrane transporters located in the PM of the cotyledon dermal cells.

Our knowledge regarding the nutrient translocation into the developing seeds of different plant species is very limited. Millar et al. 2015 showed in *Brassica napus* that unloading and transport within the CZSC can be carried out both symplastically and apoplastically. The identification of plasmodesmata is evidence for the capacity of symplastic transport. Plasmodesmata occur in three different regions within the CZSC:(i) between cells of the phloem, suggesting symplastic transport in the phloem; (ii) between phloem and parenchyma cells, suggesting symplastic unloading from the phloem into the CZSC parenchyma; and (iii) between the CZSC parenchyma cells, suggesting symplastic post-phloem unloading. Although plasmodesmata were frequently found between parenchyma cells, they were much less common between the phloem and parenchyma. The scarcity of plasmodesmata between the phloem and parenchyma would likely not be sufficient in supplying the seed with incoming nutrients; therefore, apoplastic unloading may also be present to ensure adequate nutrient transfer. Although unloading of nutrients can be mediated through bulk flow, symplastic unloading is the most common. In *Arabidopsis*, throughout ovule development, phloem unloading switches from symplastic to apoplastic and then back to symplastic (Werner et al., 2011) but throughout seed development, transport within the seed coat remains symplastic (Stadler et al., 2005). Phloem is also unloaded symplastically in legume crops such as pea (*Pisum sativum*), fava bean (*Vicia faba*), soybean (*G. max*), and common bean (*Phaseolus vulgaris*) (Ritchie et al., 2003), as well as in wheat and barley grains (Borg et al., 2009). This is compared to Grape Berry in which there is a switch from symplastic to apoplastic phloem unloading that occurs at the onset of fruit ripening (Zhang et al., 2006). In canola, although there are signs of both symplastic and apoplastic transport, the

specific mode of unloading throughout seed development still needs to be resolved. Signs of apoplastic unloading are certainly obvious in the CZSC. The abundance of mitochondria near the plasma membrane of the parenchyma cells could fuel apoplastic transport through the production of ATP required to power the active transport of plasma membrane transporter proteins (Palmgren, 2001; Sondergaard et al., 2004). It is likely that apoplastic unloading occurs within the CZSC in *B. napus*, but the role of symplastic transport in the CZSC still remains unknown. Differences in unloading mode could potentially be a result of seed coat vasculature and seed size. Depending on the size of the seed, vasculature within the seed coat varies among plant species (Radchuk and Borisjuk, 2014). Vasculature of the small *Arabidopsis* seed ends at the junction between the CZSC and funiculus (Khan et al., 2014). In the large grains of wheat and barley, the vasculature extends along the whole length of the seed coat (Radchuk and Borisjuk, 2014). *B. napus*, which produces midsize seeds, has vasculature that extends further into the CZSC than *Arabidopsis* but does not penetrate the SC. These differences could potentially account for the anatomical and molecular signs of apoplastic unloading in canola. Thus, more detailed and quantitative analyses using TEM to analyze the size and number of plasmodesmata at the unloading zone and/or GFP-tagged proteins to precisely show the location of transporters along plasma membrane is required to provide additional evidence for nutrient transport within the developing seed.

CHAPTER 2

Expression pattern of PHO1 and PHO1;H1 in the seeds of *Arabidopsis thaliana*

Evangelia Vogiatzaki[1], Célia Baroux[2], Miloslawa Jaciubek[2], Yves Poirier[1]

[1] Department for Plant Molecular Biology, Biophore Building, University of Lausanne, 1015 Lausanne, Switzerland
[2] Department of Plant Developmental Genetics, Institute of Plant Biology and Zürich-Basel Plant Science Center, University of Zürich, Zürich, Switzerland

Author contributions

E.V. and Y.P. designed experiments and Y.P. supervised the whole project. E.V. performed all experiments, except the dissection of the ovules and the gus staining for studying the PHO1 expression pattern that was performed in collaboration with M. J. and the imaging of the *Arabidopsis thaliana* ovules and seeds for studying the expression pattern of PHO1 and PHO1;H1 which were performed in collaboration with C.B.

Aim

As it is already known since several years, PHO1 and PHO1;H1 are both expressed in the root and shoot vasculature (Hamburger et al., 2002; Stefanovic et al., 2007) where they are exporting Pi into the xylem (root apoplast) (Arpat et al., 2012; Poirier et al., 1991). Belmonte et al. (2013) using laser microdissection, extracted all sub-regions and regions of seeds of the model plant *Arabidopsis*, from all the developmental stages starting from fertilization through maturity and described gene activity using microarray data. Mining of these databases (http://seedgenenetwork.net/) revealed that PHO1 (embryo) and PHO1;H1 (both embryo and seed coat) are both expressed in the seed (see Fig. 17). More precisely according to the microarray data, PHO1 is expressed in the chalazal seed coat in all the developmental stages, and in the general seed coat of the mature green stage. On the other hand, PHO1;H1 seems to be expressed only in the chalazal seed coat throughout the whole seed development. Thus, as both genes are exporting Pi into the root apoplast and they are expressed in the chalazal seed coat which is a well-known region of nutrient off-loading from the maternal plant and is symplastically isolated from the embryo (Stadler et al., 2005) we made the hypothesis that both genes could be expressed in the seeds and could export Pi into the seed apoplast. Consequently, the aim of this chapter is to identify the exact cell type(s) where PHO1 and PHO1;H1 are expressed in the seeds of *Arabidopsis* and check if their expression pattern is altered or changed under phosphate starvation conditions.

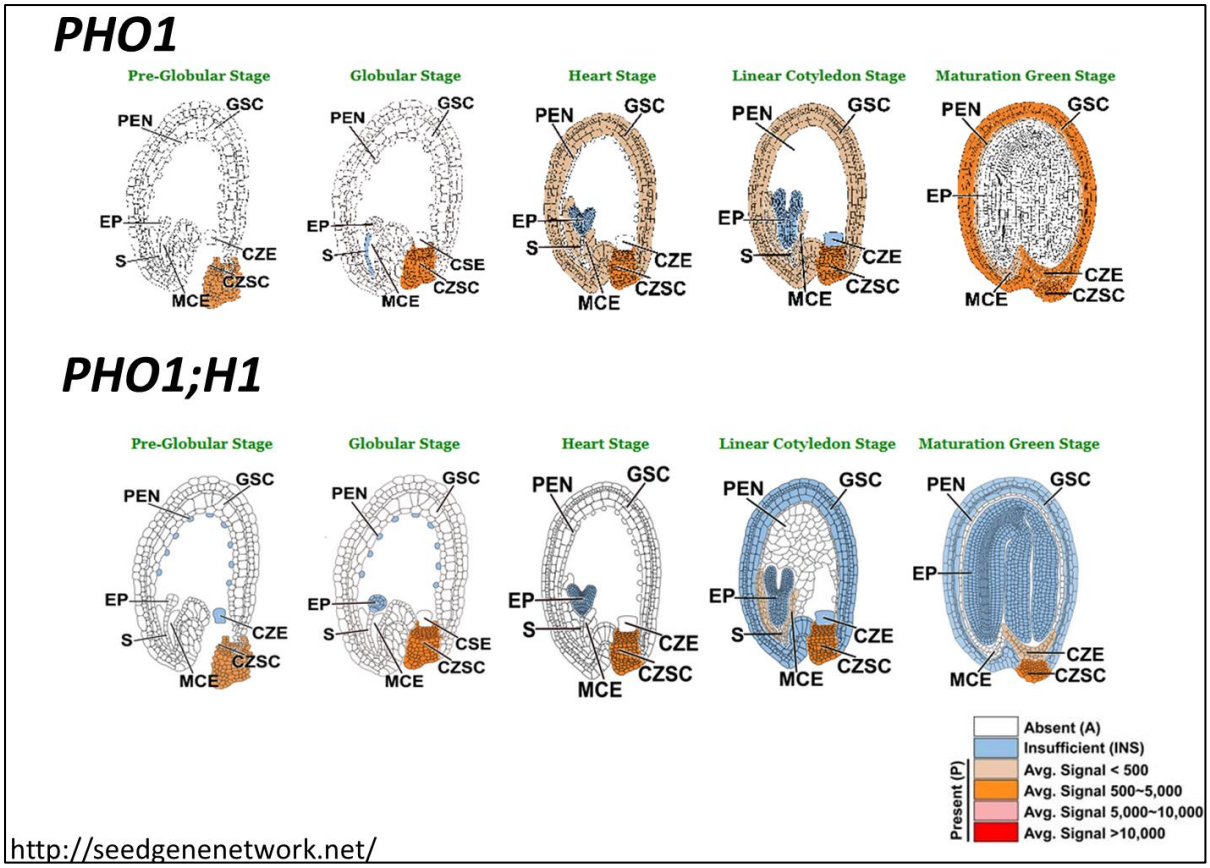

Figure 17: Expression pattern of PHO1 (up) and PHO1;H1 during the development of *Arabidopsis* seeds. Both genes are strongly expressed in the chalazal seed coat (CZSC) in all the developmental stages and only PHO1 seems to be expressed in the general seed coat (GSE) of the mature green stage embryo (http://seedgenenetwork.net/).

Material and methods

Plant material

All the *Arabidopsis thaliana* WT and mutant plants were of the Columbia ecotype (WT Col). In order to study the expression pattern of *PHO1* and *PHO1;H1* genes in the seeds we used the following transgenic lines: 1) pPHO1:gPHO1:YFP plant lines in a *pho1.2* background which were kindly supplied by Dr Tzyy-Jen Chiou (National Chung-Hsing University and Academia Sinica, Taipei 115, Taiwan) (Liu et al., 2012). 2) pPHO1;gPHO1:GFP lines in a *pho1.2* or WT background and 3) pPHO1;gPHO1;H1 in a *pho1.2* or WT background (for method see "Cloning" section). All the double mutant (DM) plants (*pho1.1/pho1.1 h1.1/h1.1*) of this study were constructed by micro-grafting.

Cloning

In order to express the whole proteins of PHO1 and PHO1;H1 we used the GATEWAY system (Curtis and Grossniklaus, 2003). The genomic sequences of *PHO1* (5483bp) and of *PHO1;H1* (3866bp) were cloned into pENTR2B vectors, using the In-Fusion technique of Clonetech. pENTR2B-PHO1 construct was made by Ji-Yul Jung. For *PHO1;H1* in pENTR2B the following primers were used: H1-F: aggaaaatgatggtgcgaattcggtaccggatccag and H1-R: gatgaagaagactactcgcggccgcactcgagatat. Using LR reaction system (Invitrogen) the genomic sequence of these genes was inserted into the binary plant expression vectors pMDC107 (expressing GFP) and pMDC163 (expressing GUS), where the 2xCaMV35S promoter was replaced by 2.1kb sequence upstream of the transcription start of *PHO1* gene or a 2kb sequence upstream of the transcription start of *PHO1;H1* gene, respectively and transformed into *Agrobacterium tumefaciens*, using the freeze-thaw method. As a standard procedure, genomic DNA was chosen both for *PHO1* and *PHO1;H1* as *PHO1* cDNA is known to be unstable in bacteria. All the constructs were stably transformed into WT and *pho1.2* plants with the flower dip method described in Logemann et al. (2006).

For the pPHO1:gPHO1:YFP lines an 8-kb genomic fragment encoding the *PHO1* coding region, spanning from 2.1 kb upstream of the start codon to 0.5 kb downstream of the stop codon, was cloned, according to Liu et al. (2012). The C-terminal YFP fusion of PHO1 was constructed with YFP inserted at nine amino acids from the C terminus of PHO1. pKGW was used as the Gateway destination vector (Karimi et al., 2002).

Bright-field microscopy

Localization of both PHO1 and PHO1;H1 proteins in *Arabidopsis* ovules and seeds was performed using either a Leica DM5000 or DM5500 microscope with transmitted light and the differential interference contrast (DIC) method. Ovules and seeds were dissected and cleared with chloral hydrate solution (40g Chloral hydrate in 10ml of H_2O and 5ml of glycerol) for several minutes (depending on the developmental stage) before imaging.

Confocal microscopy

Localization of both PHO1 and PHO1;H1 proteins in *Arabidopsis* ovules and seeds was performed using either a Zeiss LSM 700 confocal microscope with an Apochromat 63× Water immersion DIC objective with a 1.2 NA or a Zeiss LSM 710 NLO with an

Apochromat 63× Water–Oil immersion objective with a 1.2 NA or Leica SP2 laser-scanning confocal microscope (Leica Microsystems AG, Heerbrugg, Switzerland). Ovules of *Arabidopsis* plants at various stages were dissected and studied untreated in water. For the counter-staining, FM-464 was used (Final concentration: 20ug/ml). The samples, depending on the developmental stage of the ovule or the seed were dissected and incubated in 20ul FM-464 for 15min (young ovules and seeds) up to 1hour (mature seeds).

Micro-grafting Experiments

Micro-grafting experiments were performed as previously described by Zimmerli et al. (2012) with some minor additions from Marsch-Martinez et al. (2013). Plants for grafts were grown in vitro on ½ MS media, 0.5% sucrose and 0.8% plant agar for 5d in short-day conditions (8 hours light and 16 hours dark) at 26°C. During the grafting procedure, silicon tubes were used to stabilize grafts. After grafting, plants were incubated 7 additional days on the same media in short days at 26°C before being transferred to pots and continued to be grown under long day conditions (Fig. 18 A-E).

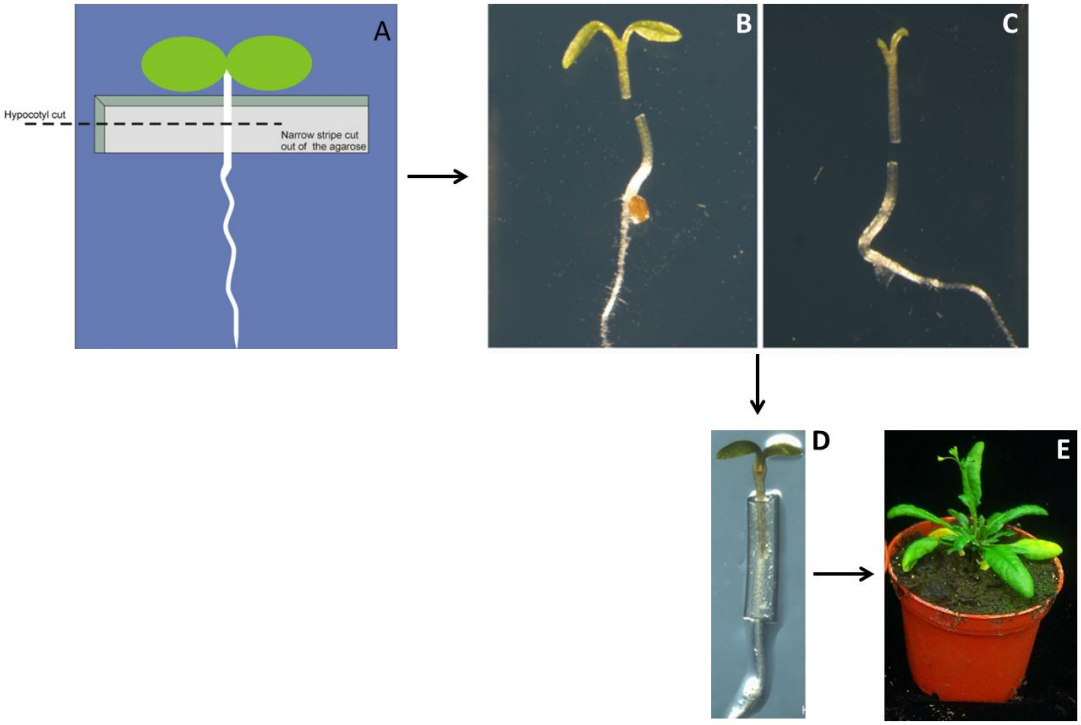

Figure 18: Micro-grafting representation for *Arabidopsis* seedlings. *Arabidopsis* seedlings are placed in a plate containing a thin layer of 0.5% agarose. Cotyledons and root remain in the agarose layer, which avoids drying of the seedling while the hypocotyl can be cut (A and B). Cotyledons are also removed (C) and the seedling is grafted with the support of a silicon tube (D). After 7 days of incubation in short days the seedling are being planted in the soil where they grow in long day conditions (E). Slightly modified from Marsch-Martinez et al. (2013) and Thieme et al. (2015).

B-Glucuronidase staining

Seedlings, ovules and seeds from the transgenic plants described above, grown in soil, were dissected and stained for GUS activity according to the protocol of Lagarde et al. (1996). The tissues were vacuum filtrated so as the solution to penetrate better the tissues and the samples were incubated at 37^{o}C overnight. Stained tissues were cleared in chloral hydrate solution (40g of chloral hydrate in 10ml of H_2O and 5ml glycerol) and analyzed using bright-field microscopy (Leica DM5000 or DM5500 microscope).

Genotyping

Genotyping for *pho1.1* and *pho1.2* alleles was done using CAPS/dCAPS technique. Genomic DNA was extracted and amplified with specifically designed dCAPS primers in order to contain restriction enzyme sites unique for each *pho1* allele (see table 2 for primers used). After the amplification the whole PCR product was digested with BsrI fast digest enzyme (ThermoFisher scientific) for the detection of *pho1.1* allele and MfeI fast digest enzyme for *pho1.2* allele and run on a 2% agarose gel. Digestion with BsrI enzyme gives 2 fragments of 143 and 183bps for the WT allele whereas it does not cut the *pho1.1* allele (326bps). Digestion with the MfeI gives 2 fragments of 204 and 37bps for the WT allele whereas it does not cut the *pho1.2* allele (241bps). For the genotyping of *pho1;h1.1* and *pho1;h1.4* alleles we used the pairs of primers presented in table 2.

Table 2: List of primers used for genotyping *pho1.1*, *pho1.2*, *pho1;h1.1* and *pho1;h1.4* alleles.

Allele name	Forward Primer	Reverse primer	
pho1.1	TGTTGAGTTGTTCAGGCGTTG	TTAACCGTCTGAGTCCCTGTC	BsrI restriction site
pho1.2	GGCAGCTCGTTGAATATGATAGC	GACCTCCTTTTATTTTACCTTATCAGAGCTGATCAATT	MfeI restriction site
pho1;h1.1	ATGGTCAAGTTCACAAAGCAATTCGA	GCAGCTTATTTCCTCCATCTGGACCATT	WT allele
pho1;h1.1 transgene	ATGGTCAAGTTCACAAAGCAATTCGA	GCGTGGACCGCTTGCTGCAACT	T-DNA
pho1;h1.4 transgene	ATGGTCAAAGTTCACAAAGCAATTCGA	ATATTGACCATCATACTCATTGC	T-DNA

Results

Expression pattern of PHO1 protein fused to GUS

In order to study the expression pattern of PHO1 we made a whole protein fusion with GUS, as the expression pattern of a gene can differ from simple promoter fusions with GUS. Furthermore, in previous work on *PHO1* (Stefanovic et al., 2007; Wang et al., 2004), where promoter of *PHO1* was fused to GUS, the expression of the gene in the seeds was never detected and its expression in the shoot vasculature was not also very clear (Hamburger et al., 2002; Zimmerli et al., 2012). As we can see from figure 19 the expression of pPHO1:gPHO1:GUS displayed β-glucuronidase (GUS) activity in the shoot vasculature (A), the developing ovules (B and C) and the vasculature of the anther filament (B), as well as in the connecting tissue between the anther locules where the vasculature of the filament ends (B).

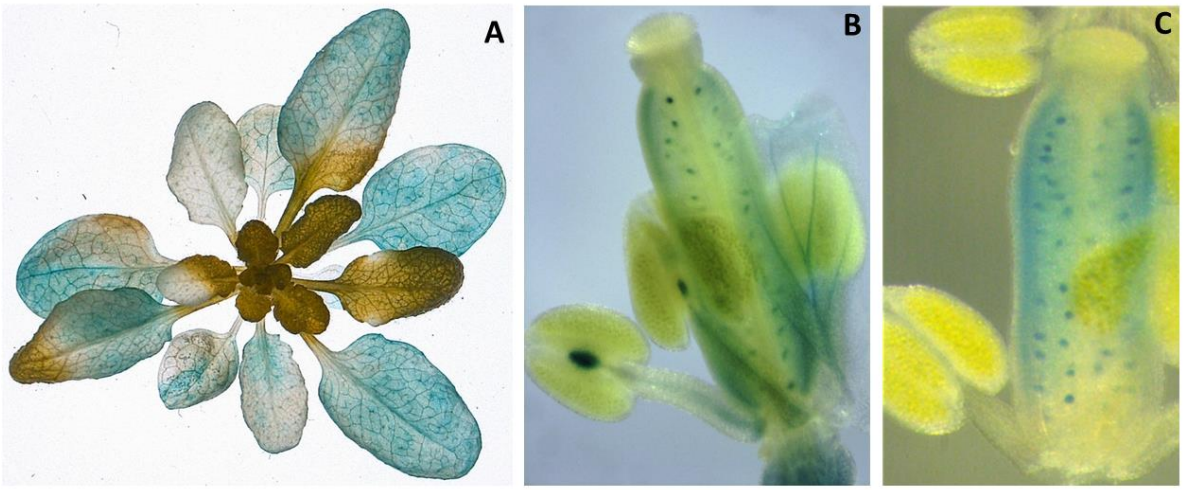

Figure 19: Expression pattern of PHO1 protein including 2Kb of promoter sequence fused to GUS. PHO1 is expressed in the vascular tissue of the shoots (A), the developing ovules (B and C), the connecting tissue of the anther and the vasculature of the anther filament (B).

After dissecting ovules of all the developmental stages and studying the PHO1 expression pattern in more detail, we noticed that PHO1 is expressed in the Megaspore Mother Cell (MMC) (Fig. 20A) and the L1 layer of the nucelus of the ovule primordia (stages 3-I until 3-V) (Fig. 20B-D), later in the development shifts and remains only in the inner integuments (I.I.) (stages 3-V until 4-II) of the developing ovules (Fig. 20E-G), as well as in the chalazal seed coat (CZSC) and the micropylar region of the developing seed (Fig. 20H).

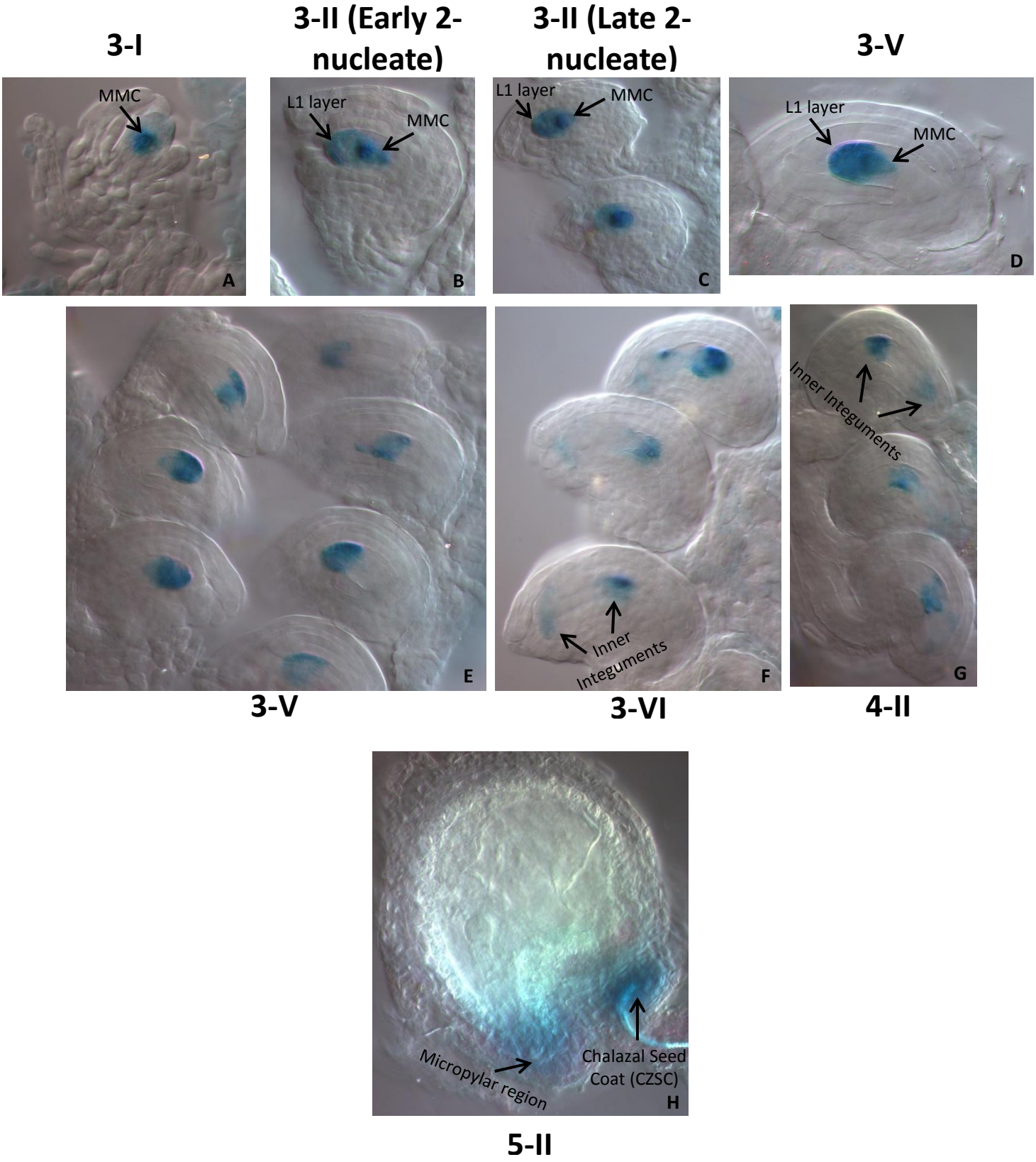

Figure 20: Expression pattern of PHO1 protein including 2Kb of promoter sequence fused to GUS. PHO1 is expressed in the Megaspore Mother Cell (MMC), the inner integuments (A-F), the chalazal seed coat and the micropylar region of the general seed coat during seed development (G).

Expression pattern of PHO1 protein fused to GFP or YFP

In order to study the expression pattern of PHO1 in more detail and confirm that it agrees with the one detected with the GUS staining method, we made a whole protein fusion with GFP or we used transgenic lines of the whole protein fused to YFP, kindly provided by Dr Tzyy-Jen Chiou (National Chung-Hsing University and Academia Sinica, Taipei 115, Taiwan). Analysis of the expression of pPHO1:gPHO1:GFP and pPHO1:gPHO1:YFP also showed that PHO1 is expressed in the megaspore mother cell (MMC) and the L1 layer of the nucelus at the young developing ovules (stages 3-I until 3-V) (Fig. 21A and B, Fig. 22A), later in the development shifts and remains only in the inner integuments (stages 3-V until 4-II) of the developing ovules (Fig. 22B and C), as well as in the chalazal seed coat (CZSC) from the globular stage until the mature stage of the embryo (Fig. 23A and B), the micropylar region only during the globular stage of the embryo (Fig. 23A) and the vasculature of the embryonic cotyledons at the mature green stage seeds (see Fig. 23B).

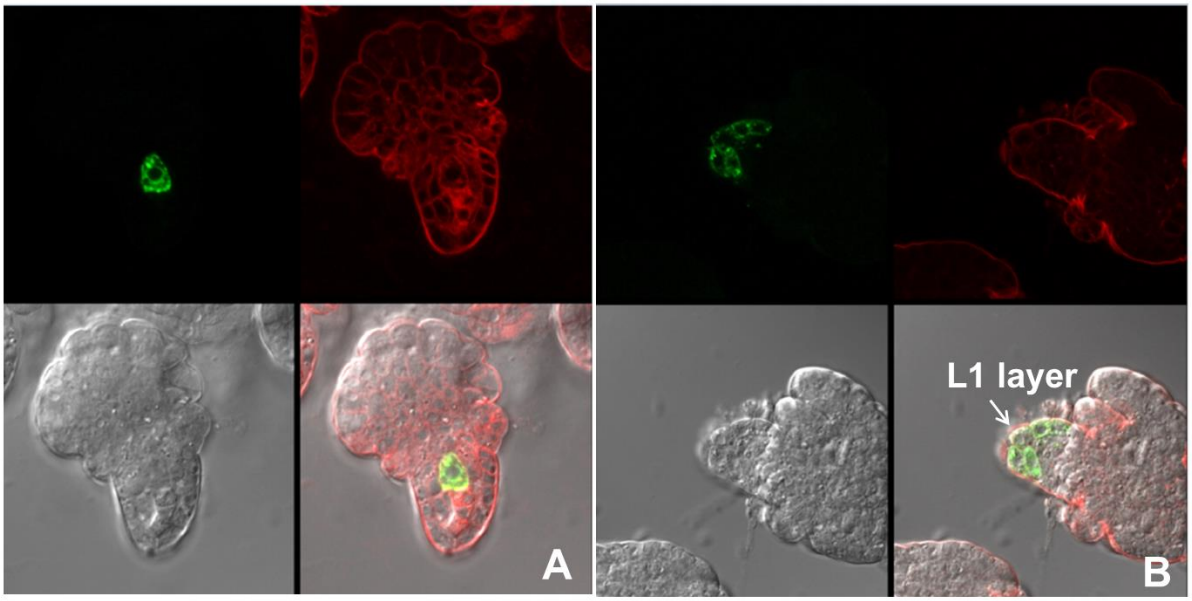

Figure 21: Expression pattern of the whole PHO1 fused to YFP and under the control of 2Kb of promoter sequence. PHO1 is expressed in the Megaspore Mother Cell (MMC) (A) and the L1 layer of the nucelus of the ovule primordia (B).

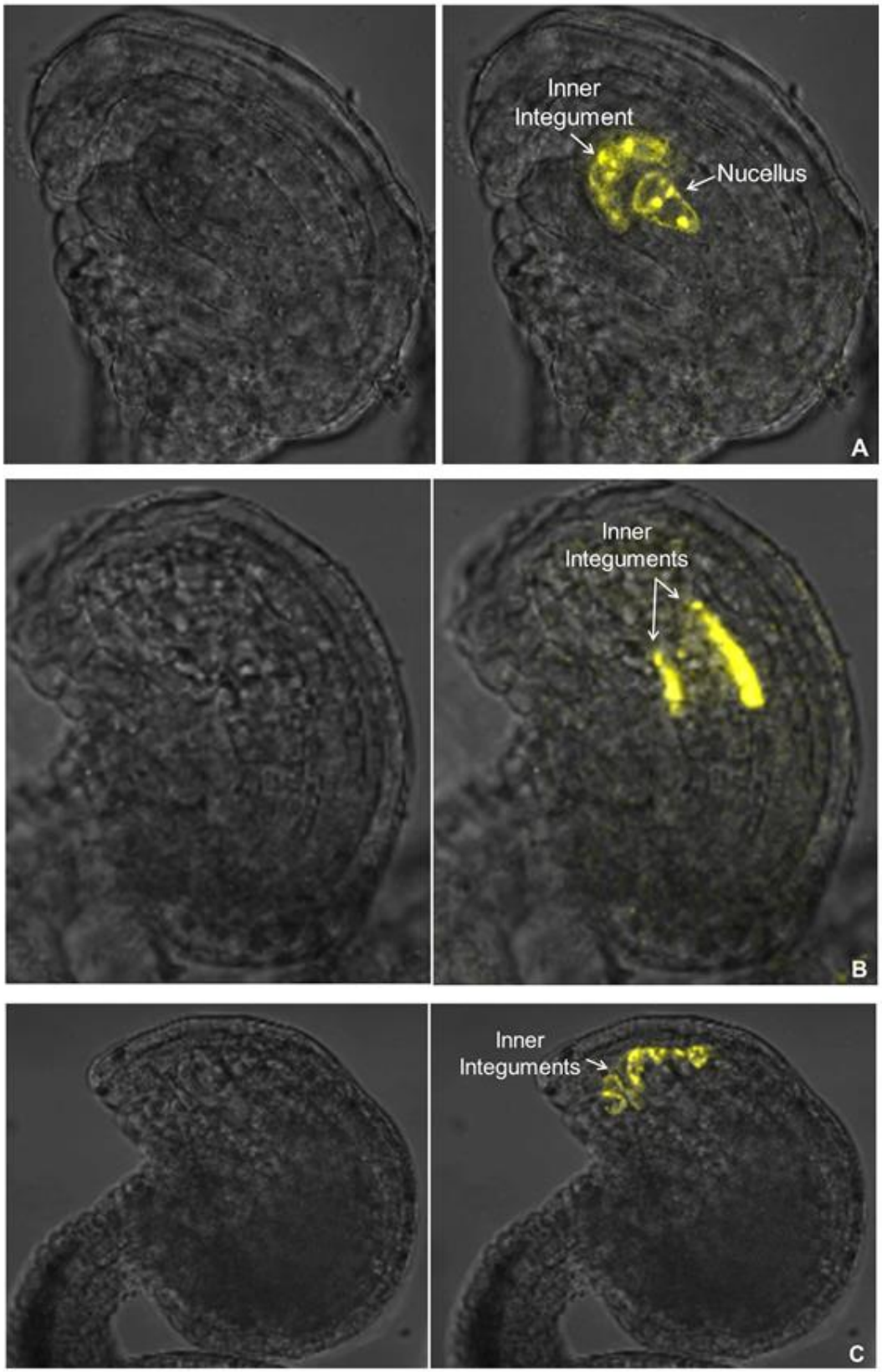

Figure 22: Expression pattern of the whole PHO1 fused to YFP and under the control of 2Kb of promoter sequence. PHO1 is expressed the inner integuments (I.I.) and the nucellus during the early stages of ovule development (A) and it remains in the I.I. during the later stages of ovule development (B and D).

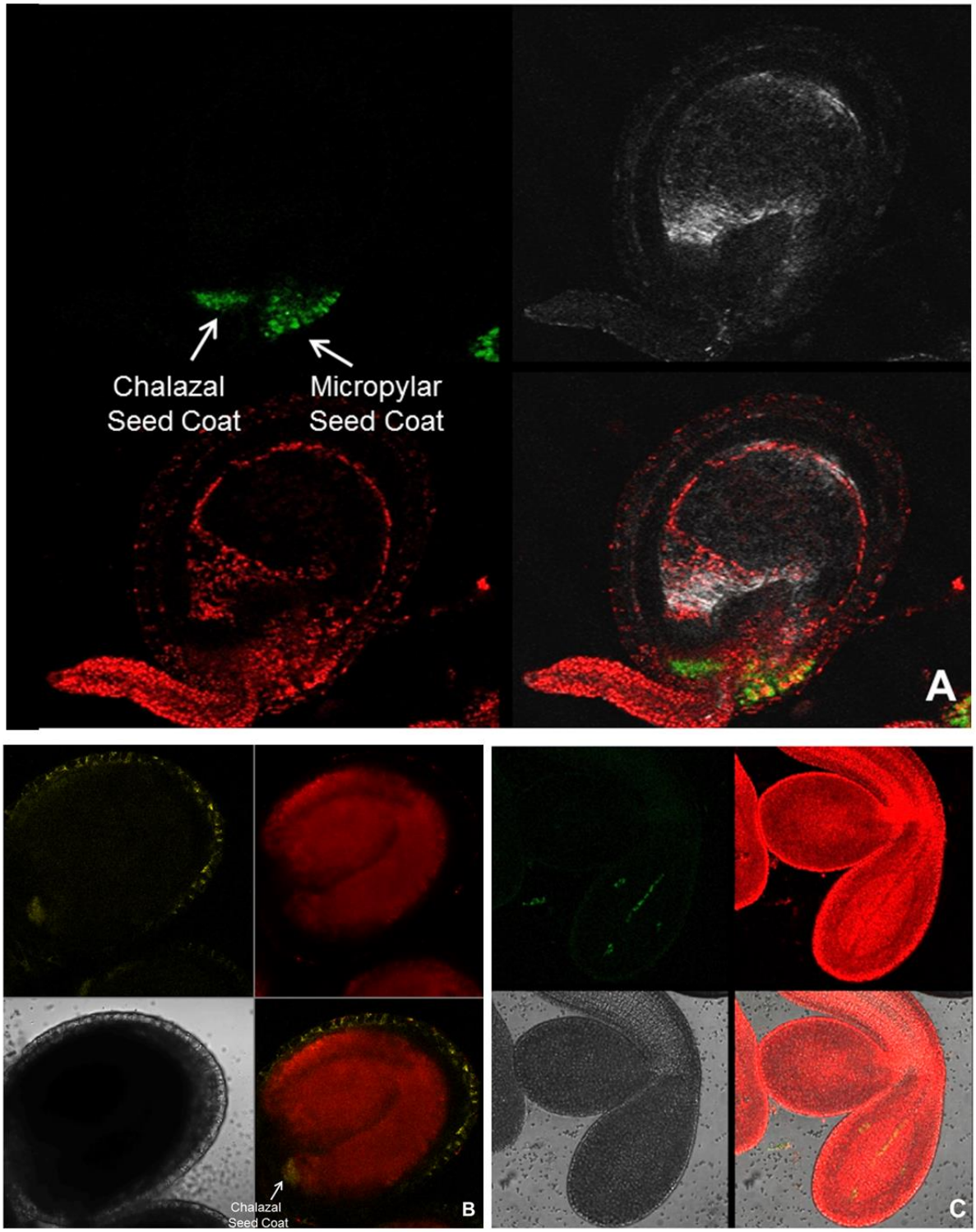

Figure 23: Expression pattern of the whole PHO1 fused to YFP and under the control of 2Kb of promoter sequence. PHO1 is expressed in the chalazal and the micropylar seed coat of the globular stage seeds (A) and in the cotyledon vasculature of the mature green stage seeds (B).

If we compare the expression pattern of PHO1 using GUS or GFP/YFP, we can conclude that the two methods give similar results regarding the expression of PHO1 in the MMC, the L1 layer of ovule primordia and the I.I. of the developing ovules (Fig. 20A-G, 21 and 22) as well as in the CZSC and the micropylar seed coat of the globular stage embryo (Fig. 20H and 23A). However, imaging seeds older than the globular stage embryo using the GUS staining and bright field method is very difficult, as the seeds start to accumulate pigments and their clearing with chloral hydrate is not very successful. Thus, using GFP or YFP lines enabled us unravel more tissues that PHO1 is expressed later in development, like the CZSC and the vasculature of the cotyledons of the developing embryo.

Expression pattern of PHO1;H1 protein with GUS staining

In order to study the expression pattern of *PHO1;H1* and be able to see in which tissue it overlaps with the one of *PHO1*, we made a whole protein fusion with GUS. The expression of pPHO1;H1:gPHO1;H1:GUS displayed β-glucuronidase (GUS) activity in the shoot vasculature (Fig. 24A and B), in the epidermis and the connecting tissue of the anther (Fig. 24C and D), as well as in the chalazal seed coat (CZSC) of the ovule primordia (Fig. 24E) and of the developing ovules and seeds (see Fig. 24F-J). Although the GUS staining was performed for the same time (overnight incubation at 37^{o}C) as for PHO1:GUS expression lines, the expression of PHO1;H1 in some tissues like the connecting tissue of the anther, the ovule primordia and the chalazal seed coat of the developing ovules and seeds was weaker comparing to the one of PHO1, which means that PHO1;H1 is less expressed in these tissues comparing to PHO1.

Figure 24: Expression pattern of the whole PHO1;H1 protein including 2Kb of promoter sequence fused to GUS. PHO1;H1 is expressed in the leaf vasculature (A and B), the connecting tissue (C) and the epidermis (D) of the anther, the chalazal region of the ovule primordia, the young ovules (E, F) and the developing seeds (H-J).

Expression pattern of PHO1;H1 protein fused to GFP

In order to study the expression pattern of *PHO1;H1* we made a whole protein construct fused to GFP. Analysis of the expression of pPHO1;H1:gPHO1;H1:GFP showed that *PHO1;H1* is expressed at the connecting tissue between the anther locules where the vasculature of the filament ends (Fig. 25A), the CZSC of the developing ovule of stage 4-II (Fig. 25B), as well as the developing seeds from the globular stage until the mature stage of the embryo (Fig. 25C and D). Finally, it is also expressed at the micropylar region of the general SC of the globular stage seed (Fig. 25C).

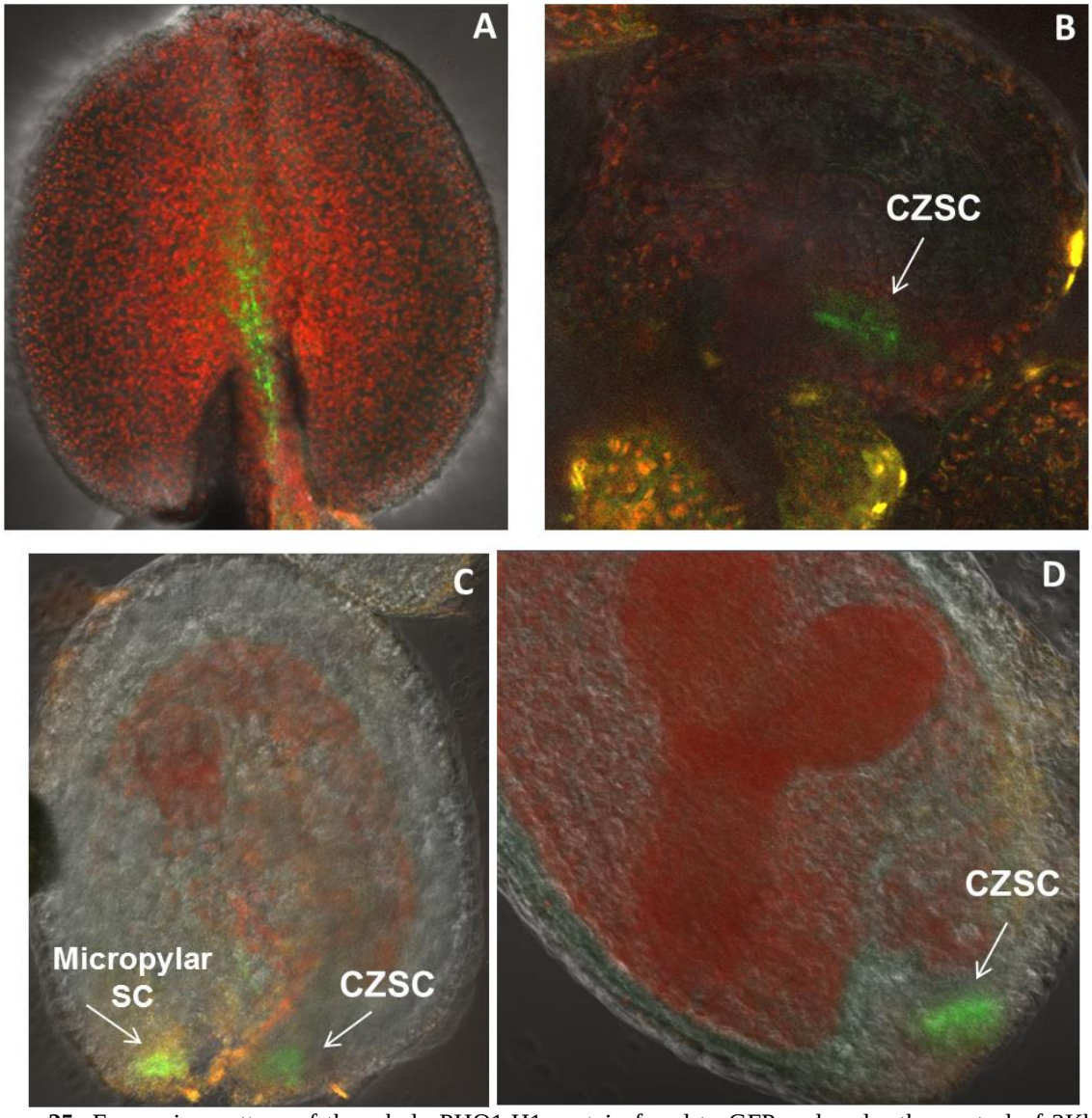

Figure 25: Expression pattern of the whole PHO1;H1 protein fused to GFP and under the control of 2Kb of promoter sequence. *PHO1;H1* is expressed in the connecting tissue (vasculature) of the anther **(A)**, the chalazal seed coat of the developing ovules of stage 4-II **(B)** and the developing seeds **(C and D)** and the micropylar region of the general seed coat of the globular stage embryo **(C)**.

If we compare the expression pattern of PHO1;H1 using GUS or GFP, we can conclude that the two methods give similar results regarding the expression of PHO1;H1 in the connecting tissue of the anther and the CZSC of the developing seeds. However, the GFP method enabled us unravel also the expression of PHO1;H1 in the CZSC of the 4-II stage developing ovules (Fig. 25B) and the micropylar seed coat of the globular stage embryo (Fig. 25C). Finally, the GUS staining method helped us detect the expression of PHO1;H1 at the CZSC of the ovule primordia, as it is more sensitive than the GFP method, where the signal was probably too weak to be detected.

Expression pattern of PHO1 fused to YFP and PHO1;H1 fused to GFP under + or - P conditions

After discovering the expression pattern of PHO1 and PHO1;H1 in the developing seeds and the ovules of *A. thaliana*, we noticed that it overlaps for both genes at the CZSC of the 4-II stage ovules (see table 10, Annex 2 for stage classification) and the developing seeds (see table 11, Anex 2 for stage classification), at the micropylar seed coat of the globular stage embryo and the connecting tissue of the anther. However, *PHO1;H1* is a well-known Pi starvation marker. As it was shown from Wang et al. (2004) it is up-regulated under Pi starvation conditions. Thus, we wanted to investigate if the expression pattern of these genes remains the same or if it changes under Pi starvation conditions.

In order to investigate if the expression pattern of PHO1 or PHO1;H1 is changing according to the P homeostasis of the plant we tried growing pPHO1;gPHO1;YFP lines in pots with clay pellets and not with soil so as to control the Pi content of the watering solution (+/- P). However, this ended in a big variation of the plant growth. Thus, we decided to use micro-grafting. When pPHO1;gPHO1;YFP shoots are grafted on WT roots, both *PHO1* and *PHO1;H1* genes are functional in the root and consequently, Pi is being transported normally to the shoots (+P conditions). On the contrary, when pPHO1;gPHO1;YFP shoots are grafted on *pho1.2* roots, only *PHO1;H1* is functional and as it was already shown from Poirier et al. (1991) not enough Pi is being transported in the *pho1* shoots thus, the shoots are Pi starved (-P conditions). The same experiment was performed using pPHO1;gPHO1;H1;GFP lines so as to study the expression pattern of *PHO1;H1* during the seed development (as *PHO1;H1* is not expressed during the ovule development).

Indicatively, in the upper part of figure 26 we can see one of the developmental stages of the ovules (stage 4-II), where PHO1 is expressed in the I.I. of the ovule, surrounding the embryo sac under P replete conditions. The expression pattern remains in the same tissue

under P starvation conditions but its expression is increased. According to our observations, the same increase in the expression of PHO1 happens in all the developmental stages of seed development. However, as we can notice at the lower part of figure 26 although, PHO1 is slightly expressed in the CZSC and in the micropylar SC of the mature seed under P replete conditions, its expression shifts and increases only in the micropylar SC under P starvation conditions.

Regarding the expression pattern of *PHO1;H1*, it remains the same both under replete or deplete P conditions (see Fig. 27).

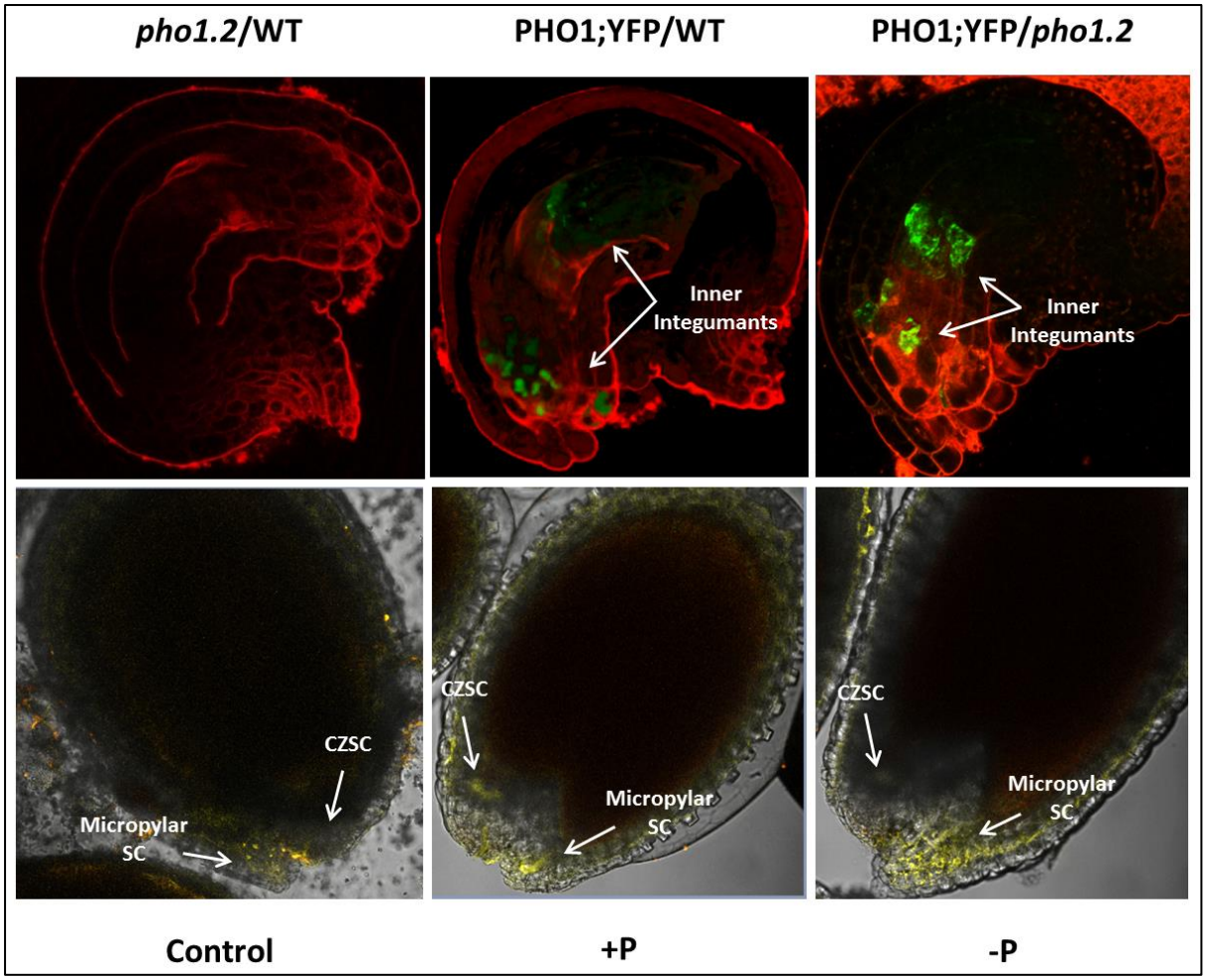

Figure 26: Expression pattern of the whole PHO1 protein fused to YFP and under the control of 2Kb of promoter sequence. PHO1 is expressed at the I.I. of the stage 4-II developing ovules under +P conditions, but its expression increases under –P conditions (up). PHO1 is expressed at the chalazal and micropylar seed coat of the developing seeds under +P conditions but its expression increases and remains only at the micropylar region of the general seed coat under –P conditions.

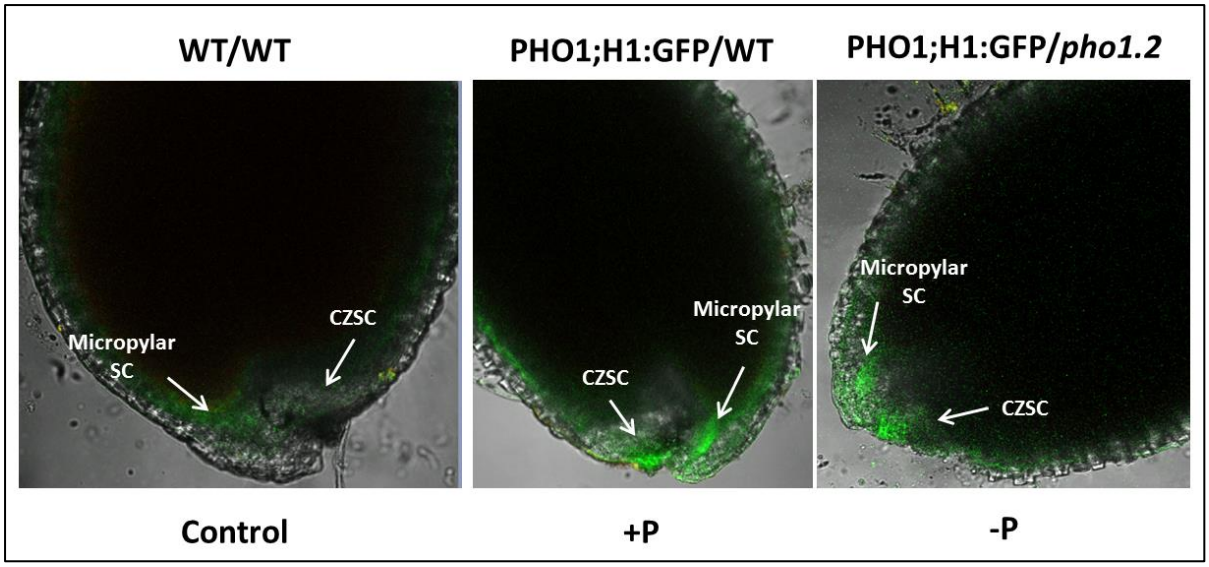

Figure 27: Expression pattern of the whole PHO1;H1 protein fused to GFP under the control of 2Kb of promoter sequence. PHO1 is expressed in the chalazal and micropylar seed coat of the developing seeds under +P conditions and its expression remains the same under –P conditions.

Embryo development of DM and *pho1* mutants

The analysis of PHO1 and PHO1;H1 expression patterns led to the identification of specific seed tissues that these genes are expressed. According to the literature, these tissues are either important for nutrient off-loading (CZSC, micropylar seed coat) or important for the embryo development (MMC, I.I.). Thus, this raises an interesting question regarding the embryo development of the single mutant of *PHO1* as well as of the DM. In order to check the embryo development in these mutants, we grew grafted *pho1.2*/WT and DM/WT plants in the soil for 3 weeks and then dissected developing ovules and seeds from each developmental stage and imaged them using bright-field microscopy.

As we can see in figure 28, the development of the embryo in both the single (*pho1.2*) and the double mutant (*pho1.1/pho1.1 pho1;h1/pho1;h1*) during all the developmental stages [globular (A-C), heart (D-F), bent cotyledon (G-I) and mature green stage (J-L)] is normal comparing to the wild type.

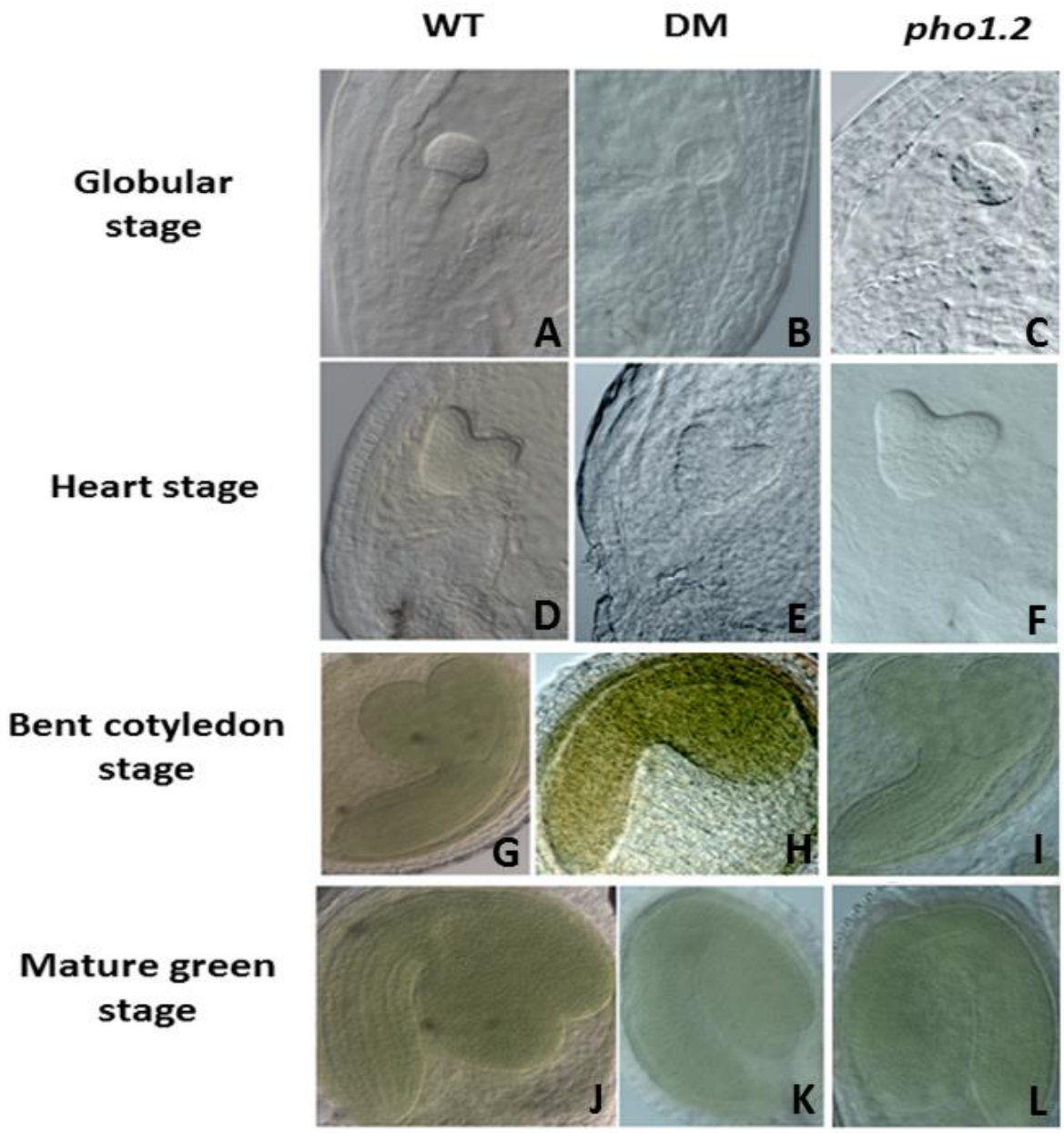

Figure 28: Embryo development of WT, DM and *pho1.2* seeds. In every developmental stage [globular (A-C), heart (D-F), bent cotyledon (G-I) and mature green stage (J-L)] the embryo develops properly comparing to the WT.

What is the role of PHO1 in the MMC?

The localization of PHO1 in the MMC that was detected both by GUS and YFP raises also the question of what could its role be in this specific tissue. As we know PHO1 is a Pi exporter and it would not be expected to export Pi from the MMC as the embryo needs Pi to grow. In order to investigate the role of PHO1 in this specific tissue, we performed reciprocal crosses between a *pho1/PHO1 pho1;h1.1/pho1;h1.1* plant and a *pho1;h1.1* plant grown under + (grafted on a WT root, as described before) or – (grafted on a *pho1.2* root) Pi conditions (see Fig. 29). This experiment allows us to test the role of *PHO1* in the fitness of the ovule.

After obtaining the seeds from these crosses we can grow the seedlings in ½ MS plates and genotype each one individually. If after the genotyping the genotype of the progeny is 50% of *pho1/PHO1* and 50% of *PHO1/PHO1*, as expected from the Mendelian genetics, it means that only one *PHO1* allele is sufficient for the fertilization and the development of the ovule. However, if we obtain a different result, this is to say a progeny of >50% *PHO1/PHO1* embryos it means that both alleles of *PHO1* are important for the development of the ovule and thus of the embryo. The experiment is still going on so we do not have the results yet.

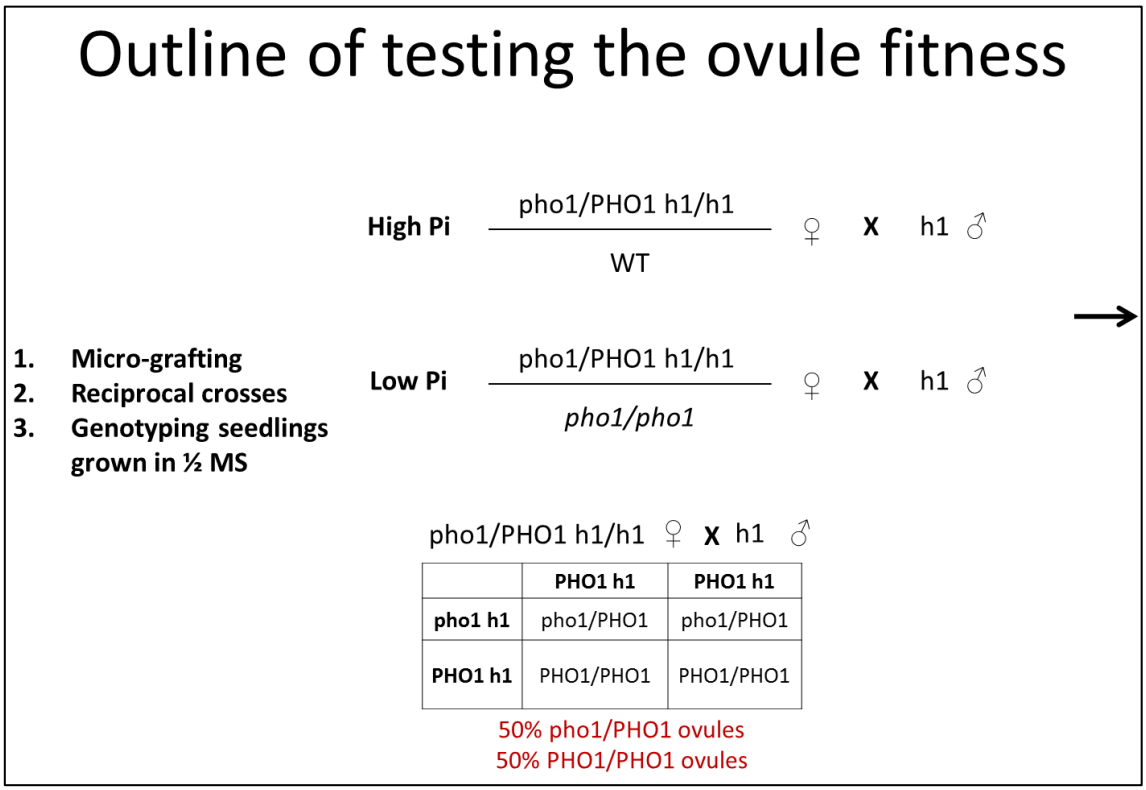

Figure 29: Experimental design of testing the role of *PHO1* in the MMC. *pho1/PHO1 pho1;h1.1/pho1;h1.1* plants were grafted either on a WT root (+ Pi conditions) or a *pho1.2* root (-P conditions). Reciprocal crosses between a *pho1/PHO1 pho1;h1.1/pho1;h1.1* plant and a *pho1;h1* plant were performed and seeds were grown in ½ MS media. The seedlings were genotyped using CAPS genotyping.

CHAPTER 3

The role of *PHO1* and *PHO1;H1* in the seeds

Evangelia Vogiatzaki[1], Ji-Yul Jung[1], Yves Poirier[1]

[1] Department for Plant Molecular Biology, Biophore Building, University of Lausanne, 1015 Lausanne, Switzerland

Author contributions

E.V. and Y.P. designed experiments and Y.P. supervised the whole project. E.V. performed all experiments, except the construction of the amiRNA PHO1 lines that were made from J-Y.J.

Aim

In chapter 2 we confirmed that indeed both *PHO1* and *PHO1;H1* genes are expressed in the developing seeds of *A. thaliana*. Since they have most likely redundant functions, it is important to look at a potential phenotype and role of these genes in the seeds of not only *pho1* and *pho1;h1* single mutants, but also in the *pho1/pho1 pho1;h1/pho1;h1* (DM). Consequently, the aim of this chapter is to identify the role of *PHO1* and *PHO1;H1* in the developing seeds of *Arabidopsis* DM plants.

Unfortunately, the double mutant plant does not give enough seeds because *PHO1* and *PHO1;H1* are not present in the root thus, not enough phosphate is transported into the shoot. The DM plants are Pi starved that grow very poorly (see up right part of Fig. 30) and even if we spray them with 1mM phosphate solution, it takes more than 4-6 months until they give a single inflorescence with 1-3 siliques. So, in order to study the role of *PHO1* and *PHO1;H1* in the developing seeds we needed a plant with a root that is able to transport Pi to the shoots, but with shoots that did not express PHO1 and PHO1;H1. In order to solve this problem and generate a DM plant that would give us enough seeds to study, we grafted *pho1/PHO1 pho1;h1/pho1;h1* or *pho1/pho1 pho1;h1/PHO1;H1* shoots on WT roots. One quarter of the seedlings were DM which did not grow normally in soil (dwarf plant, up left part of Fig. 30).We used two different alleles of *pho1* (*pho1.1* and *pho1.2*) and two of *pho1;h1* (*pho1;h1.1* and *pho1;h1.4*), so as to be sure that our results are significant and after genotyping we tried to identify a plant which had a DM shoot, a WT root and was growing normally as a WT plant (for an outline of the method see Fig. 30).

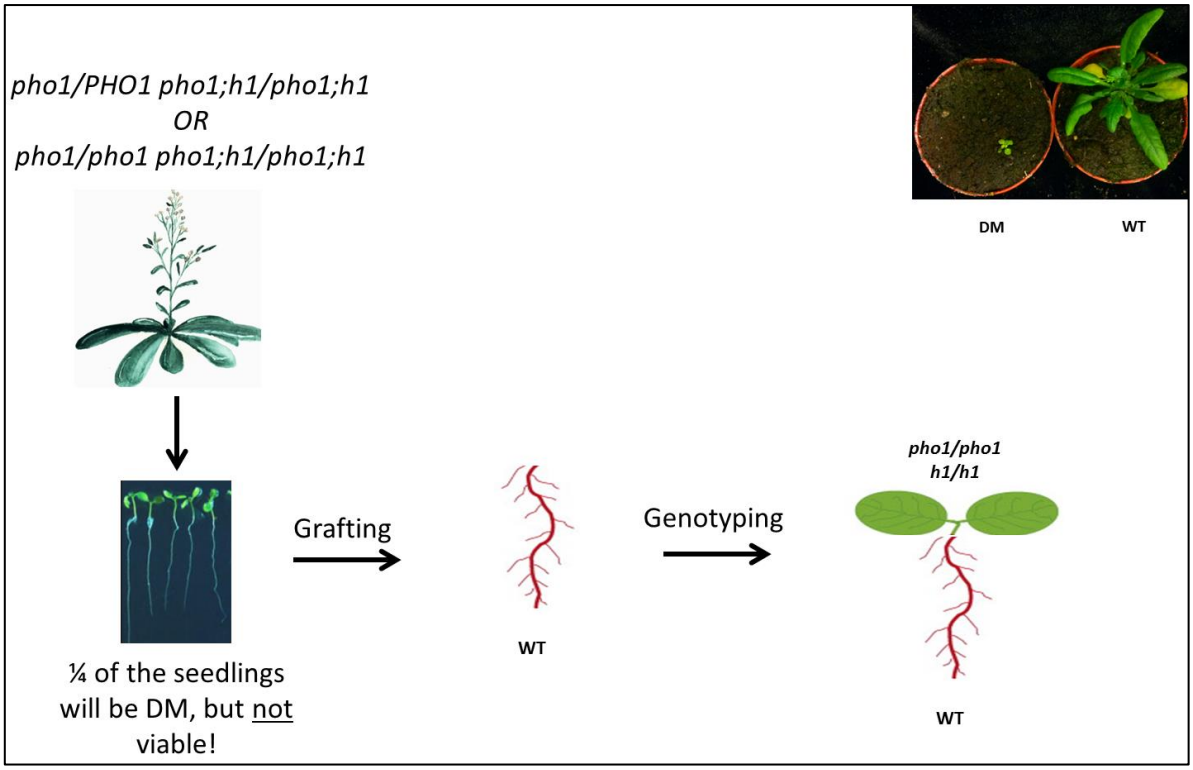

Figure 30: Outline of the procedure to identify a DM plant that grows as a WT and gives enough seeds for our study. *pho1/PHO1 pho1;h1/pho1;h1* or *pho1/pho1 pho1;h1/pho1;h1* shoots were grafted on WT roots. One quarter of the seedlings should be DM which does not grow normally in soil (dwarf, up right picture of DM). After grafting and planting the successful grafts in the soil, plants were genotyped. Plants with a DM shoot which grew as a WT plant because of the functional WT root that transported Pi into the shoot, as PHO1 and PHO1;H1 were present, were identified by genotyping and were used in this study.

Material and methods

Plant material

All the *Arabidopsis thaliana* WT and mutant plants were of the Columbia ecotype (WT Col). In order to find the role of *PHO1* gene in the seeds we used *pho1.1* and *pho1.2* alleles which have previously been described by (Delhaize and Randall, 1995; Hamburger et al., 2002; Poirier et al., 1991). *pho1;h1-1* allele was previously described by Stefanovic et al. (2007) and *pho1;h1-4* allele was obtained by the GABI-Kat T-DNA mutant database (Kleinboelting et al., 2012). All the double mutant plants of this chapter were constructed by micro-grafting using two different alleles of *pho1* and two of *pho;h1* (table 3).

Table 3: DM alleles used in this chapter.

DM name	DM genotype
DM	*pho1.1/ pho1.1 pho1;h1.1/pho1;h1.1*
DM2.4	*pho1.2/ pho1.2 pho1;h1.4/pho1;h1.4*

Micro-grafting Experiments

Micro-grafting experiments were performed as previously described by Zimmerli et al. (2012) with some minor additions from Marsch-Martinez et al. (2013). Plants for grafts were grown in vitro on ½ MS media, 0.5% sucrose and 0.8% plant agar for 5d in short-day conditions (8 hours light and 16 hours dark) at 26°C. During the grafting procedure, silicon tubes were used to stabilize grafts. After grafting, plants were incubated 7 additional days on the same media in short days at 26°C before being transferred to pots and continued to be grown under long day conditions (Fig. 18 A-E).

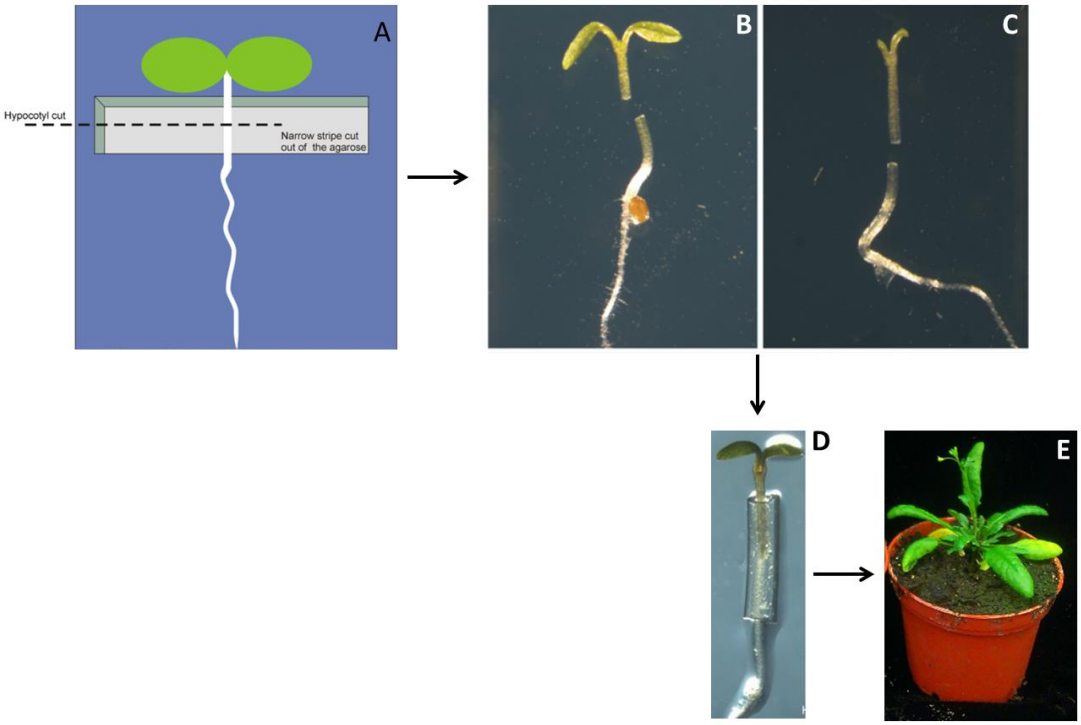

Figure 31: Micro-grafting representation for *Arabidopsis* seedlings. *Arabidopsis* seedlings are placed in a plate containing a thin layer of 0.5% agarose. Cotyledons and root remain in the agarose layer, which avoids drying of the seedling while the hypocotyl can be cut (A and B). Cotyledons are also removed (C) and the seedling is grafted with the support of a silicon tube (D). After 7 days of incubation in short days the seedling are being planted in the soil where they grow in long day conditions (E). Slightly modified from Marsch-Martinez et al. (2013) and Thieme et al. (2015).

Confocal microscopy

Localization of both PHO1 and PHO1;H1 proteins in *Arabidopsis* ovules and seeds was performed using either a Zeiss LSM 700 confocal microscope with an Apochromat 63× Water immersion DIC objective with a 1.2 NA or a Zeiss LSM 710 NLO with an Apochromat 63× Water–Oil immersion objective with a 1.2 NA or Leica SP2 laser-scanning confocal microscope (Leica Microsystems AG, Heerbrugg, Switzerland). Ovules and seeds of *Arabidopsis* plants at various stages were dissected and studied untreated in water. For the counter-staining FM-464 was used (Final concentration: 20ug/ml). The samples, depending on the developmental stage of the ovule or the seed were dissected and incubated in 20ul FM-464 for 15min (young ovules and seeds) up to 1hour (mature seeds).

Complementation of the DM using a Chalazal Seed Coat Specific Promoter

The genomic sequence of *PHO1* (5483bp) was cloned in front of the chalazal seed coat specific (CZSC) promoter pARR22 (At3g04280), previously published by Gatollin et al. (2006) and Horak et al. (2008), into the binary vector pMDC107, which contains GFP using the In-Fusion technique. The size of the amplified promoter was 1150bp using the following primers: ARR22-R: cgtaggcgcgcccttcgatttcttttctctcaag and ARR22-F: ggccagtgccaagcttgattgatacaactctatatggtt. The construct was stably transformed in DM *Arabidopsis* plants, using the floral dipping method (Logemann et al., 2006).

As the transformed plants would express PHO1 only in the CZSC of the developing seeds, the dwarf phenotype of the DM plant would not be complemented (*PHO1* and *PHO1;H1* not present in the root). Thus, planting the transformed seedlings directly in the soil would not be possible, as they would be dwarf and would not produce enough seeds necessary for our study. Consequently, the transformed plants had to be selected in media containing hygromycin (30mg/ml) and directly grafted on WT rootstocks (*PHO1* and *PHO1;H1* present). After the micro-grafting was performed, the plants were left for 7 more days in ½ MS media with carbenicillin (in order to prevent agrobacterium growth) in short day conditions and then planted in soil. In that way, after planting the successful grafts in the soil, DM plants that expressed PHO1 only in the CZSC but could grow like WT were generated (Fig. 31). The same procedure was followed for the genomic sequence of PHO1;H1:stop.

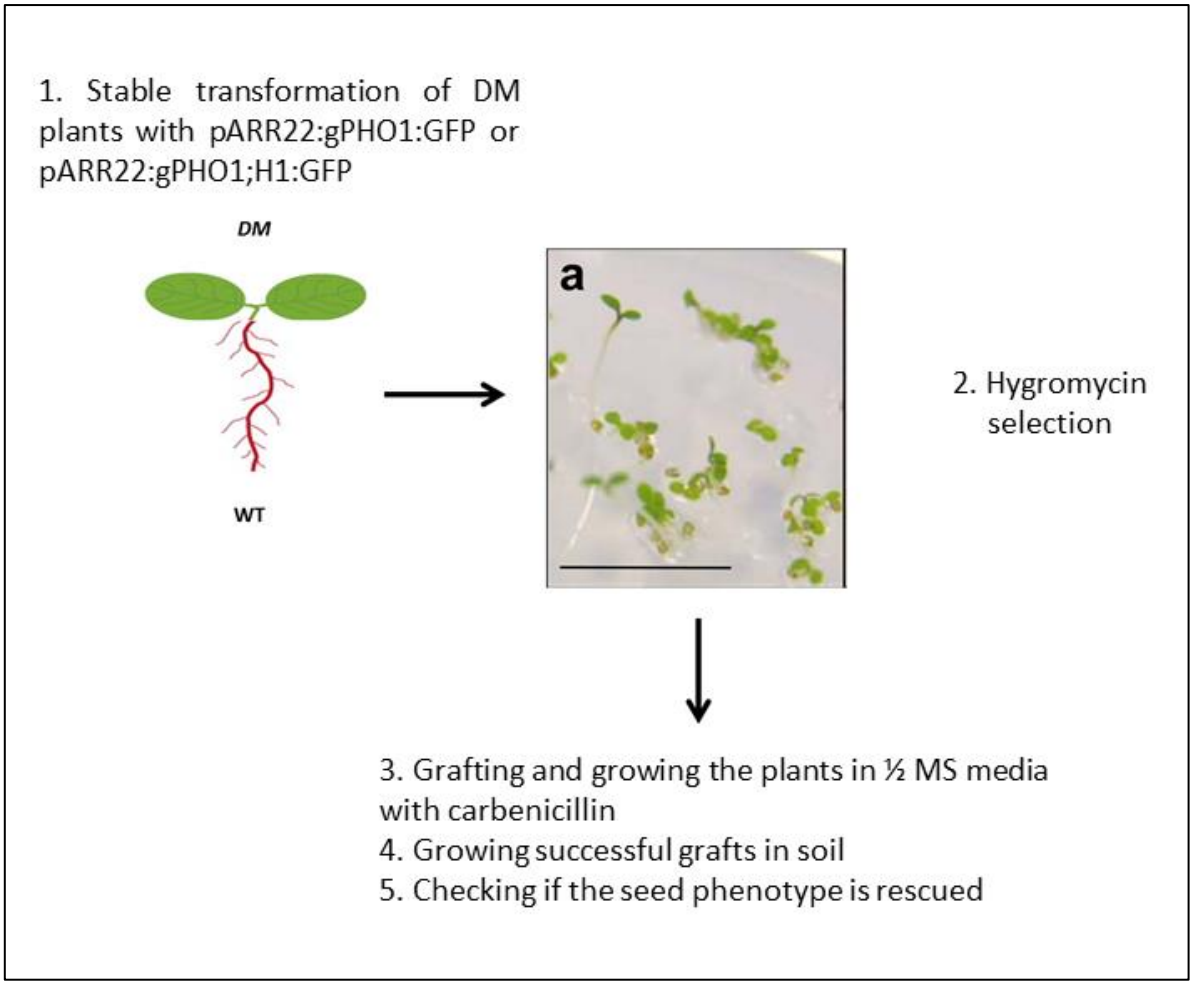

Figure 31: Description of the method used to generate complemented lines expressing specifically *gPHO1* or *gPHO1;H1* in front of the chalazal specific promoter pARR22. The constructs pARR22:gPHO1:GFP or pARR22:gPHO1;H1:GFP were stably transformed, using the floral dipping method, in DM *Arabidopsis* plants. Selection of the transformed plants by growing them in selection media with hygromycin and grafting the resistant hypocotyls on WT rootstocks (PHO1 and PHO1;H1 present). After the micro-grafting was performed, the plants were grown for 7 more days in ½ MS media with carbenicillin (in order to prevent agrobacterium growth) in short day conditions and then planted in soil.

Specific down-regulation of *PHO1* at the Chalazal Seed Coat

An amiRNA previously used from Ji-Yul Jung to effectively down-regulate *PHO1* in the background of WT and *pho1;h1.1* plants, was put in front of the pARR22 (CZSC specific) promoter in pMDC32 destination vector, in order to specifically down-regulate *PHO1* only in the seeds. Both constructs were stably transformed using *Agrobacterium tumefaciens* floral dip method in WT and *pho1;h1.1* or *pho1;h1.4* background.

To generate the pENTR2B:amiR-PHO1, Ji-Yul Jung used a pENTR2B:amiR-319 plasmid which was first constructed by the recombination of two DNA fragments as described below using a commercially available In-Fusion multiple DNA assembly cloning method (Clontech Laboratories). Then, pENTR2B:amiR-PHO1 was made by the same In-Fusion cloning method using the pENTR2B:amiR-319 plasmid as a PCR template. The

amiR-PHO1 entry vector was sequenced to make sure that no changes were introduced by PCR. The resulting entry clone was introduced into pMDC32 destination vector to yield pMDC32:amiR-PHO1. Transgenic Arabidopsis plants carrying pMDC32:amiR-PHO1 in the Col-0 background were generated by Agrobacterium-mediated transformation (Clough and Bent, 1998). The primers used for the above constructs are listed below.

1. pENTR2B:amiR-319 construct using In-Fusion method

A. Vector DNA fragment amplification by PCR using a pENTR2B vector as a PCR template

P2B-F: CACTCGAGATATCTAGACCCAGCTT

P2B-R: CGAATTCGGTACCGGATCCAGTCGA

B. Insert DNA fragment amplification by PCR using an amiR319 containing vector as a PCR template

miR319-infu-F: CCGGTACCGAATTCGacacacgctcggacgcatatt

miR319-infu-R: TAGATATCTCGAGTGtcaagcatgtttttgtgcagga

2. pENTR2B:amiR-PHO1 construct using In-Fusion method

A. Vector DNA fragment amplification by PCR using a pENTR2B:amiR-319 vector as a PCR template

amiR-U-F: ctctcttttgtattccaattttcttgattaatc

amiR-U-R: ctacatatatattcctaaaacatcaattcaaaa

B. Insert DNA fragment amplification by PCR using a pENTR2B:amiR-319 vector as a PCR template

3. amiRNA-PHO1

miRNA-PHO1-1-F: ggaatatatatgtagGTACCCATTTAACTCATTCTTtcacaggtcgtgatatgattc

miRNA-PHO1-1-R:

gaatacaaaagagagGTGCCCATTTAACACATTCTAtcaaagagaatcaatgatcca

Genotyping

Genotyping for *pho1.1* and *pho1.2* alleles was done using CAPS/dCAPS technique. Genomic DNA was extracted and amplified with specifically designed dCAPS primers in order to contain restriction enzyme sites unique for each *pho1* allele (see table 2 for primers

used). After the amplification the whole PCR product was digested with BsrI fast digest enzyme (ThermoFisher scientific) for the detection of pho1.1 allele and MfeI fast digest enzyme for pho1.2 allele and run on a 2% agarose gel. Digestion with BsrI enzyme gives 2 fragments of 143 and 183bps for the WT allele whereas it does not cut the *pho1.1* allele (326bps). Digestion with the MfeI gives 2 fragments of 204 and 37bps for the WT allele whereas it does not cut the *pho1.2* allele (241bps). For the genotyping of *pho1;h1.1* and *pho1;h1.4* alleles we used the pairs of primers presented in table 2.

P^{33} uptake measurements

In order to perform these experiments, WT, *pho1.1*, *pho1.2*, *pho1;h1.1*, *pho1;h1.4*, DM, DM2.4 and pARR22;gPHO1;GFP hypocotyls were grafted on WT rootstocks. When the plants had grown enough to produce stems and siliques, we cut a stem from each genotype and placed it in an Eppendorf tube that contained 1ml of 10uCi/ml P^{33} in water or 1ml of 10uCi/ml S^{35} in water. We incubated them overnight in a long-day growth chamber and the next morning we dissected and separated 5 seed coats and 5 embryos per sample (8-10 samples), at the mature green stage of development (12^{th} silique), in order to perform our measurements. The vials were filled with 5ml scintillation liquid (Ultima Gold, Perkin Elmer) and measured in the Perkin Elmer tri-carb 2800TF Scintillation counter. The statistical significance of the results was evaluated using student t-test.

Inorganic Phosphate measurements

For the determination of Pi content of dried seeds, 4mg of dried seeds from grafted WT/WT, *pho1.1*/WT, *pho1.2*/WT, *pho1;h1.1*/WT, *pho1;h1.4*/WT, DM/WT and DM2.4/WT plants were placed in an Eppendorf tube containing 100ul ddH_2O. The cellular content was first released into distilled water by repeated freeze-thaw cycles and the Pi concentration in the solution was then quantified by the molybdate colorimetric assay (Ames, 1966). The same procedure was used for the determination of the Pi content of whole rosettes with the difference that whole rosettes were cut and weighed and for each mg 50ul of ddH2O were added to the sample in order to release its Pi content using the freeze-thaw method. The statistical significance of the results was evaluated using student t-test and confidence interval α=0,05.

Total P measurements

In order to perform these experiments, WT, *pho1.1*, *pho1.2*, *pho1;h1.1*, *pho1;h1.4*, DM, DM2.4 and pARR22;gPHO1;GFP hypocotyls were grafted on WT rootstocks. When the plants were about 3 weeks old, we dissected and separated 5 seed coats (SCs) and 5 embryos (E), at the mature green stage of development (12^{th} silique), from every genotype (9 samples per genotype/3 samples per plant) in order to perform our measurements with a colorimetric phosphate assay, after performing a total digestion of our seeds in HNO_3 [modified by (Ames, 1966)].

Initially, the samples and a standard curve of phytic acid (PA) were incubated in borosilicate (pyrex) vials in 150ul HNO_3 at 80^oC overnight in order to completely digest the tissues. The next day, the tubes were heated at 145^oC in order to completely evaporate the HNO_3. After being cooled down at room temperature (RT), 60ul of 10% $Mg(NO_3)_2$ in ethanol were added and the tubes were heated at 100^oC in order to completely evaporate the ethanol. Following that, the tubes were transferred to a pre-heated block at 500^oC and incubated there for 2h in order to turn the tissue into ash. After the 2hours, the tubes were cooled down at RT and 300ul of 1N H_2SO_4 were added. The tubes were closed with a screw cap and incubated at 100^oC for 1h. Finally, the tubes were cooled down to RT and 700ul of 1:6 ascorbic acid:ammonium molybdate were added. The content was mixed and incubated at 45^oC for 30 minutes before the samples were measured at the wavelength 820nm in order to determine the Pi content. The statistical significance of the results was evaluated using student t-test.

Seed size measurements

Dried seeds from grafted WT, *pho1.1*, *pho1;h1.1*, DM and DM2.4 plants were collected and photographed at the Leica MZ16 FA fluorescent stereomicroscope. The photos of >100 seeds/sample were analyzed with the help of ImageJ software and the size (area) of each seed was measured. The distribution of the size area was plotted in order to check if there are any differences in the seed size between the different genotypes.

Vigor experiment

The seeds from the crosses of this experiment were grown in ½ MS media without P and sucrose complemented with 1M K_2HPO_4 for + P conditions or without K_2HPO_4 for – P conditions.

Results

1. Hypocotyl grafts

As Stefanovic et al. published in (2007) and as it was mentioned above, the double mutant of *PHO1* and *PHO1;H1* is a dwarf plant with all the symptoms of phosphate starvation. Because both genes have redundant roles, in order to study their role in the seeds we had to use their DM which does not produce seeds unless sprayed with 10mM Pi two times per week (see Fig. 32). This is why we chose to work with micro-grafted plants. If a DM shoot is grafted on a WT root, PHO1 and PHO1;H1 will be functional in the root (phosphate will be normally uploaded on the shoot) and the shoot will be DM as PHO1 and PHO1;H1 will be missing.

Figure 32: Six-week-old plants (WT and three different double mutants) grown in soil and sprayed with 10mM phosphate every second day.

Thus, in order to generate a DM plant which would give us enough seeds to study, we grafted *pho1* homozygous *pho1;h1* heterozygous or *pho1;h1* homozygous *pho1* heterozygous shoots on WT roots and after genotyping we identified a DM plant growing as the WT (see Fig. 33). As we see from the figure 33 the grafted DM plants grow as WT and produce enough seeds for our study.

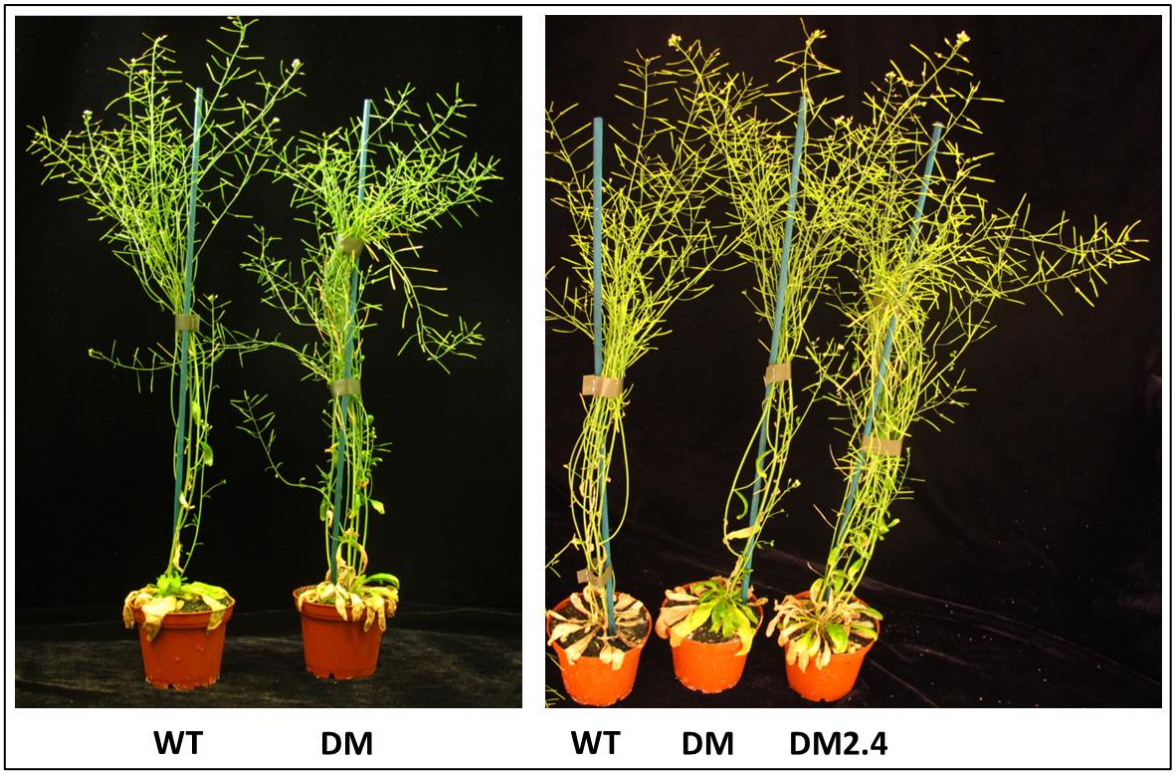

Figure 33: Phenotypes of double mutant (DM and DM2.4) plants grafted on WT roots. Their growth is equal to WT.

2. Pi content of dried seeds

In order to check if the Pi content of the whole dried seeds is the same between the WT, the DM as well as the single mutants of *pho1* and *pho1;h1*, we used grafted on WT roots plants and the colorimetric Pi assay as described in the materials and methods (p. 69). As we can see in figure 34 the Pi content between all the genotypes that were tested is equal except for the DM2.4, which is a bit higher. The fact that DM2.4 has a bit more Pi comparing to the other genotypes could be allele specific. As *pho1* and *pho1.1;h1* are mutated in different sites comparing to the DM plant, these changes could lead to different amount of Pi export into the seed or to the activation of different signaling pathways which with their turn lead to increased Pi content of the DM2.4 seeds.

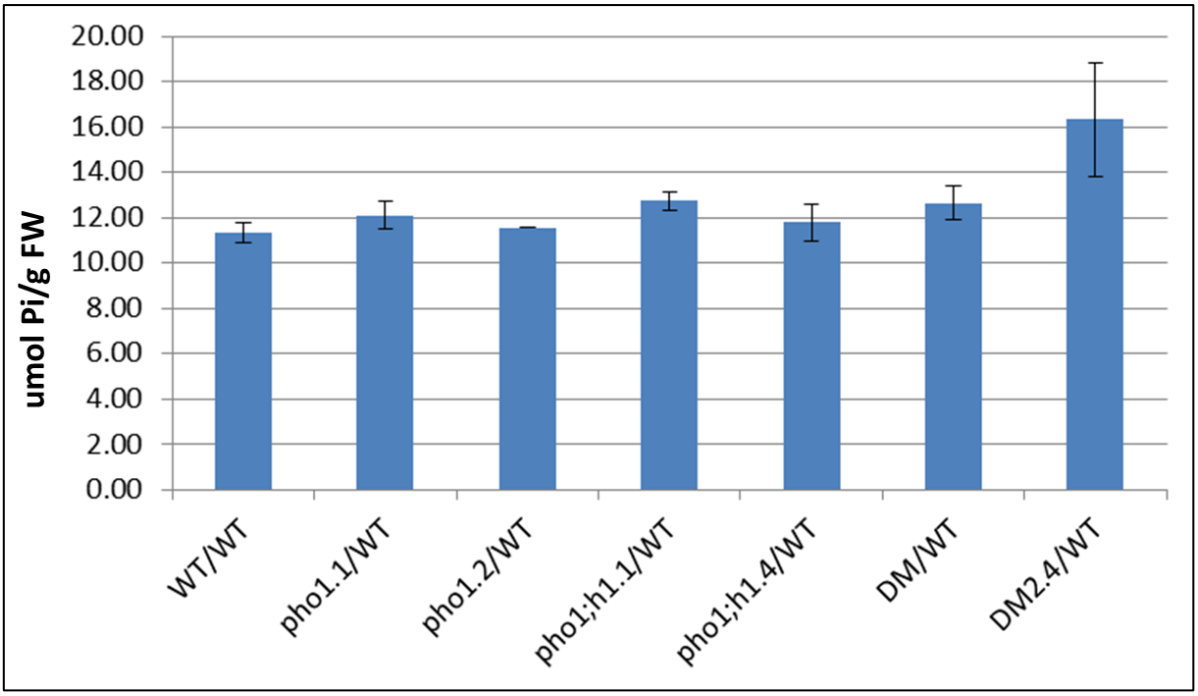

Figure 34: Inorganic P content of seeds from WT, *pho1.1*, *pho1.2*, *pho1;h1.1*, *pho1;h1.4*, DM and DM2.4 plants grafted on WT roots. Error bars denote standard deviations with n=4. There is no significant difference in the seed Pi content between the different genotypes according to confidence intervals $\alpha = 0.05$.

1. Total P content of dried seeds

The Pi content of a tissue is the indication of the free P that is contained in this tissue. Thus, this phosphate marker is not very stable when it comes to living tissues, as P is continuously used and incorporated in several molecules like DNA, lipids, proteins etc. Consequently, a more reliable P marker for measuring the P content of a tissue is the total phosphorus (P). Using 5 dried seeds from WT, DM and DM2.4 plants grafted on WT roots we measured their total P content with a protocol of complete HNO_3 digestion that was developed in our lab. As we can see in figure 35 there is no significant difference in the content of total P between the WT and the DM seeds, something that is quite astonishing if we keep in mind that *PHO1* and *PHO1;H1* are not present in the DM seeds.

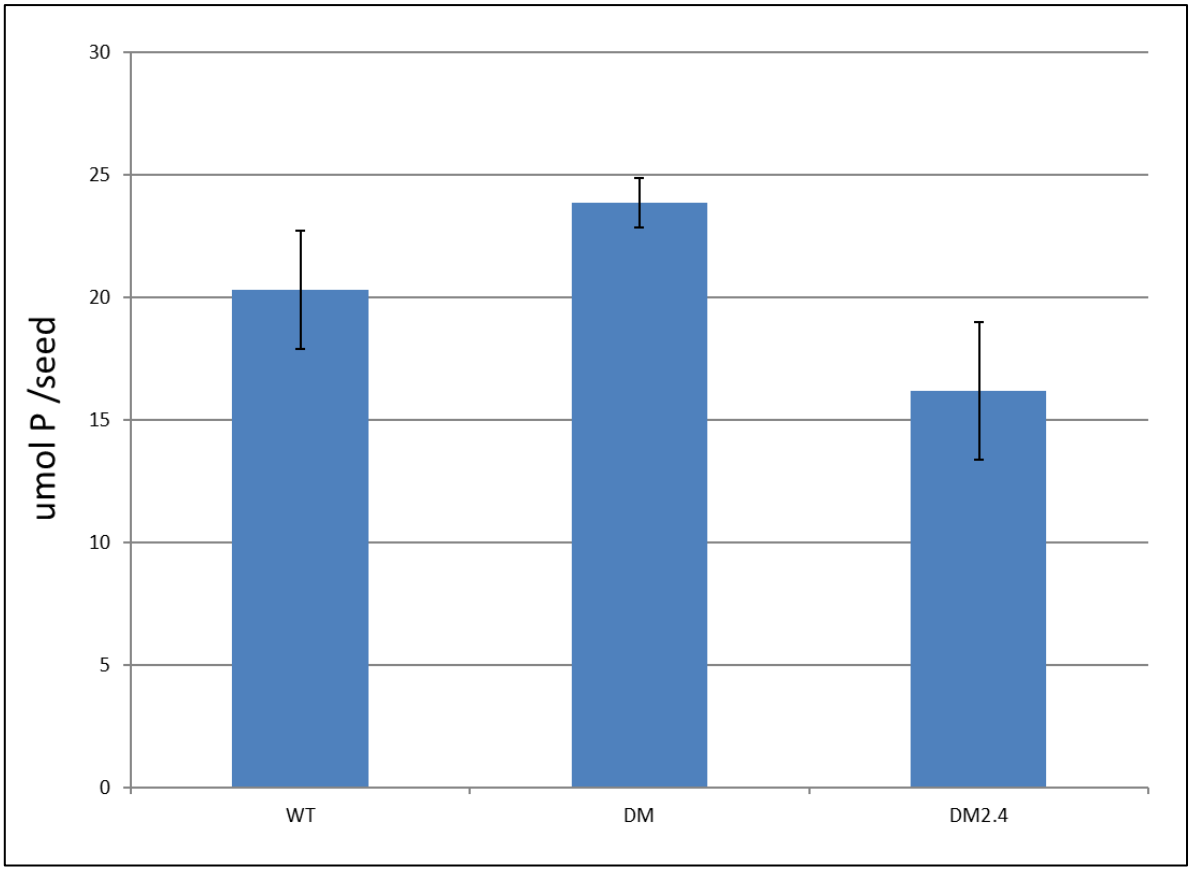

Figure 35: Total P content of seeds from WT, DM and DM2.4 plants grafted on WT roots. All the genotypes have the same total P content as the statistical difference of the total P concentrations is not significant according to the t-test ($p>0.05$). Error bars denote standard deviations with n=4.

2. Size of dried seeds

After checking the Pi and the total P content of the seeds we also wanted to check if there is any significant difference in the size of the DM and WT seeds. Thus, using dried seeds from WT, *pho1.1*, *pho1;h1.1*, DM and DM2.4 plants grafted on WT roots, we took photos of them in a stereoscope and analyzed their seed size with the help of ImageJ software. As we can see in figure 36, the distribution of the seed area of the analyzed genotypes is similar, with most of the seeds having a size of 200-250pixels. So, there is also no significant difference between the seed size of the different genotypes, something that we could expect, as the embryo development in the *pho1* single mutant and in the DM is normal in seeds that derive from grafted plants (Fig. 28, Chapter 2).

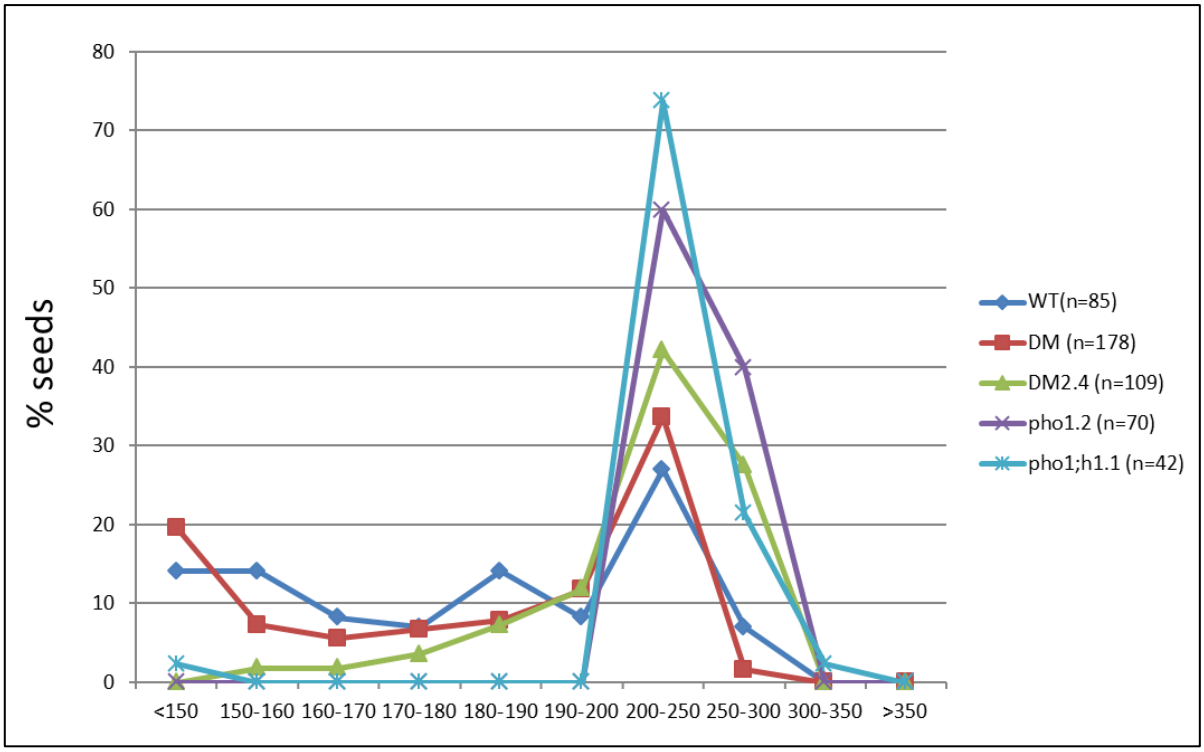

Figure 36: Distribution of seed size (area) of seeds from WT, *pho1.1*, *pho1;h1.1*, DM and DM2.4 plants grafted on WT roots. The distribution of the seed size is similar between the different genotypes.

3. Complementation of the DM using a CZSC specific promoter

As mentioned in chapter 2, the expression patterns of PHO1 and PHO1;H1 overlap in the CZSC region of the developing seeds as well as in the micropylar region of the globular stage seeds. In our effort to confirm if these regions are important for the role of *PHO1* and *PHO1;H1* in the seeds we tried to find CZSC or micropylar specific promoters and express PHO1 specifically at these regions. Unfortunately, we could not find a micropylar specific promoter neither in the published literature nor in the GENEVESTIGATOR database. However, we found a CZSC promoter called ARR22 which was previously published from Gattolin et al. (2006) and (Horak et al., 2008). ARR22 encodes an atypical subtype of the ARR (*Arabidopsis* response regulator) protein family. It is more similar to the receiver domains of hybrid kinases than other response regulators. It acts as a phosphor-histidine phosphatase when tested with phospho-AHP5 in vitro suggesting that it might be involved in a two-component phosphor-relay.

After expressing the genomic sequence of PHO1 in front of the CZSC specific promoter ARR22, fused to GFP (pARR22:gPHO1:GFP construct) and transformed it with agrobacterium mediated transformation into grafted DM plants, we selected the transformed lines in media containing hygromycin and directly grafted them on WT roots before planting them in the soil. This was done because the transformed plants would express PHO1 only in

the CZSC of the developing seeds so the dwarf phenotype of the DM plant would not be complemented (*PHO1* and *PHO1;H1* not present in the root). Thus, planting the transformed seedlings directly in the soil would not be possible, as they would be dwarf, phosphate starved and would not produce enough seeds necessary for our study. In order to check if the seeds of the transformed with pARR22:gPHO1:GFP plants expressed PHO1 only at the CZSC, we dissected seeds and we checked them under the confocal microscope.

As we can notice in figure 37, *PHO1* is successfully expressed only in the CZSC region of the seed coat. We also confirmed that the pARR22 promoter is CZSC specific by confirming that our construct was not expressed in the roots or other tissues where PHO1 is normally expressed. The same procedure was followed for the genomic sequence of PHO1;H1:stop.

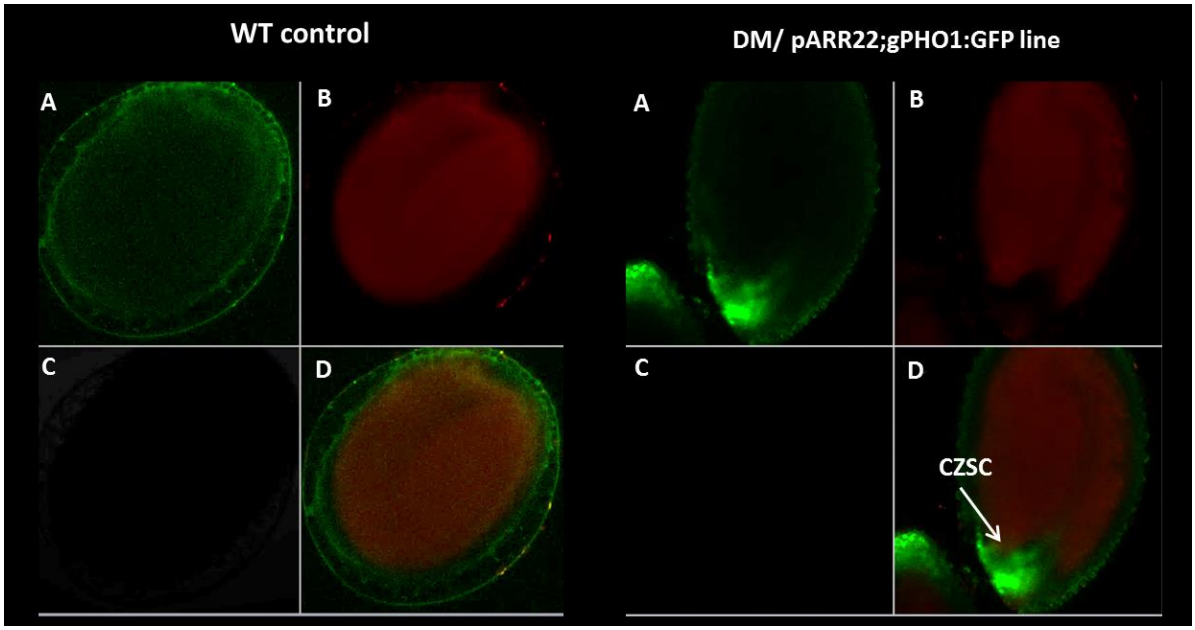

Figure 37: Expression pattern of the pARR22;gPHO1:GFP construct in a DM background. GFP laser chanel (A), mcherry laser chanel (B), Bright-field (C) and overlay (D). *PHO1* is expressed strongly in the Chalazal Seed coat of the Mature Embryo Stage of the developing seeds.

4. P^{33} uptake measurements

A. PHO1 is involved in the export of P into the seed apoplast of Arabidopsis thaliana

As we showed above, the embryo development (Fig. 28), the Pi content (Fig. 34), the total P content (Fig. 35) and the seed size (Fig. 36) of the mature dry seeds of the grafted DM and the WT plants does not differ. This raises many interesting questions: Is the distribution of P the same in the DM as in the WT? Could the P be accumulated in a specific tissue in the DM seeds? What is the exact role of PHO1 and/or PHO1;H1 in the seeds? As both genes are expressed in the CZSC and the micropylar seed coat they could export P into the apoplast, thus most of the P could be accumulated in the seed coat cells.

In our effort to identify the role of *PHO1* and *PHO1;H1* in the seed we used WT, *pho1.1*, *pho1.2*, *pho;h1.1*, *pho1;h1.4*, DM, DM2.4 and pARR22;gPHO1;GFP grafted plants on WT rootstocks. After dissecting seeds of the mature green stage (silique 12) from stems that were cut and incubated in a P^{33} solution overnight we separated the embryo from the seed coat and measured the radioactive counts of each sample.

As we can see from figures 38 and 39, P^{33} is equally distributed between the seed coat and the embryo of the WT, whereas it is accumulated in the seed coat of the *pho1.1* (67%) and *pho1.2* (74%) mutants. In the *pho1;h1.1* and *pho1;h1.4* seeds the P^{33} distribution is also equal between the seed coat and the embryo. So, according to this experiment the P^{33} increase in the seed coat of the DM could be only a result of the absence of the *pho1* allele. Finally, in the pARR22;gPHO1;GFP lines, where *PHO1* is specifically expressed in front of the CZSC promoter, the distribution of P^{33} between the seed coat and the embryo is also equal, which indicates that the specific expression of PHO1 only in the CZSC is enough to complement the DM phenotype.

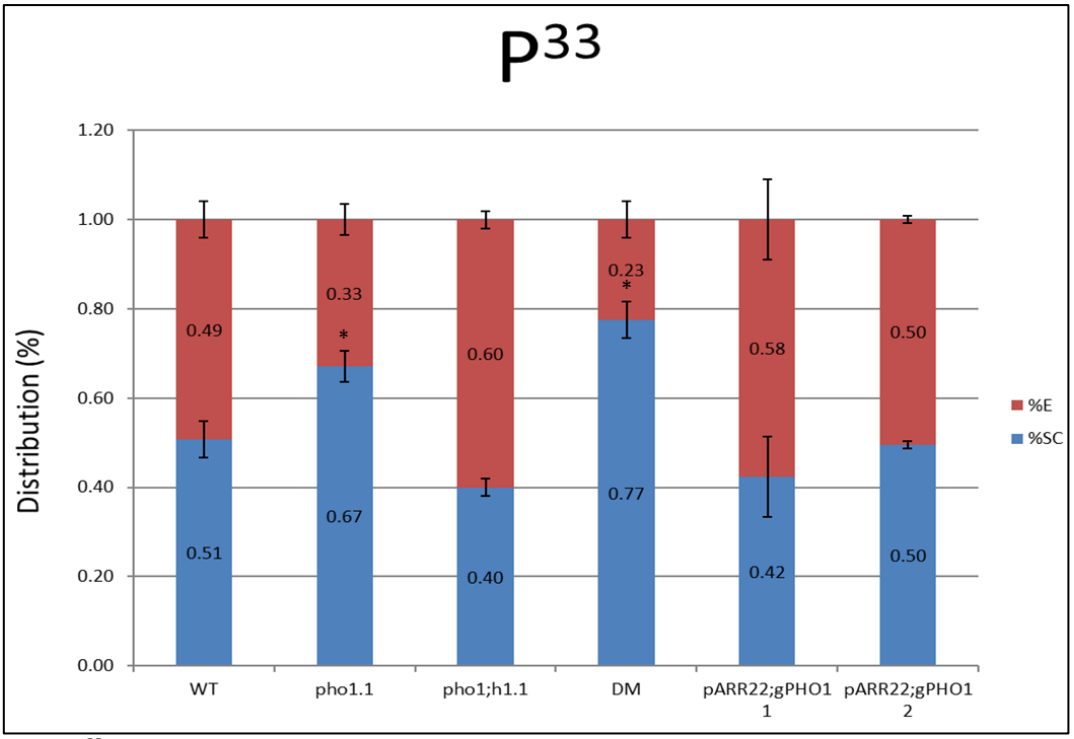

Figure 38: P^{33} uptake distribution in the Seed Coat (SC, blue) and the Embryo (E, red) of WT, *pho1.1*, *pho1;h1.1*, DM and 2 independent lines of pARR22;gPHO1;GFP. Error bars denote standard deviations with n=8-10. Statistical analysis indicates significant difference from the wild type (*p < 0.05).

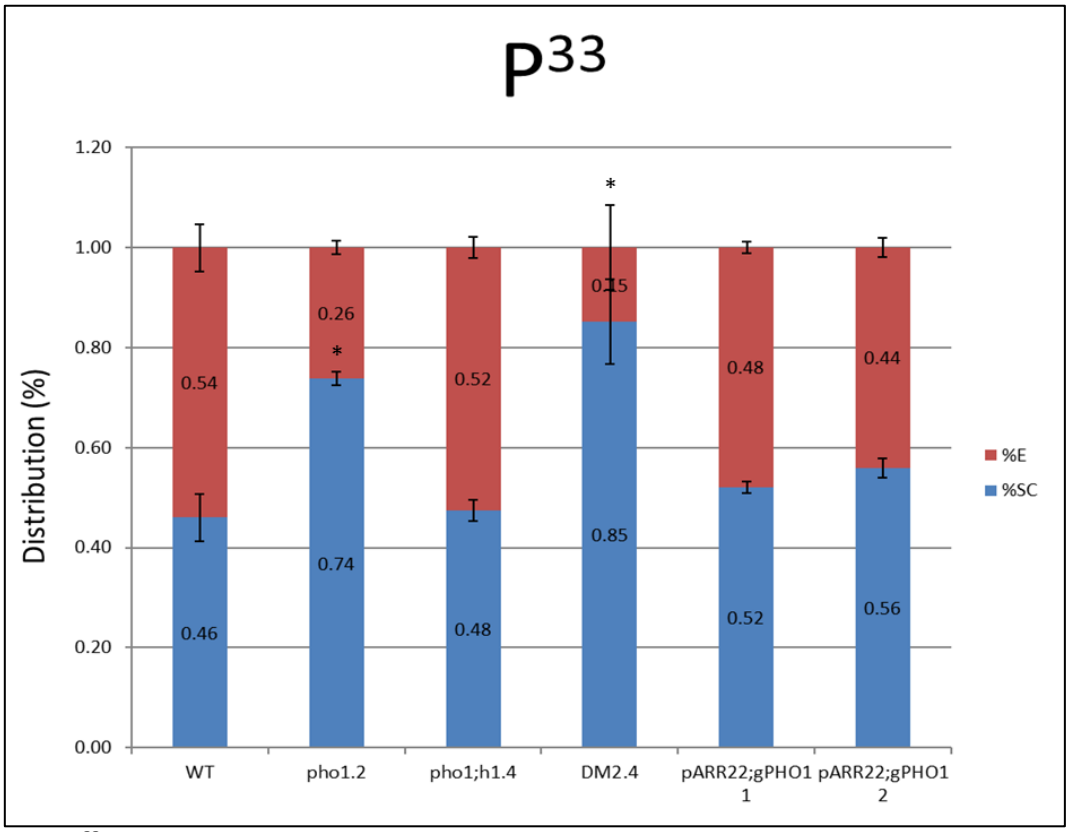

Figure 39: P^{33} uptake distribution in the Seed Coat (SC, blue) and the Embryo (E, red) of WT, *pho1.2*, *pho1;h1.4*, DM2.4 and 2 independent lines of pARR22;gPHO1;GFP. Error bars denote standard deviations with n=8-10. Statistical analysis indicates significant difference from the wild type (*p < 0.05).

In order to show that the shift we noticed in the P content of the *pho1* and DM seed coat is not a consequence of the transport of other elements except for P, we performed the same experiment using S^{35}. As we can see from figures 40 and 41 the distribution of S^{35} between the seed coat and the embryo is always equal in all the genotypes that were used. Thus, we can conclude that the shift in the P content of the seed coat that we noticed from the P^{33} transport is exclusively due to the transport of P from PHO1.

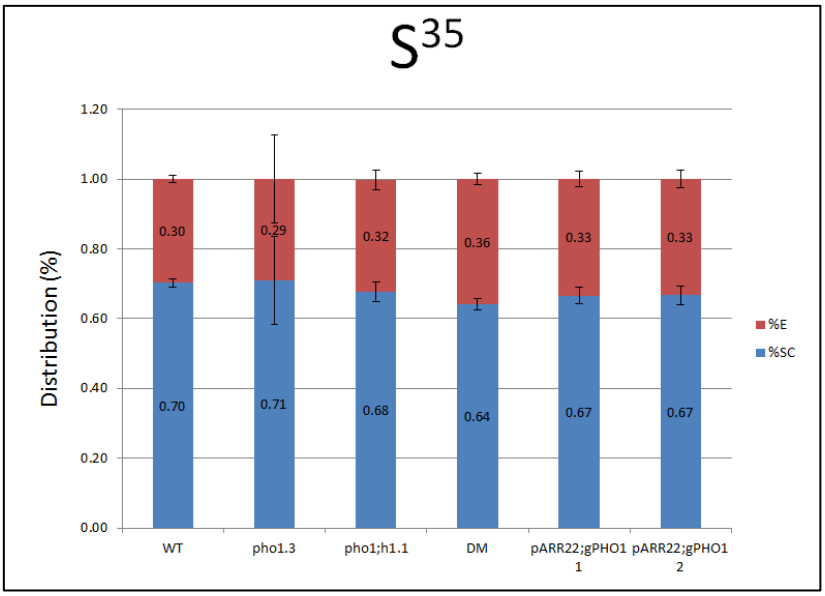

Figure 40: S^{35} uptake distribution in the Seed Coat (SC, blue) and the Embryo (E, red) of WT, *pho1.1*, *pho1;h1.1*, DM and 2 independent lines of pARR22;gPHO1;GFP. Error bars denote standard deviations with n=8-10. Statistical analysis indicates no significant difference from the wild type ($p > 0.05$).

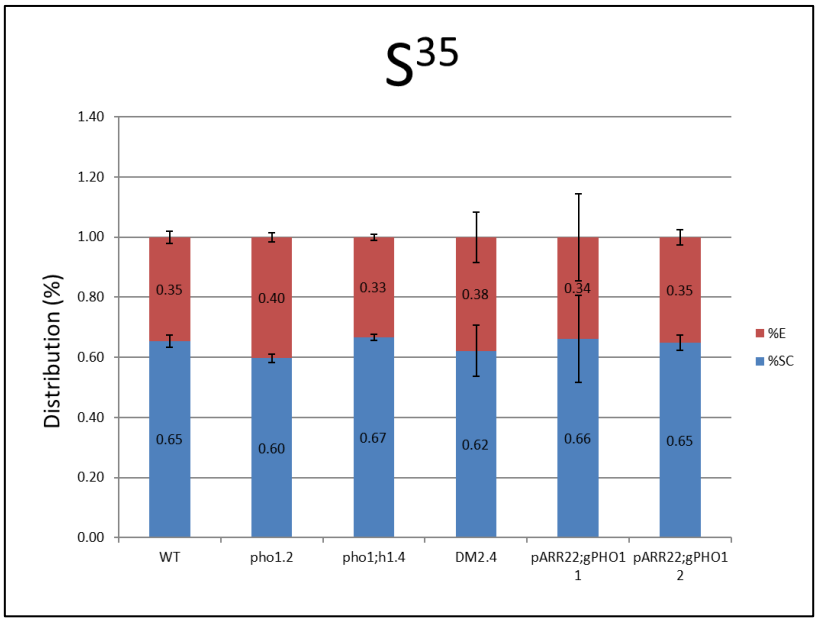

Figure 41: S^{35} uptake distribution in the Seed Coat (SC, blue) and the Embryo (E, red) of WT, *pho1.2*, *pho1;h1.4*, DM2.4 and 2 independent lines of pARR22;gPHO1;GFP. Error bars denote standard deviations with n=8-10. Statistical analysis indicates no significant difference from the wild type ($p > 0.05$).

B. Specific down-regulation of PHO1 at the Chalazal Seed Coat

B1. The PHO1amiRNA construct is functional

The *PHO1amiRNA* made by Ji-Yul Jung, was stably transformed in WT and *pho1;h1.1* plants, through *Agrobacterium* mediated transformation. As we can see in figure 42 the phenotype of the *PHO1amiRNA* in WT background looks like *pho1.2* and the one of *PHO1amiRNA* in *pho1;h1.1* background looks like the DM (see Fig. 6). Furthermore, after measuring the Pi content of whole rosettes from several lines of these plants, we showed that in the *PHO1amiRNA* down-regulated lines, the shoot Pi content is reduced comparing to the WT and is similar to the *pho1.2* single mutant (see Fig. 43). Thus, these results confirm that the *PHO1amiRNA* that we used in our down-regulation lines in front of the CZSC promoter is functional.

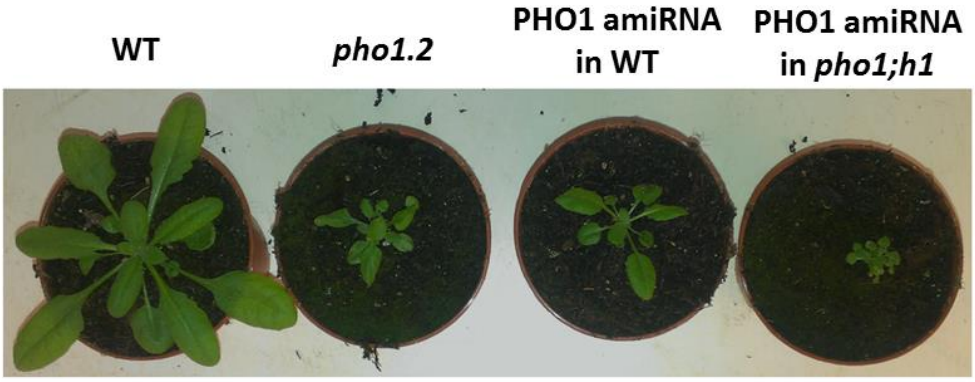

Figure 42: Down-regulation of *PHO1* gene using a *PHO1amiRNA*. From the left to the right phenotypes of: WT, *pho1.2*, *PHO1amiRNA* in WT background and *PHO1amiRNA* in *pho1;h1* background.

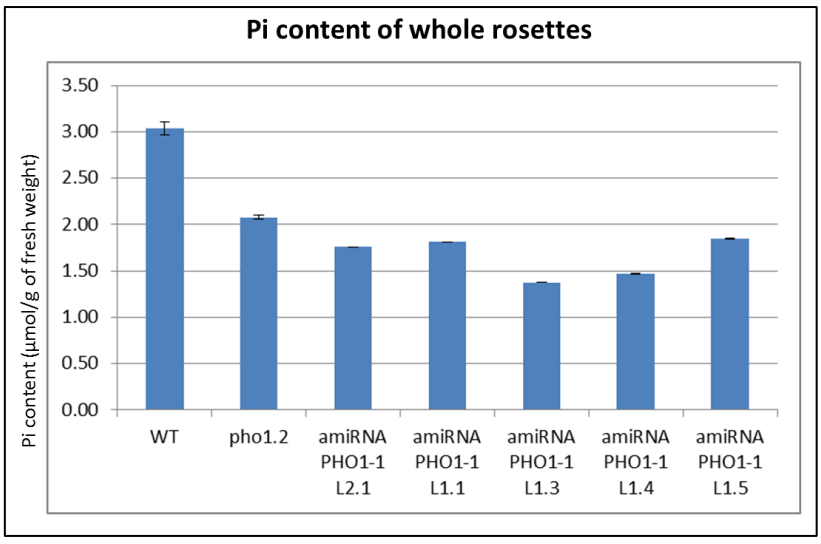

Figure 43: Analysis of inorganic phosphate (Pi) content of rosettes from wild type, *pho1-2* and transgenic lines *PHO1amiRNA* in WT and *pho1;h1.1* background, respectively. There is no significant difference in the Pi content of the whole rosettes between the different genotypes according to the t-test ($p>0.05$). Error bars denote standard deviations with n=4.

B2. PHO1 expression at the CZSC is important for Pi export

In order to show, in another way, that *PHO1* is important for the export of P, we down-regulated it only at the chalazal region of the seed coat using the pARR22 CZSC promoter and an amiRNA that targets specifically the *PHO1* gene transformed in a *pho1;h1* plant. As we can see in figure 44 in both lines, where *PHO1* was down-regulated, P^{33} is increased in the seed coat and there is much less in the embryo, comparing to the WT. From figure 45, we can see again that *PHO1* is specifically transporting P and not to S^{35}.

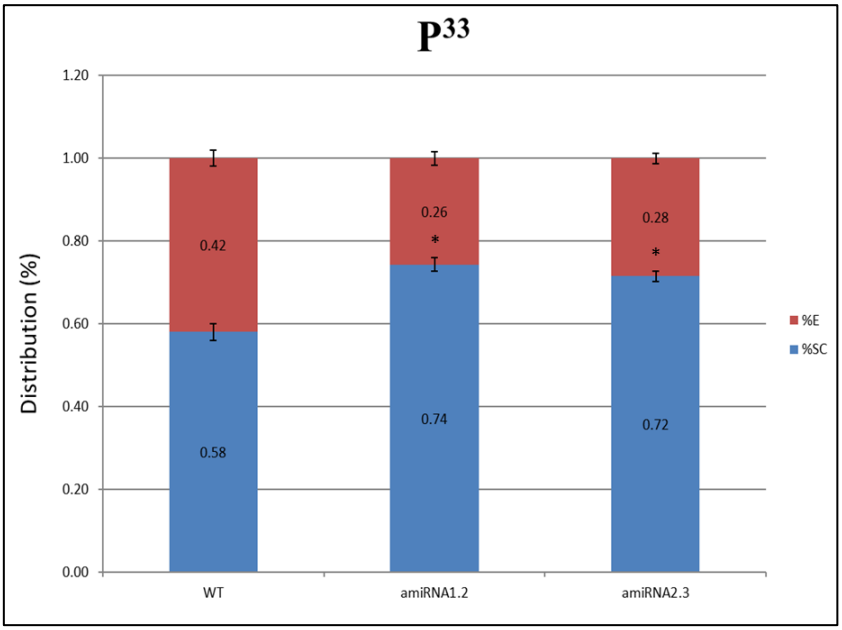

Figure 44: P^{33} uptake distribution in the Seed Coat (SC, blue) and the Embryo (E, red) of WT and 2 independent lines of WT/amiRNA (amiRNA1.2 and amiRNA2.3. Error bars denote standard deviations with n=8-10. Statistical analysis indicates significant difference from the wild type (*p < 0.05).

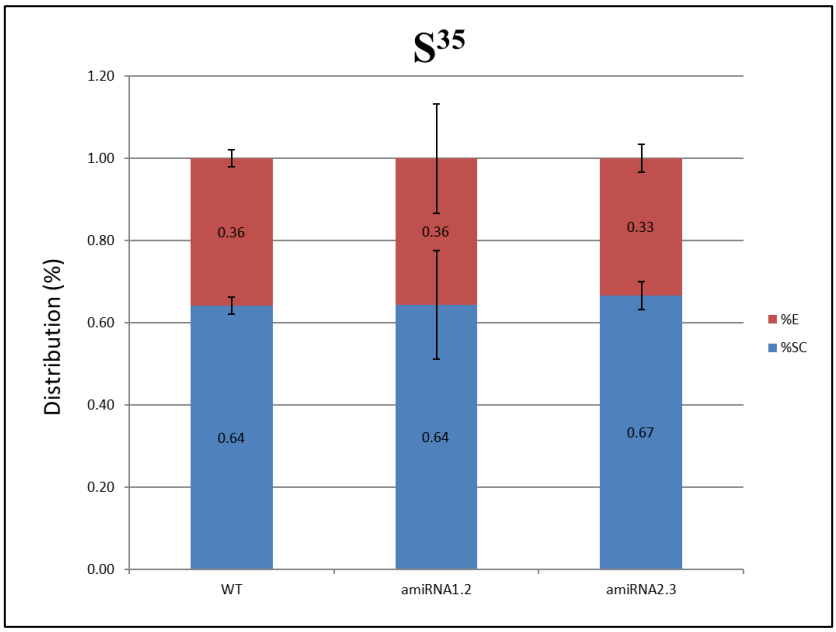

Figure 45: S^{35} uptake distribution in the Seed Coat (SC, blue) and the Embryo (E, red) of WT and 2 independent lines of WT/amiRNA (amiRNA1.2 and amiRNA2.3. Error bars denote standard deviations with n=8-10. Statistical analysis indicates no significant difference from the wild type (p > 0.05).

C. PHO1;H1 expression at the Chalazal Seed Coat is not enough to complement the DM phenotype of the P^{33} distribution

In order to check if the expression of *PHO1;H1* only at the CZSC is also enough to complement the DM phenotype, where P^{33} is accumulated in the seed coat, we used WT, DM, and pARR22;gPHO1;H1:stop (in DM background) grafted plants on WT rootstocks. As we can see from figure 46, P^{33} is equally distributed between the seed coat and the embryo of the WT, whereas it is increased in the seed coat of the DM as well as in the SC of the pARR22;gPHO1;H1:stop lines. Consequently, we can conclude that PHO1;H1 expression at the CZSC is not enough to restore the DM phenotype and decrease the P level of the SC.

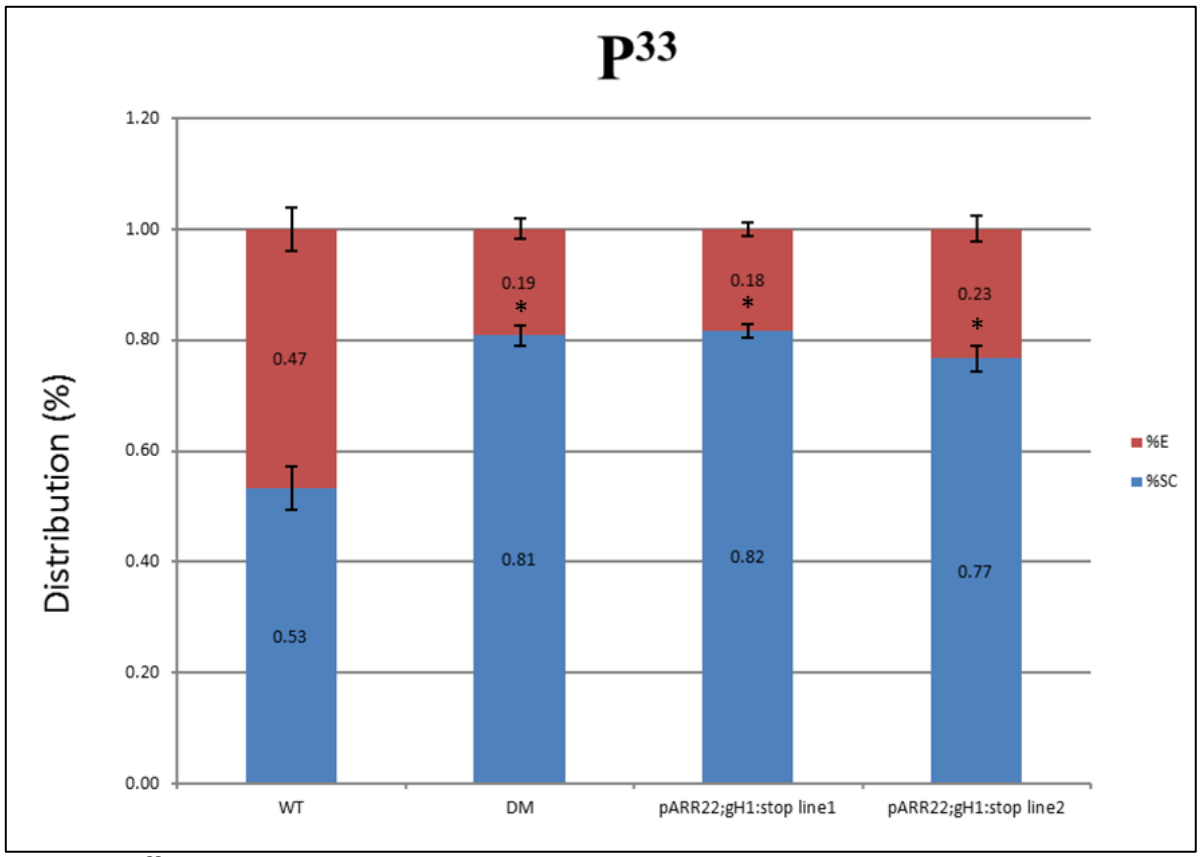

Figure 46: P^{33} uptake distribution in the Seed Coat (SC, blue) and the Embryo (E, red) of WT, DM and 2 independent lines of pARR22;gPHO1;GFP. Error bars denote standard deviations with n=8-10. Statistical analysis indicates significant difference from the wild type (*$p < 0.05$).

5. *PHO1* is involved in the export of P into the seed apoplast during the plant development

A. Total Phosphate Measurements

As we had indications that *PHO1* is involved in the phosphate export into the seed apoplast (see P^{33} uptake experiment p. 77), while phosphate is up-taken from the seeds at a particular stage of development (overnight incubation in P^{33} solution), we also wanted to check if *PHO1* had a cumulative effect on the seed P content during the plant development.

So, we collected samples (seed coat and embryo separately) from grafted plants (WT root) that had grown at least 3 weeks and we measured their total P content. In that way we did not only see what happened to the Pi but also to the total P content of the seed coat and the embryo. As we can see from figure 47, there is less P in the SC of the WT and more in the embryo. On the contrary, when *PHO1* is missing (*pho1.1* and *pho1.2* mutants), the P is increasing in the seed coat (37 and 38%, respectively). In the *pho1;h1.1* (26% in the SC and 74% in the embryo) seeds the P distribution is similar to the WT although in the *pho1;h1.4* seed coat it seems that P is increased (35%) like in the *pho1* mutants. However, this increase is not statistically significant (p-value > 0.05) according to the student t-test that we performed.

Thus, as in the P^{33} uptake experiment we can also conclude that PHO1;H1 does not play a role in the P export into the seeds. The difference between the two experiments is that in the P^{33} uptake one, we examine the effect of PHO1 on the P export during some hours, where probably not many metabolic and developmental changes happen comparing to the total P experiment which lasted three weeks and the whole development and homeostasis of the plant changed. As the amount of P in the SC of the Double Mutants [DM (48%) and DM2.4 (57%)] is more, comparing to the *pho1* single mutants it is possible that PHO1;H1 plays a minor role in the P export comparing to PHO1, or there could be other unknown genes that also contribute to the P export into the seed apoplast. Finally, in the pARR22;gPHO1;GFP lines, where *PHO1* is specifically expressed in front of the CZSC promoter, the distribution of total P between the seed coat and the embryo is similar to the WT, showing that the expression of PHO1 only in the CZSC is enough to complement the DM phenotype (P increased in the embryo).

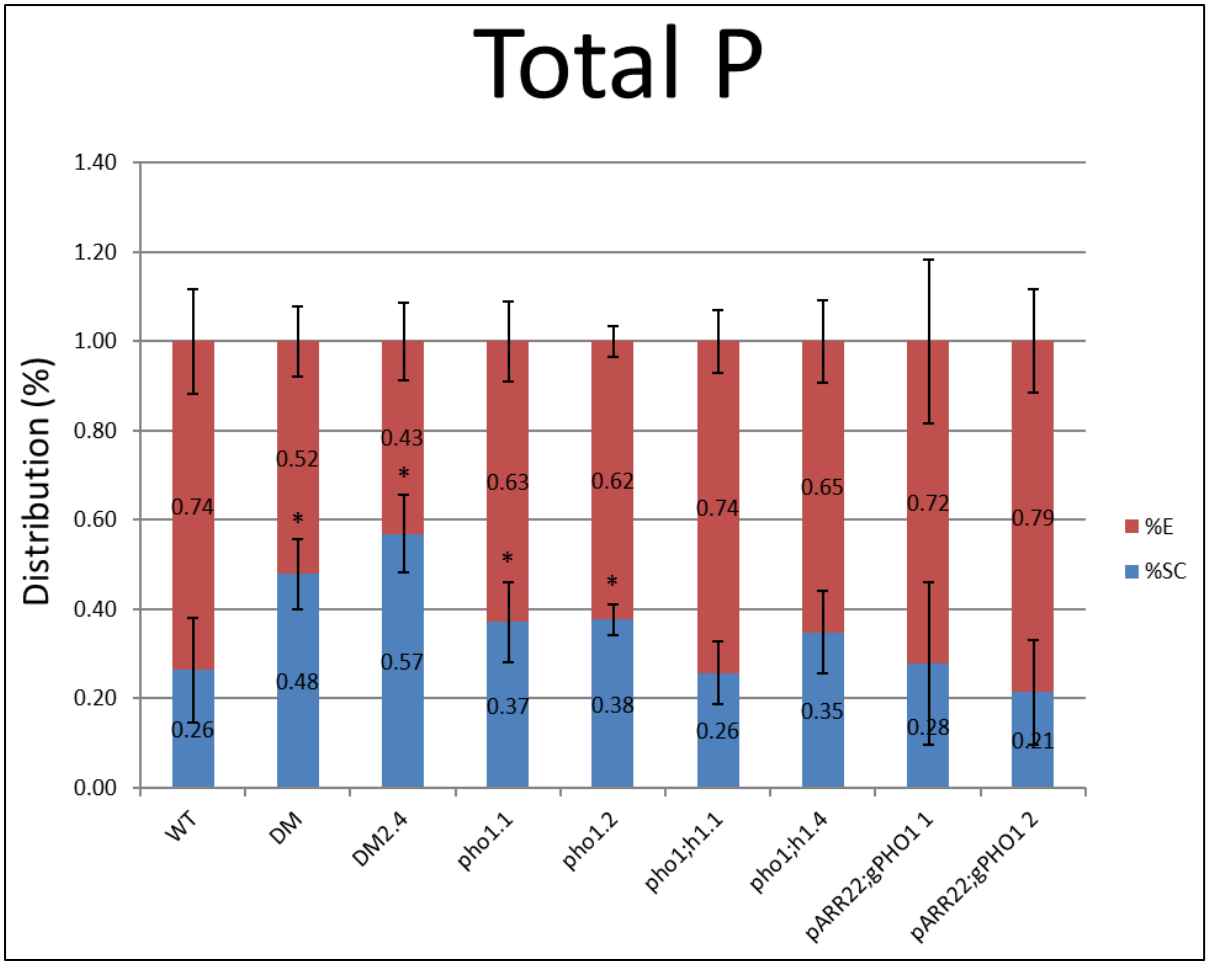

Figure 47: Total phosphorus distribution (%) between the seed coat (blue) and the embryo (red) in grafted WT, DM, DM2.4, *pho1.1*, *pho1.2*, *pho1;h1.1*, *pho1;h1.4* and 2 independent lines of pARR22;gPHO1;GFP plants. Error bars denote standard deviations with n=8-10. Statistical analysis indicates significant difference from the wild type (*$p < 0.05$).

6. Vigor Test

From the literature, it is well known that the seed coat is a maternally derived tissue. In order to check if *PHO1* plays a role in the seedling development we decided to perform reciprocal crosses using 2 different grafted DM plants (DM and DM2.4): WT x DM and DM x WT (Fig. 48). The progeny of these crosses would contain only heterozygous embryos. So, after growing these seeds under + or – P conditions we could check if the vigor of the seedlings is affected when the seed coat is WT or DM. According to the results in figure 49, there is no difference in the growth of these embryos, so *PHO1* does not play a direct role in the seedling vigor.

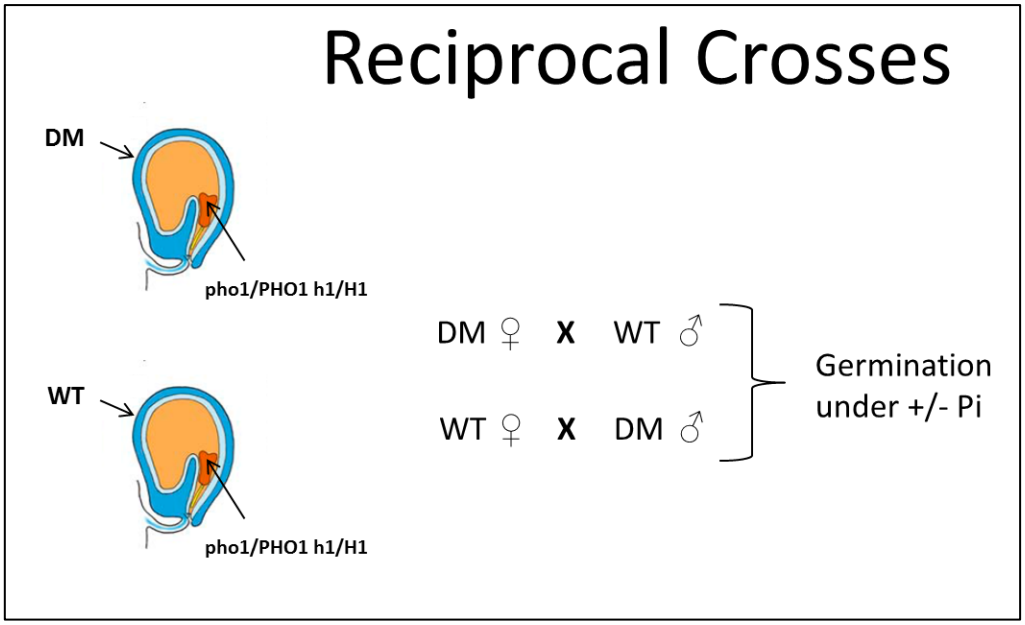

Figure 48: Reciprocal crosses between WT and 2 different DM plants (DM and DM2.4) were performed so as to test the seedling vigor of the progeny. The seeds from these crosses were grown under +/- Pi conditions.

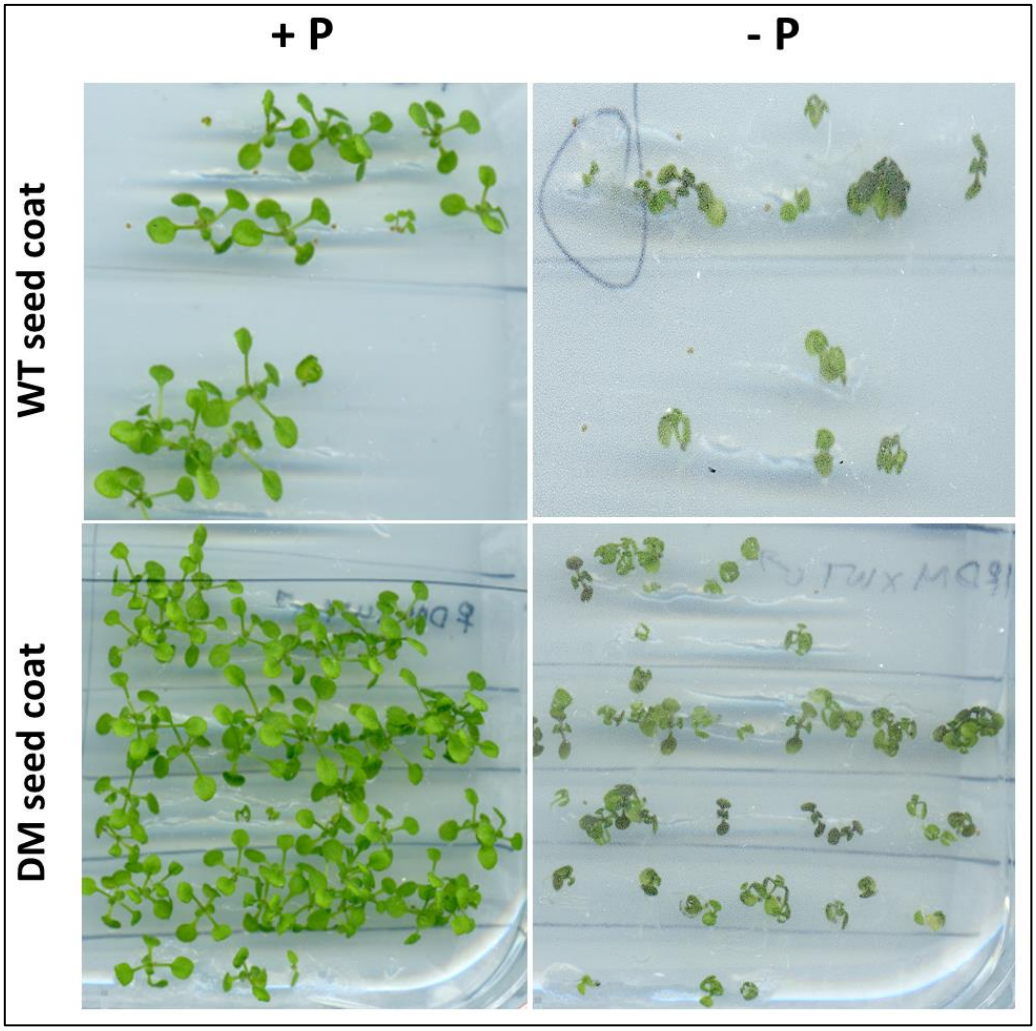

Figure 49: Vigor test of seedlings that come either from a WT x DM cross (up) or a DM x WT cross (down) and have been grown under + or – P conditions all the embryos are heterozygous, but the seed coat is either WT (up) or DM (down).

7. Tissue specific expression of nutrient transporters

In order to see if other nutrient transporters are expressed in different tissues of the seed during the seed development, we did an extended search in http://seedgenenetwork.net/, using the microarray data of the *Arabidopsis* GeneChip experiments. The results of our analysis are presented in table 4 and the annex 1.

Table 4: Tissue specific expression pattern of Phosphate, Boron, Potassium, Chlorine, Iron, Manganese, Zinc, Nitrate and Amino acid transporters using the http://seedgenenetwork.net/ microarray data.

Gene name	Locus	Biological Role	Chalazal SC	Chalazal Endosperm	Micropylar SC	Micropylar Endosperm	Outer Integument	Inner Integument	Peripheral Endosperm	Embryo
Phosphate transporters										
PHO1	AT3G23430	Phosphate transport and homeostasis	✓	✓	✓	✓	✓	✓	×	×
PHO1;H1	AT1G68740	Phosphate transport and homeostasis	✓	✓	✓	✓	✓	✓	×	×
PHO1;H2	AT2G03260	EXS family protein	×	×	×	×	×	×	×	×
PHO1;H3	AT1G14040	Pi homeostasis in response to Zn deficiency	×	×	×	×	×	×	×	✓
PHO1;H4	AT4G25350	Cryptochrome signaling	×	×	×	×	×	×	×	×
PHO1;H5	AT2G03240	EXS family protein	✓	×	×	✓	×	×	×	×
PHO1;H6	AT2G03250 (No probe in microarrays)	EXS family protein	×	×	×	×	×	×	×	×
PHO1;H7	AT1G26730	EXS family protein	×	×	×	×	×	×	×	×
PHO1;H8	AT1G35350	EXS family protein	×	×	×	×	×	×	×	×
PHO1;H9	AT3G29060 (No probe in microarrays)	EXS family protein	×	×	×	×	×	×	×	×
PHO1;H10		EXS family protein	×	×	×	×	×	×	×	×

Gene name	Locus	Biological Role	Chalazal SC	Chalazal Endosperm	Micropylar SC	Micropylar Endosperm	Outer Integument	Inner Integument	Peripheral Endosperm	Embryo
Phosphate transporters										
PHT1;1	AT5G43350	Inorganic phosphate transporter	×	×	×	×	×	×	×	×
PHT1;2	AT5G43370	cellular response to phosphate starvation, phosphate ion transport	×	×	×	×	×	×	×	×
PHT1;3	AT5G43360	Unknown	×	×	×	×	×	×	×	×
PHT1;4	AT2G38940	Response to abscisic acid	×	×	×	×	×	×	×	×
PHT1;5	AT2G32830	Phosphate ion transport	×	×	×	×	×	×	×	×
PHT1;6	AT5G43340	Unknown	×	×	×	×	×	×	×	×
PHT1;7	AT3G54700	Arsenate ion transmembrane transport	×	×	×	×	×	×	×	×
PHT1;8	AT1G20860.1	Root-to-Shoot translocation of orthophosphate	×	×	×	×	×	×	×	×
PHT1;9	AT1G76430	Arsenate ion transmembrane transport, phosphate ion transport	×	×	×	×	×	×	×	×
PHT2;1	AT3G26570	Low affinity phosphate transporter	✓	×	×	×	✓	✓	✓	×
PHT3;1	AT5G14040	Mitochondrial phosphate transporter. Modulates plant responses to salt stress.	×	×	×	×	×	×	✓	✓
PHT3;2	AT3G48850	Mitochondrial phosphate transporter. Modulates plant responses to salt stress.	×	×	×	×	×	×	×	×
PHT3;3	AT2G17270	Mitochondrial phosphate transporter. Modulates plant responses to salt stress.	×	×	×	×	×	×	×	×
PHT4;1	AT2G29650	Plastid phosphate transporter	×	×	×	×	×	×	×	×
PHT4;2	AT2G38060	Inorganic phosphate transporter	×	×	×	×	×	×	×	×

Gene name	Locus	Biological Role	Chalazal SC	Chalazal Endosperm	Micropylar SC	Micropylar Endosperm	Outer Integument	Inner Integument	Peripheral Endosperm	Embryo
Phosphate transporters										
PHT4;3	AT3G46980	Inorganic phosphate transporter	×	×	×	×	×	×	×	×
PHT4;4 (CLT2,CRT)	AT4G24460	defense response to oomycetes, glutathione transport, response to cadmium ion	✓	✓	✓	✓	✓	✓	×	×
PHT4;5	AT5G20380	Inorganic phosphate transporter	×	×	×	×	×	×	×	×
PHT4;6	AT5G44370	Inorganic phosphate transporter	×	×	×	×	×	×	×	×
Gene name	**Locus**	**Biological Role**	**Chalazal SC**	**Chalazal Endosperm**	**Micropylar SC**	**Micropylar Endosperm**	**Outer Integument**	**Inner Integument**	**Peripheral Endosperm**	**Embryo**
Boron transporters										
BOR1	AT2G47160	Boron transporter	×	×	×	×	×	×	×	×
BOR4	AT1G15460	Boron effluxer	✓	✓	×	×	×	×	×	×
Potassium transporters										
SKOR1	AT3G02850	potassium ion homeostasis, potassium ion transport, regulation of membrane potential, response to abscisic acid	×	×	×	×	×	×	×	×
KT5	AT4G32500	Regulation of membrane potential	✓	✓	✓	✓	✓	✓	✓	✓
KAT1	AT5G46240	potassium ion transport, regulation of membrane potential	×	×	×	×	×	×	✓	×
KAT2	AT4G18290	Circadian rhythm, regulation of membrane potential, response to high light intensity, stomatal movement	×	×	×	×	×	×	×	×
HAK5	AT4G13420.1	Potassium ion transport	×	×	×	×	✓	✓	×	×

Gene name	Locus	Biological Role	Chalazal SC	Chalazal Endosperm	Micropylar SC	Micropylar Endosperm	Outer Integument	Inner Integument	Peripheral Endosperm	Embryo
Potassium transporters										
AKT1 OR KT1	AT2G26650	Potassium ion import, potassium ion transport, regulation of membrane potential, regulation of stomatal closure, response to salt stress, response to water deprivation, root hair elongation	×	×	×	×	✓	✓	×	×
AKT2	AT4G22200	Regulation of membrane potential, response to abscisic acid	×	×	×	×	✓	✓	×	×
KT2	AT2G40540	Potassium ion transport, regulation of membrane potential	×	×	×	✓	×	×	✓	✓
Chlorine transporters										
SLAC1 (SLAH1)	AT1G62280	Cellular ion homeostasis	×	×	×	×	×	×	×	×
Gene name	**Locus**	**Biological Role**	**Chalazal SC**	**Chalazal Endosperm**	**Micropylar SC**	**Micropylar Endosperm**	**Outer Integument**	**Inner Integument**	**Peripheral Endosperm**	**Embryo**
Iron transporters										
IRT1	AT4G19690	cadmium ion transport, cellular iron ion homeostasis, cellular response to ethylene stimulus, to iron ion, to nitric oxide, iron ion transport, manganese ion transport, metal ion transport, nickel cation transport, response to bacterium, zinc II ion transport	×	×	×	×	×	×	×	×
IRT2	AT4G19680	iron ion transport, zinc II ion transport	×	×	×	×	×	×	×	×

Gene name	Locus	Biological Role	Chalazal SC	Chalazal Endosperm	Micropylar SC	Micropylar Endosperm	Outer Integument	Inner Integument	Peripheral Endosperm	Embryo
Iron transporters										
IRT3	AT1G60960	cation transport, iron ion transport, metal ion transport, response to nematode, zinc II ion transport	×	×	×	✓	✓	✓	✓	×
AHA1	AT2G18960	proton transport, regulation of intracellular pH, regulation of stomatal movement, response to abscisic acid, response to water deprivation	✓	✓	✓	✓	✓	✓	✓	✓
AHA2	AT4G30190 (No probe in microarrays)	regulation of intracellular pH	×	×	×	×	×	×	×	×
Mn and Zn transporters										
ZIP1	AT3G12750	response to zinc ion, zinc II ion transport	×	×	×	×	×	×	×	×
ZIP2	AT5G59520	zinc II ion transport	×	×	×	×	×	×	×	×
ZIP7	AT2G04032	cation transport, zinc II ion transmembrane transport	×	×	×	×	×	×	×	×
ZIP11	AT1G55910	cation transport, zinc II ion transmembrane transport	×	×	×	×	✓	✓	✓	×
Gene name	**Locus**	**Biological Role**	**Chalazal SC**	**Chalazal Endosperm**	**Micropylar SC**	**Micropylar Endosperm**	**Outer Integument**	**Inner Integument**	**Peripheral Endosperm**	**Embryo**
N and a.a. transporters										
LHT1	AT5G40780.2	amino acid import/ transport, response to karrikin	✓	✓	✓	✓	✓	✓	✓	×
LHT2	AT1G24400.1	Amino acid transport	×	✓	×	✓	×	×	✓	×
ANT1	AT3G11900	amino acid transport, response to nematode	✓	✓	✓	✓	✓	✓	✓	✓
CAT1 OR AAT1	AT4G21120	L-arginine, L-glutamate import, basic amino acid transport	×	×	×	×	×	×	×	×
CAT5	AT2G34960	L-arginine import, L-glutamate import	×	×	×	×	×	×	×	×

Gene name	Locus	Biological Role	Chalazal SC	Chalazal Endosperm	Micropylar SC	Micropylar Endosperm	Outer Integument	Inner Integument	Peripheral Endosperm	Embryo
N and a.a. transporters										
CAT6	AT5G04770	amino acid transmembrane transport, response to nematode	✓	✓	✓	✓	✓	✓	✓	×
BAC1	AT2G33820	L-lysine and basic amino acid transmembrane transport, mitochondrial transport	×	×	×	×	×	×	✓	✓
BAC2	AT1G79900.1	L-arginine import, hyperosmotic response, mitochondrial transport, proline biosynthetic process, translation	×	×	×	×	×	×	×	×
NRT1	AT1G12110	nitrate transport, response to nitrate, response to water deprivation	×	×	×	×	×	×	×	×
UmamiT11	AT2G40900 (No probe in the microarrays)	amino acid transmembrane export, seed development	✓	×	×	×	×	×	×	×
UmamiT14	AT2G39510.1	L-glutamate import across plasma membrane, amino acid transmembrane export, seed development	✓	×	×	×	×	×	×	×
UmamiT28	AT1G01070	amino acid transmembrane export, seed development	×	×	×	×	×	×	✓	×
UmamiT29	AT4G01430	amino acid transmembrane export, seed development	✓	✓	×	×	✓	✓	×	×

Discussion

As it is already known from our previous published data, *PHO1* and *PHO1;H1* are expressed in the vascular tissue of both the root and the shoot (Stefanovic et al., 2007). Our main interest was to uncover their expression in the seeds, because as we noticed from the publicly available microarray databases *PHO1* and *PHO1;H1* are both expressed in the seed, mainly in the general seed coat (SC) and the chalazal seed coat (CZSC). However, according to our GUS-staining and fluorescence data both *PHO1* and *PHO1;H1* are expressed mostly in the CZSC and not in the general SC. The CZSC is the end of the funiculus, the organ that connects the maternal vasculature with the seed coat and it is known to be the unloading region of nutrients from the mother plant in several plant species, with its most compelling feature being the terminating xylem and phloem-unloading domain (Costa et al., 2012; Dermastia et al., 2009; Gomez et al., 2009; Millar et al., 2015; Salanenka et al., 2009; Sreenivasulu et al., 2010; Thorne, 1985). This region constitutes a sort of delivery zone where amino acids and other solutes arrive in large amounts via the phloem. From the phloem, the solutes are symplasmically unloaded and can migrate within the cells of the seed coat, which are connected by plasmodesmata (Imlau et al., 1999; Stadler et al., 2005). In contrast, no or few symplasmic connections exist between the maternal seed coat and the filial tissue. It has been shown in *Citrus paradisi* (Espelie et al., 1980) as well as in the cucumber seeds (Salanenka et al., 2009) that the cells of the chalazal region are suberized and lignified (Salanenka et al., 2009). This lingo-suberization is required during the late stages of seed development (after the globular stage) to isolate the embryo from the uncontrolled import of nutrients through the vascular traces (Espelie et al., 1980). Thus, nutrients have to be exported into the apoplasmic space first, to be available for the adjacent cells that allocate the nutrients toward the sites of utilization (Stadler et al., 2005; Thorne, 1985).

There are also two studies in *Arabidopsis* seeds that characterized the molecular function of the CZSC. The first one revealed populations of mRNAs accumulated specifically in the CZSC and not in other seed regions and provided strong evidence that the CZSC is a transcriptionally distinct sub-region of the maternal seed coat and is controlled by dynamic sets of actively transcribed genes (Belmonte et al., 2013). The second one, by Khan et al. (2014) analyzed the *Arabidopsis* CZSC transcriptome and its underlying transcriptional circuitry at a higher resolution by employing vigorous bioinformatic analyses. Using a systems biology approach, the CZSC transcriptome was compared to the SC transcriptome in both space and time, revealing profound differences in the molecular machinery controlling

adjacent seed coat sub-regions at the transcriptional level. They showed that transcripts involved in the transport of sugar, water, amino acids, lipids, and hormonal regulation are expressed in the CZSC at specific stages of seed development that coincide with the timing of integral processes associated with embryonic growth, and oil and protein accumulation. In addition, funiculus vasculature was shown to terminate at the CZSC, suggesting that the CZSC is an unloading zone in *Arabidopsis* and is likely involved in the control of information into the seed from the maternal plant.

The specific expression of both *PHO1* and *PHO1;H1* in cells of the chalazal region indicates their involvement in the export of inorganic phosphate from these cells. *PHO1* and *PHO1;H1* probably function in the release of phosphate into the apoplasmic space in the chalazal region, from where it is subsequently available for import into adjacent cells of the endosperm and the embryo. *PHO1* is also expressed in the CZSC region in mature green stage seeds although the symplasmic offloading remains switched on according to Werner et al. (2011).

Furthermore, *PHO1* is also expressed in the micropylar region of the developing seeds during the globular stage. According to Stadler et al. (2005), the unique vascular bundle that translocates photoassimilates to an *Arabidopsis* seed terminates at the end of the funiculus and releases its content into the testa proximal to the micropyle, where the abscission zone (the hilum) will be formed in the mature seed (Robinson-Beers et al., 1992). Until the globular stage, the suspensor is forming a symplastic continuum with the embryo. However, it is not yet very clear which is the role of the micropylar region later in the development of the *Arabidopsis* seeds, regarding the transport of nutrients. Only Salanenka et al. (2009) showed in cucumber seeds that the cells of this region are also ligno-suberized, like the cells of the chalazal region, but this ligno-suberization already occurs before the globular stage shortly after fertilization of the egg within the ovule. The only information that we have about the micropylar region is that it acts as a barrier for the radicle emergence during germination and is studied in many species such as tomato (*Solanum lycopersicum*) (Groot and Karssen, 1987; Nonogaki and Morohashi, 1996), lettuce (*Lactuca sativa*) (Ikuma and Thimann., 1963), pepper (*Capsicum annuum*) (Watkins et al., 1985), and tobacco (*Nicotiana tabacum*) (1996; Leubner-Metzger et al., 1995), but not in *Arabidopsis*. Finally, the only study where it was shown that sucrose can move via the micropylar endosperm was performed by (Morley-Smith et al., 2008) in oilseed rape. In their experiments in which [^{14}C]-sucrose was supplied to intact oilseed rape (*Brassica napus*) siliques they showed that

import of sugars into developing embryos occurs via the micropylar rather than the chalazal endosperm.

During our study of the expression pattern of *PHO1*, we also noticed that it is expressed in the developing ovules. This specific expression of *PHO1* in the Megaspore Mother Cell (MMC) and the L1 layer of the nucelus is quite surprising. According to Werner et al. (2011) at early stages of ovule development, there is only symplastic phloem unloading and post-phloem transport of nutrients. The phloem unloading mode in ovules of *A. thaliana* is a highly regulated process and is most likely tightly connected with changes in the architecture of plasmodesmata (Werner et al., 2011). It was also never mentioned before that a nutrient tranporter, except from *PIN1* gene that is an auxin transporter (Pagnussat et al., 2009), is expressed in the developing ovule integuments. As we know *PHO1* is a phosphate exporter and its' expression in the MMC is difficult to be explained. We would expect Pi import in this cell rather than Pi export. A hypothesis that we could make is that it probably plays similar role as it does in the guard cells of the stomata. Zimmerli et al. (2012) showed that *PHO1* expression in the guard cells of *Arabidopsis thaliana* is required for full stomatal responses to ABA. They proposed that Pi efflux mediated by *PHO1* may, together with Cl, NO^-_3, and malate2, participate in the depolarization of the plasma membrane and the down-regulation of osmotic pressure during stomatal closure mediated by ABA. So, *PHO1* expression in the MMC could also contribute to the activation of transient membrane depolarization cascades related to signaling. However, the expression of *PHO1* in the L1 layer of the ovule primordia and the Inner Integuments (I.I.) surrounding the embryo sac during the later stages of the ovule development (stages 3-V until 4-II) could be more easily explained (for a summary of stages of ovule development in *A. thaliana* see table 10, annex 2). Werner et al. (2011) showed strong evidence that there is a reduced cell-to-cell connectivity in the post-phloem pathway between the megaspore mother cell and the surrounding tissue (outer and inner integuments) in developing ovules of stage 11 flowers (for summary of stages of flower development in *Arabidopsis thaliana* see table 11, annex 2). Thus, we would expect that *PHO1* is exporting phosphate from the L1 layer and the ovule integuments into the apoplast, from where it is then imported into the MMC or the embryo sac, respectively. However, its absence in the *pho1* mutants does not have any effect in the ovule development according to our study.

Subsequently, the interesting expression pattern of PHO1 and PHO1;H1 motivated us to search more extensively the role of these genes in the *Arabidopsis* seeds. As the embryo development (Fig. 28), the Pi content (Fig. 34), the total P content (Fig. 35) and the seed size

(Fig. 36) of the mature dry seeds of the grafted DM and the WT plants did not differ, we tried to identify the exact tissues that P could be accumulated in the DM mutants as PHO1 and PHO1;H1 were absent in these seeds. Having in mind that both genes have redundant roles related to Pi export, we speculated that P could be accumulated at the seed coat of the *pho1* and DM mutants. In the P^{33} uptake experiment, we showed that P^{33} is equally distributed between the seed coat and the embryo of the WT, but is increased at the seed coat of the *pho1* single and double mutants (Fig. 38 and 39) which indicates that *PHO1* expression in the CZSC and micropylar region is important for the export of phosphate from the mother plant. On the contrary, *PHO1;H1* does not seem to play any significant role in the phosphate export as P^{33} is equally distributed between the seed coat and the embryo of both *pho1;h1.1* and *pho1;h1.4* mutants (Fig. 38 and 39). However, the P^{33} uptake experiment was performed in cut stems of grafted *Arabidopsis* plants that were incubated in radioactive solution overnight. So, from this experiment we can only observe the amount of P that is transported from the mother plant into the seeds only during some hours. The total P experiment which was performed on whole grafted plants which were grown in a 3 weeks period allows us to observe what happens at the plant P status during a longer period of the plant development. From that experiment we also confirmed that *PHO1* expression in the seed coat is necessary for the delivery of Pi into the seed apoplasm and that *PHO1;H1* does not play a significant role in the export of P during the plant development. However, PHO1;H1 could play a role in the P export into the seed apoplasm under P starvation conditions, as it does in the root (Stefanovic et al., 2007; Wang et al., 2004). Unfortunately, when we tried to check this hypothesis, using grafted on *pho1* roots (P starvation conditions) WT, *pho1*, DM and *pho1;h1* plants, we obtained too high variation in our measurements, due to the fact that the grafted plants were too stressed, were flowering at very different time points or not at all and could only produce one or two stems with very few siliques.

Regarding the results from the complementation lines (DM background) pARR22;gPHO1;GFP (Fig. 38 and 39) and pARR22;gPHO1;H1:stop (Fig. 46), we can conclude that *PHO1* expression only at the CZSC is enough to complement the DM phenotype were P^{33} is accumulated at the SC, whereas *PHO1;H1* not (Fig. 46). This could be due to many different reasons. Either the role of *PHO1;H1* could be to participate in a signaling cascade which regulates P export or other unknown gene pathways, or *PHO1;H1* needs specific post-transcriptional modifications in order to be active. Furthermore, in our laboratory we have preliminary evidence, using the bimolecular fluorescence

complementation (BiFC) technique, that PHO1;H1 can create heterodimers with PHO1. Thus, maybe in order for PHO1;H1 to be functional PHO1 should be present.

Finally, we also confirmed that *PHO1* down-regulation only at the CZSC is enough for the P^{33} to increase again at the SC at similar levels as in the DM (Fig. 44). Consequently, we clearly showed that *PHO1* plays the major role for the phosphate export in the seeds as it does in the roots and probably *PHO1;H1* has a secondary role, or is activated under phosphate starvation or under different stress conditions. Another interesting finding is that the expression of *PHO1* at the chalazal region of the seed coat is necessary for the right amount of Pi to be exported into the apoplastic space of the seed. This is because when *PHO1* is absent or down-regulated, the P is accumulated in the SC like in the *pho1* and DM plants analyzed in the P^{33} and total P experiments (Fig. 38, 39 and 47) as well as the down-regulation experiment of *PHO1* (Fig. 44). Finally, we also proved that PHO1 expression only at the CZSC is sufficient to restore the DM phenotype were P is accumulated in the seed coat (Fig. 38, 39 and 47, pARR22:gPHO1:GFP complementation lines).

From the literature (Chen et al., 2015; Muller et al., 2015; Olsen et al., 2016; Stadler et al., 2005) it is quite clear that the CZSC region is very important for nutrient offloading. However, it is not very clear yet if it is the only region that plays an important role for nutrient offloading and what is the functional role of the micropylar region. As discussed before (see p. 91), the micropylar region is composed by lingo-suberized cells and is not symplastically connected with the embryo. Thus, our finding that the expression of PHO1 is not only increased, but also shifted to the micropylar region of the mature stage seeds during P starvation conditions (see Fig. 26) is very interesting and raises new questions regarding the function of this region under P starvation conditions, or other biotic or abiotic conditions.

Finally, in order to answer if the expression of *PHO1* in the seed coat, which is a maternally derived tissue, plays a role in the vigor of the next generation progeny, we performed a vigor test using reciprocal crosses: WT x DM and DM x WT. The progeny of both of these crosses is only heterozygous embryos, whereas the seed coat is WT (WT x DM cross) or DM (DM x WT cross), respectively. So, after growing these seeds under + or – P conditions we could not find any obvious difference in the growth of these embryos. This leads us to conclude that the genotype of the seed coat does not play any important role for the growth of the seedling, probably because all the layers of the seed coat, except the aleurone, are crushed when the seeds reach maturity and all the nutrients are released so as the vigor and the survival of the next generation to be ensured. Thus, even if the mature seeds of the DM have most of the P accumulated in the seed coat, during germination all the seed

coat layers will be crushed so as all the P to be released in the surrounding environment and the embryo to be provided with sufficient P for its vigor and survival.

Conclusions – Future prospects

Together, our data demonstrate a critical role of *PHO1* in the P release from the seed coat and more specifically the chalazal seed coat into the seed apoplast in order to supply the developing embryo. However, the fact that the development of the embryo in a grafted DM/WT plant is normal (Fig. 28) is quite surprising, as we showed that P is accumulated in the seed coat. This could be explained by two different hypotheses: 1) The Pi can reach the embryo via the bulk flow of nutrients that are transported through the phloem and the xylem. This hypothesis is supported from the fact that in several studies (Waters and Grusak, 2008; Waters and Sankaran, 2011a; Waters et al., 2009), seed micronutrients did not derive totally from recycled sources, suggesting that plants continue to take up and translocate minerals, from the soil or the roots, into seeds over the seed filling period (Waters and Sankaran, 2011a). 2) There are other known or unknown Pi transporters that export Pi into the embryo, so as to ensure the survival and the vigor of the progeny (see table 4). Thus, it would be interesting to find out in the future, using RNAseq which other transporters are expressed in the embryo and are used for the uptake of Pi or are expressed in the seed coat and are also participating in the Pi export into the seed apoplasm.

The importance of the CZSC as an offloading region of Pi was also shown. According to the literature, it seems that most of the seed coat layers of several plant species are crushed either during the maturation of the seeds or during their germination (Aniszewski, 2009; Beeckman et al., 2000; Bouman, 1975; Corner, 1976; Haughn and Chaudhury, 2005; Miller et al., 1999; van Caseele et al., 1982). However, it is not very clear from the literature if this happens in all species. If this is not the case for some crop species or other economically important species, the role of PHO1 in the Pi export into the seed apoplast would be of high importance. Therefore, it would be very interesting to study the PHO1 function in these species and possibly construct plants with improved P homeostasis mechanisms that can utilize better the P and can survive in soils with low P availability.

Furthermore, the increase of the expression of *PHO1* in the micropylar region of the mature seeds under P starvation conditions is a new and interesting finding that raises new questions regarding the role of the micropylar region under Pi starvation or other stress

conditions (biotic or abiotic) and would be worthy of further investigation. The use of a micropylar specific promoter to express or down-regulate *PHO1* and *PHO1;H1* specifically in that region would be very interesting in order to unravel the function of these genes at the micropylar region. Furthermore, testing the expression pattern of PHO1 under P starvation conditions could also add more information to our knowledge regarding the role of this region under such conditions. Finally, the study of other still unknown transporters that are specifically expressed in the micropylar region under different biotic or abiotic stresses could contribute to our knowledge regarding the role of this region.

Our data show that PHO1 is one of the major Pi transporters in the seeds but it is also clear that there could be complementary mechanisms for Pi transport into the embryo. As we can notice from table 4 some other Pi transporters are also expressed in the seeds of *A. thaliana*, according to the open access microarray data. For instance, PHO1;H3 is expressed in the embryo and PHO1;H5 in the CZSC and the micropylar endosperm. It is also quite impressive that not many members of the PHT family are expressed, except for PHT2;1, PHT3;1 and PHT4;4. Among these three genes *PHT2;1* seems to be the most promising one. Although it is a chloroplastic transporter, it has been shown that it influences allocation of phosphate within the plant under Pi starvation in *Arabidopsis* (Versaw and Harrison, 2002) and in wheat (Guo et al., 2013) as well as it plays a role in auto-and heterotrophic tissues in potato and *Arabidopsis* (Rausch et al., 2004). Furthermore, according to the microarray data it is expressed in the CZSC, the Outer Integuments (O.I.), the Inner Integuments (I.I.) and the Peripheral Endosperm (PEN). It was also shown to be expressed highly in the shoots of *A. thaliana* and because of its fairly high Km for Pi (0.4 mM) and high mRNA content in the shoot, especially in leaves, was suggested to play a role in Pi loading (Daram et al., 1999). Thus, it would be interesting to investigate if it has any role related to the seed P homeostasis. On the contrary, PHT3;1 is a mitochondrial gene and PHT4;4 has been shown to be activated against oomycetes. Thus, studying the expression pattern and the role of these Pi transporters would not be very promising to unravel new mechanisms for the Pi transfer into the seeds. Interestingly, there were some new vacuolar transporters identified recently (Liu et al., 2016a; Liu et al., 2016b) which regulate cytoplasmic Pi homeostasis and are required for fitness and plant growth. The study of the function of these transporters could also shed light on the seed P homeostasis as the vacuole is an important subcellular compartment for phosphate storage in plants. Finally, there are still numerous genes in *Arabidopsis* that have not yet been attributed with a function and could be potential P exporters or importers in the seeds and could be important for making more sustainable and bio-fortified crops.

CHAPTER 4

What is the role of *PHO1* and *PHO1;H1* genes in the leaves of *Arabidopis thaliana*?

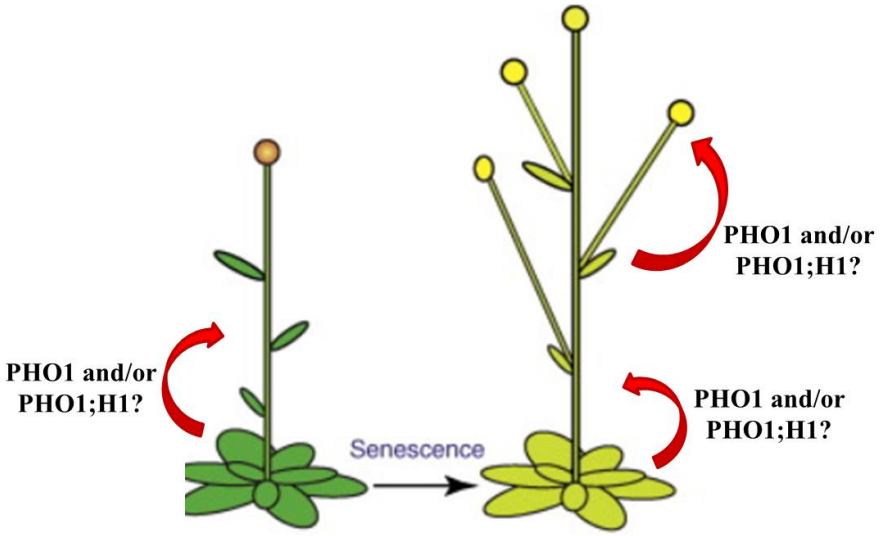

Introduction

Remobilization of nutrients from the roots to the shoots

The knowledge of resource allocation within plants, and between plants and associated organisms, is essential for plant, crop and ecosystem management. However, it is still an unresolved issue (Thornley and Parsons, 2014). While plants are senescing, remobilization (i.e. net export of stored or recycled nutrients) of some nutrients occurs from vegetative tissues, such as leaves and stems. At the end of growing seasons, mass senescence typically occurs in leaves and other tissues. Nutrients are being re-mobilized from the senescing leaves to other plant parts, e.g., newly developed vegetative tissue, developing seeds, or storage organs (Buchanan-Wollaston and Ainsworth, 1997), and so the senescence and seed import are synchronized to provide source-sink relationships. This strategy can be of particular importance to plants growing under poor nutrient conditions, as nutrient recycling reduces the need for nutrient uptake from the environment (Aerts, 1990).

Although it is well established that N remobilization in wheat and barley is a major source of seed protein components (Cakmak, 2008; Pfeiffer and McClafferty, 2007; White and Broadley, 2009), data for other mineral elements is more scarce. Older studies demonstrated remobilization of Cu, Fe, and Zn in legumes (Hocking and Pate, 1977; Pate and Hocking, 1978), and wheat (Hill, 1980; Hocking, 1994; Miller et al., 1994), and some newer studies have found similar results (Garnett and Graham, 2005; Maillard et al., 2015; Waters et al., 2009; Yoneyama et al., 2015). When Fe and Zn micronutrients were withheld from the hydroponic solution post-anthesis, their remobilization increased indicating that recycling mechanisms might be upregulated under nutrient inadequacy (Waters et al., 2009). Mineral element concentrations decrease during the development in *Arabidopsis thaliana* senescing rosette leaves (Himelblau and Amasino, 2001; Waters and Grusak, 2008). This clearly suggests nutrient remobilization from these leaves, which may be used to supply seeds. Quantitative analysis of *Arabidopsis* plants in different developmental stages also indicated that up to 30% of the total Cu, Fe, and Zn in *Arabidopsis* seeds derived from remobilized nutrients (Waters and Grusak, 2008). Future crop breeding or development of strategies to produce different varieties may include modifications that result in increased efficiency of remobilization to generate bio-fortified seeds. However, in all of the studies mentioned above, seed micronutrients did not derive totally from recycled sources, suggesting that plants

continue to take up and translocate minerals into seeds over the seed filling period (Waters and Sankaran, 2011a).

Regarding the remobilization of Pi, functional characterization of the single mutants *pht1;1* and *pht1;4* confirmed their roles in Pi acquisition (Shin et al., 2004). Poirier et al. (1991) showed that after Pi is transported into root epidermal cells, it is loaded into the xylem for distribution to shoot tissues. Several studies have characterized mutants that are unable to mobilize Pi from source (older leaves) to sink (roots and younger leaves) organs (Aung et al., 2006; Chiou et al., 2006; Delhaize and Randall, 1995; Versaw and Harrison, 2002). Under long term Pi deprivation, Pi is redistributed from older leaves towards the sink organs (young leaves, growing roots, and developing seeds) by a process that requires its transfer through phloem vessels (Bucher et al., 2001; Raghothama, 2000). As mentioned before an important process in plant growth and development is the efficient nutrient remobilization from older, senescing leaves in order to scavenge resources that may be scarce in nature or they require a lot of energy in order to be absorbed (Leopold, 1961). In this context, it has been demonstrated that up to 78% of stored Pi is remobilized from older leaves in *Arabidopsis* (Himelblau and Amasino, 2001). Therefore, the translocation of Pi into sink tissues/cells is important for sustaining growth under low-Pi conditions.

Phosphate Remobilization during Leaf Senescence

During leaf development, leaves emerge and expand while converting solar energy into chemical energy via the process of photosynthesis. However, as the plant matures the aging leaves face respiratory problems as well as diminishing light conditions due to self-shading, which results in a reduced production of assimilates. Although the senescing leaves are no longer a photosynthetic asset for the plant, they are useful as pools of nutrients (Veneklaas et al., 2012). When the aging leaves enter senescence, nutrient redistribution to the sink tissues occurs before they finally die. The procedure could be vital to the overall fitness of the plant, particularly in environments where it is energetically costly to acquire nutrients from the soil or there is a scarcity of nutrients. Therefore, the efficiency of nutrient remobilization from senescing leaves to developing tissues is important so that precious nutrients, such as Pi, are not lost to the environment. Pi recovery from older leaves has the obvious adaptive value that reduces the need to take up Pi from the soil which may be poorly available and energetically costly (Veneklaas et al., 2012). The initial target of senescence-mediated catabolism is the vacuole; this organelle serves as the main source of the Pi and

other nutrients (Veneklaas et al., 2012). Small senescence-associated vacuoles with intense proteolytic activity accumulate in leaves of several plant species, and although senescence-associated vacuoles appear to play a key role in nitrogen (N) remobilization (Veneklaas et al., 2012), future research needs to be done regarding their role in Pi remobilization. Indeed, Pi remobilization from senescing leaves is much less studied comparing to N remobilization, although a recent review of Smith et al. (2015) has shed light on this understudied, yet critical, topic.

Arabidopsis thaliana has become a valuable model plant species for studies of nutrient mobilization during senescence as its entire genome sequence is available and it is an easy tool for several genomic applications. During *Arabidopsis* leaf senescence, the total amount of N decreases by 85% as cellular proteins are catabolized and the resulting amino acids are exported to other tissues (Himelblau and Amasino, 2001). Likewise, total P levels drop by about 75%, while nutrients such as copper, iron, chromium and potassium decrease by greater than 40% during senescence (Himelblau and Amasino, 2001; Robinson et al., 2012). However, not all plants have the same abilities of nutrient recycling (see Table 5). Extremophile species which can grow in severely Pi-impoverished soils, such as *Banksia serrata* and *Hakea prostrata* (harsh hakea) typically recycle 85%–95% of their total P from senescing leaves, whereas species such as soybean (*Glycine max*) and *Acacia truncata* remobilize less than 50% (Crafts-Brandner, 1992; De Campos et al., 2013; Lambers et al., 2015; Shane et al., 2004). Stigter and Plaxton (2015), hypothesize that species that highly efficient species capable of remobilizing Pi from their senescing leaves have evolved many adaptive advantages that allow them to survive in Pi poor soils that are typically found. Such adaptations could include more effective hydrolytic enzymes, such as nucleases and phosphatases, which play a key role in releasing Pi from macromolecules and/or low molecular weight Pi-monoesters and anhydrides during senescence. Interestingly, while there is plenty of information about P resorption efficiency for extremophile species, which are found in soils such as the highly Pi-deficient soils of Western Australia and the severe sub-arctic climate, there is very little data regarding P resorption efficiencies of common crop species cultivated under usual agricultural conditions. It would be of great interest to perform a comprehensive study that would compare P resorption efficiencies of senescing leaves for various crop species, particularly due to the possibility that traits enabling phosphorus-use efficiency (PUE) may have been out-selected in modern crop varieties as a consequence of selecting for maximal yields with maximal fertilizer inputs. Another interesting aspect of nutrient recycling is the fact that has emerged from several studies which conclude that the

greater the green-leaf nutrient concentration, the less efficient the nutrient resorption from senescing leaves will be (Kobe et al., 2005; Vergutz et al., 2012), something which is also a negative impact of increased fertilizer use; P resorption efficiency is reduced two-fold with only moderate increases in green-leaf P concentration (Vergutz et al., 2012). Therefore, the use of fertilizers in agricultural practices may boost efficient crop growth, but could consequently inhibit efficient Pi recycling, the overall PUE and possibly selection of less PUE efficient species.

Species (Common Name)	Phosphorus Resorption Efficiency (%)
Acacia truncata (angle-leafed wattle)	41
Acacia xanthine (white-stemmed wattle)	36
Arabidopsis thaliana (thale cress)	75
Artabotrys hongkongensis (talon wild vine)	41
Banksia attenuate (slender banksia)	69
Banksia chamaephyton (fishbone banksia)	82
Banksia serrata (saw banksia)	95
Calophyllum polyanthum (sirpoon tree)	53
Cladium jamaicense (Jamaica swamp grass)	78
Empertrum hermaphroditum (mountain crowberry)	70
Eriophorum vaginatum (tussock cottongrass)	90
Glyceria maxima (reed mannagrass)	22
Glycine max (soybean)	50
Hakea prostrata (harsh hakea)	85
Michelia floribunda	80
Phragmites australis (common reed)	50
Vaccinium uliginosum (bog blueberry)	40

Table 5: A comparison of phosphorus (P) resorption efficiencies across a variety of plant species, where P resorption efficiency is defined as the amount of total P resorbed during senescence (expressed as a percentage of the total amount of P present in a fully-expanded, leaf relative to a fully senesced leaf) (Aerts, 1996).

Transcriptome changes promote phosphorus remobilization during leaf senescence

Many studies have investigated by analyzing genome-wide transcriptomes of senescing leaves the gene expression changes that occur at this final phase of development. A wealth of knowledge through large-scale comparisons of genes and gene families that are up-regulated or down-regulated during senescence has been the outcome of these studies. Thus, many key genes have been identified for further study to enrich our understanding of the plant senescence program. Genome-wide comparisons among various species including *Arabidopsis* (Balazadeh et al., 2008; Breeze et al., 2011; Buchanan-Wollaston et al., 2003;

Gepstein et al., 2003; Guo et al., 2004), wheat (*Triticum aestivum*) (Gregersen and Holm, 2007), rice (*Oryza sativa*) (Liu et al., 2008), maize (*Zea mays*) (Zhang et al., 2014), and cotton (*Gossypium hirsutum*) (Lin et al., 2015) exhibit overlapping senescence-related loci, which could be indicative of conserved leaf senescence programs. Many studies have also contributed to the indentification of regulators of senescence, such as transcription factors and hormones. However, the downstream targets for many of these regulatory elements have yet to be elucidated and their relationship to nutrient transporters has yet to be unraveled.

Differential gene expression over the course of senescence

The transition from a living photosynthetic organ to a senescing tissue requires numerous molecular and genetic changes. Many hormones and transcription factors are involved regulating downstream protein targets so as to remobilize nutrients such as Pi to sink tissues. The regulation of the senescence program is so complex that the expression of some transcription factors changes rapidly (Balazadeh et al., 2008; Breeze et al., 2011). For example, when most of the leaf is still green, many transcription factors from the *NAC* family are expressed (Breeze et al., 2011). In *Arabidopsis*, the *AtNAP (NAC2)* transcription factor is involved in triggering the start of senescence (Guo et al., 2004). The *nap* null mutant is delayed in leaf senescence and demonstrated a strong reduction in the expression of the senescence-specific marker gene *SAG12* (Guo and Gan, 2006). Many NAC transcription factors are also involved in the abscisic acid (ABA)-inducible gene expression, which probably triggers the increase of the expression of many ABA-related genes which have been detected during the onset of senescence (Balazadeh et al., 2008; Breeze et al., 2011). Furthermore, genes related to jasmonic acid (JA) signaling and biosynthesis, as well as their potential targets, are also up-regulated during senescence (Breeze et al., 2011). For instance, *ORE1* expression increases during early senescence (Balazadeh et al., 2008) promoting the expression of *AtBFN1*, a nuclease that breaks down single-stranded nucleic acids (Matallana-Ramirez et al., 2013) and thus, contributing to the remobilization of Pi from macromolecules. In turn, *AtORE1* promotes the expression of *AtSWEET15/SAG29*, which is involved in sucrose transport, and of *AtSINA1*, which is involved in protein ubiquitination (Matallana-Ramirez et al., 2013), associating *AtORE1* not only with the regulation of Pi remobilization but also with other nutrients.

With the advancement of leaf senescence, the transcriptome profile changes. Many of the same transcription factor families, such as the *NAC* family and the *WRKY* transcription

factor family (Breeze et al., 2011) are being up or down-regulated. Senescence induces the expression of *WRKY53* (Hinderhofer and Zentgraf, 2001) and its mutant delays leaf senescence (Miao et al., 2004). *WRKY53* is also activated by MEKK1 an upstream mitogen-activated protein kinase kinase kinase, which binds to the *WRKY53* promoter and phosphorylates the WRKY53 protein regulating the DNA-binding activity of this transcription factor (Miao et al., 2007). There have also been found more than 60 putative target genes, including other members of the *WRKY* gene family (Miao et al., 2004), that can be regulated by WRKY53, something that suggests WRKY53 as a key regulator of a transcription factor signaling cascade.

Interestingly, *SQD1* a gene involved in sulfolipid biosynthesis could be another potential target of WRKY53 (Miao et al., 2004). Understanding the role of *SQD1*, would enhance our understanding of Pi recycling regulation, as it is known that Pi is being reused through the replacement of phospholipids with sulpholipids at the cell membranes (Misson et al., 2005). *WRKY6* is involved in the signaling cascades that modulate the senescence program and is strongly induced in senescing leaves (Robatzek and Somssich, 2002). It can both activate and repress other WRKY genes and it activates directly the SIRK/FRK1 promoter. Moreover, *WRKY6* is also involved in the regulation of *PHO1* expression during Pi starvation (Chen et al., 2009). Consequently, PHO1 could participate in the Pi remobilization during leaf senescence, either as a transporter or as a regulator of Pi transporters belonging to the *PHT1* gene family in *Arabidopsis* (Chen et al., 2009). At the middle of the senescence process, an increase in the expression of genes involved in membrane lipid degradation, cell wall degradation, and metal ion binding has been also observed (Breeze et al., 2011; Buchanan-Wollaston et al., 2003), indicating the continuous catabolism of macromolecules to free nutrients such as Pi for transport to other tissues.

A complete understanding of Pi remobilization during senescence is important and will facilitate the development of effective biotechnological strategies to improve crop PUE, and reduce society's dependency on Pi-containing fertilizers, leading also to the reduction of the pollution of water bodies.

Aim

PHO1 and *PHO1;H1* are Pi exporters that are expressed in the vascular tissue of the shoots (stems and leaves, see Fig. 6). Thus, our working hypothesis is that they could contribute to the remobilization of phosphate from the old to the young leaves or from the leaves to the seeds. Therefore, the aim of this chapter is to identify the role of these two genes in the transfer of Pi to the phloem so as it can be recycled from the source to the sink leaves.

Material and methods

Plant material

As mentioned before, PHO1 and PHO1;H1 have redundant functions in the root of *A. thaliana* thus, in order to find their role in the leaves we should study their DM. However, the DM plants grow poorly and are Pi starved so, we needed a plant that expresses PHO1 and PHO1;H1 only in the roots and not at the aerial part. To achieve that we thought to use two different approaches: 1) Micro-grafting and 2) Transgenic plants were we tried to express *PHO1* or *PHO1;H1* in front of a Root Pericycle Specific Promoter (RPSP).

The following plant lines: *pho1.1*, *pho1.2* and *pho1.3* alleles have previously been described by Poirier et al. (1991), Delhaize and Randall (1995) and Hamburger et al. (2002). *pho1;h1-1* allele was previously described by Stefanovic et al. (2007) and *pho1;h1-4* allele was obtained by the GABI-Kat T-DNA mutant database (Kleinboelting et al., 2012). The double mutants used in this study (see table 6) were constructed as described in chapters 2 and 3 (p. 45 and 63).

Table 6: DM alleles used in this chapter.

DM name	DM genotype
DM	*pho1.1/ pho1.1 h1.1/h1.1*
DM3.1	*pho1.3/ pho1.3 h1.1/h1.1*

Cloning

A. Expression of whole *PHO1* and *PHO1;H1* in front of a Root Pericycle Specific Promoter

In order to express the whole proteins of *PHO1* and *PHO1;H1* in front of a RPSP we used the GATEWAY system (Curtis and Grossniklaus, 2003). The genomic sequences of *PHO1* (5483bp) and of *PHO1;H1* (3866bp) were cloned into pENTR2B vectors, using the

InFusion technique of Clonetech. pENTR2B-PHO1 construct was made by Ji-Yul Jung. For *PHO1;H1* in pENTR2B the following primers were used: H1-F: aggaaaatgatggtgcgaattcggtaccggatccag and H1-R: gatgaagaagactactcgcggccgcactcgagatat. Using LR reaction system (Invitrogen) the genomic sequence of these genes was inserted into the binary plant expression vector pMDC163 (expressing GUS), where the 2xCaMV35S promoter was replaced by a RPSP (identified through GENEVESTIGATOR, see Fig. 50), using restriction enzymes and transformed into *Agrobacterium tumefaciens*, using the freeze-thaw method. As a standard procedure, genomic DNA was chosen both for *PHO1* and *PHO1;H1* as *PHO1* cDNA is known to be unstable in bacteria (see Fig. 59 and 60, Annex 3 for representative graphic maps of the constructs). All the constructs were stably transformed into WT and DM plants with the flower dip method described in Logemann et al. (2006). The names of the RPSPs and the primers used for the cloning can be found in table 7 (Baerson et al., 2005; Bailey et al., 2003; Boutrot et al., 2008; Drechsler et al., 2015; Heim et al., 2003; Hsieh et al., 2008; Hsieh and Goodman, 2005; Liu et al., 2006; Toledo-Ortiz et al., 2003).

Table 7: Root Pericyle Specific Promoters used in this study. In this table their name, function and the primers used for their cloning are presented.

Gene Ontology name	Function	RPSP name	Forward Primer	Reverse primer	Publiced from:
at3g02850 (SKOR1)	Root to shoot K loading	RPSP1	ccggtcacggttcgatacacctccgaatcacgataccagataatc	cctcgagggggggcctagacatgggaccattttgtatgttacaag	Liu et al. 2006, Drechsler et al. 2015
at2g37870	Bifunctional inhibitor/lipid-transfer protein	RPSP2	ccggtcacggttcgagtgtgtctttatttgatgaaaccatatgttg	cctcgagggggggccACCTTGTTACATTGgacgtttgttttgtat	Boutrot et al. 2008, Baerson et al. 2005
at1g31050	Basic helix-loop-helix (bHLH) DNA-binding superfamily protein, regulation of transcription	RPSP3	ccggtcacggttcgatcgtgtcaccaaacaagtaagcatcaaatt	cctcgagggggggccaaaggatagaagctcgaaaaagaaaaacga	Bailey et al. 2003, Toledo-Ortiz et al. 2003, Heim et al. 2003
at2g26930	Kinase	RPSP5	gctgaagcttATAACTTTTCAATAATGGATCTCGGCT	cgatgggcccCAAATAAAAAAAAACAATCTTAGTTCT	Hsieh et al. 2005;2008

Figure 50: Identification of Root Pericycle Specific Promoter Genes using GENEVESTIGATOR. Only the 4 first genes that are expressed at the root pericycle and steel were selected (https://genevestigator.com/gv/).

B. Expression of the *PHO1* and *PHO1;H1* synthetic cDNA in front of a Root Pericycle Specific Promoter

The cDNA of *PHO1* and *PHO1;H1* was synthesized from GeneScript, in a pUC18 vector with attR sites around the insert and including intron 6 for *PHO1* and intron 4 for *PHO1;H1* (see Fig. 51). Using LR reaction system (Invitrogen) the synthetic cDNA of these genes was inserted into the binary plant expression vector pMDC163 (expressing GUS), where the 2xCaMV35S promoter was replaced by a one of the four RPSPs (identified through GENEVESTIGATOR, see Fig. 50), using restriction enzymes and transformed into *Agrobacterium tumefaciens*, using the freeze-thaw method. All the constructs were stably transformed into WT and DM plants with the flower dip method described in Logemann et al. (2006).

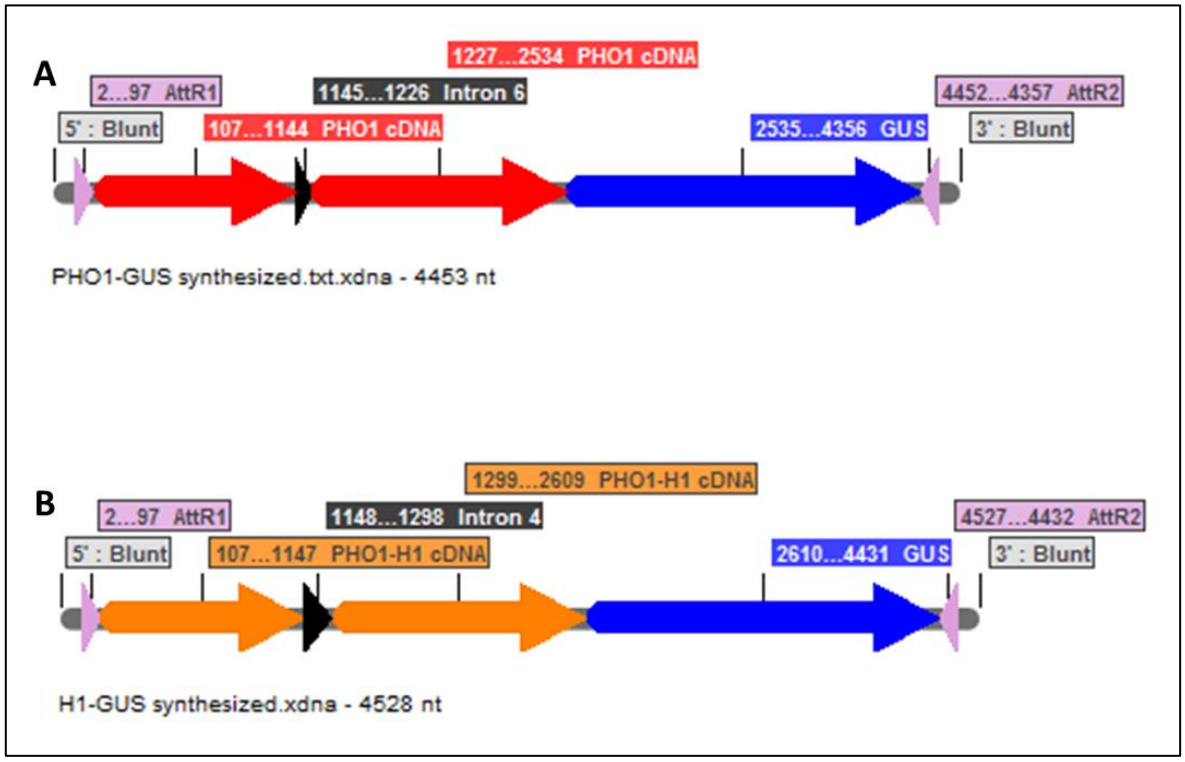

Figure 51: Schematic representation of the synthesized PHO1 and PHO1;H1 cDNAs containing an intron (intron 6 for PHO1 and intron 4 for PHO1;H1) and AttR1 and AttR2 sites.

Inorganic Phosphate measurements

In order to find the role of *PHO1* and *PHO1;H1* in the shoots, we grew plants in three different conditions:

1) in soil, under short day conditions so as to avoid early flowering (Fig. 53A),

2) in red or white pellets (+/- Pi), under short day conditions so as to avoid early flowering (Fig. 53 B1-B3) and

3) in soil or in red or white pellets (+/- Pi) and under induced senescence (IDL) (Weaver and Amasino, 2001), by covering 3 leaves of the same number/position [according to (Mousavi et al., 2013), Fig. 53C].

Then we compared the Pi content of WT and DM rosettes from plants grown in soil or under +/- P conditions and of individual leaves from plants grown under IDL. For the determination of the Pi content, whole rosettes or individual leaves were cut and weighed and for each mg, 50ul of ddH2O were added to the sample in order to release its Pi content using the freeze-thaw method. The Pi concentration in the solution was then quantified by the molybdate assay (Ames, 1966). The statistical significance of the results was evaluated using student t-test.

Figure 53: Growth conditions for Pi measurements. Grafted WT and DM plants were grown either in soil (A), or in red or grey pellets (B1-B3) were a silicon tube or an Eppendorf tube containing very little amount of soil, in order to maintain the right humidity for the root, were used to place the seedling in the middle of the pot and to control the +/- P conditions. In order to induce the senescence we grew up the plants in soil and we covered the 3 leaves of the same number/position.

P^{33} transfer from the shoot to the root

In order to identify the potential role of *PHO1* and/or *PHO1;H1* in the leaves we quantified the transfer of P^{33} from the shoots to the roots of WT and DM seedlings. We used grafted WT and DM seedlings, constructed as in p. 63 and grown in ½ MS plates with 0.5% sucrose under short day conditions for 15 days. After the establishment of the graft (about 5 days after the initial micro – grafting) we cut the root tip in order to induce lateral root initiation. When the plants had grown enough to produce several leaves (about 1 week after the cut of the root tip), we split the roots of each seedling and placed half of the root on a cover slip with ½ MS liquid medium without phosphate and the other on a cover slip with 10uCi/ml P^{33} in K_2HPO_4 buffer (see Fig. 52). We incubated them for 1 hour, removed the root that was in the P^{33} solution and measured the other part of the root (attached to the shoot) and the shoot, separately in a Scintillation counter. The vials were filled with 5ml scintillation liquid (Ultima Gold, Perkin Elmer) and measured in the Perkin Elmer tri-carb 2800TF Scintillation counter. The statistical significance of the results was evaluated using student t-test.

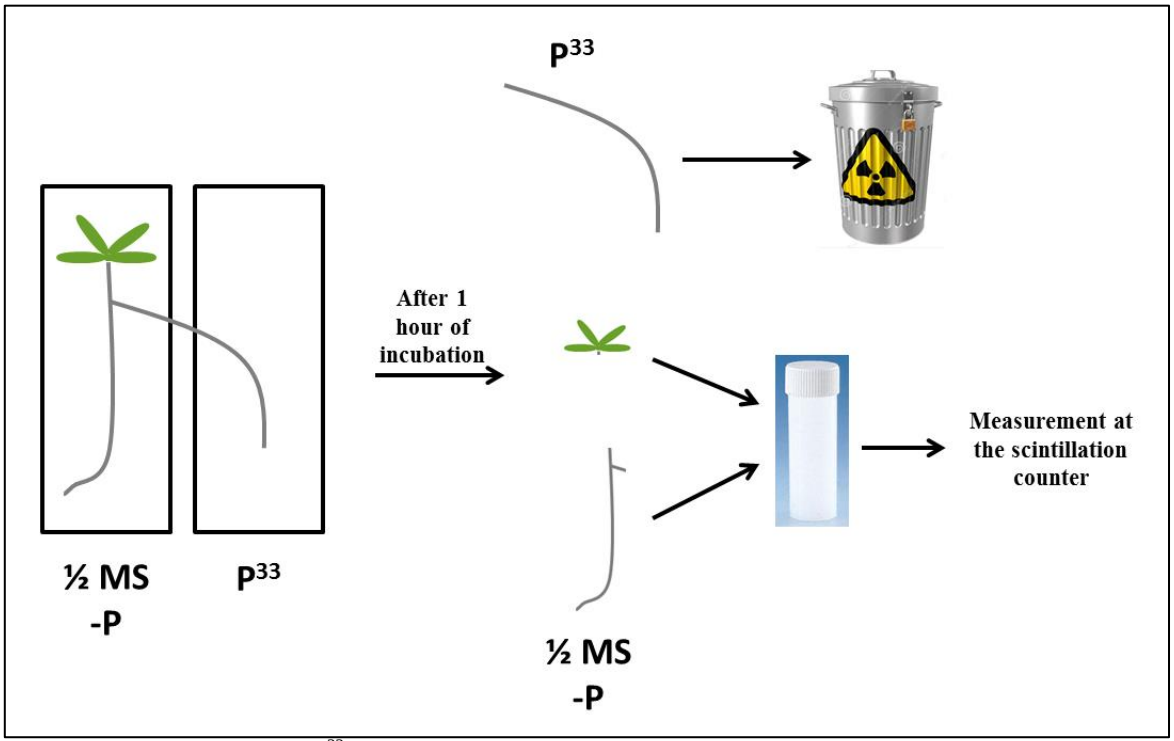

Figure 52: Representation of P^{33} transfer experiment. One half of the seedling (root and shoot) was placed on the left cover slip with ½ MS solution without phosphate and the other half (only root) was placed on the other cover slip with P^{33} solution in K_2HPO_4 buffer. After one hour of incubation the root that was in the P^{33} solution was removed and the other part of the root and the shoot was separated and measured in a scintillation counter.

RT-PCR

In order to check if the RPSPs that we identified using the GENEVESTIGATOR software were only expressed in the roots, we isolated total RNA from homogenized *Arabidopsis* leaves, roots, inflorescence and petioles of WT *Arabidopsis* plants grown red pellets (so to isolate more easily the roots). We performed a reverse transcription PCR (RT-PCR) using oligo-dT primers in order to produce cDNA from these tissues. Following that, we amplified each RPSP from every tissue using the same primers from table 8.

Table 8: Root Pericyle Specific Promoters used in this study. In this table their name, function and the primers used for their cloning are presented.

Gene Ontology name	RPSP name	Primers
at3g02850(SKOR1)	RPSP1-F	ATGGGGAAACACACCTCTTGATG
	RPSP1-R	TTGTCCATCACTTATCAAATCTA
at2g37870	RPSP2-F	ATGAAGTGTTGTAAGTTTGTTGC
	RPSP2-R	TTAAGAAAAACATCTCATATTGT
at1g31050	RPSP3-F	CCTGGTAGAAGCTTAGGAGATCA
	RPSP3-R	TGTTGTTCCCAGTCTCACTGCTG
at2g26930	RPSP5-F	gctgaagcttATAACTTTTCAATAATGGATCTCGGCT
	RPSP5-R	cgatgggcccCAAATAAAAAAAAACAATCTTAGTTCT

B-Glucuronidase staining

Leaves from the transgenic plants described above (RPSP lines), grown in soil, were stained for GUS activity according to the protocol of Lagarde et al. (1996). The tissues were vacuum filtrated for 10 minutes so as the solution to penetrate better the tissues and the samples were incubated at 37^{o}C overnight. Stained tissues were cleared with sequential washes in ethanol solutions (70%, 50% and 10%) starting from the highest and incubated for 30 minutes in each solution. The samples were analyzed using bright-field microscopy (Leica MZ16 FA).

Results

1st Approach: Micro-Grafting

Inorganic Phosphate measurements

1. Whole rosettes

As explained in the previous chapters we had to use grafted on WT roots DM plants in order to find the role of PHO1 and PHO1;H1, as these genes have redundant functions in Pi loading into the xylem and we needed plants that would have a functional root (PHO1 and PHO;H1 present) but DM shoots. In this chapter, so as to check if there is any difference in the Pi content of WT and DM rosettes we also tried to use grafted plants and compare the Pi content of WT and DM plants. Initially, we grew the grafted plants in soil or in red or grey pellets [so as to control the watering with (+) or without (–) phosphate]. As we can see in figure 54, there is no significant difference between the Pi content of WT and DM rosettes and the variation of measurements between the different DM plants is very big. This could be due to the fact that plants were grown in soil where the Pi content of each pot can differ or because the establishment of each graft is different and thus each plant can have significant differences in its P homeostasis and overall development.

Unfortunately, the same variation of Pi content was observed also in WT and DM rosettes from plants grown in red or grey pellets (data not presented) where the watering with + or – Pi was controlled. Consequently, we can conclude that the main reason for this variation is the dissimilarity that emerges from the establishment of the graft junction.

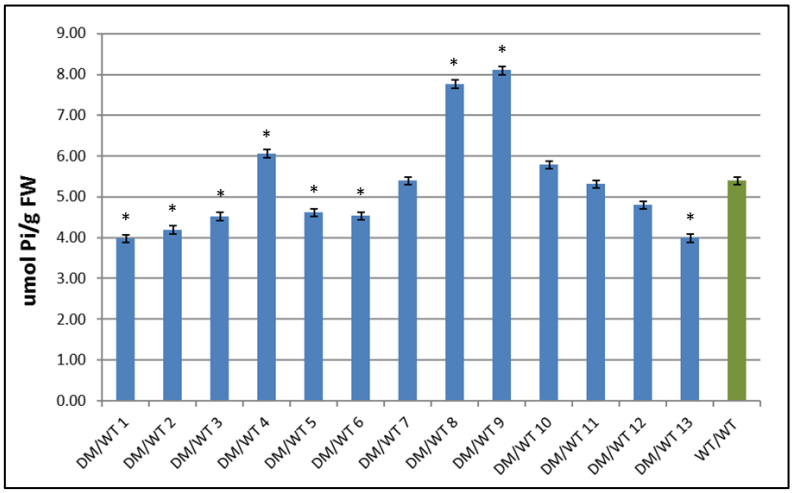

Figure 54: Pi content of whole rosettes from grafted WT (green) and DM (blue) plants grown in soil. Error bars denote standard deviations with n=3. Statistical analysis indicates significant difference from the wild type (*p < 0.05).

2. Individual leaves

Although in the previous experiment we obtained high variation in the Pi content of whole rosettes, it could be possible that the Pi content of whole rosettes does not differ between WT and DM plants. Thus, we hypothesized that source (older) leaves could remobilize their Pi to sink (younger) leaves with the help of PHO1 and/or PHO1;H1. Thus, in our effort to check if PHO1 and PHO1;H1 contribute to the Pi remobilization from the source to the sink leaves we checked the Pi content of individual rosette leaves using again grafted WT and DM plants on WT roots. After numbering and collecting individual leaves according to Mousavi et al. (2013) from WT and DM grafted plants grown only in soil we measured their Pi content using a colorimetric assay. Unfortunately, in this experiment we also obtained high variation in our measurements, which was probably a result of the dissimilarity that emerges from the establishment of the graft junction.

In this experiment we did not use any red or grey pellets [so as to control watering with (+) or without (–) phosphate] because from the previous experiment (p. 113) we noticed that most of the grafted plants could not survive under these conditions. This was probably due to an extra stress (drought or thickness of the pellets) added on the already stressed grafted roots. Even though, we tried to use a silicon tube filled with some soil, which would help at the early establishment of the seedlings, the grafted plants could not survive probably due to some toxic compounds that were being released from the tubes.

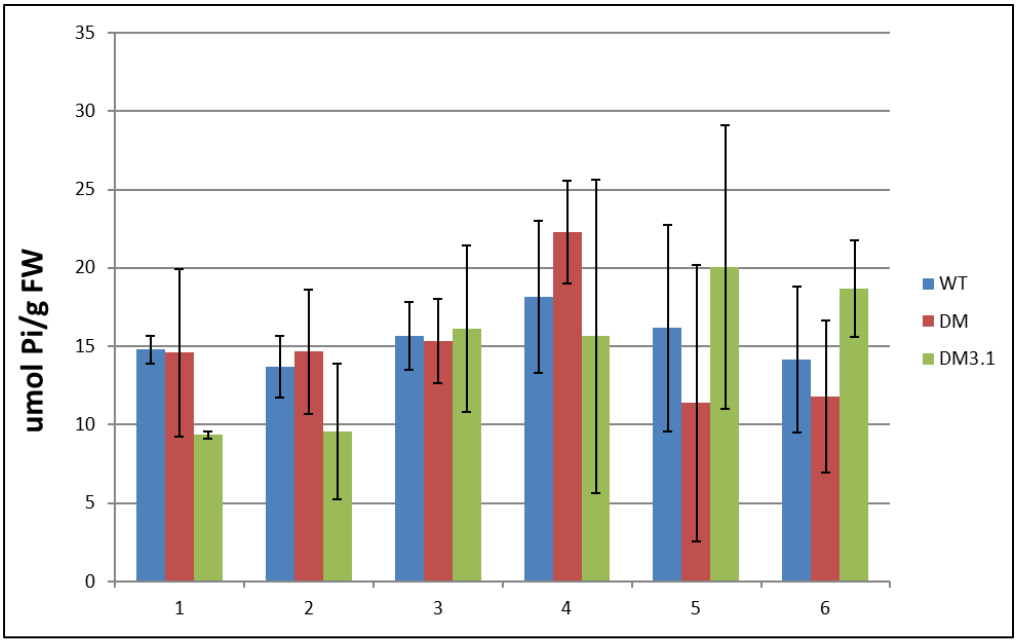

Figure 55: Pi content of individual leaves (1-7) from grafted WT (blue) DM (red) and DM3.1 (green) plants grown in soil. Error bars denote standard deviations with n=3. Statistical analysis indicates no significant difference from the wild type ($p > 0.05$).

3. Induced senescence (IDL)

Another experiment that we performed in order to test the same hypothesis, if PHO1 and PHO1;H1 play a role in the Pi remobilization from the source to the sink leaves, was to induce senescence as it is well known that when leaves start senescing there is nutrient remobilization from the senescing leaves to the younger leaves or to the seeds. Thus, after grafting WT and DM shoots on WT roots and growing the plants in soil we induced senescence to the same number and position of leaves (see Material and Methods p. 110) and measured the Pi content of individual leaves. Our results contained high variation once more (see Fig. 56) and thus it was very difficult to draw any conclusions.

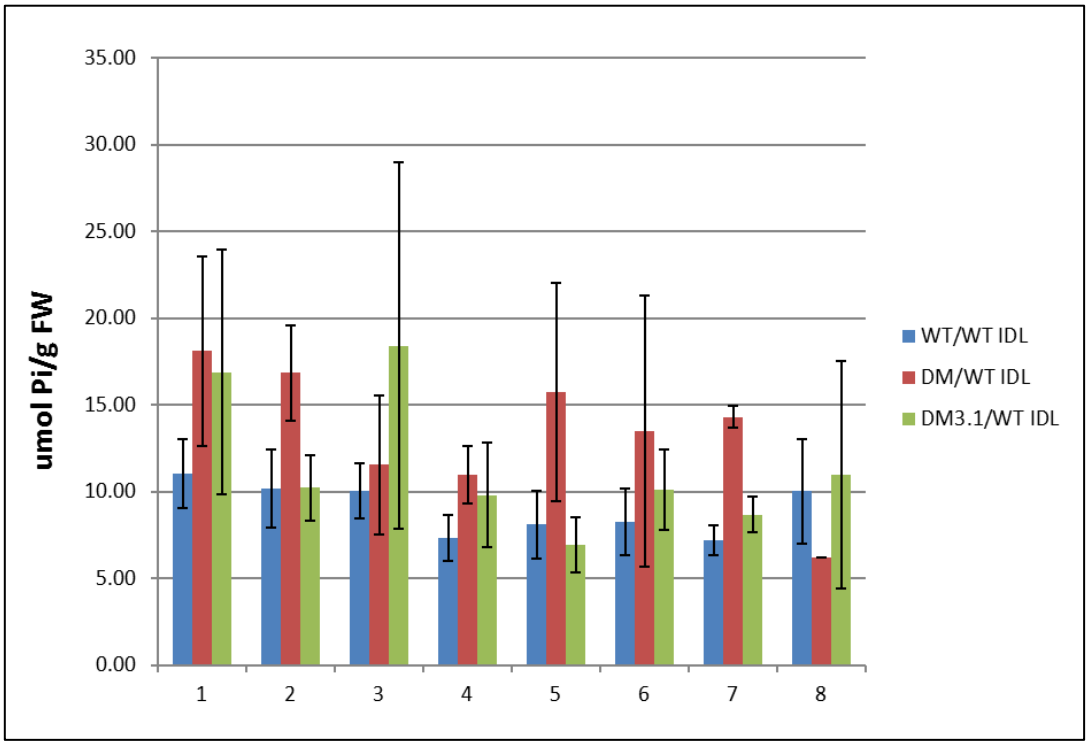

Figure 56: Pi content of individual leaves (1-7) from grafted WT (blue), DM (red) and DM3.1 (green) plants grown in soil and under induced senescence. Error bars denote standard deviations with n=3. Statistical analysis indicates no significant difference from the wild type ($p > 0.05$).

P^{33} transfer from the shoot to the root

As it is already known, in a WT plant PHO1 and PHO1;H1 are expressed in the root where they export Pi into the root apoplast. However, in a DM plant they are absent from the root and thus, Pi cannot be uploaded to the leaves. In our last effort to find their role in the leaves using grafted plants, we tried to test if they remobilize Pi from the leaves into the phloem from where it can be either uploaded in the aerial part of the plant or it can be transported to the root. Thus, after grafting plants and inducing secondary root development (see. Material and Methods p. 111), we split the roots of each seedling and placed half of the root on a cover slip with ½ MS liquid medium without phosphate and the other on a cover slip with 10uCi/ml P33 in K_2HPO_4 buffer (see Fig. 52). We incubated them for 1 hour, removed the root that was in the P^{33} solution and measured the other part of the root (attached to the shoot) and the shoot, separately in a Scintillation counter. Unfortunately, the results of this experiment were not clear enough to conclude something about the role of *PHO1* or *PHO1;H1* in the transport of phosphate from the shoot to the root (see table 9), possibly also due to the dissimilarity that emerges from the establishment of the graft junction.

Table 9: Results of P^{33} transfer measurements in CPM, under + or – phosphate conditions. S+R=Shoot + Root (Total), R/S+R= Root/Total, S/S+R= Shoot/Total.

	CPM S+R	CPM R/ S+R	CPM S/ S+R	
WT 1a	1541.00	0.09	0.91	**+Pi**
WT 2a	3860.00	0.03	0.97	
WT 3a	2523.00	0.06	0.94	
h1 1a	4921.00	0.05	0.95	
h1 2a	2457.00	0.13	0.87	
h1 3a	5871.00	0.12	0.88	
pho1.2 1a	11207.00	0.15	0.85	
pho1.2 2a	13417.00	0.11	0.89	
DM 1a	3593.00	0.06	0.94	
DM 2a	1543.00	0.32	0.68	
DM 3a	6932.00	0.00	1.00	
WT 1a	1393.00	0.04	0.96	**-Pi**
WT 2a	1667.00	0.10	0.90	
WT 3a	4318.00	0.01	0.99	
h1 1a	953.00	0.12	0.88	
h1 2a	1057.00	0.09	0.91	
h1 3a	10272.00	0.06	0.94	
pho1.2 1a	21798.00	0.12	0.88	
pho1.2 2a	13719.00	0.17	0.83	
DM 1a	2122.00	0.02	0.98	
DM 2a	3499.00	0.22	0.78	

2nd Approach: Root Pericycle Specific Promoters

RT-PCR

Due to the fact that we were getting high variation by the measurements that we performed using grafted plants but we still needed plants that would not be Pi starved and would grow as a WT, we decided to express *PHO1* only in the roots of DM plants using four different Root Pericycle Specific Promoters (RPSPs) that we identified using the GENEVESTIGATOR software. In that way, the roots would be functional (as PHO1 would be specifically expressed in the root) and the shoots would be Pi starved (PHO1 and PHO1;H1 absent). Before we started cloning the RPSPs, we checked their expression in different plant tissues (i.e: roots, leaves, petiols and inflorescence, Fig. 57) of WT plants grown in soil, in order to ensure that they are specifically expressed only in the roots.

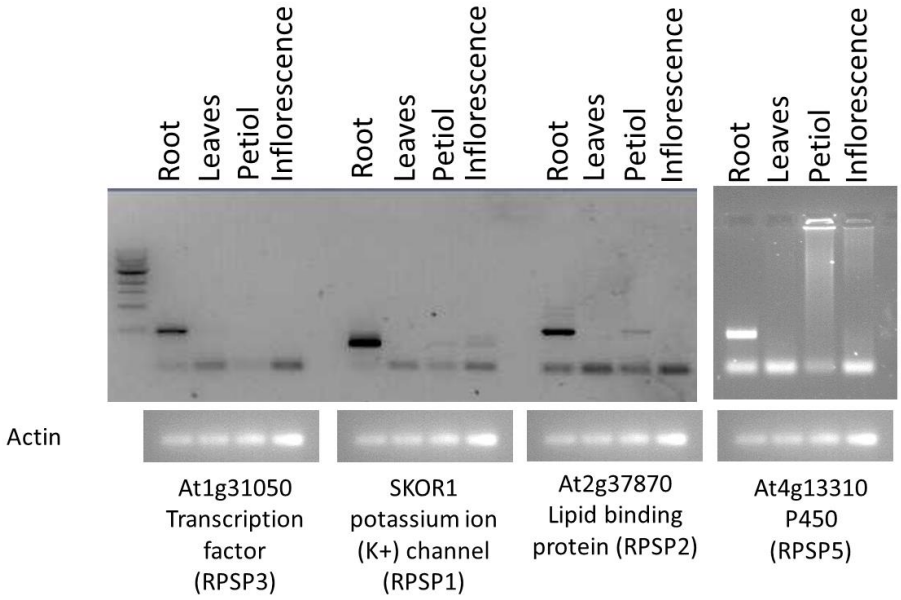

Figure 57: RT-PCR (35 cycles) of RPSP1,2,3 and 5 in different plant tissues (roots, leaves, petiols and inflorescence). As we can see all of the promoters are specifically expressed only in the roots and not in the aerial parts of the plant.

Unfortunately, after cloning the genomic sequence of *PHO1* fused to GUS in front of all these RPSPs and testing their expression with GUS staining we noticed that they were expressed (Fig. 58) in all the tissues where these genes are normally expressed under the PHO1 promoter (see the expression pattern of PHO1 in Chapter 2). In order to confirm that this result was not an artifact we also checked with RT-PCR (see Fig. 59) that the transgenes which contained the RPSPs were expressed.

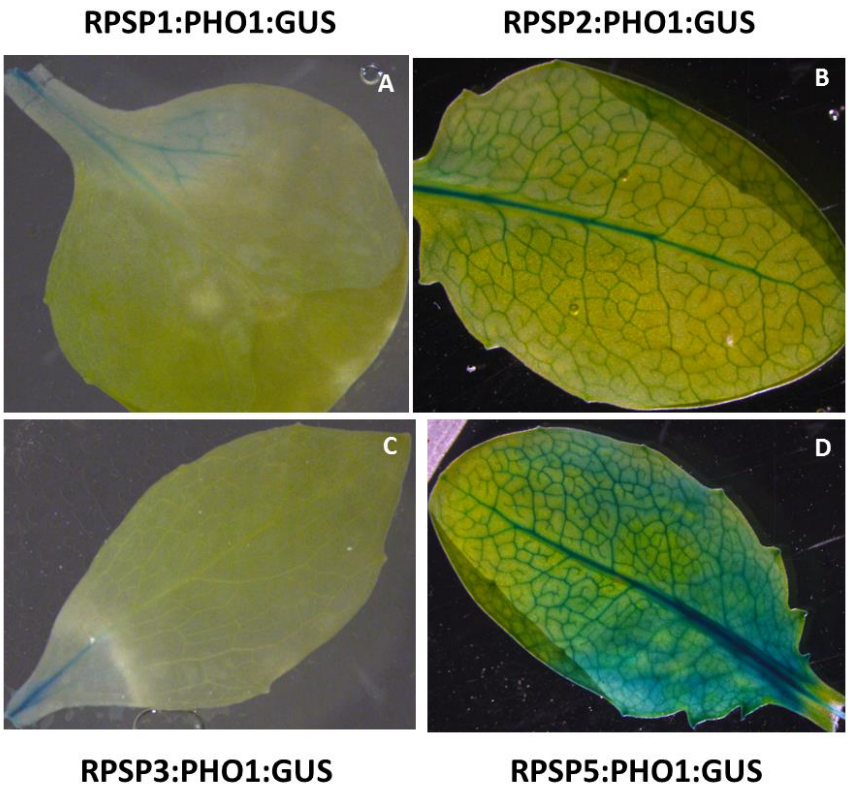

Figure 58: GUS expression of PHO1 in leaves of the transgenic lines that contained different root pericycle specific promoters fused to the genomic sequence of PHO1 and GUS (RPSP;PHO1;GUS). (A) RPSP1, (B) RPSP2, (C) RPSP3 and (D) RPSP5.

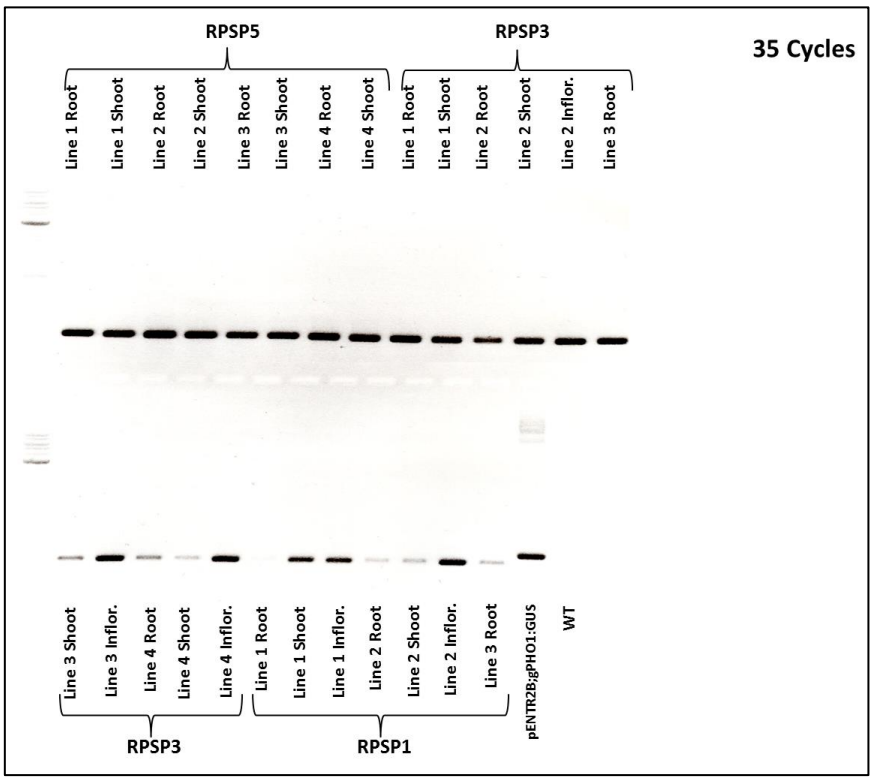

Figure 59: RT-PCR (35 cycles) of *PHO1* in roots and shoots of the transgenic lines that contained RPSP;PHO1;GUS. As a control we used pENTR2BlgPHO1;GUS and WT.

After obtaining the above results, we thought that either the RPSPs are not specifically expressed only in the root, although some of them are already published (i.e. SKOR1=RPSP1) or, probably *PHO1* contains some regulatory elements in its' genomic sequence (i.e. introns, enhancers protein or transcription factor binding sites as the UTR regions were not included in our construct design) that regulate its expression in specific tissues. Thus, we thought to clone the cDNA of these genes in front of a RPSP. However, it is already known that the cDNA of both PHO1 and PHO1;H1 is unstable in bacteria. Thus, maintaining an intron in the cDNA sequence would prevent the protein from being expressed in the bacteria but it could be functional in the plants as they contain the splicing machinery and they could splice the intron out. However, we were careful to maintain a small intron from both genes so as to avoid possible regulation of expression in all the tissues that these genes are normally expressed. When we tried to clone the cDNA of *PHO1* with intron 6 and the cDNA of *PHO1;H1* with intron 4 in front of the four RPSPs it was impossible as we were getting deletions or mutations in the cDNA sequence. Consequently, we decided to get it synthesized by GeneScript (http://www.genscript.com/).

After getting both cDNAs with one intron synthesized and cloned in front of a RPSP, we transformed the constructs into a DM background. When we checked the transgenic lines for *PHO1* or *PHO1;H1* expression in other tissues except the root, we also found that in the lines that PHO1 or PHO1;H1 was expressed in front of the RPSP5 both genes were expressed in the same tissues as *PHO1* and *PHO1;H1* are normally expressed under the PHO1 or PHO1;H1 promoter. Regarding the other three RPSPs (1, 2 and 3) the transgenic plants did not survive. This means that our constructs were not functional in the plants and thus the DM phenotype was not rescued (no viable plants).

Discussion

Our efforts to decipher the role of *PHO1* and *PHO1;H1* in the shoot of *Arabidopsis thaliana*, were not successful because we could not obtain the appropriate plants. In our first approach, the grafted plants gave us too much of variation in our measurements. This is because every grafted plant is different, depending on how well the hypocotyl junction was established. Furthermore, the grafted plants are more stressed comparing to the non-grafted ones, which leads to early flowering and thus complete change of the plant metabolism and nutrient remobilization.

Regarding the transgenic plants, using the RPSPs, they did not express *PHO1* and *PHO1;H1* only in the root. It seems that either these promoters are not root specific (although some of them have been published and we could identify all of them in GENEVESTIGATOR as root specific) or that *PHO1* and *PHO1;H1* have regulatory elements in their sequence (i.e. introns, enhancers, protein or transcription binding domains) that control and direct their expression in specific plant tissues. If the latter is true, many interesting questions and hypotheses could be raised regarding the role of these genes in the overall Pi homeostasis of the plant. How crucial are these genes for the survival of the plant? What is the exact mechanism of their regulation and how could we modulate it?

Thus, for the moment we do not have the technology to investigate the role of these genes in the shoot of *Arabidopsis thaliana*. Ideally, a root pericycle or a mesophyll specific promoter cloned behind the sequence of *PHO1* or *PHO1;H1* would be enough to study the role of these genes in the shoot. However, if our hypothesis about the regulatory elements on the genomic sequence of these genes which may control their expression is true, even if the root or mesophyll specific promoters are available, it will not be possible to express these genes only in one tissue. So, another possible approach would be to study a double mutant of one of these genes and of another still un-known gene that is related to phosphate export. Of course this double mutant should be a plant that grows well enough to produce enough leaves and seeds for analysis without being grafted. Furthermore, if indeed *PHO1* and/or *PHO1;H1* contain regulatory elements on their genomic sequence, it would be important to find them and understand the regulatory mechanism behind them. Cloning small parts of the whole genomic sequence of these genes (i.e.: SPX, EXS or trans-membrane domains) fused to GUS or GFP and checking their expression *in planta*, would help us narrow down which region of these sequences contains these regulatory elements. Once this region is found, we could check if it contains any particular motif, for instance a transcription factor binding motif and mutate it in order to check its importance on the expression of these genes.

Phloem loading is a determining process for the plant growth and development and therefore, for the crop yield. It is a process that carbohydrates and other nutrients from leaves are being exported (Lalonde et al., 2003; Schulz, 2005; Turgeon, 2006; Turgeon and Ayre, 2005) and is considered to be different among various plant families. Loading of sugars and amino acids into the phloem has been shown to follow three different pathways: a symplasmic and passive step (through plasmodesmata and cell cytosols), an active apoplasmic step (across plasma membranes via intervening cell walls) which requires transporters (influx or efflux) or a passive symplasmic transfer followed by polymer trapping

as was recently described by Rennie and Turgeon (2009). However, depending on the species or the growth conditions there can be a switch from symplastic to apoplastic transport (Gil et al., 2011). In the literature there are plenty of studies that have described how sugars and amino acids are being loaded or unloaded in the phloem. However, there is still a need to discover the transport mechanisms of other necessary nutrients like P, Zn or Fe. PHO1 and PHO1;H1 could be key players in the phloem loading of P as they are both Pi exporters and thus, they could actively export Pi into the leaf apoplasm. Although they have never been localized in the plasma membrane, like NRT1.7 which is responsible for remobilizing N from the older leaves to the N-demanding tissues, they could be loading Pi into Golgi-derived vesicles, followed by release of Pi to the extracellular space via exocytosis and recycling of PHO1 and/or PHO1;H1 away from the plasma membrane (Arpat et al., 2012; Wege and Poirier, 2014).

There are some interesting experiments that could be performed in order to find the role of these two genes in the phloem loading. Staining of the sieve plates with aniline blue followed by localization of PHO1 and PHO1;H1 with a fluorescent marker could show us if they are expressed next to the sieve plates. This would be a strong indication that they can participate in the P loading into the phloem. Immunolocalisation of these genes could also be useful. As it was shown for NRT1.7 (Fan et al., 2009), a nitrate transporter which is remobilizing N from source-to-sink tissues, its immunolocalization in the companion cell and sieve element complex is strong evidence for its possible role in the phloem loading, particularly in the mature leaves.

Another common experiment that is performed in order to detect the effect of a gene in nutrient remobilization from the source to the sink tissues is checking its diurnal regulation by qRT-PCR. As it was previously done for NRT1.7 (Fan et al., 2009) and OsPTR9 (Fang et al., 2013), leaves of WT plants grown under + or – P conditions, could be harvested at different time points during the day and the night and the expression of PHO1 could be checked by qRT-PCR. If PHO1 expression is diurnally regulated (higher at night, lower during the day), just as it was shown for NRT1.7 and OsPTR9, it would be a strong indication that it is participating in excess Pi export during the night. Furthermore, for most plants, the amount of sucrose exported from the source leaves during the night is similar to or slightly lower than the amount exported during the day (Mitchell et al., 1992; Pate et al., 1979). The sucrose exported during the night comes from hydrolysis of starch stored during the day. Since nitrate, phosphate and sucrose remobilization use the same phloem path for transport, and PHO1 expression is upregulated by sucrose (Ribot et al., 2008), there could be a common

feedback regulatory mechanism(s) for C/P balance, something that could also be true according to Ciereszko and Kleczkowski (2005) who showed that ADP-glucose and UDP-glucose pyrophosphorylases (enzymes directly involved in Pi recycling) as well as invertases (sucrose hydrolysis) are transcriptionally regulated by Pi-deficiency, which may play a role in homeostatic mechanisms that acclimate the plant to the Pi-stress conditions.

Finally, another possible solution to study the role of *PHO1* and *PHO1;H1* in Pi remobilization would be to study it in different plant species apart from *Arabidopsis*. For instance, the *PHO1* homologues are already known in rice (Jabnoune et al., 2013; Wang et al., 2004) and they could be identified in maize where their role could be more easily studied as it was recently done for carbon utilization (Czedik-Eysenberg et al., 2016). Similarly, several zones of a developing leaf could be analyzed and together with its transcriptome and/or metabolome we could obtain an idea of how Pi is being used and remobilized during the plant development.

References

Addy, K., and Green, L. (1996). "Phosphorus and Lake Aging."

Aerts, R. (1990). Nutrient Use Efficiency in Evergreen and Deciduous Species from Heathlands. *Oecologia* **84**, 391-397.

Aerts, R. (1996). Nutrient resorption from senescing leaves of perennials: Are there general patterns? *J. Ecol.* **84**, 597–608.

Ames, B. N. (1966). Assay of inorganic phosphate, total phosphate and phosphatases. *Methods Enzymol.* **8**, 115–118.

Anderson, D. M., Glibert, P. M., and Burkholder, J. M. (2002). Harmful algal blooms and eutrophication: Nutrient sources, composition, and consequences. *Estuaries* **25**, 704-726.

Aniszewski, T. (2009). Phaseolus lunatus testa topography and biometrics of crushed cells. *Seed Sci Technol* **37**, 121-131.

Archetti, M., Doring, T. F., Hagen, S. B., Hughes, N. M., Leather, S. R., Lee, D. W., Lev-Yadun, S., Manetas, Y., Ougham, H. J., Schaberg, P. G., and Thomas, H. (2009). Unravelling the evolution of autumn colours: an interdisciplinary approach. *Trends Ecol Evol* **24**, 166-73.

Arpat, A. B., Magliano, P., Wege, S., Rouached, H., Stefanovic, A., and Poirier, Y. (2012). Functional expression of PHO1 to the Golgi and trans-Golgi network and its role in export of inorganic phosphate. *Plant J* **71**, 479-91.

Aung, K., Lin, S. I., Wu, C. C., Huang, Y. T., Su, C. L., and Chiou, T. J. (2006). pho2, a phosphate overaccumulator, is caused by a nonsense mutation in a microRNA399 target gene. *Plant Physiol* **141**, 1000-11.

Baerson, S. R., Sanchez-Moreiras, A., Pedrol-Bonjoch, N., Schulz, M., Kagan, I. A., Agarwal, A. K., Reigosa, M. J., and Duke, S. O. (2005). Detoxification and transcriptome response in *Arabidopsis* seedlings exposed to the allelochemical benzoxazolin-2(3H)-one. *J Biol Chem* **280**, 21867-81.

Bailey, P. C., Martin, C., Toledo-Ortiz, G., Quail, P. H., Huq, E., Heim, M. A., Jakoby, M., Werber, M., and Weisshaar, B. (2003). Update on the basic helix-loop-helix transcription factor gene family in Arabidopsis thaliana. *Plant Cell* **15**, 2497-502.

Balazadeh, S., Riano-Pachon, D. M., and Mueller-Roeber, B. (2008). Transcription factors regulating leaf senescence in *Arabidopsis thaliana*. *Plant Biol* **10**, 63-75.

Barberon, M., and Geldner, N. (2014). Radial Transport of Nutrients: The Plant Root as a Polarized Epithelium. *Plant Physiol* **166**, 528-537.

Barberon, M., Zelazny, E., Robert, S., Conejero, G., Curie, C., Friml, J., and Vert, G. (2011). Monoubiquitin-dependent endocytosis of the IRON-REGULATED TRANSPORTER 1 (IRT1) transporter controls iron uptake in plants. *PNAS* **108**, E450-E458.

Barbier-Brygoo, H., Vinauger, M., Colcombet, J., Ephritikhine, G., Frachisse, J., and Maurel, C. (2000). Anion channels in higher plants: functional characterization, molecular structure and physiological role. *Biochim Biophys Acta* **1465**, 199-218.

Barton, L. (1961). Seed preservation and longevity. London: Hill.

Beeckman, T., Rycke, R. D., Viane, R., and D., I. (2000). Histological study of seed coat development in Arabidopsis thaliana. *J. Plant Res.* , 139–148.

Beeton, A. M., and Edmondso, W. (1972). Eutrophication Problem. *J Fish Res Board Can* **29**, 673-&.

Belmonte, M. F., Kirkbride, R. C., Stone, S. L., Pelletier, J. M., Bui, A. Q., Yeung, E. C., Hashimoto, M., Fei, J., Harada, C. M., Munoz, M. D., Le, B. H., Drews, G. N., Brady, S. M., Goldberg, R. B., and Harada, J. J. (2013). Comprehensive developmental

profiles of gene activity in regions and subregions of the *Arabidopsis* seed. *Proc Natl Acad Sci U S A* **110**, E435-44.

Bennet, E., Carpenter, S., and Caraco, N. (2001). Human Impact on Erodable Phosphorus and Eutrophication: A Global Perspective. *Bioscience* **51**, 227-232.

Bewley, J. D. (1997). Seed Germination and Dormancy. *Plant Cell* **9**, 1055-1066.

Bolland, M. D. A., and Baker, M. J. (1988). High phosphorus concentrations in seed of wheat and annual medic are related to higher rates of dry-matter production of seedlings and plants. *Aust J Exp Agr* **28**, 765-770.

Borg, S., Brinch-Pedersen, H., Tauris, B., and Holm, P. B. (2009). Iron transport, depositionand bioavailability in the wheat and barley grain. *Plant Soil* **325**, 15-24.

Borisjuk L., W. H., Panitz R., Manteuffel R., Wobus U. (1995). Embryogenesis of *V. faba* histodifferentiation in relation to starch and storage protein synthesis. *J Plant Physiol* **147**, 203–18.

Bouman, F. (1975). Integument initiation and testa development in some *Cruciferae*. *Bot J Linn Soc* **70**, 213–299.

Boutrot, F., Chantret, N., and Gautier, M. F. (2008). Genome-wide analysis of the rice and *Arabidopsis* non-specific lipid transfer protein (nsLtp) gene families and identification of wheat nsLtp genes by EST data mining. *BMC Genomics* **9**, 86.

Bradford, K., and H., N. (2007). Seed Development, Dormancy and Germination. Vol. 27, pp. 26, Oxford, UK: Blackwell Publishing.

Breeze, E., Harrison, E., McHattie, S., Hughes, L., Hickman, R., Hill, C., Kiddle, S., Kim, Y. S., Penfold, C. A., Jenkins, D., Zhang, C., Morris, K., Jenner, C., Jackson, S., Thomas, B., Tabrett, A., Legaie, R., Moore, J. D., Wild, D. L., Ott, S., Rand, D., Beynon, J., Denby, K., Mead, A., and Buchanan-Wollaston, V. (2011). High-resolution temporal profiling of transcripts during *Arabidopsis* leaf senescence reveals a distinct chronology of processes and regulation. *Plant Cell* **23**, 873-94.

Brown, R. C., Lemmon, B. E., Nguyen, H., and Olsen, O. A. (1999). Development of endosperm in *Arabidopsis thaliana*. *Sex Plant Reprod* **12**, 32-42.

Buchanan-Wollaston, V., and Ainsworth, C. (1997). Leaf senescence in Brassica napus: cloning of senescence related genes by subtractive hybridisation. *Plant Mol Biol* **33**, 821-34.

Buchanan-Wollaston, V., Earl, S., Harrison, E., Mathas, E., Navabpour, S., Page, T., and Pink, D. (2003). The molecular analysis of leaf senescence: a genomics approach. *Plant Biotechnol J* **1**, 3-22.

Bucher, M., Rausch, C., and Daram, P. (2001). Molecular and biochemical mechanisms of phosphorus uptake into plants. *J Plant Nutr Soil Sc* **164**, 209-217.

Burch-Smith, T. M., and Zambryski, P. C. (2012). Plasmodesmata paradigm shift: regulation from without versus within. *Annu Rev Plant Biol* **63**, 239-60.

Cakmak, I. (2008). Zinc crops 2007: improving crop production and human health. *Plant Soil* **306**.

Carpenter, S. R., and Lathrop, R. C. (2008). Probabilistic estimate of a threshold for eutrophication. *Ecosystems* **11**, 601-613.

Chen, L. Q., Hou, B. H., Lalonde, S., Takanaga, H., Hartung, M. L., Qu, X. Q., Guo, W. J., Kim, J. G., Underwood, W., Chaudhuri, B., Chermak, D., Antony, G., White, F. F., Somerville, S. C., Mudgett, M. B., and Frommer, W. B. (2010). Sugar transporters for intercellular exchange and nutrition of pathogens. *Nature* **468**, 527-32.

Chen, L. Q., Lin, I. W., Qu, X. Q., Sosso, D., McFarlane, H. E., Londono, A., Samuels, A. L., and Frommer, W. B. (2015). A cascade of sequentially expressed sucrose transporters in the seed coat and endosperm provides nutrition for the *Arabidopsis* embryo. *Plant Cell* **27**, 607-19.

Chen, Y. F., Li, L. Q., Xu, Q., Kong, Y. H., Wang, H., and Wu, W. H. (2009). The WRKY6 transcription factor modulates PHOSPHATE1 expression in response to low Pi stress in *Arabidopsis*. *Plant Cell* **21**, 3554-66.

Chiou, T. J., Aung, K., Lin, S. I., Wu, C. C., Chiang, S. F., and Su, C. L. (2006). Regulation of phosphate homeostasis by MicroRNA in *Arabidopsis*. *Plant Cell* **18**, 412-21.

Chiou, T. J., Liu, H., and Harrison, M. J. (2001). The spatial expression patterns of a phosphate transporter (MtPT1) from *Medicago truncatula* indicate a role in phosphate transport at the root/soil interface. *Plant J* **25**, 281-293.

Christensen, C. A., King, E. J., Jordan, J. R., and Drews, G. N. (1997). Megagametogenesis in *Arabidopsis* wild type and the Gf mutant. *Sex Plant Reprod* **10**, 49-64.

Ciereszko, I., and Kleczkowski, L. A. (2005). Expression of several genes involved in sucrose/starch metabolism as affected by different strategies to induce phosphate deficiency in *Arabidopsis*. *Acta Physiol Plant* **27**, 147-155.

Clough, S. J., and Bent, A. F. (1998). Floral dip: a simplified method for Agrobacterium-mediated transformation of *Arabidopsis thaliana*. *Plant J* **16**, 735-43.

Cogliatti, D. H., and Clarkson, D. T. (1983). Physiological changes in, and phosphate uptake by potato plants during development of, and recovery from phosphate deficiency. *Physiol Plant* **25**, 287-294.

Corner, E. (1976). The seeds of dicotyledons. *Cambridge University Press, London* **II**.

Costa, L. M., Yuan, J., Rouster, J., Paul, W., Dickinson, H., and Gutierrez-Marcos, J. F. (2012). Maternal control of nutrient allocation in plant seeds by genomic imprinting. *Curr Biol* **22**, 160-5.

Crafts-Brandner, S. J. (1992). Phosphorus nutrition influence on leaf senescence in soybean. *Plant Physiol* **98**, 1128-32.

Curtis, M. D., and Grossniklaus, U. (2003). A gateway cloning vector set for high-throughput functional analysis of genes in planta. *Plant Physiol* **133**, 462-469.

Czedik-Eysenberg, A. B., Arrivault, S., Lohse, M. A., Feil, R., Krohn, N., Encke, B., Nunes-Nesi, A., Fernie, A. R., Lunn, J. E., Sulpice, R., and Stitt, M. (2016). The interplay between carbon availability and growth in different zones of the growing maize leaf. *Plant Physiol*.

Daram, P., Brunner, S., Rausch, C., Steiner, C., Amrhein, N., and Bucher, M. (1999). *pht2;1* encodes a low-affinity phosphate transporter from *Arabidopsis*. *Plant Cell* **11**, 2153-66.

De Campos, M. C. R., Pearse, S. J., Oliveira, R. S., and Lambers, H. (2013). Downregulation of new phosphorus-uptake capacity is inversely related to leaf phosphorus-resorption proficiency in four species from a phosphorus-impoverished environment. *Ann. Bot.* **111**, 445-54.

De Marco, D. (1990). Effect of seed weight, and seed phosphorus and nitrogen concentrations on the early growth of wheat seedlings. *Aust J Exp Agric* **30**, 545–549.

Debeaujon, I., Nesi, N., Perez, P., Devic, M., Grandjean, O., Caboche, M., and Lepiniec, L. (2003). Proanthocyanidin-accumulating cells in *Arabidopsis* testa: regulation of differentiation and role in seed development. *Plant Cell* **15**, 2514-31.

Dejardin, A., Rochat, C., Maugenest, S., and Boutin, J. P. (1997). Purification, characterization and physiological role of sucrose synthase in the pea seed coat (*Pisum sativum L.*). *Planta* **201**, 128-37.

Delhaize, E., and Randall, P. J. (1995). Characterization of a Phosphate-Accumulator Mutant of *Arabidopsis thaliana*. *Plant Physiol* **107**, 207-213.

Dermastia, M., Kladnik, A., Dolenc Koce, J., and Chourey, P. S. (2009). A cellular study of teosinte *Zea mays* subsp. parviglumis (*Poaceae*) caryopsis development showing several processes conserved in maize. *Am J Bot* **96**, 1798-807.

Dixon, R. A., Xie, D. Y., and Sharma, S. B. (2005). Proanthocyanidins--a final frontier in flavonoid research? *New Phytol* **165**, 9-28.

Drechsler, N., Zheng, Y., Bohner, A., Nobmann, B., von Wiren, N., Kunze, R., and Rausch, C. (2015). Nitrate-Dependent Control of Shoot K Homeostasis by the Nitrate Transporter1/Peptide Transporter Family Member NPF7.3/NRT1.5 and the Stelar K+ Outward Rectifier SKOR in *Arabidopsis*. *Plant Physiol* **169**, 2832-47.

Dresselhaus, T. (2006). Cell-cell communication during double fertilization. *Curr Opin Plant Biol* **9**, 41-47.

Drew, M. C., Saker, L. R., Barber, S. A., and Jenkins, W. (1984). Changes in the kinetics of phosphate and potassium absorption in nutrient-deficient barley roots measured by a solution-depletion technique. *Planta* **160**, 490-9.

Drews, G. N., and Koltunow, A. M. (2011). The female gametophyte. *Arabidopsis Book* **9**, e0155.

Epstein, E., and Hagen, C. E. (1952). A Kinetic Study of the Absorption of Alkali Cations by Barley Roots. *Plant Physiol* **27**, 457-74.

Epstein, E., Rains, D. W., and Elzam, O. E. (1963). Resolution of Dual Mechanisms of Potassium Absorption by Barley Roots. *Proc Natl Acad Sci U S A* **49**, 684-92.

Espelie, K. E., Davis, R. W., and Kolattukudy, P. E. (1980). Composition, ultrastructure and function of the cutin- and suberin-containing layers in the leaf, fruit peel, juice-sac and inner seed coat of grapefruit (*Citrus paradisi Macfed*.). *Planta* **149**, 498-511.

Fan, S. C., Lin, C. S., Hsu, P. K., Lin, S. H., and Tsay, Y. F. (2009). The Arabidopsis Nitrate Transporter NRT1.7, Expressed in Phloem, Is Responsible for Source-to-Sink Remobilization of Nitrate. *Plant Cell* **21**, 2750-2761.

Fang, Z., Xia, K., Yang, X., Grotemeyer, M. S., Meier, S., Rentsch, D., Xu, X., and Zhang, M. (2013). Altered expression of the *PTR/NRT1* homologue *OsPTR9* affects nitrogen utilization efficiency, growth and grain yield in rice. *Plant Biotechnol J* **11**, 446-58.

Fisher, D. B., and Oparka, K. J. (1996). Post-phloem transport: Principles and problems. *J Exp Bot* **47**, 1141-1154.

Garnett, T. P., and Graham, R. D. (2005). Distribution and remobilization of iron and copper in wheat. *Ann Bot* **95**, 817-826.

Gasser, C. S., and Robinson-Beers, K. (1993). Pistil Development. *Plant Cell* **5**, 1231-1239.

Gattolin, S., Alandete-Saez, M., Elliott, K., Gonzalez-Carranza, Z., Naomab, E., Powell, C., and Roberts, J. A. (2006). Spatial and temporal expression of the response regulators ARR22 and ARR24 in *Arabidopsis thaliana*. *J Exp Bot* **57**, 4225-33.

Gepstein, S., Sabehi, G., Carp, M. J., Hajouj, T., Nesher, M. F., Yariv, I., Dor, C., and Bassani, M. (2003). Large-scale identification of leaf senescence-associated genes. *Plant J* **36**, 629-42.

Gil, L., Yaron, I., Shalitin, D., Sauer, N., Turgeon, R., and Wolf, S. (2011). Sucrose transporter plays a role in phloem loading in CMV-infected melon plants that are defined as symplastic loaders. *Plant J* **66**, 366-74.

Gomez, E., Royo, J., Muniz, L. M., Sellam, O., Paul, W., Gerentes, D., Barrero, C., Lopez, M., Perez, P., and Hueros, G. (2009). The maize transcription factor myb-related protein-1 is a key regulator of the differentiation of transfer cells. *Plant Cell* **21**, 2022-35.

Grant, C. A., Flaten, D. N., Tomasiewicz, D. J., and Sheppard, S. C. (2001). The importance of early season phosphorus nutrition. *Can J Plant Sci* **81**, 211-224.

Gregersen, P. L., and Holm, P. B. (2007). Transcriptome analysis of senescence in the flag leaf of wheat (*Triticum aestivum L.*). *Plant Biotechnol J* **5**, 192-206.

Grime, J. P. (1977). Evidence for the existence of three primary strategies in plants and its relevance to ecological and evolutionary theory. *Am Nat* **111**, 1169–1194.

Groot, S. P., and Karssen, C. M. (1987). Gibberellins regulate seed germination in tomato by endosperm weakening: a study with gibberellin-deficient mutants. *Planta* **171**, 525-31.

Guo, C., Zhao, X., Liu, X., Zhang, L., Gu, J., Li, X., Lu, W., and Xiao, K. (2013). Function of wheat phosphate transporter gene TaPHT2;1 in Pi translocation and plant growth regulation under replete and limited Pi supply conditions. *Planta* **237**, 1163-78.

Guo, Y., Cai, Z., and Gan, S. (2004). Transcriptome of *Arabidopsis* leaf senescence. *Plant Cell Environ* **27**, 521–549.

Guo, Y., and Gan, S. (2006). AtNAP, a NAC family transcription factor, has an important role in leaf senescence. *Plant J* **46**, 601-12.

Hamburger, D., Rezzonico, E., Petetot, J. M. C., Somerville, C., and Poirier, Y. (2002). Identification and characterization of the *Arabidopsis PHO1* gene involved in phosphate loading to the xylem. *Plant Cell* **14**, 889-902.

Haughn, G., and Chaudhury, A. (2005). Genetic analysis of seed coat development in *Arabidopsis*. *Trends Plant Sci* **10**, 472-7.

Heim, M. A., Jakoby, M., Werber, M., Martin, C., Weisshaar, B., and Bailey, P. C. (2003). The basic helix-loop-helix transcription factor family in plants: a genome-wide study of protein structure and functional diversity. *Mol Biol Evol* **20**, 735-47.

Heim, U., Weber, H., Baumlein, H., and Wobus, U. (1993). A sucrose-synthase gene of *Vicia faba L.*: expression pattern in developing seeds in relation to starch synthesis and metabolic regulation. *Planta* **191**, 394-401.

Herrera-Estrella, L., and Lopez-Arredondo, D. (2016). Phosphorus: the underrated element for feeding the world. *Trends Plant Sci* **21**, 461-3.

Hill, J. (1980). The Remobilization of Nutrients from Leaves. *J Plant Nutr* **2**, 407-444.

Himelblau, E., and Amasino, R. M. (2001). Nutrients mobilized from leaves of *Arabidopsis thaliana* during leaf senescence. *J Plant Physiol* **158**, 1317-1323.

Hinderhofer, K., and Zentgraf, U. (2001). Identification of a transcription factor specifically expressed at the onset of leaf senescence. *Planta* **213**, 469-73.

Hocking, P. J. (1994). Dry-Matter Production, Mineral Nutrient Concentrations, and Nutrient Distribution and Redistribution in Irrigated Spring Wheat. *J Plant Nutr* **17**, 1289-1308.

Hocking, P. J., and Pate, J. S. (1977). Mobilization of Minerals to Developing Seeds of Legumes. *Ann Bot* **41**, 1259-1278.

Horak, J., Grefen, C., Berendzen, K. W., Hahn, A., Stierhof, Y. D., Stadelhofer, B., Stahl, M., Koncz, C., and Harter, K. (2008). The *Arabidopsis thaliana* response regulator ARR22 is a putative AHP phospho-histidine phosphatase expressed in the chalaza of developing seeds. *BMC Plant Biol* **8**, 77.

Hsieh, M. H., Chang, C. Y., Hsu, S. J., and Chen, J. J. (2008). Chloroplast localization of methylerythritol 4-phosphate pathway enzymes and regulation of mitochondrial genes in ispD and ispE albino mutants in *Arabidopsis*. *Plant Mol Biol* **66**, 663-73.

Hsieh, M. H., and Goodman, H. M. (2005). The *Arabidopsis* IspH homolog is involved in the plastid nonmevalonate pathway of isoprenoid biosynthesis. *Plant Physiol* **138**, 641-53.

Hulskamp, M., Schneitz, K., and Pruitt, R. E. (1995). Genetic Evidence for a Long-Range Activity That Directs Pollen Tube Guidance in *Arabidopsis*. *Plant Cell* **7**, 57-64.

Ikuma, H., and Thimann., K. V. (1963). The role of the seed coat in germination of photosensitive lettuce seeds. *Plant Cell Physiol.* **4**, 169–185.

Imlau, A., Truernit, E., and Sauer, N. (1999). Cell-to-cell and long-distance trafficking of the green fluorescent protein in the phloem and symplastic unloading of the protein into sink tissues. *Plant Cell* **11**, 309-22.

Jabnoune, M., Secco, D., Lecampion, C., Robaglia, C., Shu, Q., and Poirier, Y. (2013). A rice cis-natural antisense RNA acts as a translational enhancer for its cognate mRNA and contributes to phosphate homeostasis and plant fitness. *Plant Cell* **25**, 4166-82.

Jenner, C. F., Ugalde, T. D., and Aspinall, D. (1991). The Physiology of Starch and Protein Deposition in the Endosperm of Wheat. *Australian Journal of Plant Physiology* **18**, 211-226.

Karimi, M., Inze, D., and Depicker, A. (2002). GATEWAY vectors for Agrobacterium-mediated plant transformation. *Trends Plant Sci* **7**, 193-5.

Karthikeyan, A. S., Varadarajan, D. K., Mukatira, U. T., D'Urzo, M. P., Damsz, B., and Raghothama, K. G. (2002). Regulated expression of *Arabidopsis* phosphate transporters. *Plant Physiol* **130**, 221-33.

Kermicle, J. L. (1969). Androgenesis conditioned by a mutation in maize. *Science* **166**, 1422-4.

Khan, D., Millar, J. L., Girard, I. J., and Belmonte, M. F. (2014). Transcriptional circuitry underlying seed coat development in *Arabidopsis*. *Plant Sci* **219-220**, 51-60.

Kleinboelting, N., Huep, G., Kloetgen, A., Viehoever, P., and Weisshaar, B. (2012). GABI-Kat SimpleSearch: new features of the *Arabidopsis thaliana* T-DNA mutant database. *Nucleic Acids Res* **40**, D1211-5.

Kobayashi, M., and Tsunewaki, K. (1980). Haploid Induction and Its Genetic Mechanism in Alloplasmic Common Wheat. *J Hered* **71**, 9-14.

Kobe, R. K., Lepczyk, C. A., and Iyer, M. (2005). Resorption efficiency decreases with increasing green leaf nutrients in a global data set. *Ecology* **86**, 2780–2792.

Krol, E., and Trebacz, K. (2000). Ways of ion channel gating in plant cells. *Ann Bot* **86**, 449-469.

Lalonde, S., Boles, E., Hellmann, H., Barker, L., Patrick, J. W., Frommer, W. B., and Ward, J. M. (1999). The dual function of sugar carriers. Transport and sugar sensing. *Plant Cell* **11**, 707-26.

Lalonde, S., Tegeder, M., Throne-Holst, M., Frommer, W., and Patrick, J. (2003). Phloem loading and unloading of sugars and amino acids. Vol. Plant, Cell & Environment pp. 37–56.

Lambers, H., Finnegan, P. M., Jost, R., Plaxton, W. C., Shane, M. W., and Stitt, M. (2015). Phosphorus nutrition in Proteaceae and beyond. *Nat Plants* **1**, 15109.

Leopold, A. C. (1961). Senescence in Plant Development: The death of plants or plant parts may be of positive ecological or physiological value. *Science* **134**, 1727-32.

Leubner-Metzger, G., Fruendt, C., and Meins, F. (1996). Effects of gibberellins, darkness and osmotica on endosperm rupture and class I beta-1,3-glucanase induction in tobacco seed germination. *Planta* **199**, 282-288.

Leubner-Metzger, G., Frundt, C., Vogeli-Lange, R., and Meins, F., Jr. (1995). Class I [beta]-1,3-Glucanases in the Endosperm of Tobacco during Germination. *Plant Physiol* **109**, 751-759.

Lin, M., Pang, C., Fan, S., Song, M., Wei, H., and Yu, S. (2015). Global analysis of the *Gossypium hirsutum L.* Transcriptome during leaf senescence by RNA-Seq. *BMC Plant Biol* **15**, 43.

Lin, W. Y., Lin, S. I., and Chiou, T. J. (2009). Molecular regulators of phosphate homeostasis in plants. *J Exp Bot* **60**, 1427-1438.

Litke, D. W. (1999). Review of phosphorus control measures in the US and their effects on water quality. *In* "National Water Quality Assessment Program: Water-Resources Investigations Report".

Liu, J., Fu, S., Yang, L., Luan, M., Zhao, F., Luan, S., and Lan, W. (2016a). Vacuolar SPX-MFS transporters are essential for phosphate adaptation in plants. *Plant Signal Behav* **11**, e1213474.

Liu, K., Li, L., and Luan, S. (2006). Intracellular K+ sensing of SKOR, a Shaker-type K+ channel from *Arabidopsis*. *Plant J* **46**, 260-8.

Liu, L., Zhou, Y., Zhou, G., Ye, R., Zhao, L., Li, X., and Lin, Y. (2008). Identification of early senescence-associated genes in rice flag leaves. *Plant Mol Biol* **67**, 37-55.

Liu, T. Y., Huang, T. K., Tseng, C. Y., Lai, Y. S., Lin, S. I., Lin, W. Y., Chen, J. W., and Chiou, T. J. (2012). PHO2-dependent degradation of PHO1 modulates phosphate homeostasis in *Arabidopsis*. *Plant Cell* **24**, 2168-2183.

Liu, T. Y., Huang, T. K., Yang, S. Y., Hong, Y. T., Huang, S. M., Wang, F. N., Chiang, S. F., Tsai, S. Y., Lu, W. C., and Chiou, T. J. (2016b). Identification of plant vacuolar transporters mediating phosphate storage. *Nat Commun* **7**, 11095.

Lofke, C., Luschnig, C., and Kleine-Vehn, J. (2013). Posttranslational modification and trafficking of PIN auxin efflux carriers. *Mech Dev* **130**, 82-94.

Logemann, E., Birkenbihl, R. P., Ulker, B., and Somssich, I. E. (2006). An improved method for preparing Agrobacterium cells that simplifies the *Arabidopsis* transformation protocol. *Plant Methods* **2**, 16.

Lund, J. W. G. (1974). Phosphorus and Eutrophication Problem. *Nature* **249**, 797-797.

Maheshwari, P., and Johri, B. M. (1950). Development of the Embryo Sac, Embryo and Endosperm in *Helixanthera ligustrina* (Wall) Dans. *Nature* **165**, 978-979.

Maillard, A., Diquelou, S., Billard, V., Laine, P., Garnica, M., Prudent, M., Garcia-Mina, J. M., Yvin, J. C., and Ourry, A. (2015). Leaf mineral nutrient remobilization during leaf senescence and modulation by nutrient deficiency. *Front Plant Sci* **6**, 317.

Marsch-Martinez, N., Franken, J., Gonzalez-Aguilera, K. L., de Folter, S., Angenent, G., and Alvarez-Buylla, E. R. (2013). An efficient flat-surface collar-free grafting method for *Arabidopsis thaliana* seedlings. *Plant Methods* **9**, 14.

Marschner, H. (1995). "Mineral nutrition of higher plants," Academic Press, London.

Matallana-Ramirez, L. P., Rauf, M., Farage-Barhom, S., Dortay, H., Xue, G. P., Droge-Laser, W., Lers, A., Balazadeh, S., and Mueller-Roeber, B. (2013). NAC transcription factor ORE1 and senescence-induced BIFUNCTIONAL NUCLEASE1 (BFN1) constitute a regulatory cascade in *Arabidopsis*. *Mol Plant* **6**, 1438-52.

Miao, Y., Laun, T., Zimmermann, P., and Zentgraf, U. (2004). Targets of the WRKY53 transcription factor and its role during leaf senescence in *Arabidopsis*. *Plant Mol Biol* **55**, 853-67.

Miao, Y., Laun, T. M., Smykowski, A., and Zentgraf, U. (2007). *Arabidopsis* MEKK1 can take a short cut: it can directly interact with senescence-related WRKY53 transcription factor on the protein level and can bind to its promoter. *Plant Mol Biol* **65**, 63-76.

Millar, J. L., Khan, D., Becker, M. G., Chan, A., Dufresne, A., Sumner, M., and Belmonte, M. F. (2015). Chalazal seed coat development in *Brassica napus*. *Plant Sci* **241**, 45-54.

Miller, R. O., Jacobsen, J. S., and Skogley, E. O. (1994). Aerial Accumulation and Partitioning of Nutrients by Hard Red Spring Wheat. *Commun Soil Sci Plant Anal* **25**, 1891-1911.

Miller, S. S., Bowman, L. A., Gijzen, M., and Miki, B. L. A. (1999). Early development of the seed coat of soybean (*Glycine max*). *Ann Bot*, 297–304.

Mimura, T. (1999). Regulation of phosphate transport and homeostasis in plant cells. *Int Rev Cytol* **191**, 149-200.

Misson, J., Raghothama, K. G., Jain, A., Jouhet, J., Block, M. A., Bligny, R., Ortet, P., Creff, A., Somerville, S., Rolland, N., Doumas, P., Nacry, P., Herrerra-Estrella, L., Nussaume, L., and Thibaud, M. C. (2005). A genome-wide transcriptional analysis using *Arabidopsis thaliana* Affymetrix gene chips determined plant responses to phosphate deprivation. *Proc Natl Acad Sci U S A* **102**, 11934-9.

Mitchell, D. E., Gadus, M. V., and Madore, M. A. (1992). Patterns of assimilate production and translocation in Muskmelon (*Cucumis melo L.*) : I. Diurnal Patterns. *Plant Physiol* **99**, 959-65.

Morley-Smith, E. R., Pike, M. J., Findlay, K., Kockenberger, W., Hill, L. M., Smith, A. M., and Rawsthorne, S. (2008). The transport of sugars to developing embryos is not via the bulk endosperm in oilseed rape seeds. *Plant Physiol* **147**, 2121-30.

Mousavi, S. A., Chauvin, A., Pascaud, F., Kellenberger, S., and Farmer, E. E. (2013). GLUTAMATE RECEPTOR-LIKE genes mediate leaf-to-leaf wound signalling. *Nature* **500**, 422-6.

Muchhal, U. S., Pardo, J. M., and Raghothama, K. G. (1996). Phosphate transporters from the higher plant *Arabidopsis thaliana*. *PNAS* **93**, 10519-10523.

Mudge, S. R., Rae, A. L., Diatloff, E., and Smith, F. W. (2002). Expression analysis suggests novel roles for members of the Pht1 family of phosphate transporters in *Arabidopsis*. *Plant J* **31**, 341-53.

Muller, B., Fastner, A., Karmann, J., Mansch, V., Hoffmann, T., Schwab, W., Suter-Grotemeyer, M., Rentsch, D., Truernit, E., Ladwig, F., Bleckmann, A., Dresselhaus, T., and Hammes, U. Z. (2015). Amino Acid Export in Developing *Arabidopsis* Seeds Depends on UmamiT Facilitators. *Curr Biol* **25**, 3126-31.

Murray, D. R. (1987). Nutritive role of seed coats in developing legume seeds. *Am J Bot* **74**, 1122–1137.

Nonogaki, H., and Morohashi, Y. (1996). An Endo-[beta]-Mannanase Develops Exclusively in the Micropylar Endosperm of Tomato Seeds Prior to Radicle Emergence. *Plant Physiol* **110**, 555-559.

Offler, C. E., Nerlich, S. M., and Patrick, J. W. (1989). Pathway of photosynthate transfer in the developing seed of *Vicia faba L.* Transfer in relation to seed anatomy. *J Exp Bot* **40**, 769–780.

Ohad, N., Margossian, L., Hsu, Y. C., Williams, C., Repetti, P., and Fischer, R. L. (1996). A mutation that allows endosperm development without fertilization. *PNAS* **93**, 5319-5324.

Olsen, L. I., Hansen, T. H., Larue, C., Osterberg, J. T., Hoffmann, R. D., Liesche, J., Kramer, U., Surble, S., Cadarsi, S., Samson, V. A., Grolimund, D., Husted, S., and Palmgren, M. (2016). Mother-plant-mediated pumping of zinc into the developing seed. *Nat Plants* **2**, 16036.

Oparka, K., and Gates, P. (1984). Sink anatomy in relation to solute movement in rice (*Oryza sativa L.*): a summary of findings. *Plant Growth Regul.* **2**, 297–307.

Oparka, K. J. (1990). What Is Phloem Unloading. *Plant Physiol* **94**, 393-396.

Pagnussat, G. C., Alandete-Saez, M., Bowman, J. L., and Sundaresan, V. (2009). Auxin-dependent patterning and gamete specification in the *Arabidopsis* female gametophyte. *Science* **324**, 1684-9.

Palmgren, M. G. (2001). Plant plasma membrane H^+-ATPases: powerhouses fornutrient uptake. *Annu Rev Plant Physiol Plant Mol Biol*, 817–845.

Park, S., and Harada, J. J. (2008). *Arabidopsis* embryogenesis. *Methods Mol Biol* **427**, 3-16.

Pate, J. S., Atkins, C. A., Hamel, K., McNeil, D. L., and Layzell, D. B. (1979). Transport of organic solutes in Phloem and xylem of a nodulated legume. *Plant Physiol* **63**, 1082-8.

Pate, J. S., and Hocking, P. J. (1978). Phloem and xylem transport in supply of minerals to a developing legume (*Lupinus albus L.*) fruit. *Ann Bot* **42**, 911-921.
Patrick, J. W. (1997). Phloem unloading: Sieve element unloading and post-sieve element transport. *Annu Rev Plant Physiol Plant Mol Biol* **48**, 191-222.
Patrick, J. W., and Offler, C. E. (1995). Post-sieve element transport of sucrose in developing seeds. *Aust J Plant Physiol* **22**, 681-702.
Patrick, J. W., and Offler, C. E. (2001). Compartmentation of transport and transfer events in developing seeds. *J Exp Bot* **52**, 551-564.
Pfeiffer, W. H., and McClafferty, B. (2007). HarvestPlus: Breeding crops for better nutrition. *Crop Sci* **47**, S88-S105.
Poirier, Y., and Bucher, M. (2002). Phosphate transport and homeostasis in *Arabidopsis*. *The Arabidopsis book* **1**, e0024.
Poirier, Y., and Jung, J.-Y. (2015). Phosphate transporters. *Annual Plant Reviews* **48**, 125-158.
Poirier, Y., Thoma, S., Somerville, C., and Schiefelbein, J. (1991). Mutant of *Arabidopsis* deficient in xylem loading of phosphate. *Plant Physiol* **97**, 1087-93.
Radchuk, V., and Borisjuk, L. (2014). Physical, metabolic and developmental functions of the seed coat. *Front Plant Sci* **5**, 510.
Raghothama, K. G. (1999). Phosphate acquisition. *Annu Rev Plant Physiol Plant Mol Biol* **50**, 665-693.
Raghothama, K. G. (2000). Phosphate transport and signaling. *Curr Opin Plant Biol* **3**, 182-187.
Rausch, C., and Bucher, M. (2002). Molecular mechanisms of phosphate transport in plants. *Planta* **216**, 23-37.
Rausch, C., Zimmermann, P., Amrhein, N., and Bucher, M. (2004). Expression analysis suggests novel roles for the plastidic phosphate transporter *pht2;1* in auto- and heterotrophic tissues in potato and *Arabidopsis*. *Plant J* **39**, 13-28.
Rennie, E. A., and Turgeon, R. (2009). A comprehensive picture of phloem loading strategies. *PNAS* **106**, 14162-14167.
Ribot, C., Wang, Y., and Poirier, Y. (2008). Expression analyses of three members of the AtPHO1 family reveal differential interactions between signaling pathways involved in phosphate deficiency and the responses to auxin, cytokinin, and abscisic acid. *Planta* **227**, 1025-36.
Ritchie, R. J., Fieuw-Makaroff, S., and Patrick, J. W. (2003). Sugar retrieval by coats of developing seeds of *Phaseolus vulgaris L.* and *Vicia faba L. Plant Cell Physiol* **44**, 163-72.
Robatzek, S., and Somssich, I. E. (2002). Targets of AtWRKY6 regulation during plant senescence and pathogen defense. *Genes Dev* **16**, 1139-49.
Roberts, S. K. (2006). Plasma membrane anion channels in higher plants and their putative functions in roots. *New Phytologist* **169**, 647-666.
Robinson-Beers, K., Pruitt, R. E., and Gasser, C. S. (1992). Ovule Development in Wild Type *Arabidopsis* and Two Female Sterile Mutants. *Plant Cell* **4**, 1237-1249.
Robinson, W. D., Carson, I., Ying, S., Ellis, K., and Plaxton, W. C. (2012). Eliminating the purple acid phosphatase AtPAP26 in *Arabidopsis thaliana* delays leaf senescence and impairs phosphorus remobilization. *New Phytol* **196**, 1024-9.
Rochat, C., Wuilleme, S., Boutin, J. P., and Hedley, C. L. (1995). A mutation at the rb gene, lowering ADPGPPase activity, affects storage product metabolism of pea seed coats. *J. Exp. Bot.* **46**, 415–21.

Ros, C., Bell, R. W., and White, P. F. (1997). Effect of seed phosphorus and soil phosphorus applications on early growth of rice (*Oryza sativa L.*) cv. IR66. *Soil Sci Plant Nutr* **43**, 499-509.

Ruan, Y. L. (2005). Recent advances in understanding cotton fibre and seed development. *Seed Sci Res* **15**, 269-280.

Rudall, P. J. (2006). How many nuclei make an embryo sac in flowering plants? *Bioessays* **28**, 1067-1071.

Russell, S. D. (1993). The Egg Cell: Development and Role in Fertilization and Early Embryogenesis. *Plant Cell* **5**, 1349-1359.

Sakano, K. (1990). Proton/phosphate stoichiometry in uptake of inorganic phosphate by cultured cells of *Catharanthus roseus (L.)* G. Don. *Plant Physiol* **93**, 479-83.

Salanenka, Y. A., Goffinet, M. C., and Taylor, A. G. (2009). Structure and histochemistry of the micropylar and chalazal regions of the perisperm–endosperm envelope of cucumber seed associated with solute permeability and germination. *J. Amer. Soc. Hort. Sci.* **134**, 479–487.

SAMAB (1996). (Southern Appalachian Man and the Biosphere). *The Southern Appalachian Assessment Aquatics Technical Report Atlanta: USDA Forest Service, Southern Region*, Report nr 2 of 5.

Sattari, S. Z., Bouwman, A. F., Martinez Rodriguez, R., Beusen, A. H., and van Ittersum, M. K. (2016). Negative global phosphorus budgets challenge sustainable intensification of grasslands. *Nat Commun* **7**, 10696.

Schachtman, D. P., Reid, R. J., and Ayling, S. M. (1998). Phosphorus uptake by plants: from soil to cell. *Plant Physiol* **116**, 447-53.

Schneitz, K., Baker, S. C., Gasser, C. S., and Redweik, A. (1998). Pattern formation and growth during floral organogenesis: HUELLENLOS and AINTEGUMENTA are required for the formation of the proximal region of the ovule primordium in *Arabidopsis thaliana*. *Development* **125**, 2555-63.

Schneitz, K., Hulskamp, M., and Pruitt, R. E. (1995). Wild-type ovule development in *Arabidopsis thaliana*: a light microscope study of cleared whole-mount tissue. *Plant J* **7**, 731-749.

Schroeder, J. I. (1995). Anion channels as central mechanisms for signal transduction in guard cells and putative functions in roots for plant-soil interactions. *Plant Mol Biol* **28**, 353-61.

Schulz, A. (2005). Role of plasmodesmata in solute loading and unloading. *Plasmodesmata* **18**, 135-161.

Schulz, A., Kuhn, C., Riesmeier, J. W., and Frommer, W. R. (1998). Ultrastructural effects in potato leaves due to antisense-inhibition of the sucrose transporter indicate an apoplasmic mode of phloem loading. *Planta* **206**, 533-543.

Shane, M. W., Cramer, M. D., Funayama-Noguchi, S., Cawthray, G. R., Millar, A. H., Day, D. A., and Lambers, H. (2004). Developmental physiology of cluster-root carboxylate synthesis and exudation in harsh hakea. Expression of phosphoenolpyruvate carboxylase and the alternative oxidase. *Plant Physiol* **135**, 549-60.

Sharma, P. D. (2009). "

Shin, H., Shin, H. S., Dewbre, G. R., and Harrison, M. J. (2004). Phosphate transport in *Arabidopsis*: Pht1;1 and Pht1;4 play a major role in phosphate acquisition from both low- and high-phosphate environments. *Plant J* **39**, 629-42.

Smaya (TJ. 2008). Complexity in the eutrophication—harmful algal bloom relationship, with comment on the importance of grazing. *Harmful Algae* **8**, 140-151.

Smith, A. P., Fontenot, E. B., Zahraeifard, S., and Feuer DiTusa, S. (2015). Molecular components that drive phosphorus-remobilisation during leaf senescence. *Annu. Plant Rev.* **48**, 159–186.

Smith, V. H., Tilman, G. D., and Nekola, J. C. (1999). Eutrophication: impacts of excess nutrient inputs on freshwater, marine, and terrestrial ecosystems. *Environ Pollut* **100**, 179-96.

Smyth, D. R., Bowman, J. L., and Meyerowitz, E. M. (1990). Early flower development in *Arabidopsis*. *Plant Cell* **2**, 755-67.

Sondergaard, T. E., Schulz, A., and Palmgren, M. G. (2004). Energization of transport processes in plants. roles of the plasma membrane H^+-ATPase. *Plant Physiol* **136**, 2475-82.

Sreenivasulu, N., Borisjuk, L., Junker, B. H., Mock, H. P., Rolletschek, H., Seiffert, U., Weschke, W., and Wobus, U. (2010). Barley grain development toward an integrative view. *Int Rev Cell Mol Biol* **281**, 49-89.

Stadler, R., Lauterbach, C., and Sauer, N. (2005). Cell-to-cell movement of green fluorescent protein reveals post-phloem transport in the outer integument and identifies symplastic domains in *Arabidopsis* seeds and embryos. *Plant Physiol* **139**, 701-712.

Stefanovic, A., Ribot, C., Rouached, H., Wang, Y., Chong, J., Belbahri, L., Delessert, S., and Poirier, Y. (2007). Members of the PHO1 gene family show limited functional redundancy in phosphate transfer to the shoot, and are regulated by phosphate deficiency via distinct pathways. *Plant J* **50**, 982-94.

Stigter, K. A., and Plaxton, W. C. (2015). Molecular mechanisms of phosphorus metabolism and transport during leaf senescence. *Plants* **4**, 773-98.

Sze, H., Li, X., and Palmgren, M. G. (1999). Energization of plant cell membranes by H+-pumping ATPases. Regulation and biosynthesis. *Plant Cell* **11**, 677-90.

Teakle, N. L., and Tyerman, S. D. (2010). Mechanisms of Cl- transport contributing to salt tolerance. *Plant Cell Environ* **33**, 566-589.

Thibaud, J. B., Davidian, J. C., Sentenac, H., Soler, A., and Grignon, C. (1988). H^+ cotransports in corn roots as related to the surface pH shift induced by active H^+ excretion. *Plant Physiol* **88**, 1469-73.

Thieme, C. J., Rojas-Triana, M., Stecyk, E., Schudoma, C., Zhang, W., Yang, L., Miñambres, M., Walther, D., Schulze, W. X., Paz-Ares, J., Scheible, W.-R., and Kragler, F. (2015). Endogenous *Arabidopsis* messenger RNAs transported to distant tissues. *Nature Plants* **1**, 15025.

Thompson, A. J., Bown, D., Yaish, S., and Gatehouse, J. A. (1991). Differential expression of seed storage protein genes in the pea-legJ subfamily; sequence of gene-legK. *Biochem Physiol Pflanz* **187**, 1-12.

Thomson, C. J., and Bolger, T. P. (1993). Effect of seed phosphorus concentration on the emergence and growth of subterranean clover (*Trifolium subterraneum*). *In* "Plant Nutrition: From Genetic Engineering to Field Practice", pp. 353-356. Kluwer Academic Publishers, Dordrecht.

Thorne, J. H. (1985). Phloem unloading of C-assimilates and N-assimilates in developing seeds. *Annu Rev Plant Physiol Plant Mol Biol* **36**, 317-343.

Thornley, J. H., and Parsons, A. J. (2014). Allocation of new growth between shoot, root and mycorrhiza in relation to carbon, nitrogen and phosphate supply: teleonomy with maximum growth rate. *J Theor Biol* **342**, 1-14.

Ticconi, C. A., and Abel, S. (2004). Short on phosphate: plant surveillance and countermeasures. *Trends in Plant Science* **9**, 548-555.

Toledo-Ortiz, G., Huq, E., and Quail, P. H. (2003). The *Arabidopsis* basic/helix-loop-helix transcription factor family. *Plant Cell* **15**, 1749-70.

Tsunewaki, K., and Mukai, Y. (1990). Wheat Haploids Through the Salmon Method. *In* "Wheat", Vol. 13, pp. pp 460-478.

Turgeon, R. (2006). Phloem loading: How leaves gain their independence. *Bioscience* **56**, 15-24.

Turgeon, R., and Ayre, B. (2005). Pathways and mechanisms of phloem loading, in Vascular Transport in Plants. *In* "Elsevier/Academic, Oxford".

Tyerman, S. D. (1992). Anion channels in plants. *Annu Rev Plant Physiol Plant Mol Biol* **43**, 351-373.

U.S. (Geological Survey 2016). Mineral commodity summaries. 202.

Ullrich-Eberius, C. I., Novacky, A., and van Bel, A. J. E. (1984). Phosphate uptake in *Lemna gibba* G1: energetics and kinetics. . *Planta* **161**, 46-52.

van Caseele, L., Mills, J., Sunner, M., and Gillespie, R. (1982). Cytological study of palisade development in the seed coat of Candle canola. *Can J Bot* **60**, 2469–2475.

Veneklaas, E. J., Lambers, H., Bragg, J., Finnegan, P. M., Lovelock, C. E., Plaxton, W. C., Price, C. A., Scheible, W. R., Shane, M. W., White, P. J., and Raven, J. A. (2012). Opportunities for improving phosphorus-use efficiency in crop plants. *New Phytol* **195**, 306-20.

Vergutz, L., Manzoni, S., Porporato, A., Novais, R. F., and Jackson, R. B. (2012). Global resorption efficiencies and concentrations of carbon and nutrients in leaves of terrestrial plants. *Ecol. Monogr.* **82**, 205–220.

Versaw, W. K., and Harrison, M. J. (2002). A chloroplast phosphate transporter, PHT2;1, influences allocation of phosphate within the plant and phosphate-starvation responses. *Plant Cell* **14**, 1751-66.

Viola, R., Roberts, A. G., Haupt, S., Gazzani, S., Hancock, R. D., Marmiroli, N., Machray, G. C., and Oparka, K. J. (2001). Tuberization in potato involves a switch from apoplastic to symplastic phloem unloading. *Plant Cell* **13**, 385-398.

Walker, N. A., Patrick, J. W., Zhang, W. H., and Fieuw, S. (1995). Efflux of photosynthate and acid from developing seed coats of *Phaseolus vulgaris L.* - a chemiosmotic analysis of pump-driven efflux. *J Exp Bot* **46**, 539-549.

Wang, T. L., and Hedley, C. L. (1993). Genetic and developmental analysis of the seed. *In* "In Peas: Genetics, Molecular Biology and Biochemistry". Cambridge, UK: CAB Intl.

Wang, Y., Ribot, C., Rezzonico, E., and Poirier, Y. (2004). Structure and expression profile of the *Arabidopsis* PHO1 gene family indicates a broad role in inorganic phosphate homeostasis. *Plant Physiol* **135**, 400-11.

Waters, B. M., and Grusak, M. A. (2008). Whole-plant mineral partitioning throughout the life cycle in *Arabidopsis thaliana* ecotypes Columbia, Landsberg erecta, Cape Verde Islands, and the mutant line ysl1ysl3. *New Phytologist* **177**, 389-405.

Waters, B. M., and Sankaran, R. P. (2011a). Moving micronutrients from the soil to the seeds: genes and physiological processes from a biofortification perspective. *Plant Sci* **180**, 562-74.

Waters, B. M., and Sankaran, R. P. (2011b). Moving micronutrients from the soil to the seeds: Genes and physiological processes from a biofortification perspective. *Plant Science* **180**, 562-574.

Waters, B. M., Uauy, C., Dubcovsky, J., and Grusak, M. A. (2009). Wheat (*Triticum aestivum*) NAM proteins regulate the translocation of iron, zinc, and nitrogen compounds from vegetative tissues to grain. *J Exp Bot* **60**, 4263-4274.

Watkins, J. T., Cantliffe, D. J., D.J., H., and Nell, T. A. (1985). Gibberellic acid stimulated degradation of endosperm in pepper *J. Amer. Soc. Hort. Sci.* **110**, 61-65.

Weaver, L. M., and Amasino, R. M. (2001). Senescence is induced in individually darkened Arabidopsis leaves, but inhibited in whole darkened plants. *Plant Physiol* **127**, 876-86.

Webb, M. C., and Gunning, B. E. S. (1990). Embryo sac development in *Arabidopsis thaliana* I. Megasporogenesis, including the microtubular cytoskeleton. *Sex Plant Reprod* **3**, 244-256.

Weber, H., Borisjuk, L., Heim, U., Buchner, P., and Wobus, U. (1995). Seed coat-associated invertases of fava bean control both unloading and storage functions: cloning of cDNAs and cell type-specific expression. *Plant Cell* **7**, 1835-46.

Weber, H., Borisjuk, L., and Wobus, U. (1997). Sugar import and metabolism during seed development. *Trends Plant Sci* **2**, 169-174.

Weber, H., Borisjuk, L., and Wobus, U. (2005). Molecular physiology of legume seed development. *Annu Rev Plant Biol* **56**, 253-279.

Wege, S., Khan, G. A., Jung, J. Y., Vogiatzaki, E., Pradervand, S., Aller, I., Meyer, A. J., and Poirier, Y. (2016). The EXS Domain of PHO1 Participates in the Response of Shoots to Phosphate Deficiency via a Root-to-Shoot Signal. *Plant Physiol* **170**, 385-400.

Wege, S., and Poirier, Y. (2014). Expression of the mammalian Xenotropic Polytropic Virus Receptor 1 (XPR1) in tobacco leaves leads to phosphate export. *FEBS Lett* **588**, 482-9.

Werner, D., Gerlitz, N., and Stadler, R. (2011). A dual switch in phloem unloading during ovule development in *Arabidopsis*. *Protoplasma* **248**, 225-35.

Western, T. L., Skinner, D. J., and Haughn, G. W. (2000). Differentiation of mucilage secretory cells of the *Arabidopsis* seed coat. *Plant Physiol* **122**, 345-56.

White, P. J., and Broadley, M. R. (2001). Chloride in soils and its uptake and movement within the plant: A review. *Ann Bot* **88**, 967-988.

White, P. J., and Broadley, M. R. (2009). Biofortification of crops with seven mineral elements often lacking in human diets - iron, zinc, copper, calcium, magnesium, selenium and iodine. *New Phytologist* **182**, 49-84.

Willemse, M. T. M., and van Went, J. L. (1984). The female gametophyte. *In Embryology of Angiosperms B.M. Johri, ed (Berlin: Springer-Verlag)*, 159–196.

Windsor, J. B., Symonds, V. V., Mendenhall, J., and Lloyd, A. M. (2000). *Arabidopsis* seed coat development: morphological differentiation of the outer integument. *Plant J* **22**, 483-93.

Wolswinkel, P., Ammerlaan, A., and Koerselmankooij, J. (1992). Effect of the osmotic environment on K^+ and $Mg^{-}2^+$ release from the seed coat and cotyledons of developing seeds of *Vicia faba* and *Pisum sativum*: Evidence for a stimulation of efflux from the vacuole at high cell turgor. *J Exp Bot* **43**, 681-693.

Xu, Y., Tao, Y., Cheung, L. S., Fan, C., Chen, L. Q., Xu, S., Perry, K., Frommer, W. B., and Feng, L. (2014). Structures of bacterial homologues of SWEET transporters in two distinct conformations. *Nature* **515**, 448-52.

Yoneyama, T., Ishikawa, S., and Fujimaki, S. (2015). Route and Regulation of Zinc, Cadmium, and Iron Transport in Rice Plants (*Oryza sativa L.*) during Vegetative Growth and Grain Filling: Metal Transporters, Metal Speciation, Grain Cd Reduction and Zn and Fe Biofortification. *Int J Mol Sci* **16**, 19111-29.

Zhang, M., Nyborg, M., and Mcgill, W. B. (1990). Phosphorus concentration in Barley (*Hordeum vulgare L.*) seed - Influence on seedling growth and dry-matter production. *Plant Soil* **122**, 79-83.

Zhang, W. H., Zhou, Y. C., Dibley, K. E., Tyerman, S. D., Furbank, R. T., and Patrick, J. W. (2007). Nutrient loading of developing seeds. *Funct Plant Biol* **34**, 314-331.

Zhang, W. Y., Xu, Y. C., Li, W. L., Yang, L., Yue, X., Zhang, X. S., and Zhao, X. Y. (2014). Transcriptional analyses of natural leaf senescence in maize. *PLoS One* **9**, e115617.

Zhang, X. Y., Wang, X. L., Wang, X. F., Xia, G. H., Pan, Q. H., Fan, R. C., Wu, F. Q., Yu, X. C., and Zhang, D. P. (2006). A shift of Phloem unloading from symplasmic to apoplasmic pathway is involved in developmental onset of ripening in grape berry. *Plant Physiol* **142**, 220-32.

Zhou, Y., Qu, H., Dibley, K. E., Offler, C. E., and Patrick, J. W. (2007). A suite of sucrose transporters expressed in coats of developing legume seeds includes novel pH-independent facilitators. *Plant J* **49**, 750-64.

Zhu, Y. G., and Smith, S. E. (2001). Seed phosphorus (P) content affects growth, and P uptake of wheat plants and their association with arbuscular mycorrhizal (AM) fungi. *Plant Soil* **231**, 105-112.

Zimmerli, C., Ribot, C., Vavasseur, A., Bauer, H., Hedrich, R., and Poirier, Y. (2012). PHO1 expression in guard cells mediates the stomatal response to abscisic acid in *Arabidopsis*. *Plant J* **72**, 199-211.

Annex 1

In this annex, all the nutrient transporters that are included in table 4 of page 85 are represented schematically according to the http://seedgenenetwork.net/.

Phosphate Transporters

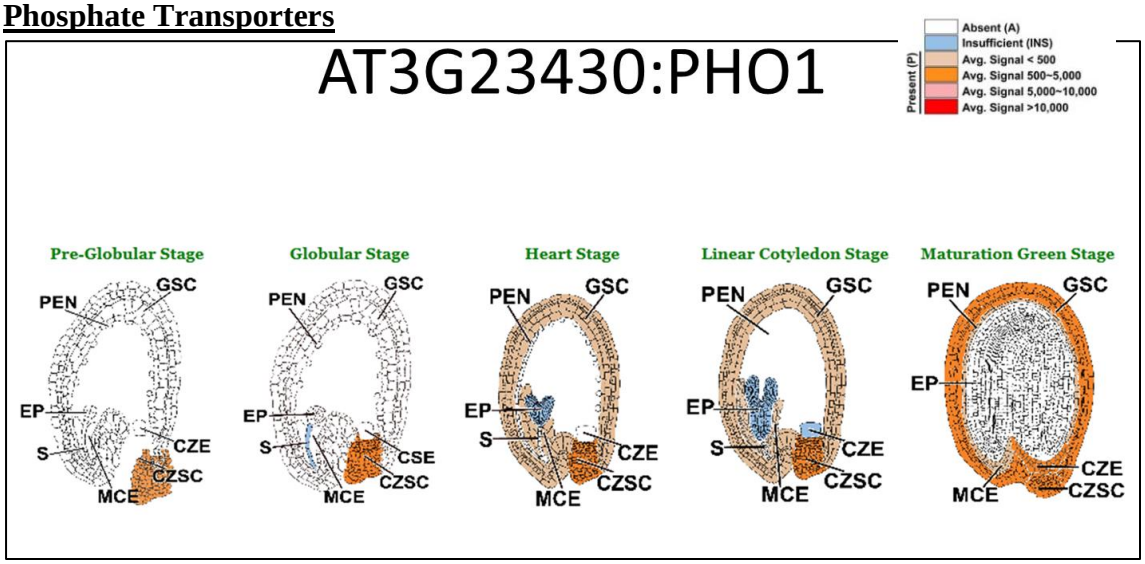

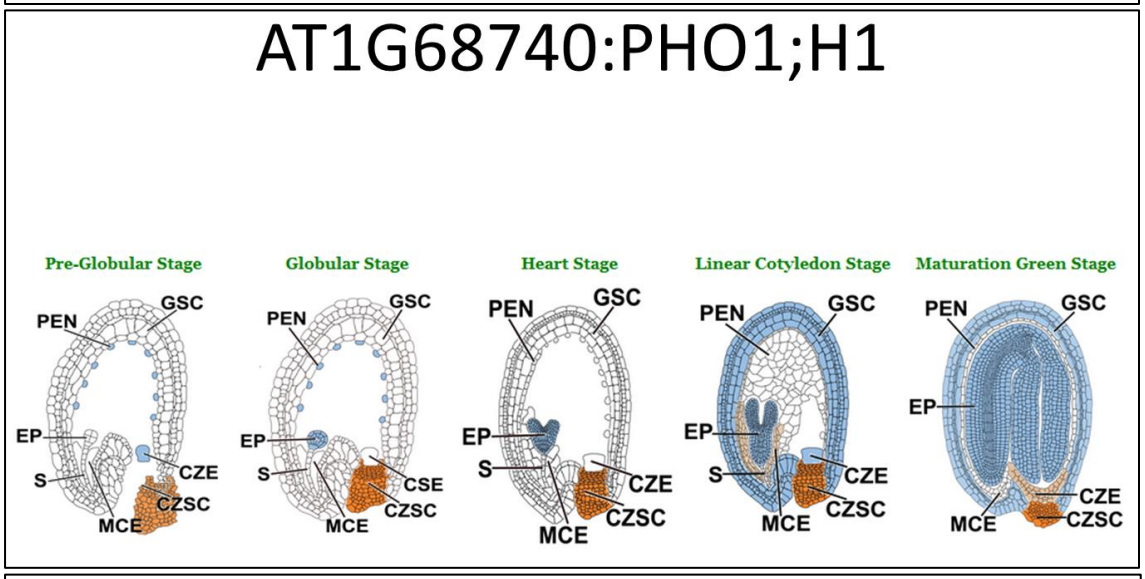

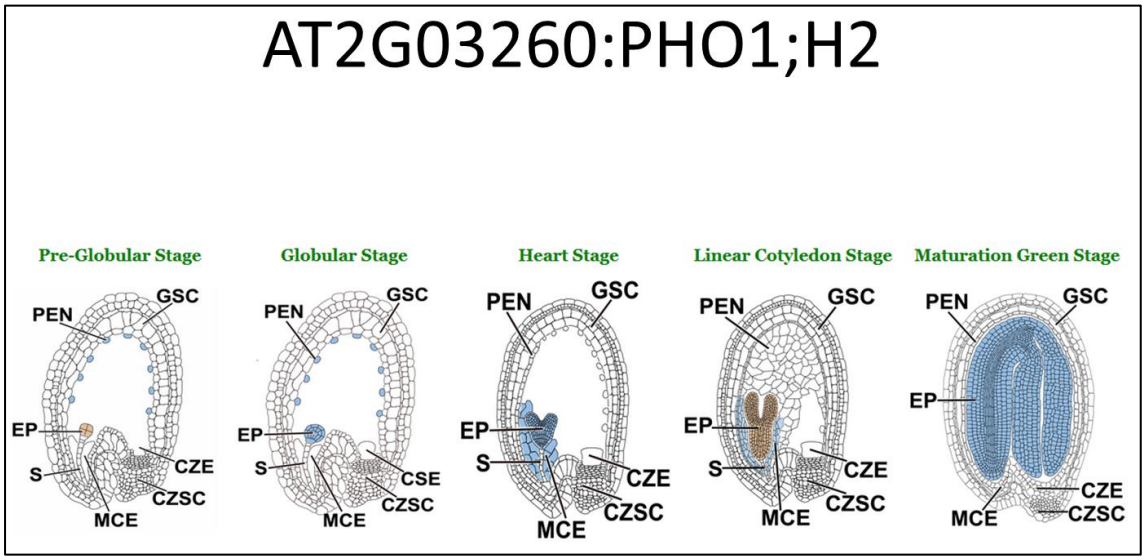

AT1G14040:PHO1;H3

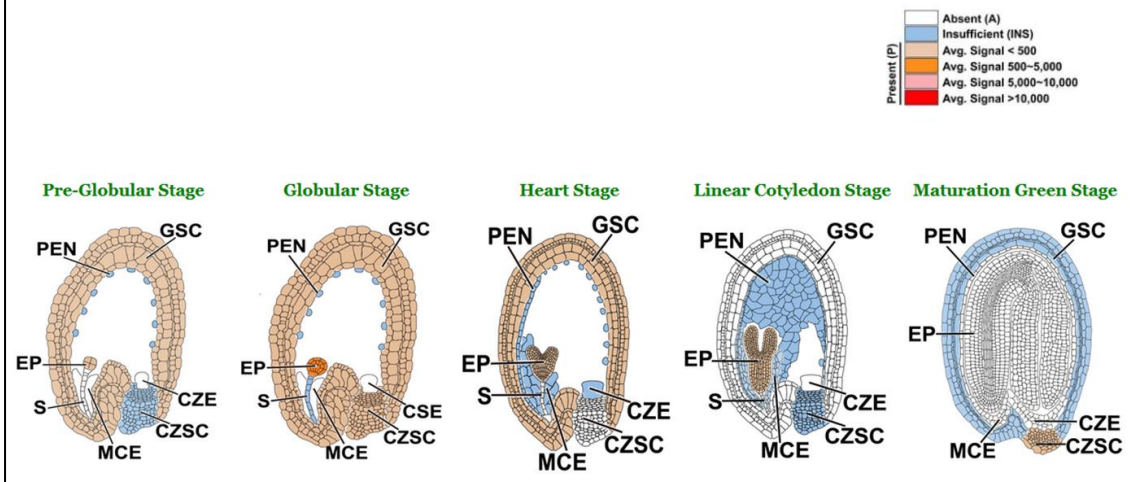

AT4G25350:PHO1;H4

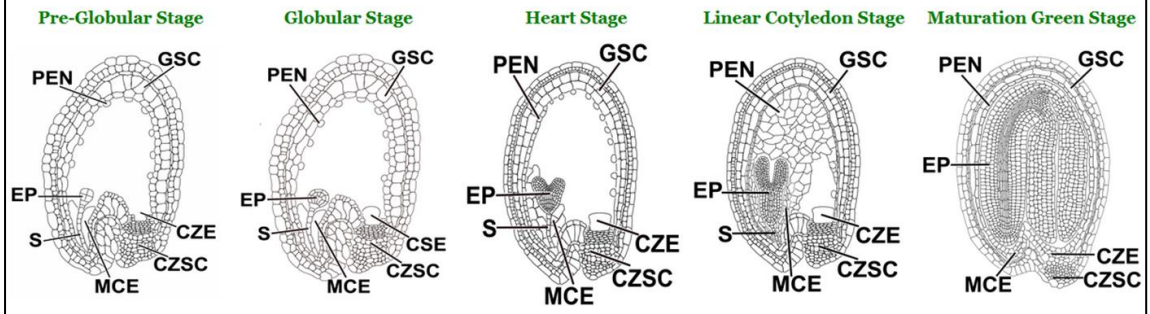

AT2G03240:PHO1;H5

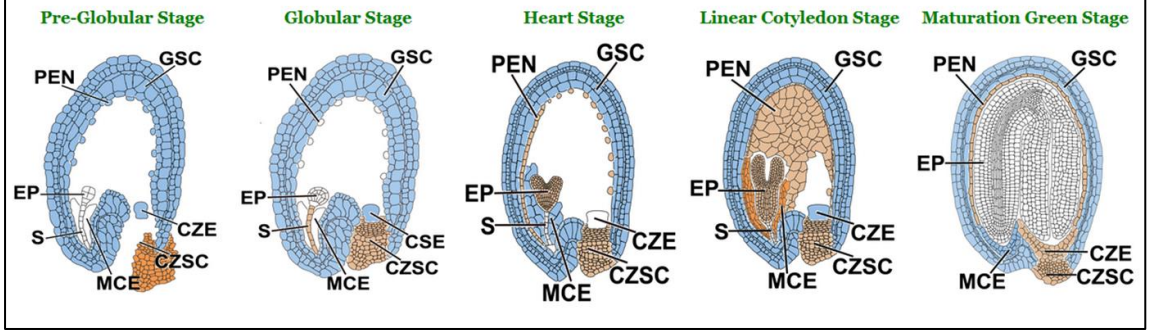

AT1G26730:PHO1;H7

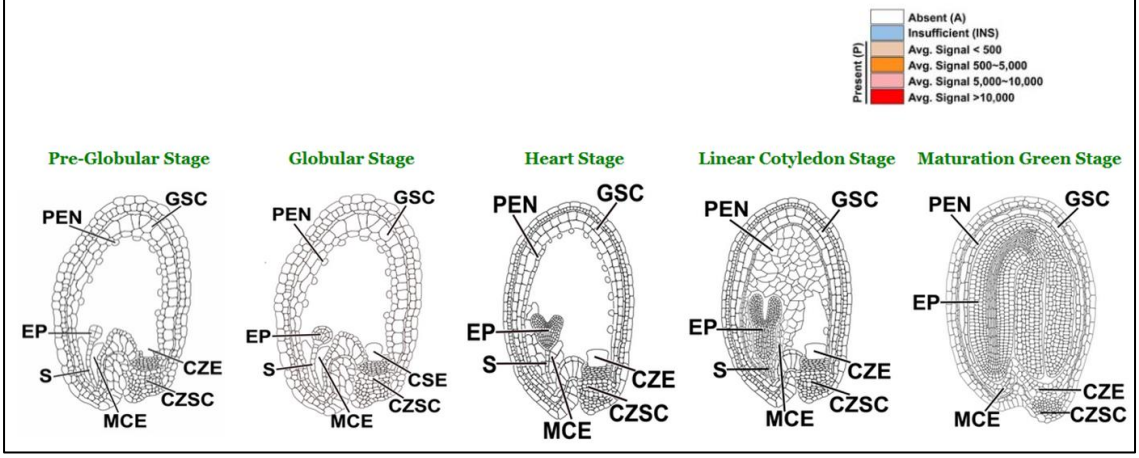

AT1G35350:PHO1;H8

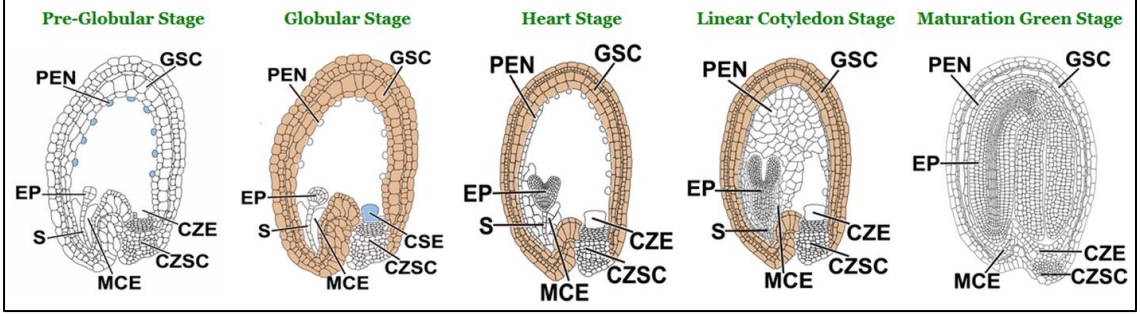

AT1G69480:PHO1;H10

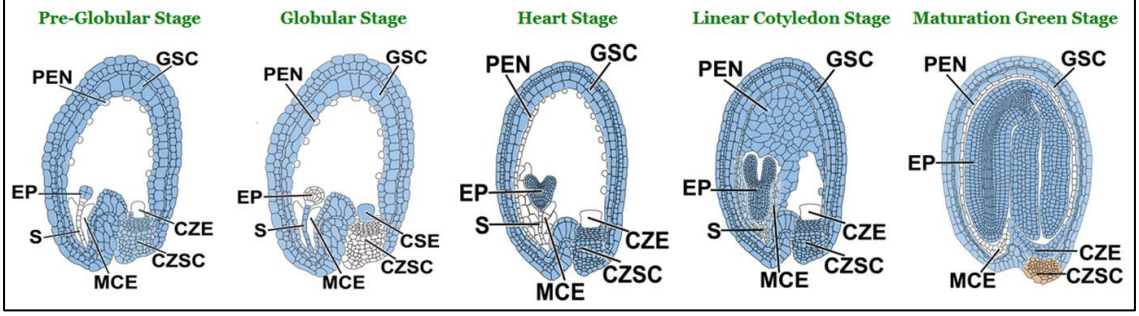

AT5G43350:PHT1.1(AtPT1)

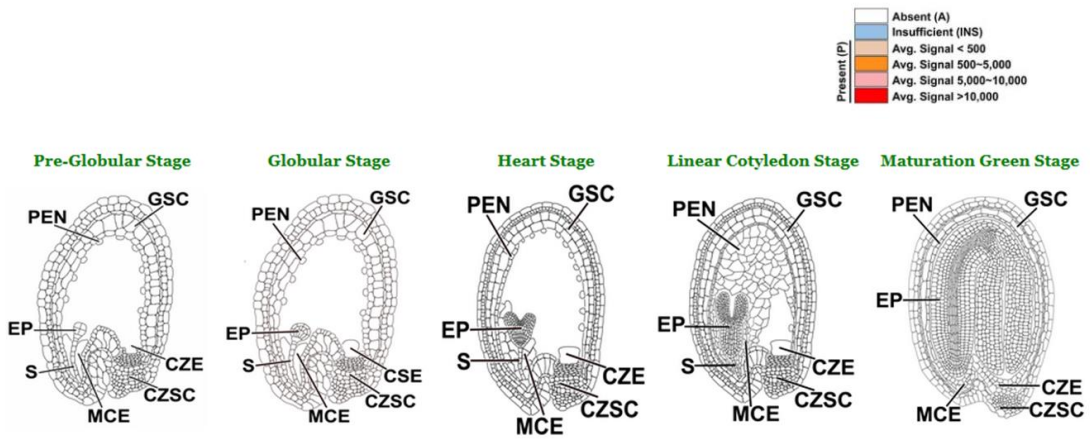

AT5G43370:PHT1.2

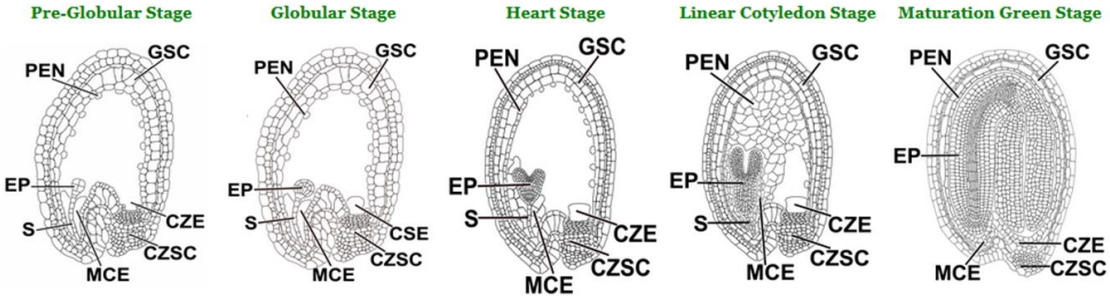

AT5G43360:PHT1.3(AtPT4)

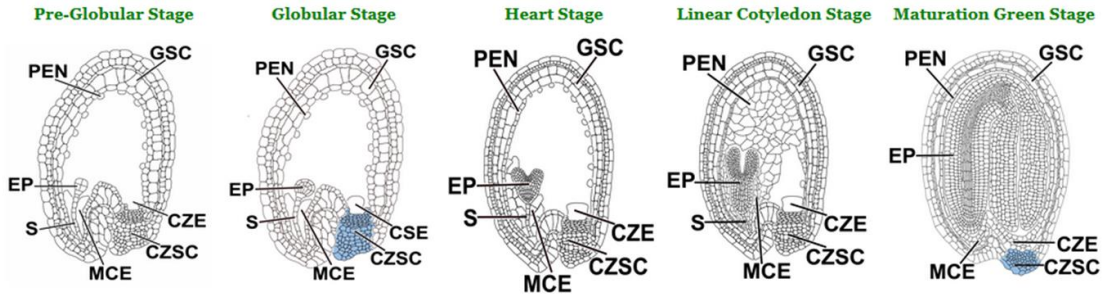

AT2G38940:PHT1.4(AtPT2)

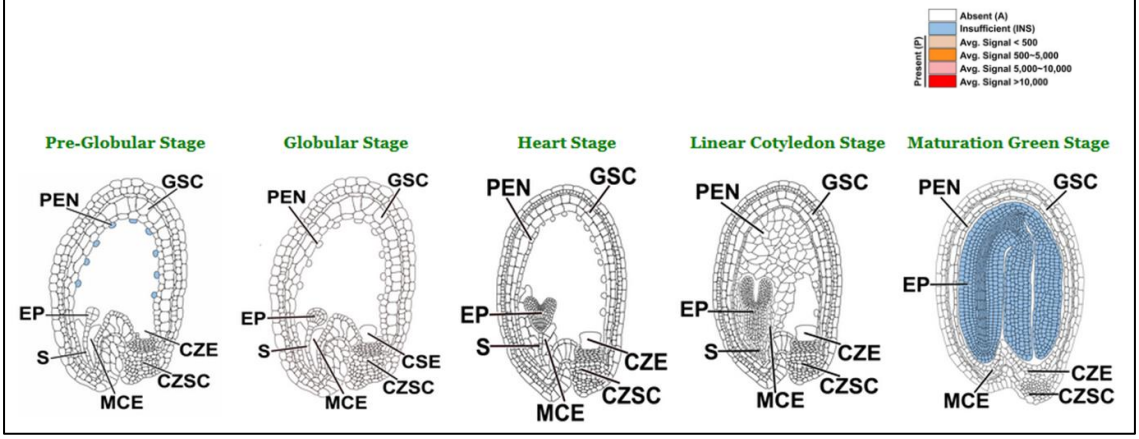

AT2G32830:PHT1.5

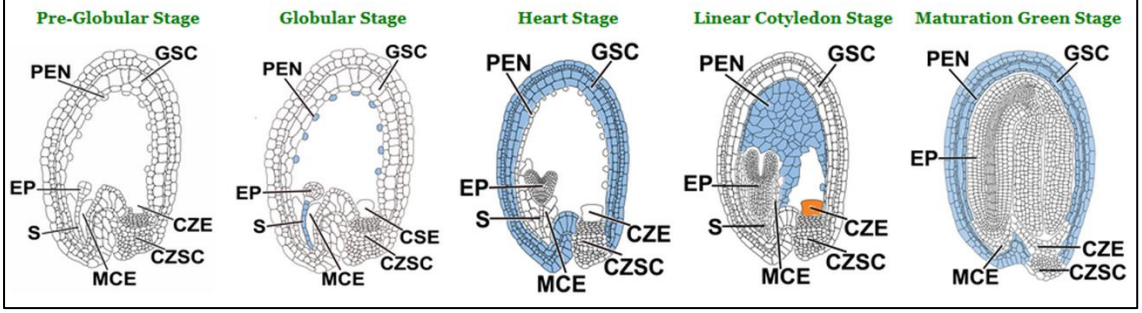

AT5G43340:PHT1.6

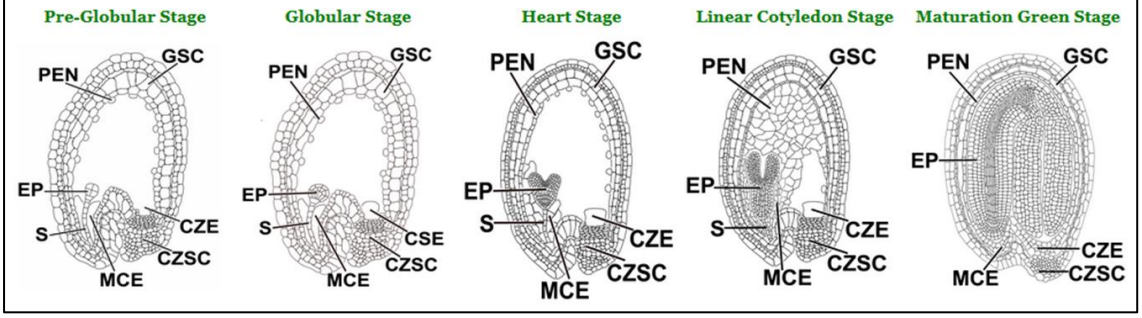

AT3G54700:PHT1.7

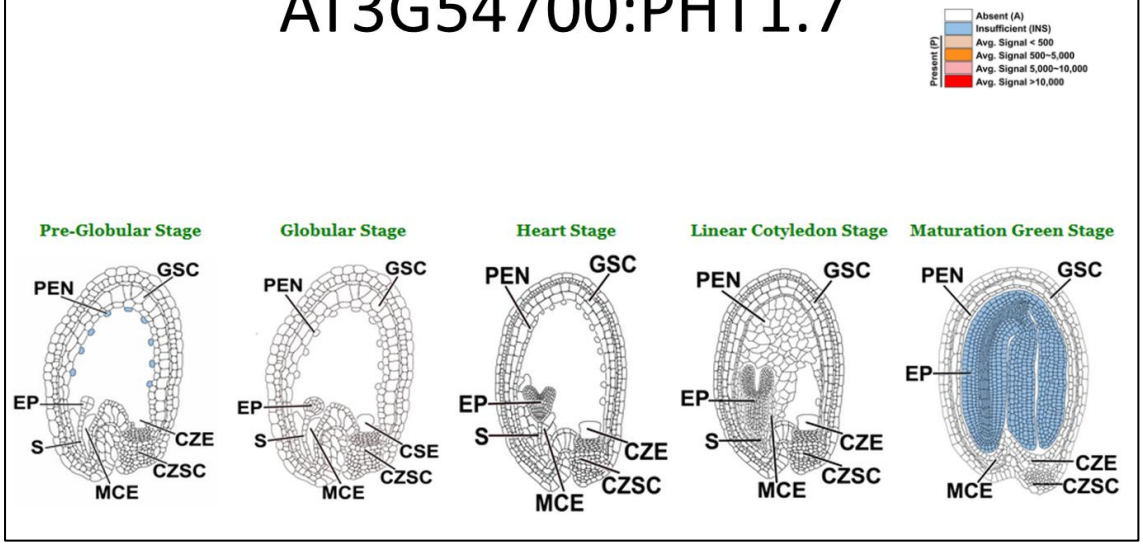

AT1G20860.1 :PHT1.8

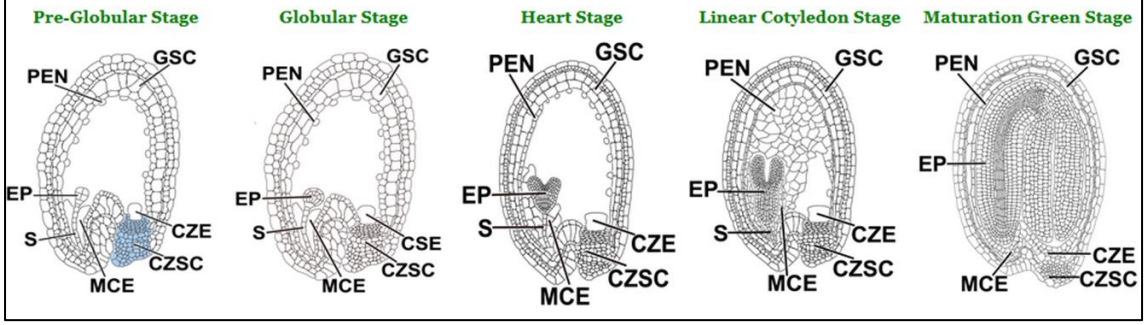

AT1G76430:PHT1.9

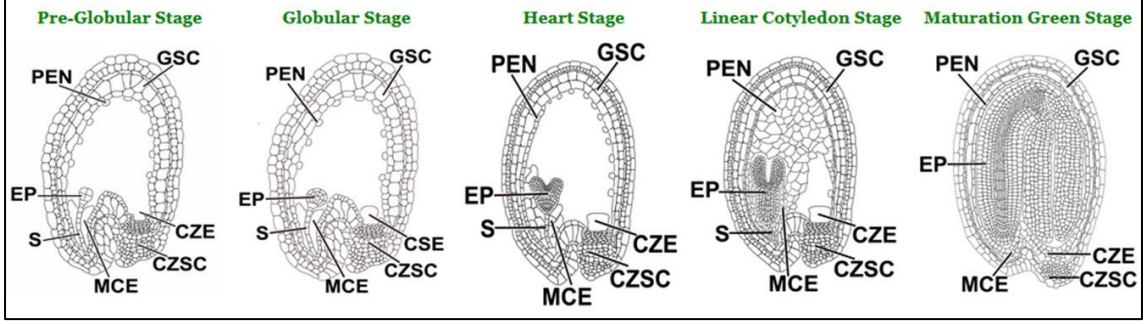

AT3G26570:PHT2.1

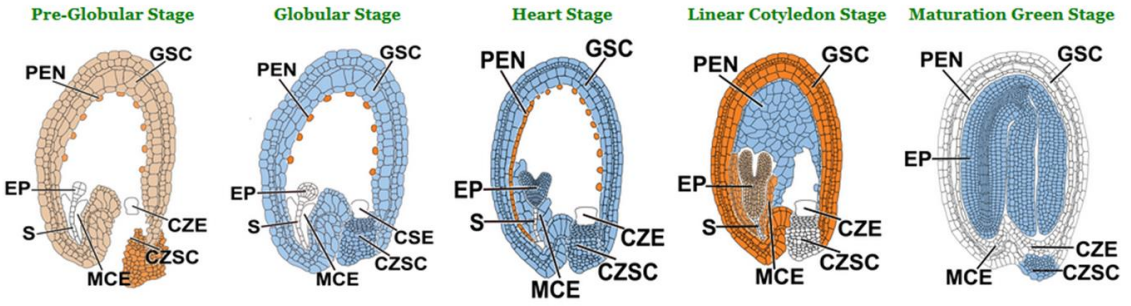

AT5G14040:PHT3.1

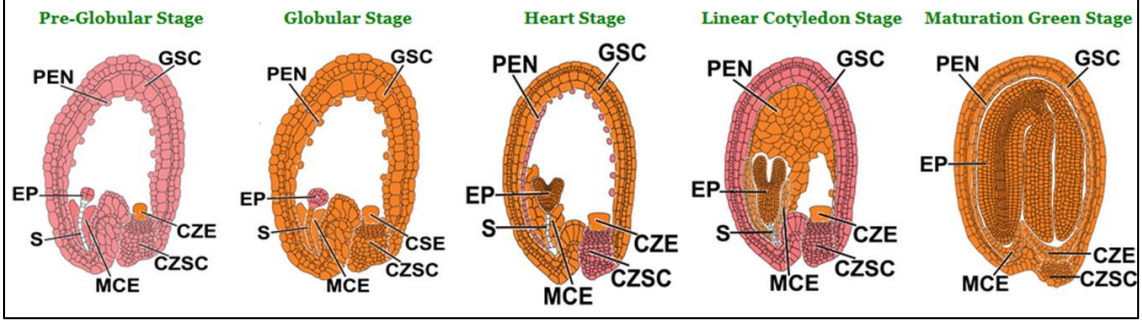

AT3G48850:PHT3.2

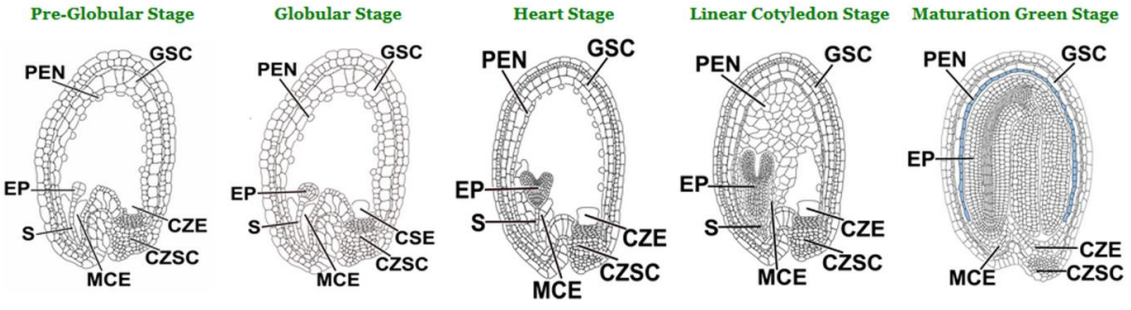

AT2G17270:PHT3.3

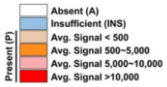

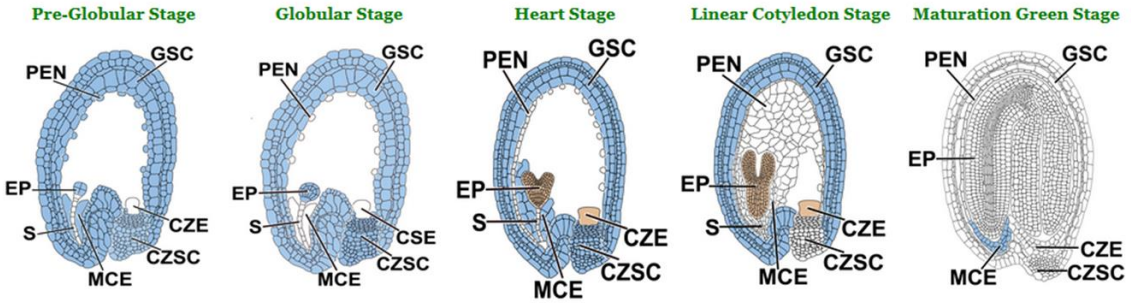

AT2G29650:PHT4.1

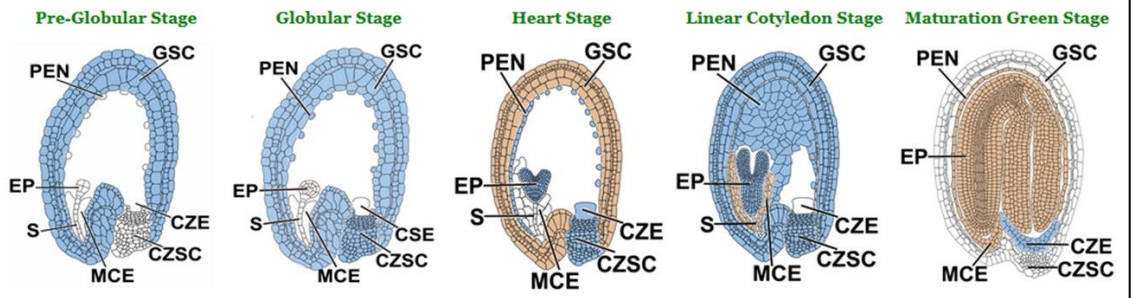

AT2G38060:PHT4.2

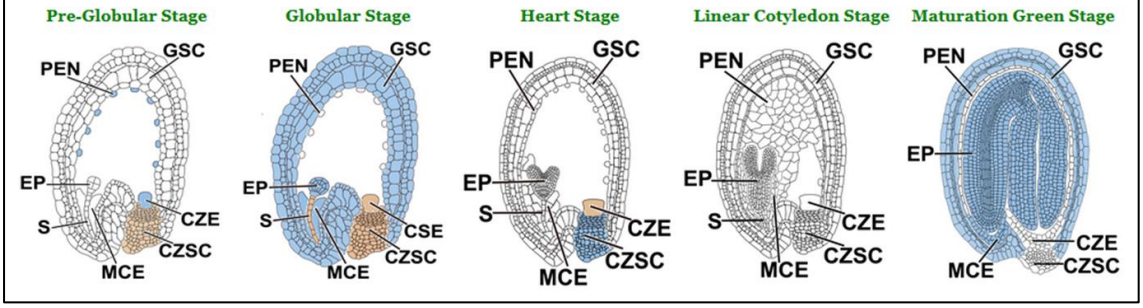

AT3G46980:PHT4.3

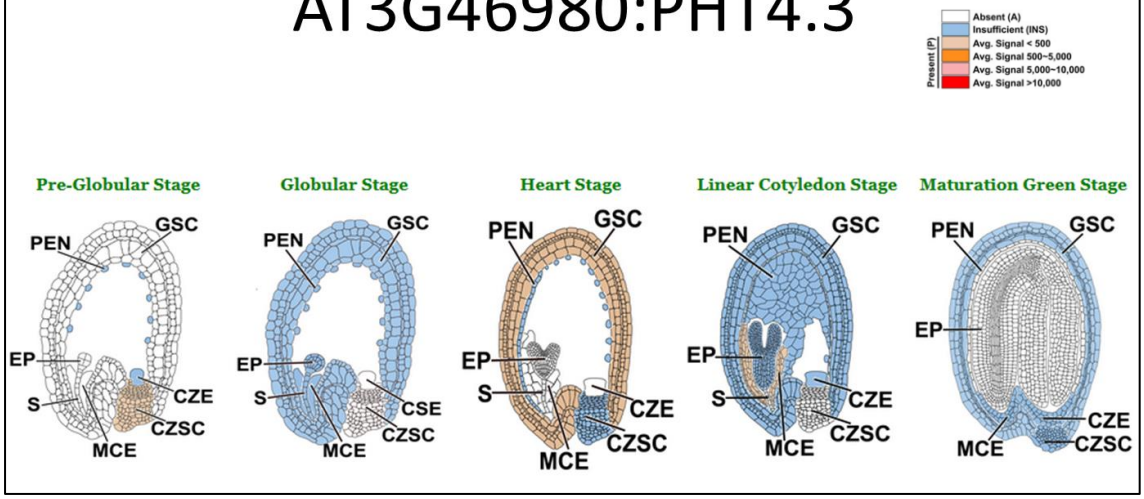

AT4G24460:PHT4.4

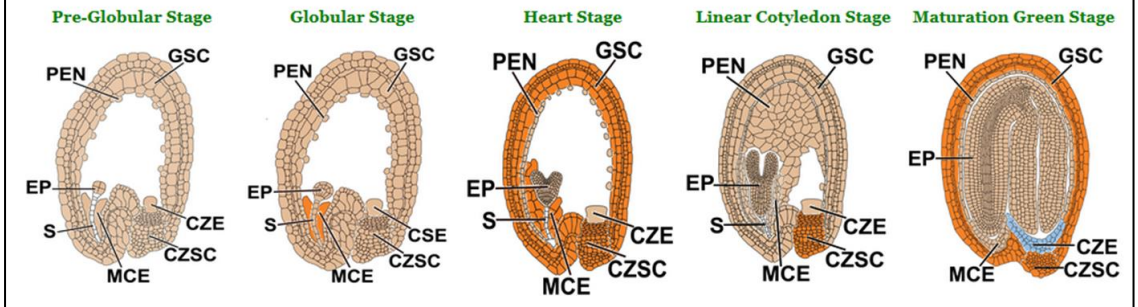

AT5G20380:PHT4.5

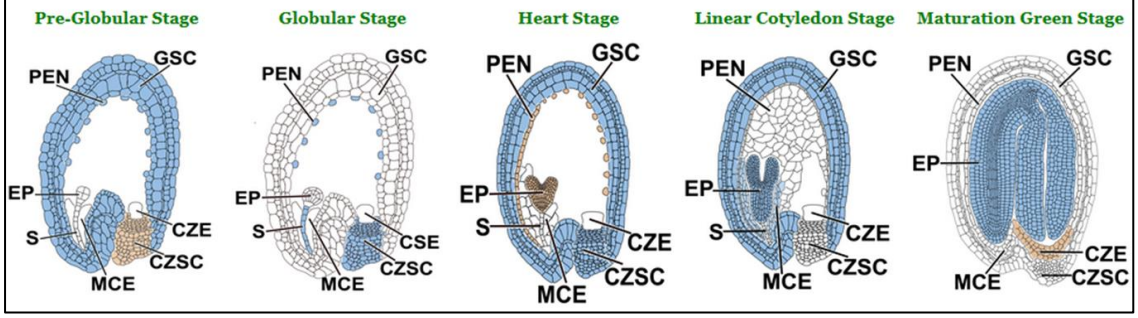

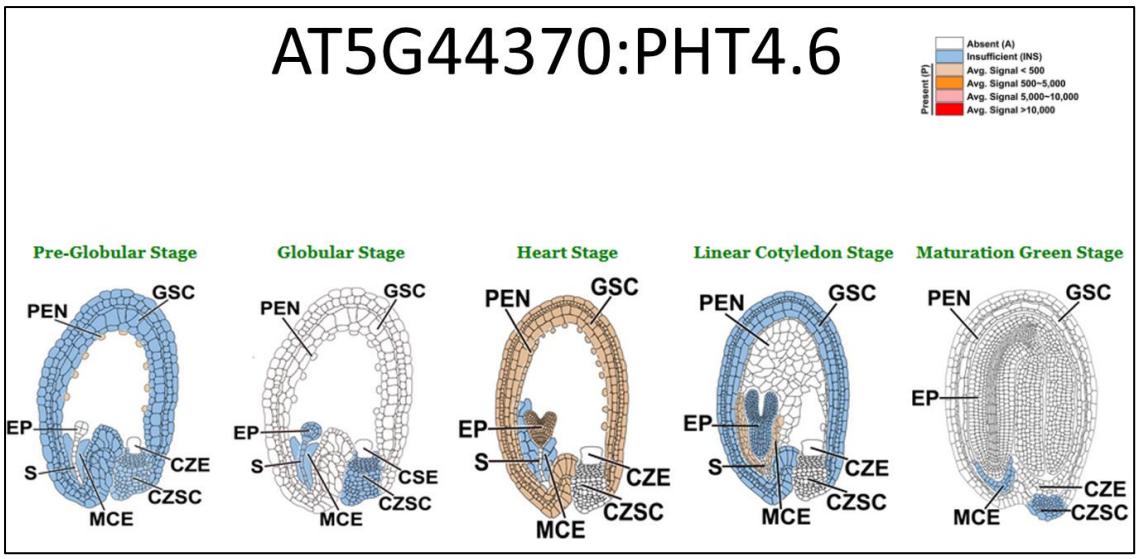

Boron transporters

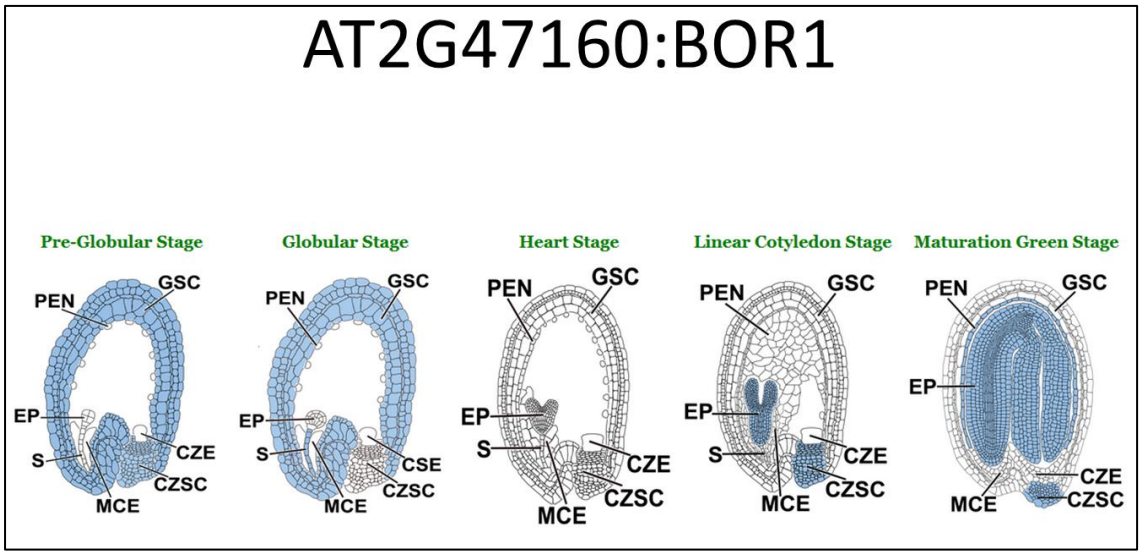

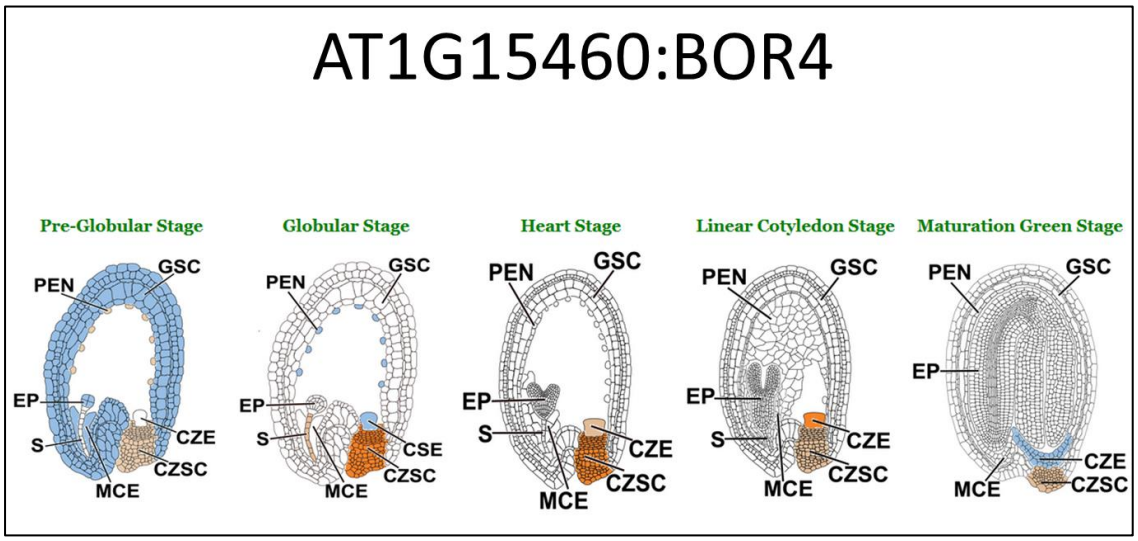

Potassium transporters

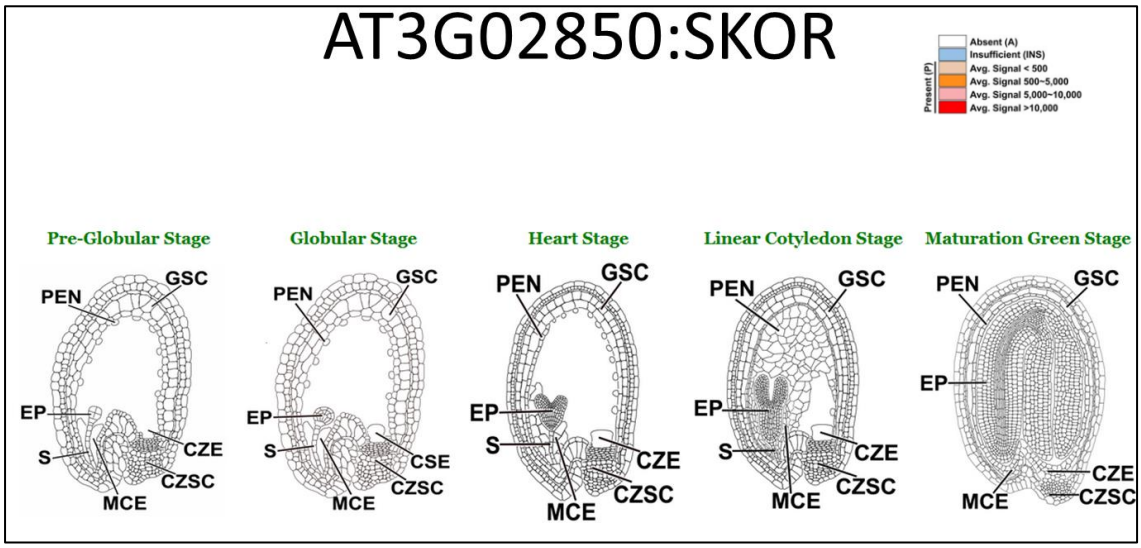

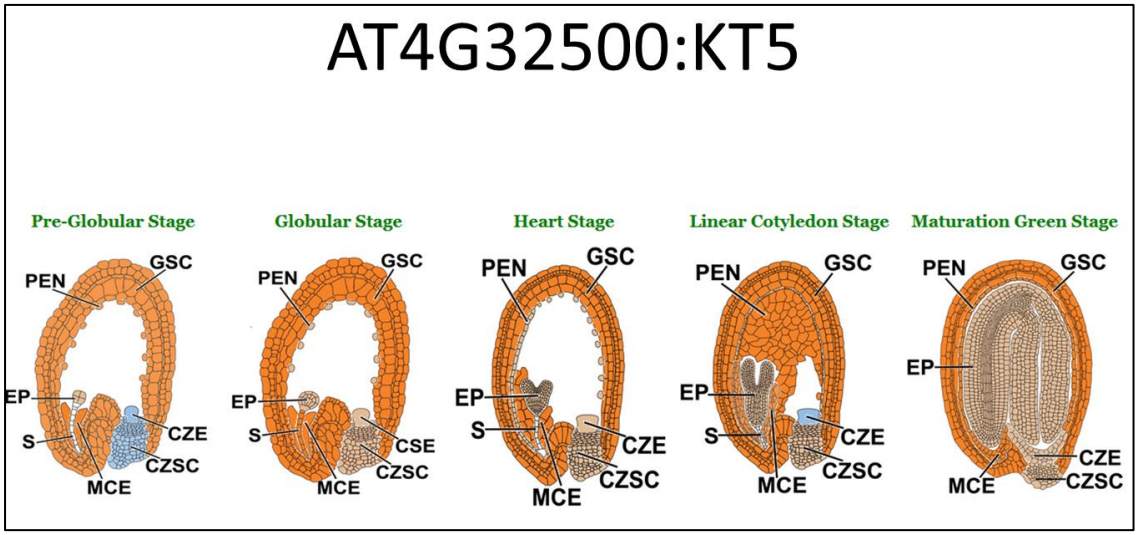

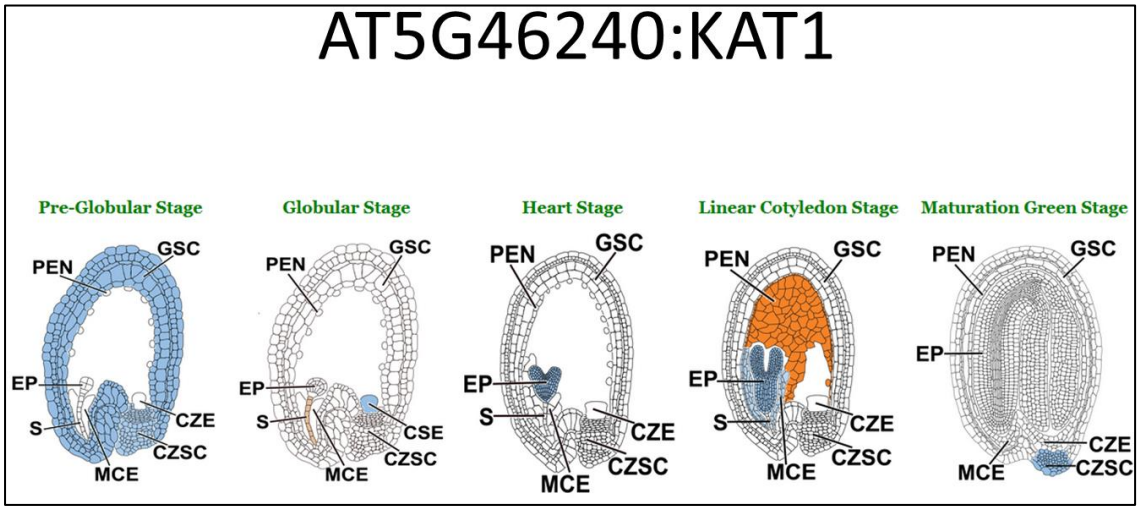

AT4G18290:KAT2

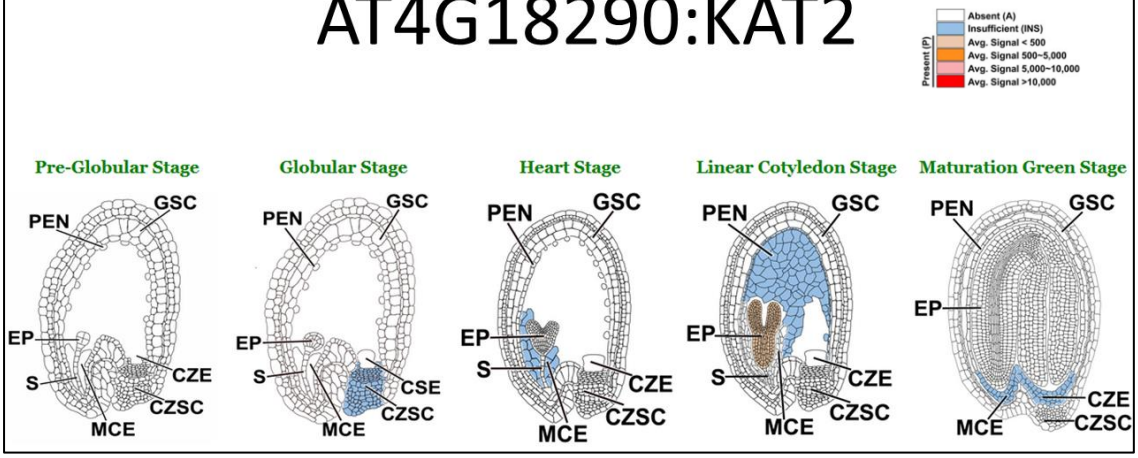

AT4G13420.1:HAK5

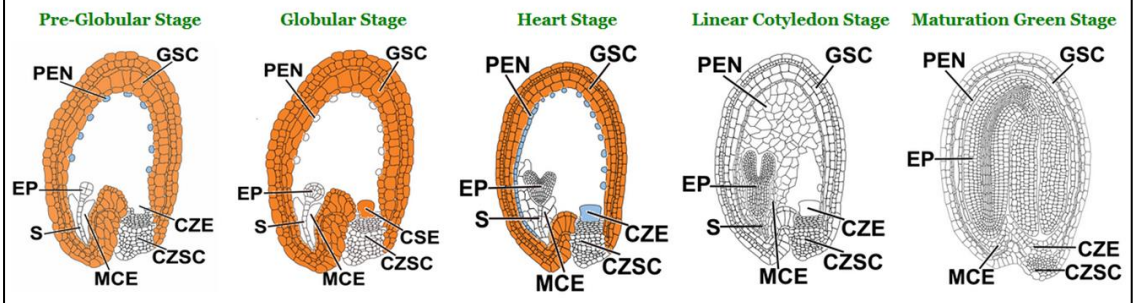

AT2G26650:AKT1 OR KT1

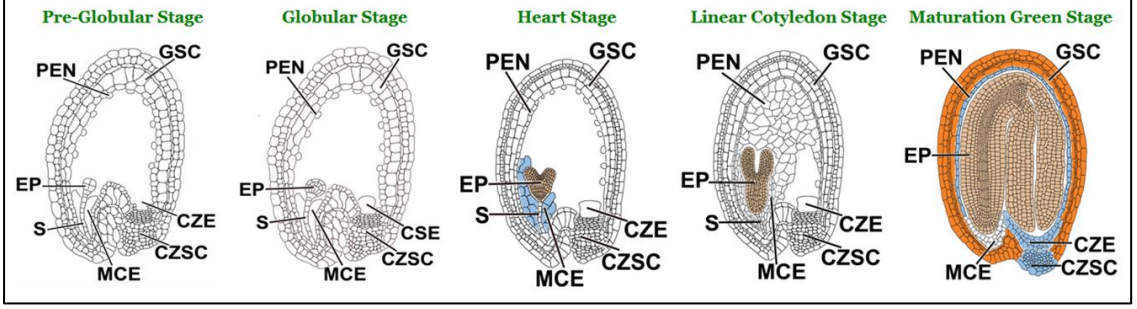

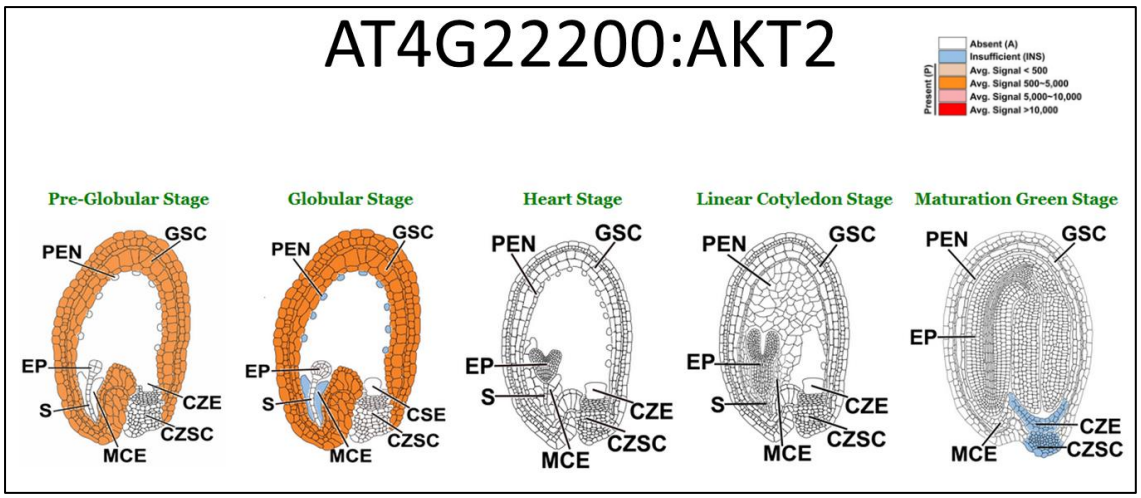

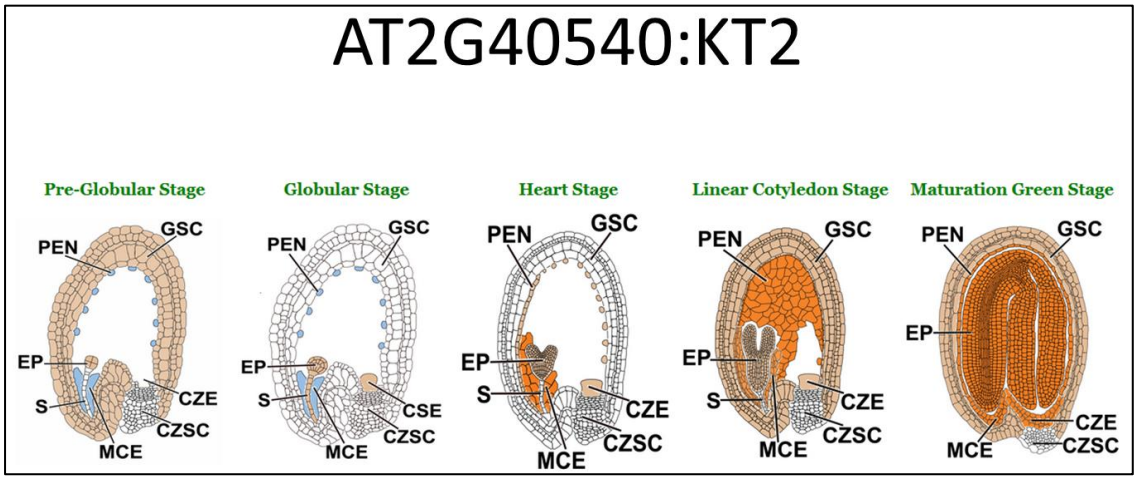

Chlorine transporters

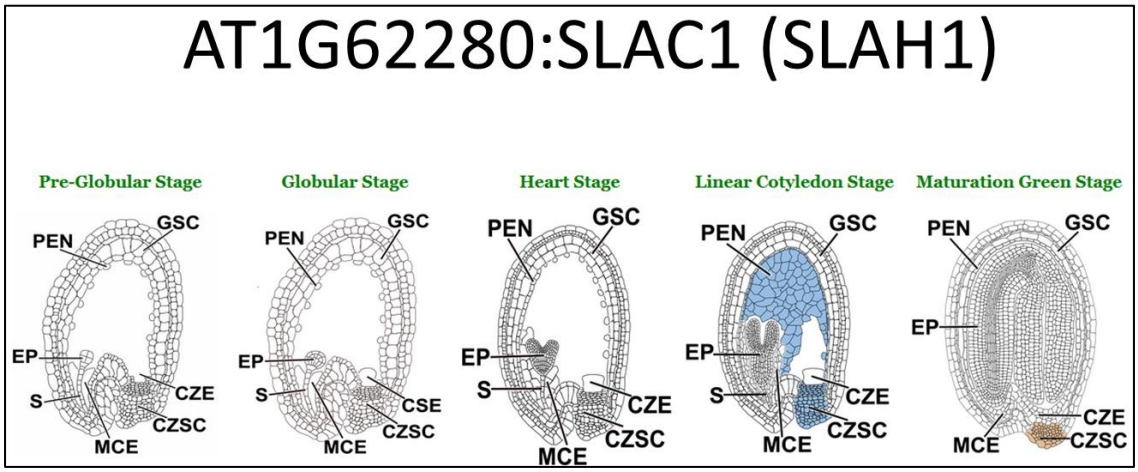

Iron transporters

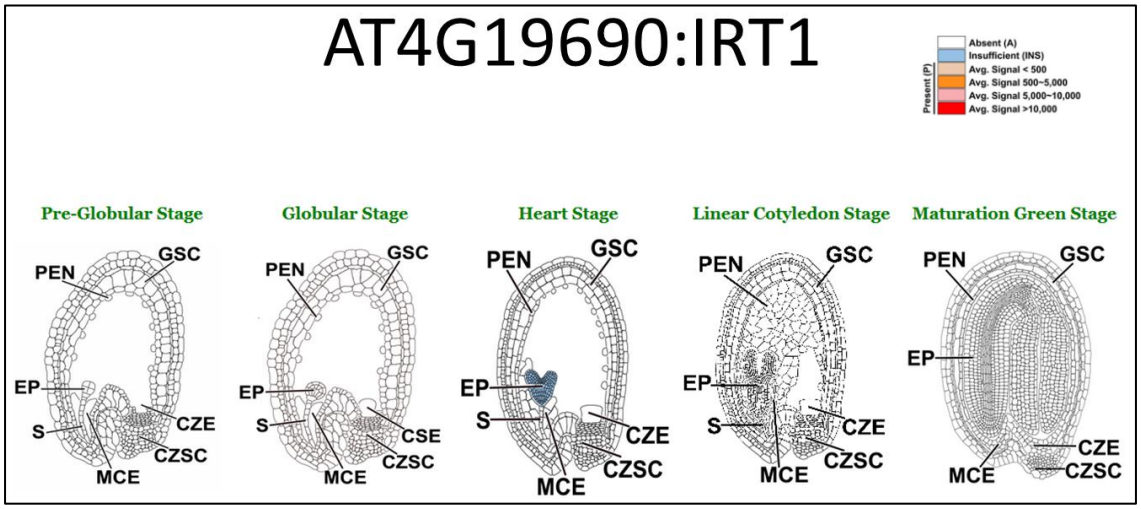

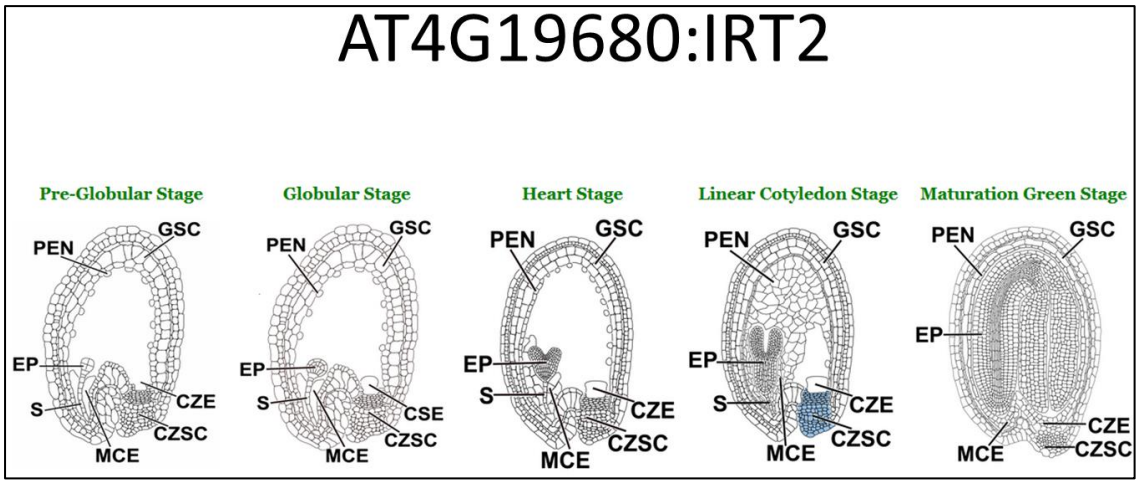

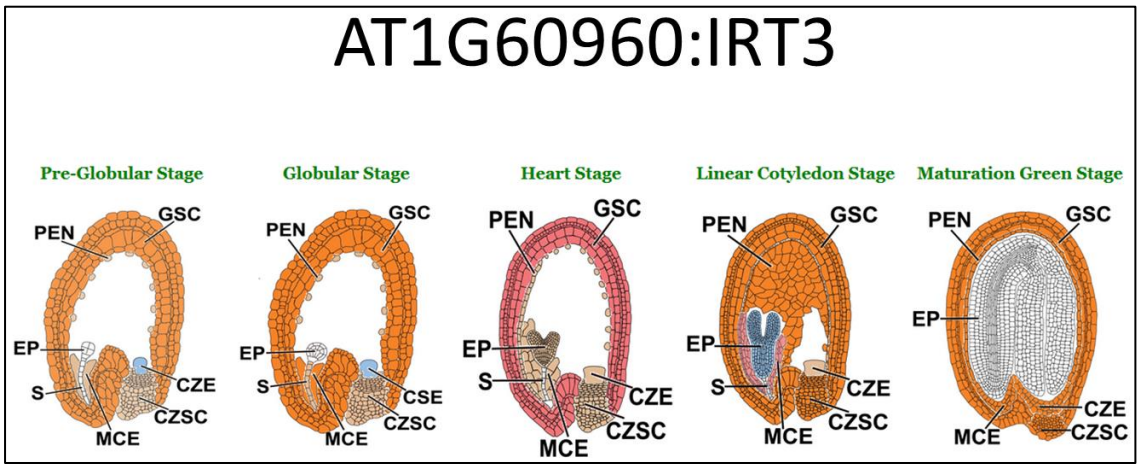

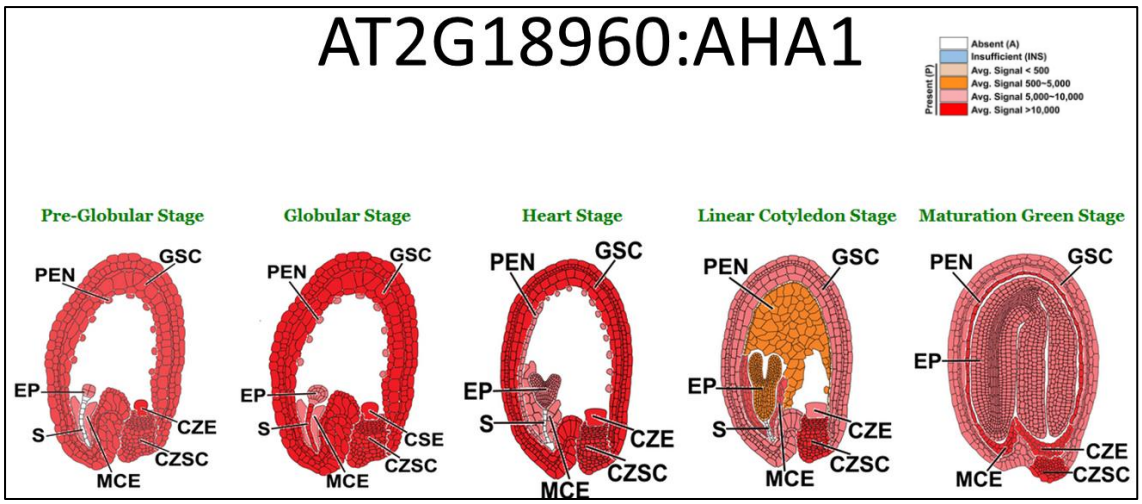

Mn and Zn transporters

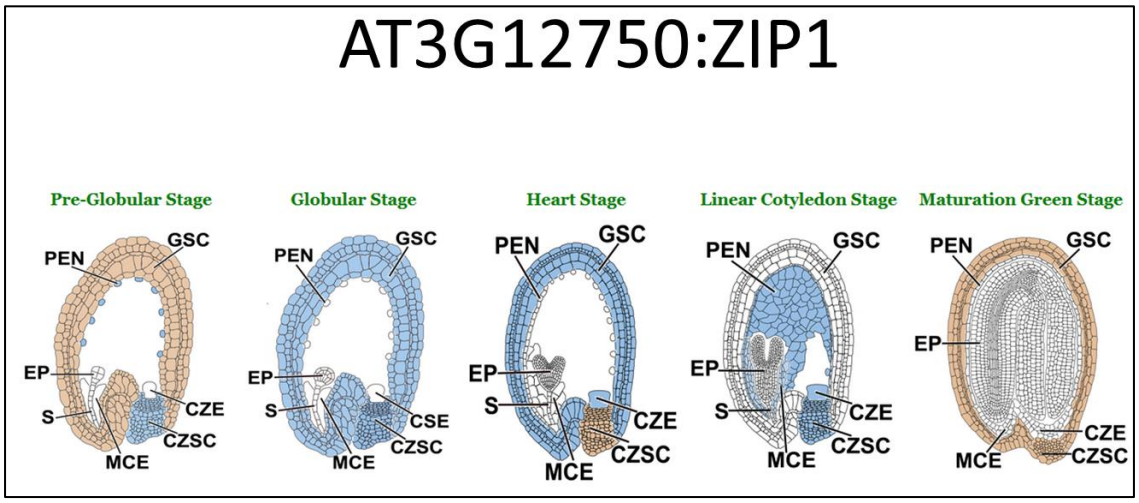

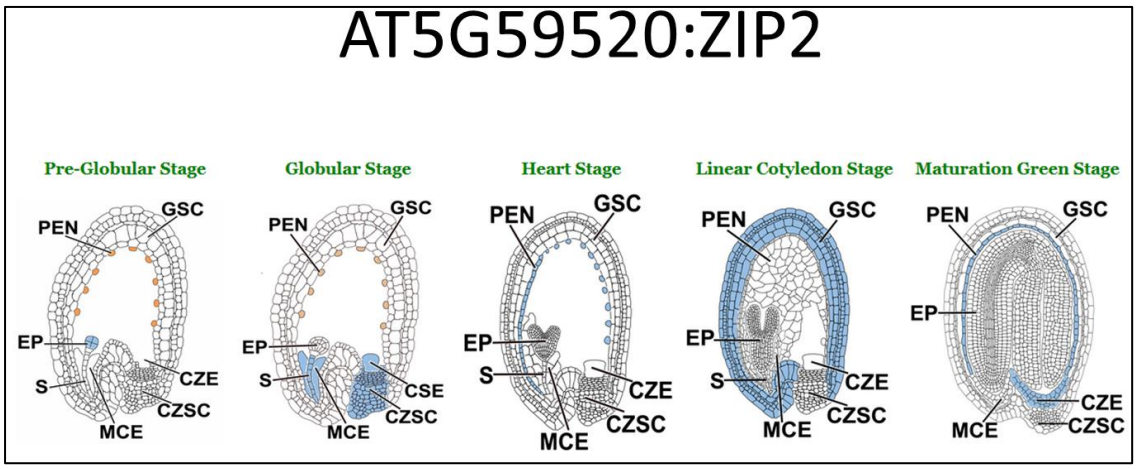

AT2G04032:ZIP7

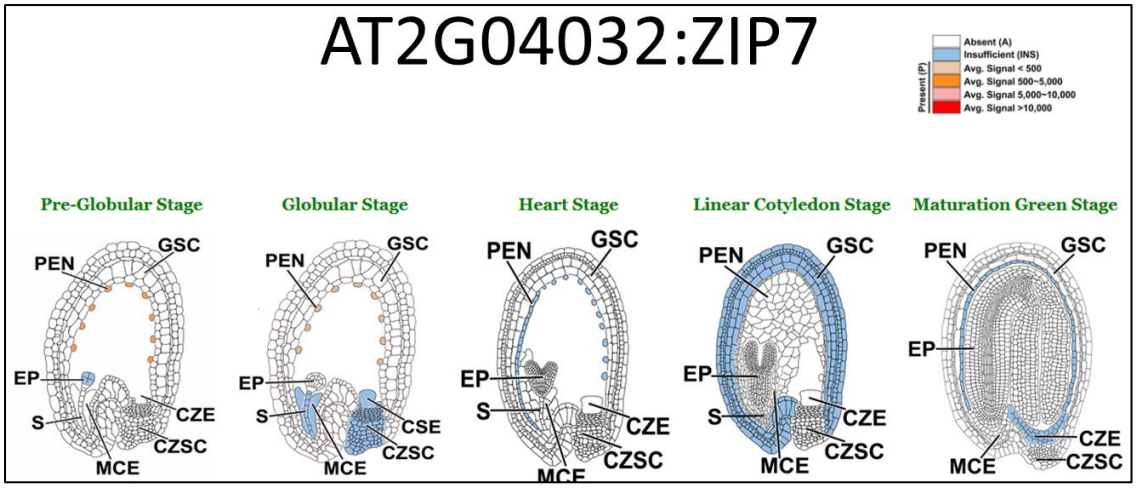

AT1G55910:ZIP11

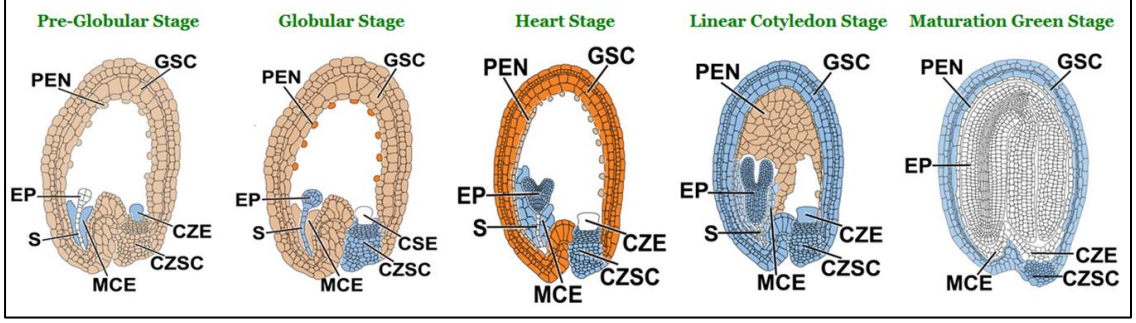

Nitrogen and Amino acid transporters

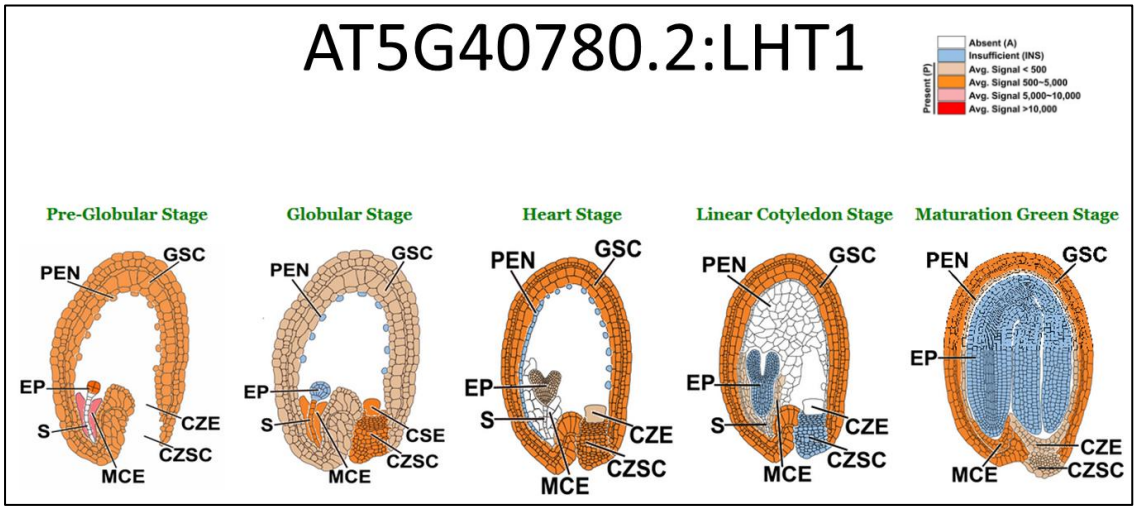

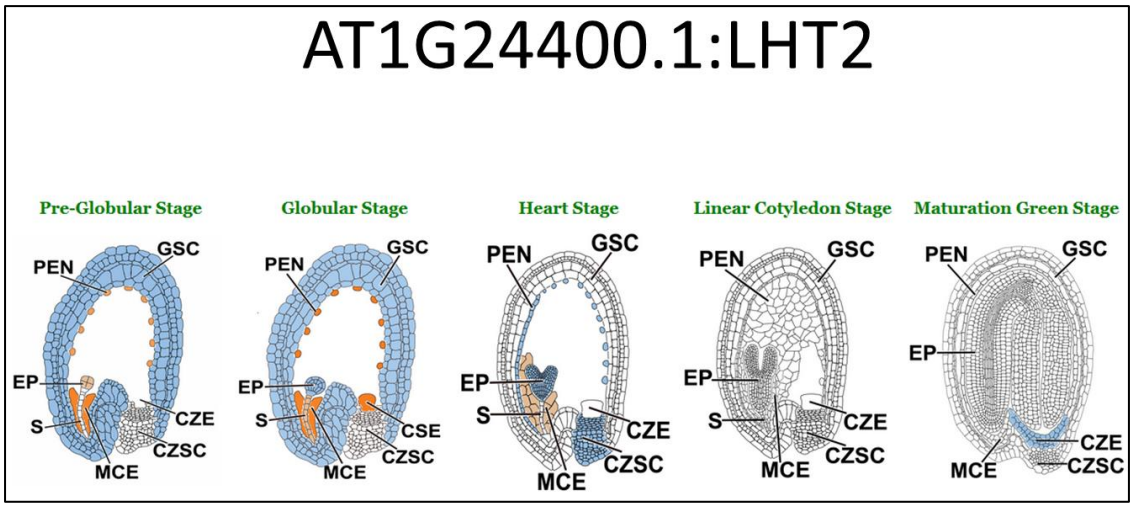

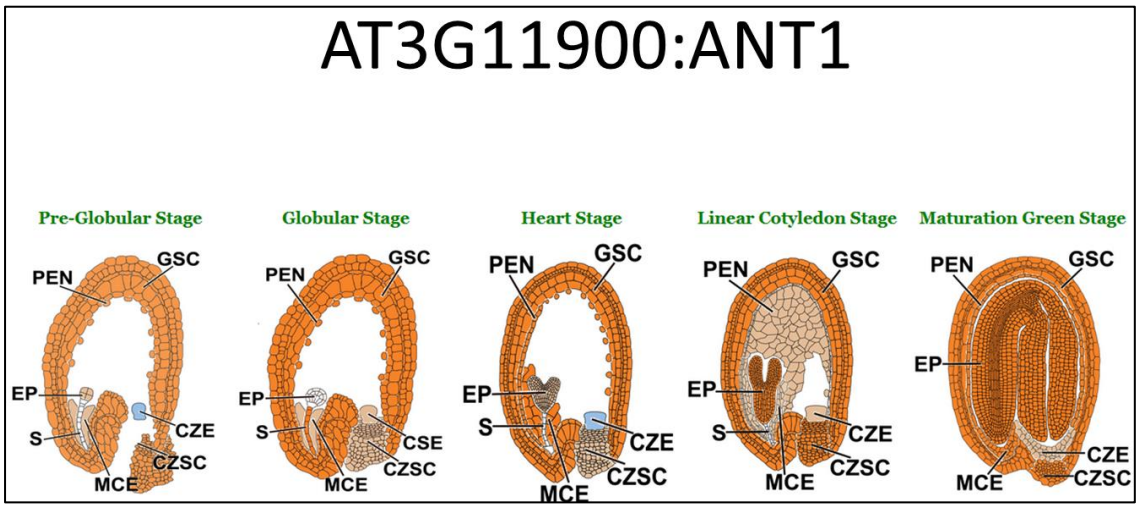

AT4G21120:CAT1 or AAT1

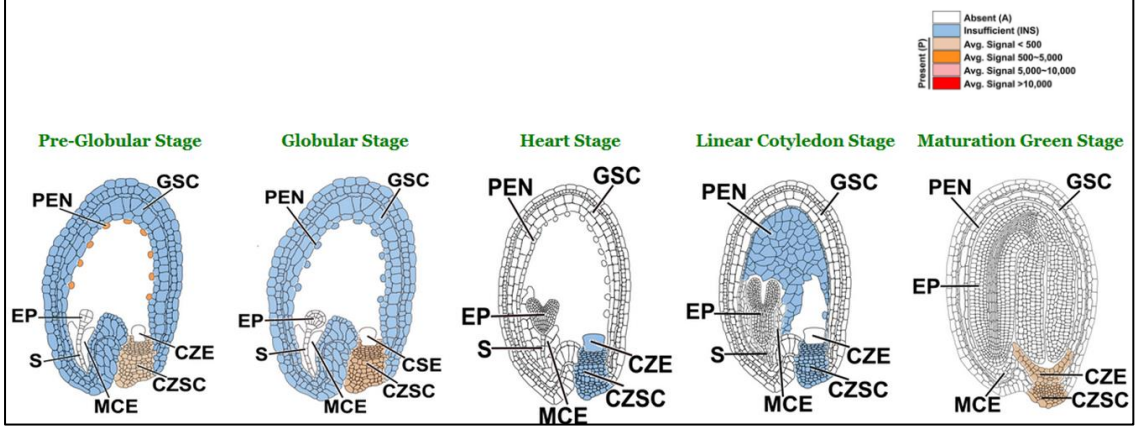

AT2G34960:CAT5

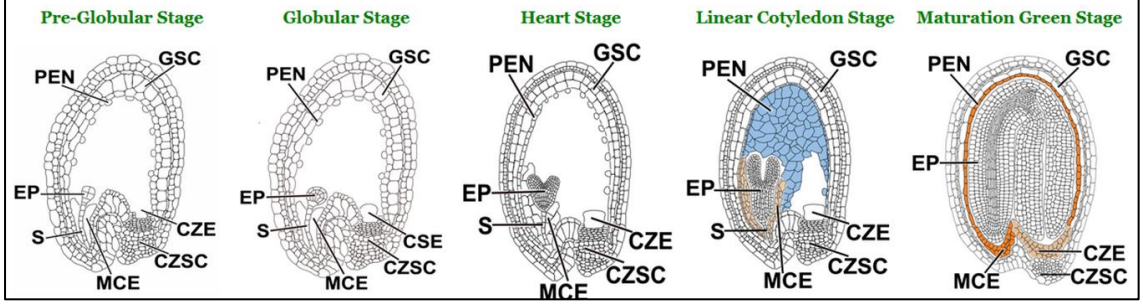

AT5G04770:CAT6

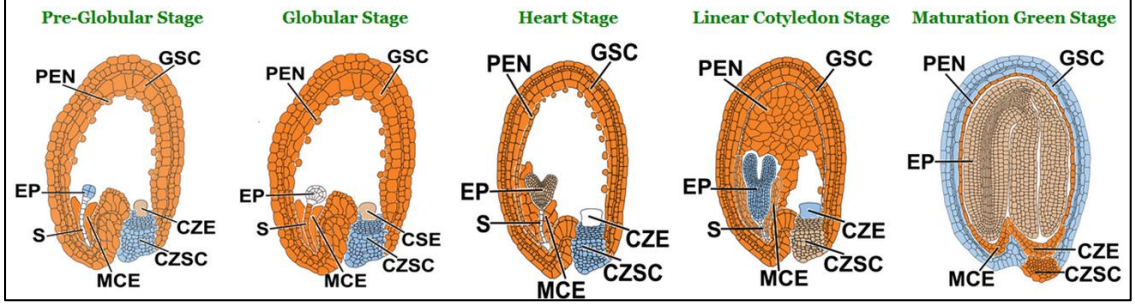

AT2G33820:BAC1

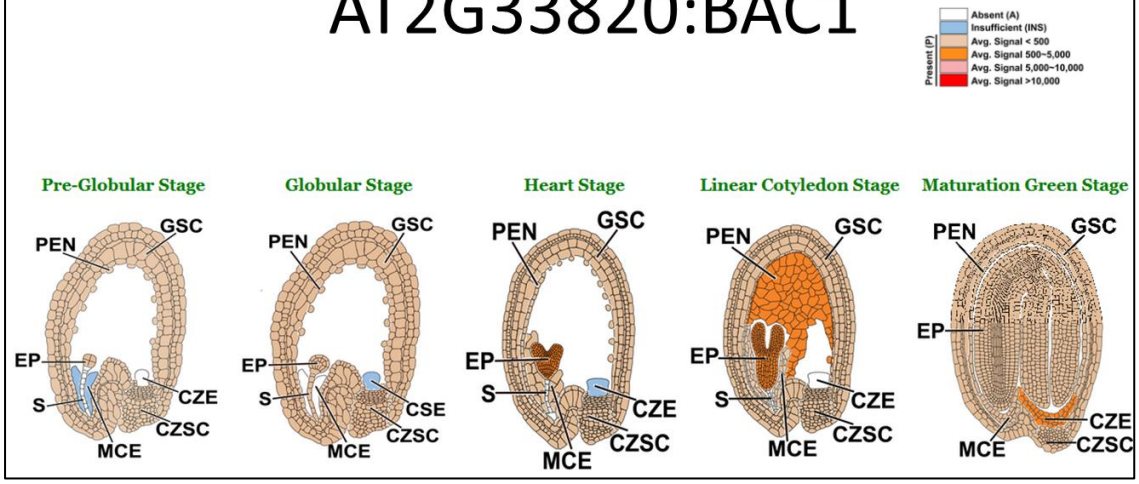

AT1G79900.1:BAC2

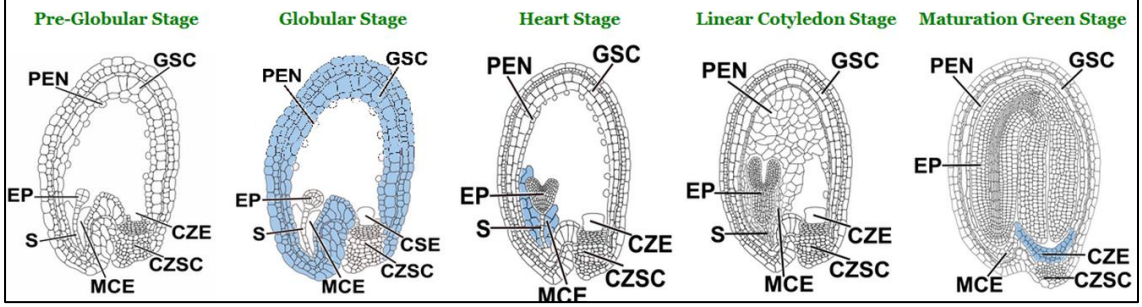

AT1G12110:NRT1

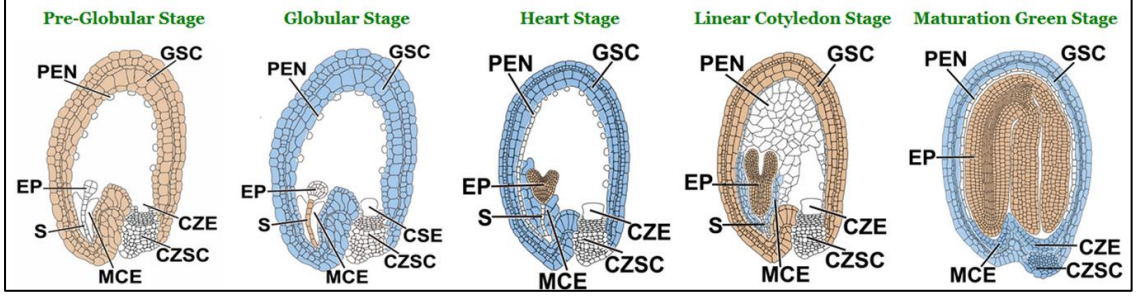

AT2G39510.1:UmamiT14

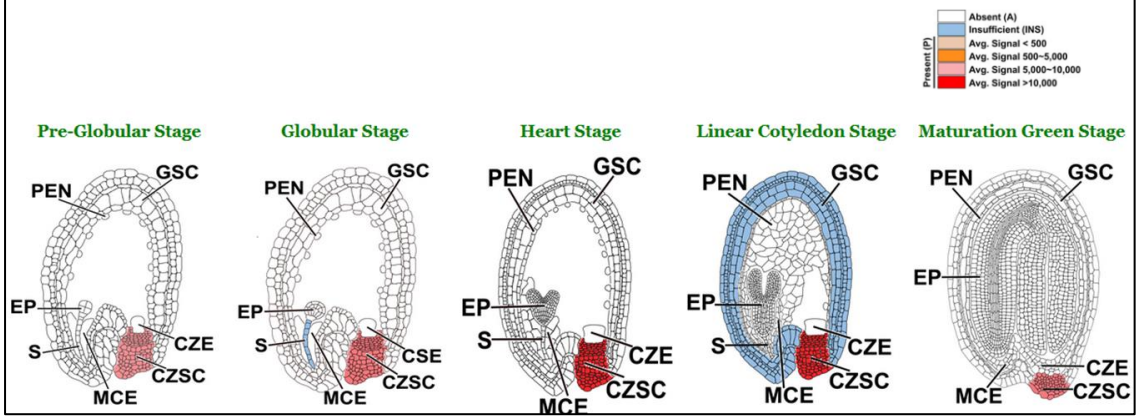

AT1G01070:UmamiT28

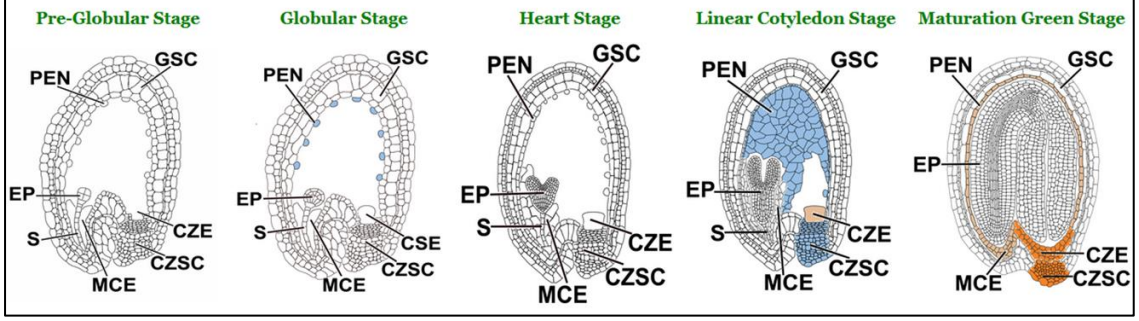

AT4G01430:UmamiT29

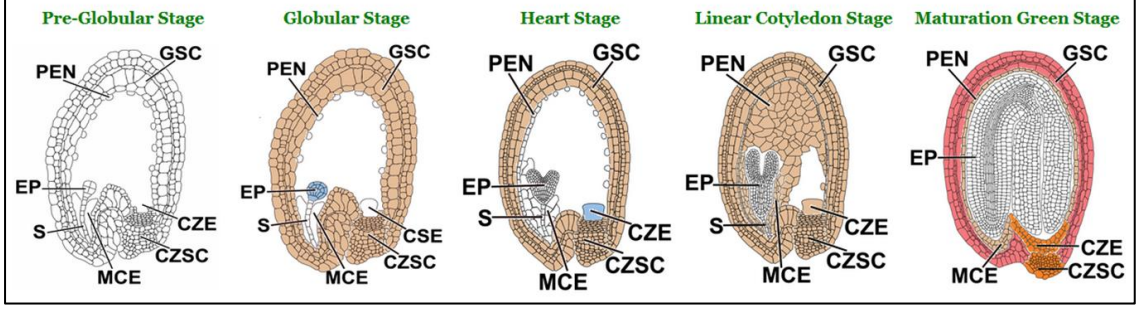

Annex 2

In annex 2 information related to the stages of flower development according to Smyth et al. (1990) and Schneitz et al. (1995) are provided.

Table 10: Summary of stages of ovule development in *A. thaliana* (Schneitz et al., 1995).

Ovule stages	Ovule development		Floral development		
	Embryo sac and endosperm development	Sporophytic tissue development	Gynoecium development[a]	Floral landmarks of corresponding floral stages[b,c]	Duration (h)[b,c]
1. Early phase of ovule development					
1-I		Protrusions arise	Open cylinder	Locules appear in long stamens (floral stage 8)	24
1-II		Protrusions elongated	Cylinder constricted at apex	Petal primoridia stalked at base (floral stage 9)	60
2. Megasporogenesis					
2-I	Megaspore mother cell enlarges		Cylinder closed	Petals level with short stamens (floral stage 10)	12
2-II		Inner integument initiates			
2-III		Outer integument initiates, chalazal nucellus divides			
2-IV	Meiosis	Chalazal nucellus enlarges	First immature papillar cells which do not cover all of the stigma yet, lateral vasculature visible as lighter strip	Filaments start to elongate, anthers green (floral stage 11)	30
2-V	Tetrad formation	Integuments extend toward the apex of the nucellus			
3. Megametogenesis					
3-I	Degenerating tetrad with mono-nuclear embryo sac	Outer integument envelops the nucellus and the inner integument, funiculus and nucellus curve			
3-II	Two-nuclear embryo sac	Outer integument surrounds nucellus, micropylar end pointing more than 90° away from funiculus, further differential growth of integuments	Papillar cells small and covering all the stigma, style recognizable, valves almost visible as distinct structures	Petals level with long stamens, anthers turn yellow (floral stage 12)	42
3-III	Vacuole appears	Micropylar end points away about 90° from funiculus	Papillar cells grow longer		
3-IV	Four-nuclear embryo sac	Inner integument surrounds nucellus, endothelium differentiates	Valves more pronounced		
3-V	Eight-nuclear embryo sac, cellularization				
3-VI	Central cell nuclei fuse, antipodal cells degenerate	Additional cell layer initiated in inner integument	Well-extended papillar cells, prominent style and valves		

Table 11: Summary of stages of flower development in *A. thaliana*, listing the landmark events that define the beginning events of each stage and its approximate duration (Smyth et al., 1990).

Stage	Landmark Event at Beginning of Stage	Duration[a] (hr)	Age of Flower at End of Stage[a] (days)
1	Flower buttress arises	24	1
2	Flower primordium forms	30	2.25
3	Sepal primordia arise	18	3
4	Sepals overlie flower meristem	18	3.75
5	Petal and stamen primordia arise	6	4
6	Sepals enclose bud	30	5.25
7	Long stamen primordia stalked at base	24	6.25
8	Locules appear in long stamens	24	7.25
9	Petal primordia stalked at base	60	9.75
10	Petals level with short stamens	12	10.25
11	Stigmatic papillae appear	30	11.5
12	Petals level with long stamens	42	13.25
13[b]	Bud opens, petals visible, anthesis	6	0.5
14	Long anthers extend above stigma	18	1
15	Stigma extends above long anthers	24	2
16	Petals and sepals withering	12	2.5
17	All organs fall from green siliques	192	10.5
18	Siliques turn yellow	36	12
19	Valves separate from dry siliques	up to 24	13
20	Seeds fall		

[a] Estimated to nearest 6 hr.
[b] Results for stages 13 to 20 (after the flower opens) are summarized from Müller (1961) where they were named B3 to B10. Their timings are given separately because a different strain was grown under different conditions from those used in the present study.

Annex 3

Schematic representations of the constructs containing a RPSP and the genomic *PHO1* or *PHO1;H1* sequence fused to GUS.

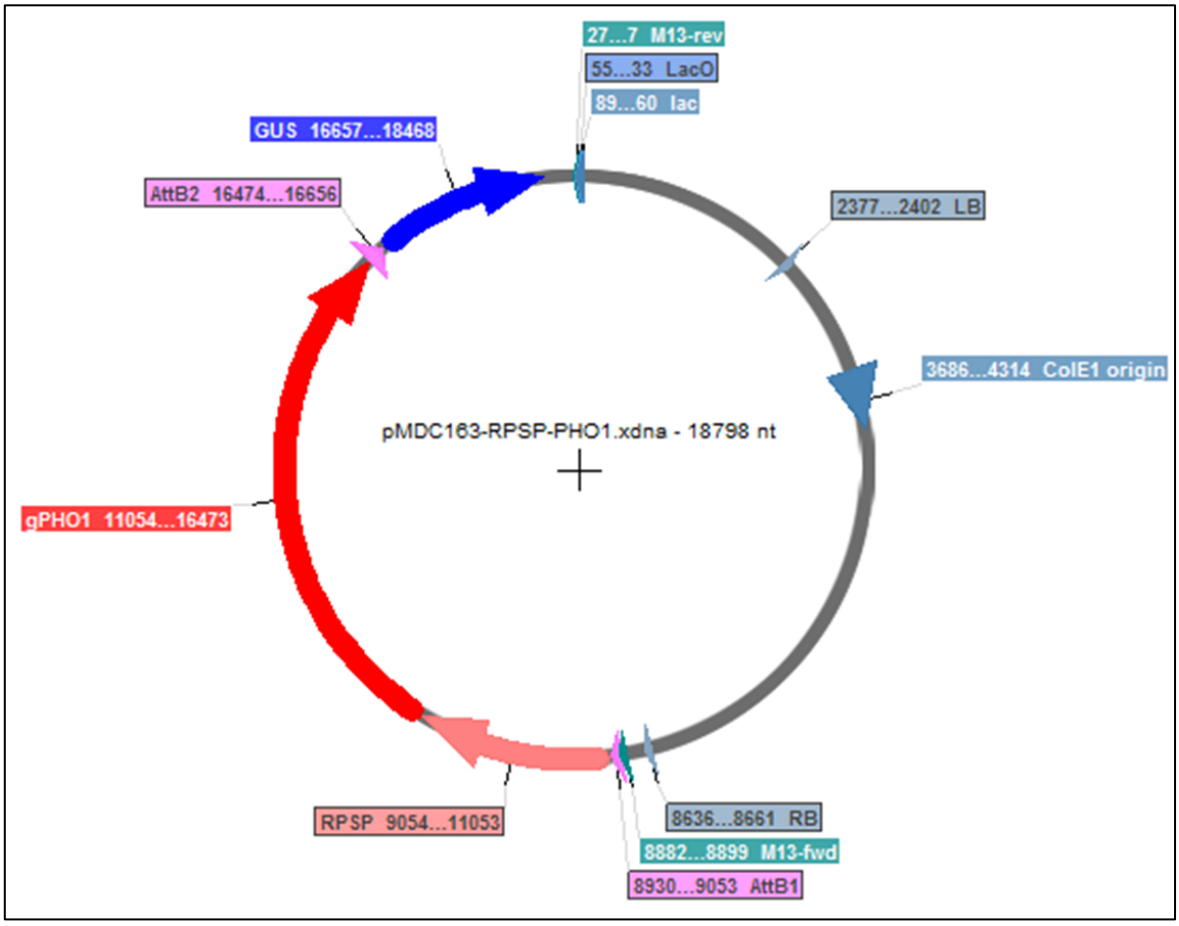

Figure 59: Schematic representation of the constructs containing the genomic sequence of *PHO1* fused to GUS in front of one of the four RPSPs identified with the help of GENEVESTIGATOR. The graph was made using SerialCloner 2.6.1 software.

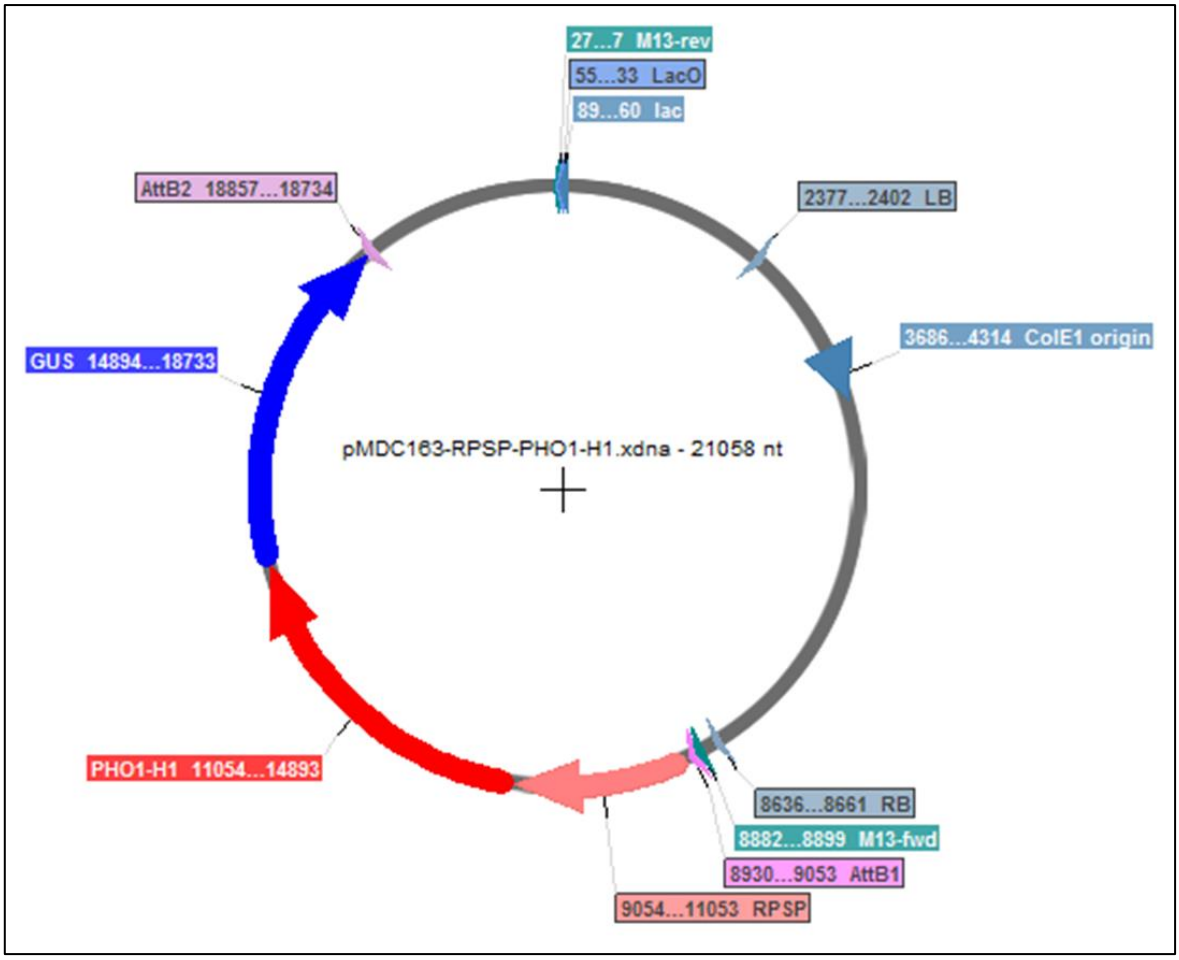

Figure 60: Schematic representation of the constructs containing the genomic sequence of *PHO1;H1* fused to GUS in front of one of the four RPSPs identified with the help of GENEVESTIGATOR. The graph was made using SerialCloner 2.6.1 software.